MYB IS REQUIRED FOR β-SELECTION DURING THYMOPOIESIS

Amanda Katherine Duley
Westminster, Maryland

B.S., University of Delaware, 2001

A Dissertation presented to the Graduate Faculty
of the University of Virginia in Candidacy for the Degree of
Doctor of Philosophy

Department of Microbiology

University of Virginia
August, 2009

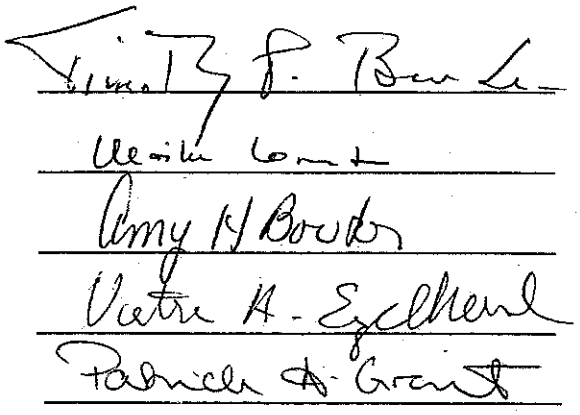

Abstract

c-Myb is a transcription factor required during hematopoiesis and is crucial for multiple stages of thymopoiesis. Understanding c-Myb function during hematopoiesis has been greatly impeded due to the lack of a tractable genetic system. We have used the Cre/loxP approach to conditional mutagenesis to study c-Myb function during thymopoiesis. Thymocyte specific inactivation of the *Myb* locus demonstrated a block in DN3 to DN4 differentiation concomitant with impaired Vβ to DJβ recombination of the *Tcrb* locus suggesting that the inability to generate a TCRβ protein blocked DN3 differentiation. However, some DN3 thymocytes expressed a TCRβ protein but very few thymocytes transitioned to the DN4 stage suggesting that c-Myb is required for DN3 to DN4 differentiation. To determine if c-Myb plays additional role(s) during transition from the DN3 to DN4 stage of thymocyte differentiation, we bred mice with either *Myb*^{ff} *cwlckCre Rag2*$^{-/-}$ or *Myb*^{ff} *cwlckCre Rag2*$^{-/-}$ *Tcrb-Tg* genotypes. c-Myb does not appear to be required for maintenance of the DN3E compartment in *Rag2*-deficient thymocytes, and defective V(D)J recombination in the *Myb*$^{f/f}$ *C* mice is not simply a consequence of reduced survival and the inability to complete V(D)J recombination. Moreover, the presence of a *Tcrb* transgene (Tg) was not able to rescue DN3 to DN4 differentiation in the absence of c-Myb, demonstrating for the first time that c-Myb is required for normal β-selection independent of the impairment in V(D)J recombination. We present evidence that c-Myb deficient thymocytes can initiate some events associated with pre-TCR signaling and up-regulate surface markers indicative of β-selection such as CD5, CD2 and CD27. In addition, *Myb*- and *Rag2*$^{-/-}$ doubly deficient mice are able to respond to pre-TCR stimulation by anti-CD3ε treatment to down-regulate CD25 and up-regulate CD8. However, survival of pre-TCR+ DN3

thymocytes is impaired in the absence of c-Myb which is not rescued by expression of a *Bcl-2*-transgene or loss of *p53*. Moreover, in DN4 thymocytes both survival and proliferation is impaired. The inability of DN4 thymocytes to proliferate could be due to the massive amount of cell death that was occurring; however, pre-TCR+ DN and ISP thymocytes fail to receive signals to enter the cell cycle and do not express cyclin D3. Despite recent studies that demonstrated that mature B lymphocytes can proliferate without c-Myb, we demonstrate that c-Myb is required for proliferation during β-selection of DN4 and ISP thymocytes. We performed gene expression microarrays on several DN subsets from *Myb*$^{f/f}$ *cwlckCre* and control mice to gain insight into how c-Myb regulates proliferation and survival during β-selection. The microarrays suggest changes in expression of genes involved in interaction with the thymic microenvironment which could cause the impaired proliferation and survival in c-Myb-deficient thymocytes. Moreover, we provide preliminary data that suggests that c-Myb may be involved in migration to CXCL12 and in interaction with extracellular matrix protein laminin. Thus, we provide evidence that c-Myb plays multiple roles during differentiation of DN3 thymocytes independent of V(D)J recombination that is most likely due to the altered expression of multiple transcriptional targets of c-Myb.

Acknowledgments

I have learned a great deal pursuing my doctorate degree at the University of Virginia and I have really enjoyed meeting wonderful students, postdocs, faculty and support staff. I am thankful that I worked on my thesis dissertation in a wonderful laboratory environment with great individuals both past and present. I would like to thank my mentor, Timothy P. Bender, for giving me the opportunity to work in his lab. I made his project my own and its complexity was a great challenge. He has taught me how to think critically about science and he has prepared me for career in science. We also formed a great friendship and I am very thankful for the hellebores, lawnmower and use of the tiller and tent. I would also like to thank our technicians Chris Kremer and Rowena Crittenden for their expert advice on scientific techniques and on the meaning of life. Rowena has been a wonderful pillar of support and praise these past 4 years and I am very thankful that she chose to join our lab. I would also like to thank all the wonderful graduate students that have been a part of our lab. My senior graduate student, Matt Thomas, continues to give me advice and support and I am very thankful for all of his help and his friendship. For the past 7 years, I have worked with Joan Yuan and I have appreciated her Chinese/Swedish outlook on life. We have worked so long and well together and we have worked at desks that face each other that we can communicate without words. We had read some place on the internet that people have work spouses and we joke that we are each other's lab spouse. I would also like to thank Erin Yarde for all her support and for general knowledge about cooking, style and wine and for those extra pounds I gained from helping her test new recipes for baked goods. Shawn Fahl has also provided me with hours of laughs,

stories and field trips to the Corner and cafeteria. He is always ready to take a punch, joke around and climb on the beach tops. I would also like to thank our undergraduate helper Katie Shi from Haiti for helping with all of my genotyping and general lab stuff and for making me smile everytime she would leave and sweetly say, “Goodbye, Dr. Bender”. We have a great dynamic in the laboratory and I am thankful for all the lunches spent together, all the stories shared and all the lab jokes played on everyone including our fearless leader. There are too many people to name that are a part of other laboratories that I am thankful for their friendship and scientific advice; however, I would like to thank Paul Trampont for all of his scientific help and advice on life. He is always willing to help and he is extremely knowledgeable and will take the time to answer all of my many questions. I am very thankful for the hours spent discussing each other’s blocks in DN3 differentiation.

I would not have been able to come this far without the support from my parents, family and friends. My parents loved and supported me to go for whatever I wanted in life. I would also like to thank my sister who always challenged me mentally and was also very supportive. I am also very grateful to my husband who has been with me since day one of graduate school and he has been encouraging, patient and understanding through the years. He has readily picked up where I have slacked and we made a great team together going through my graduate school. I would also like to thank all the wonderful friends I have met in Charlottesville. I do not think I would have been able to accomplish my goal without their love, support and field trips to ski and mountain bike.

Table of Contents

List of Figures

Chapter I.

Chapter II.

Chapter III.

List of Tables

List of Abbreviations

7AAD	**7-aminoacetomycin D**
Ada	**Adenosine deaminase**
AEBSF	**4-(2-Aminoethyl) benzenesulfonyl fluoride hydrochloride**
Akt	**thymoma viral proto-oncogene**
αMEM	**alpha-Minimum Essential Medium**
AMV	**Avian Myleoblastosis Virus**
APC	**Adenomatous Polyposis Coli**
AP-1	**Activator protein 1**
Axin	**Axis Inhibitor**
BCA	**Bicinchoninic acid**
BCR	**B Cell Receptor**
Bp	**base pairs**
BrdU	**5-bromo-2'-deoxyuridine**
BSA	**Bovine Serum Albumin**
CBP	**CREB binding protein**
CCCP	**Carbonyl cyanide chlorophenylhydrazone**
Cdk	**Cyclin dependent kinase**
Ck1	**Casein Kinase 1**
cDNA	**complementary DNA**
C/EBPβ	**CCAAT/enhancer binding protein beta**
CFSE	**5-(and-6)-carboxyfluorescein diacetate, succinimidyl ester**
ChIP	**Chromatin Immunoprecipitation**

CLP	**Common Lymphoid Progenitor**
CREB	**cAMP response element binding**
D	**Diversity**
dCTP	**Deoxycytidine Triphosphate**
DBD	**DNA binding domain**
DISC	**Death-inducing signaling complex**
DL	**Delta like**
DMEM	**Dulbecco's Modified Eagle Medium**
DN	**Double Negative**
DNA	**Deoxyribonucleic Acid**
DP	**Double positive**
DSB	**Double-stranded-break**
ECL	**Enhanced Chemiluminescence**
ECM	**Extracellular Matrix**
EDTA	**Ethylenediaminetetraacetic acid**
eEF2	**Eukaryotic elongation factor 2**
Egr	**Early growth response**
ERK	**Extracellular signal-regulated kinase**
ETP	**Early T lineage Progenitors**
FACS	**Fluorescence Activated Cell Sorter**
FADD	**Fas associated death domain**
FBS	**Fetal Bovine Serum**
FDR	**False Discovery Rate**
FSC	**Forward side scatter**

FZ	**Frizzled**
GCRMA	**GC Robust Multi-array Average**
GEM	**Glycoprotein-enriched microdomains**
Grb-2	**Growth factor receptor-bound protein 2**
GTPase	**Guanosine triphosphatase**
GSK3β	**Glycogen synthase kinase-3β**
H2A.Z	**H2A histone Z**
HLR	**Heptad leucine repeat**
HRP	**Horseradish Peroxidase**
HSC	**Hematopoietic stem cell**
IAP	**Inhibitors of apoptosis**
ICN	**Intracellular Notch**
IL	**Interleukin**
IMDM	**Iscove's Modified Dulbecco's Medium**
ISP	**Immature single positive**
ITAM	**Immunoreceptor tyrosine-based activation motif**
J	**Joining**
Kb	**Kilobase**
kD	**Kilodalton**
LAT	**Linker for activation of T cells**
Lck	**Lymphocyte protein tyrosine kinase**
LEF	**Lymphocyte-enhancer-binding factor**
Lpr	**Lymphoproliferative**
LPR5, LPR6	**Low-density-lipoprotein-receptor-related-protein**

MACS	**Magnetic Cell Sorting**
MAM	**Mastermind**
MAPK	**Mitogen activated protein kinase**
Mat2a	**Methionine adenyl-transferase II, alpha**
MBS	**Myb Binding Sequence**
MCL-1	**Myeloid cell leukemia sequence 1**
MFI	**Mean Fluorescence Intensity**
MLP	**Mouse Lineage Panel**
MPP	**Multipotent Progenitor**
MHC	**Major Histocompatiblity complex**
MRE	**Myb Responsive Element**
mRNA	**messenger RNA**
NFAT	**NF of activated T cells**
NF-kB	**Nuclear Factor kB**
NHEJ	**Nonhomologous DNA end-joining**
NRD	**Negative Regulatory Domain**
PAGE	**Polyacrylamide gel electrophoresis**
PBA	**PBS plus 0.5% BSA and 0.01% Sodium Azide**
PBS	**Phosphate Buffered Saline**
PBST	**PBS plus 0.05% Tween**
PCR	**Polymerase Chain Reaction**
PI	**Propidium Iodide**
PI3K	**Phosphatidylinositol-3-OH kinase**
PLCγ1	**Phospholipase C-γ1**

PMA	**Phorbyl myristate acetate**
PMSF	**Phenylmethylsulfonyl fluoride**
PP1	**Protein phosphatase 1**
PP2	**Protein phosphatase 2**
PS	**Phosphatidylserine**
PSGL	**P-selectin glycoprotein ligand**
PTEN	**Phosphatase and tensin homolog**
qPCR	**Quantitative Real Time Polymerase Chain Reaction**
Rac-1	**Ras-related C3 botulinum toxin substrate 1**
Raf	**v-raf-leukemia viral oncogene 1**
Rb	**Retinoblastoma protein**
RBP-J	**Recombination signal binding protein for immunoglobulin kappa J region**
RCN	**Relative cell number**
RNA	**Ribonucleic Acid**
RPMI	**Roswell Park Memorial Institute**
RSS	**Recombination Signal Sequence**
RT	**Room Temperature**
RT-PCR	**Reverse Transcriptase PCR**
SCID	**Severe Combined Immunodeficiency mutation**
SDS	**Sodium Dodecyl Sulfate**
SLP-76	**SH2-domain-containing leukocyte protein of 76kD**
Sos	**Son of sevenless**
SP	**Single positive**

SSC	**Side light scatter**
SUMO-1	**SMT3 suppressor of mif two 3 homolog 1**
TCF	**T cell factor**
TCR	**T cell receptor**
Tdt	**Terminal deoxynucleotidyl transferase**
Tg	**Transgene**
TIF1β	**Transcription intermediary factor 1-beta**
TNFRSF	**Tumor Necrosis Factor Receptor Superfamily**
V	**Variable**
VCAM	**Vascular cell adhesion molecule 1**
ZAP-70	**Zeta-chain (TCR) associated protein kinase**

Chapter I. Introduction

T Cell Development.

T cell mediated immunity is based on the ability of T cells to recognize and respond with effector functions to a plethora of foreign antigens that the host might encounter over a lifetime. An individual contains billions of T cells but each αβ-T cell expresses a unique αβ-T cell receptor (TCR) that recognizes a single antigen. Mature T cells also have a limited lifespan and must be renewed throughout the life of an individual. The complex process of generating new T cells is called thymopoiesis and the diversity of the αβ-TCR repertoire is generated during this process. However, the generation of new T cells and their TCRs is a somewhat random process allowing for diversity. Checkpoints are in place at different stages of thymopoiesis to test if a TCRβ protein was successfully produced and to test the self reactivity of the αβ-TCR.

Thymopoiesis occurs in the thymus and can be divided into distinct stages of differentiation based on cell surface expression of the TCR and co-receptors, CD4 and CD8, and rearrangement status of the αβ-TCR chains (Figure 1). The thymus does not contain self renewing hematopoietic stem cells and is seeded by bone marrow-derived pregenitor cells that migrate via the bloodstream throughout the lifetime of the individual [5-7]. The earliest thymic progenitor cells are referred to as double negative (DN) because they express neither CD4 nor CD8 and comprise 5% of the total

Figure 1. Outline of T cell developmental in the thymus. T cell development can be divided into stages based on expression of CD4, CD8, CD25, CD44, CD117 and CD3 and rearrangement status of the V, D and J gene segments of the *Tcra* and *Tcrb* loci. Also presented are the β-selection and Positive and Negative Selection check points.

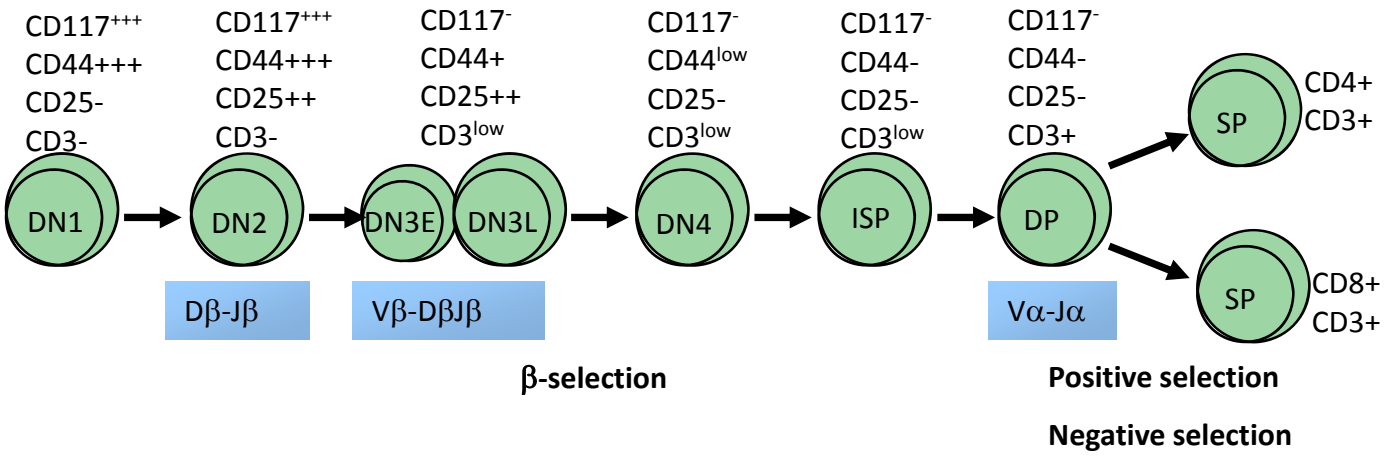
CD117+++
CD44+++
CD25-
CD3-
DN1
CD117+++
CD44+++
CD25++
CD3-
DN2
Dβ-Jβ
CD117-
CD44+
CD25++
CD3low
DN3E
DN3L
Vβ-DβJβ
β-selection
CD117-
CD44low
CD25-
CD3low
DN4
CD117-
CD44-
CD25-
CD3low
ISP
CD117-
CD44-
CD25-
CD3+
DP
Vα-Jα
Positive selection
Negative selection
SP
CD4+
CD3+
SP
CD8+
CD3+

thymocytes. DN thymocytes differentiate to become CD8+ immature single positive (ISP) thymocytes before expressing CD4 to become CD4+CD8+ double positive (DP) thymocytes which constitute 80% of total thymocytes. DP thymocytes differentiate to become mature CD4 or CD8 single positive (SP) thymocytes.

The DN population can be further subdivided based on expression of CD44, CD25 and CD117, beginning with the most immature subset as CD44+CD25-CD117+ (DN1), CD44+CD25+CD117+ (DN2), CD44-CD25+CD117- (DN3) and CD44-CD25-CD117- (DN4) as the more mature DN subset [15]. Cells that seed the thymus from the bone marrow are not committed to the T cell lineage and DN1 thymocytes retain myeloid lineage potential [16]. Development of DN1 and DN2 thymocytes is driven by interactions with cytokines and the thymic microenvironment to initiate a T-lineage transcriptional program while down-regulating genes required of non-T-lineage differentiation [17, 18]. DN1 and DN2 thymocytes proliferate to increase the number of T cell progenitor cells [19]. During the late DN2 stage upon down-regulation of CD117, proliferation ceases and thymocytes initiate generation of the β-chain of the TCR [20, 21].

To generate a functional TCRβ chain, the *Tcrb* locus undergoes V(D)J recombination of its gene segments variable (V), diversity (D) and joining (J) which are widely spread over 500kb to generate a single coding segment. V(D)J recombination is initiated by the recombinase activating proteins encoded by the recombinase activating

genes, Rag-1 and Rag-2 which are only expressed in cells undergoing antigenic receptor rearrangement [22-24]. Rag proteins bind to recombination signal sequences (RSSs) that flank the V, D and J gene segments and initiate double-strand breaks (DSB) [25]. Double-strand break repair proteins, known as nonhomologous DNA end-joining (NHEJ) proteins, process and rejoin the ends of the gene segments.

In DN2 thymocytes, rearrangement of the Dβ to Jβ gene segments takes place on both alleles [26]. As cells differentiate to the DN3 stage, recombination of Vβ-DJβ gene segments occurs on one allele at a time until a functional TCRβ-chain is made [26, 27]. The process of V(D)J recombination is imprecise which contributes to the diversity of the TCR repertoire but it often results in aberrant TCRβ rearrangements [28]. To prevent the accumulation of thymocytes with aberrant TCRβ-chains, the β-selection checkpoint is in place [29]. Thymocytes unable to productively rearrange their *Tcrb* loci do not receive signals to advance beyond the DN3 stage of development [30]. In order to receive signals to mature, the nascent TCRβ-chain forms a complex with CD3ε, γ, η/ξ signaling molecules and an invariant pre-Tα (pTα) chain, to form the pre-TCR [31]. Signals downstream of the pre-TCR complex, as well as interaction with the thymic microenvironment, are required to traverse the β-selection checkpoint [32-39]. Pre-TCR signaling drives a series of maturation events that include proliferation, survival, differentiation to the DP stage, and allelic exclusion of the *Tcrb* locus ceasing further rearrangement at the *Tcrb* locus [22, 27, 40-42]. This contributes to the diversity of the

αβ-TCR repertoire by expanding the number of cells that produce a given TCRβ chain which can then pair with different TCRα chains [43].

Rearrangement of gene segments Vα to Jα of the *Tcra* locus occurs at the DP stage. The newly generated TCRα-chain replaces the preTα chain to pair with the TCRβ chain to form the mature αβ-TCR. The αβ-TCR is expressed on the cell surface in conjunction with CD3γ, δ, ε, and ζ signaling molecules [44]. Surface expression of the αβ-TCR initiates a second checkpoint to test the ability of the αβ-TCR to interact with self-peptides complexed with major histocompatibility complex (MHC) molecules [45-47]. If DP thymocytes generate a TCR with low avidity or are unable to interact with the MHC molecules they undergo apoptosis via a process referred to as "death by neglect". Thymocytes that produce an αβ-TCR with moderate avidity for peptide/self-MHC complexes receive positive selection signals to differentiate while SP thymocytes with strong avidity for peptide/self-MHC complexes receive negative selection signals to die [47]. If DP thymocytes are positively selected, they down regulate either CD8 or CD4 to become a SP thymocyte based on their ability to interact with MHC class I or II, respectively [48]. CD4 and CD8 SP T cells migrate from the thymus to the periphery to form the peripheral T cell compartment.

β-selection

β-selection refers to the maturation signals provided by the pre-TCR and thymocyte:stromal cell interactions during differentiation of DN3 thymocytes to the DP stage. The DN3 compartment is heterogeneous in that it contains non-proliferating cells that are actively undergoing V(D)J recombination at the *Tcrb* loci as well as proliferating cells that have successfully completed V(D)J recombination and produce a TCRβ protein. DN3 thymocytes that are actively carrying out V(D)J recombination are small in size and referred to as 'E' for 'expected size' (DN3E) [2]. Thymocytes that are unable to perform V(D)J recombination due to the absence of RAG proteins [23, 24, 30] or that lack components involved in DNA repair (severe combined immunodeficiency mutation [SCID]) [49] are blocked to differentiation beyond the DN3E stage [2]. The DN3 subset also includes cells that have successfully completed V(D)J recombination at one of the *Tcrb* loci, produce a TCRβ protein, form a pre-TCR and proliferate and survive in response to pre-TCR mediated signals. These cells are large and are referred to as 'L' for 'larger than expected' (DN3L) [2]. The pre-TCR also provides signals to differentiate beyond the DN3L stage [40, 50-53]. DN3L thymocytes down-regulate CD25 to become DN4 thymocytes, up-regulate CD8 to become ISP thymocytes and subsequently up-regulate CD4 to become DP thymocytes [27, 40-42]. Interestingly, the pre-TCR also signals allelic exclusion of the *Tcrb* locus inhibiting further rearrangement at the *Tcrb* locus while providing signals that result in initiation of Vα to Jα rearrangement of the *Tcra* locus [22, 54-56].

Pre-TCR signaling is inherently different from signals provided by the mature αβ-TCR despite some shared downstream outcomes like survival, proliferation, and differentiation [31]. In the absence of a pTα, expression of a TCRα transgene in DN thymocytes is unable to induce effective proliferation, survival and differentiation during β-selection demonstrating the specificity of the pre-TCR signal [57]. These differences could be attributed to the difference in usage of CD3 signaling components. The CD3δ chain is dispensable for activation of the extracellular signal-regulated kinase (ERK) signaling pathway during pre-TCR signaling but is essential for αβ-TCR activation of ERK to mediate positive selection [58, 59]. The differences between αβ-TCR and pre-TCR signaling could also be attributed to the differences in the nature of the self-oligomerization signal generated by the pre-TCR versus the ligand-receptor signaling of the αβ-TCR at the cell surface [60, 61].

The purpose of the self-oligomerization of the pre-TCR, which is mediated by preTα, is to crosslink the CD3 chains [61]. This has been demonstrated in *Rag*-null mice treated with anti-CD3ε antibody *in vivo,* which induces β-selection signaling bypassing the need for the pre-TCR [62, 63]. It is also thought that pre-TCR signaling occurs in glycolipid-enriched microdomains (GEMs) to facilitate interaction with downstream signaling molecules found in GEMs such as Lck (lymphocyte protein tyrosine kinase) and the adapter protein LAT (linker for activation of T cells) [64]. Disruption of the plasma membrane lipid structure in pre-TCR^{+} cell lines reduced the phosphorylation of tyrosine

kinases downstream of the pre-TCR [64, 65]. However, targeting CD3 to the GEMs by fusing CD3ε to LAT did not drive β-selection events whereas expression of a constitutively dimerizing CD3ε did drive β-selection events [60]. It is possible that the pre-TCR localizes to the GEMs as a result of β-selection signaling and localization to GEMs may be required for downstream signaling events but it does not appear to initiate pre-TCR signaling [61].

Self-oligomerization of the pre-TCR and crosslinking of the CD3 signaling chains results in phosphorylation of the conserved tyrosine residues in the cytoplasmic domains of the CD3 chains referred to as immunoreceptor tyrosine-based activation motives (ITAMs) by the Src-family of protein tyrosine kinases, Lck and Fyn (Figure 2). The phosphorylated ITAMs act as docking sites for the SH2 domain containing Syk/ZAP-70 (zeta-chain [TCR] associated protein) protein tyrosine kinase family. Lck then phosphorylates and activates ZAP-70 which in turn phosphorylates adapter proteins LAT and SLP-76 (SH2-domain-containing leukocyte protein of 76kD). Deficiencies in Lck and Fyn [66], Zap-70 and Syk [67], LAT [68] and SLP-76 [69] blocked β-selection demonstrating the crucial roles of these kinases and adapter proteins during pre-TCR signaling.

Other proteins recruited to the SLP-76/LAT adapter complex include Grb-2 (growth factor receptor-bound protein 2), Sos (Son of sevenless) and Vav-1. Vav-1 is a guanine nucleotide exchange factor that recruits and activates the GTPase (Guanosine

Figure 2. Schematic of pre-TCR signaling network. The pre-TCR is composed of a pTα protein, a TCRβ protein, and CD3 δ, γ, ε, and ζ signaling proteins which contain ITAMs. Signaling molecules involved in the pre-TCR signaling cascade provide signals for thymocytes to survive, proliferate, differentiate, and undergo allelic exclusion. Signals downstream of death receptor family TNFRSF may also be blocked by pre-TCR signaling (adapted from [12]).

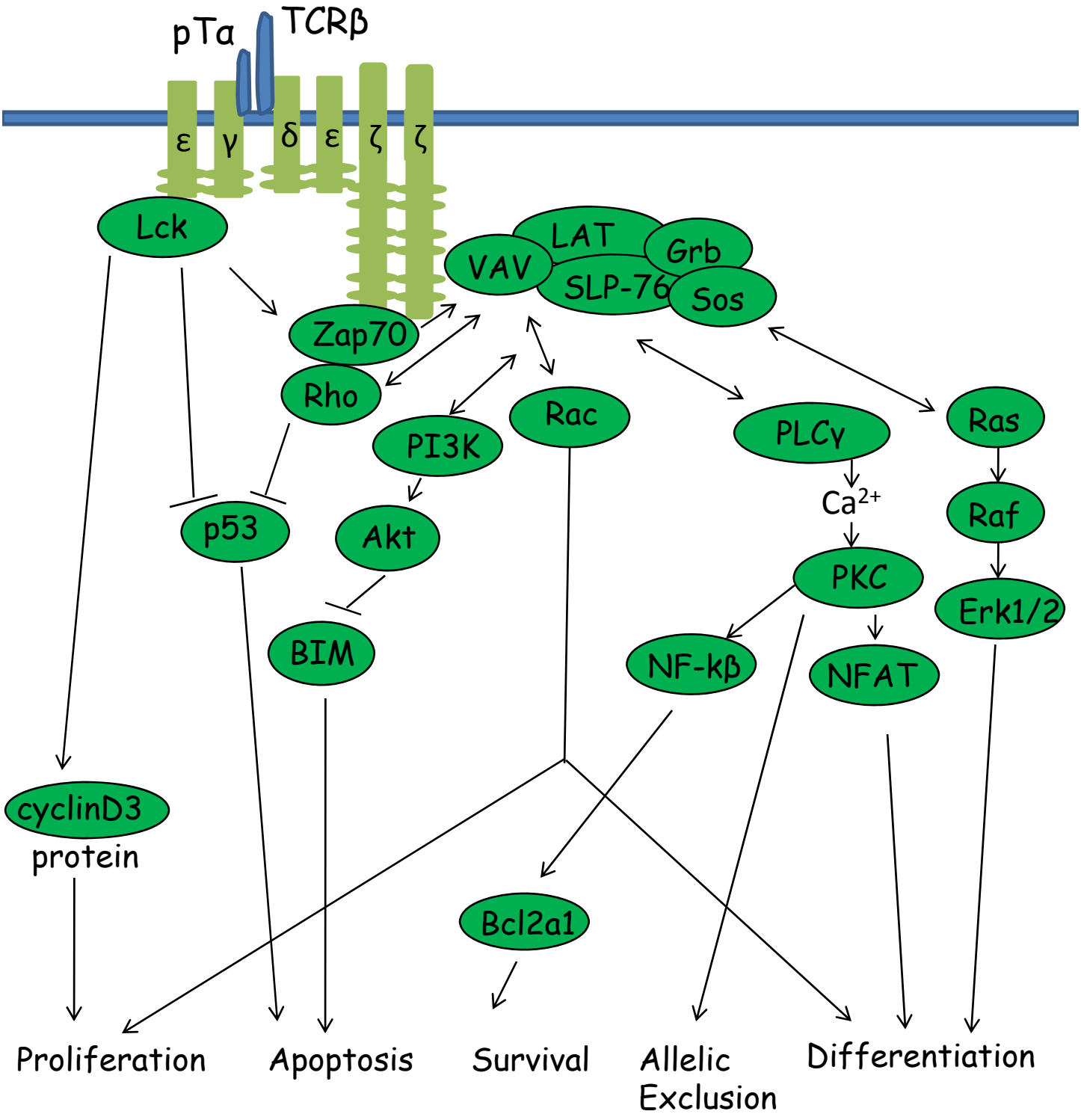
pTα
TCRβ
ε
γ
δ
ε
ζ
ζ
Lck
LAT
Grb
VAV
SLP-76
Sos
Zap70
Rho
Rac
PI3K
PLCγ
Ras
Ca2+
Raf
p53
Akt
PKC
Erk1/2
BIM
NF-kβ
NFAT
cyclinD3
protein
Bcl2a1
Proliferation
Apoptosis
Survival
Allelic
Exclusion
Differentiation

triphosphatase) Rac-1 (Ras-related C3 botulinum toxin substrate 1). Rac-1 mediates β-selection proliferation and differentiation signals possibly through regulation of the actin cytoskeleton [70, 71]. Grb-2 is an adapter protein that recruits the guanine nucleotide exchange factor Sos which activates the Ras GTPase [72]. Ras subsequently activates the serine-threonine kinase Raf (v-raf-leukemia viral oncogene 1) and ERK1 and ERK2 mitogen activated protein kinases (MAPKs) resulting in proliferation and differentiation signals [73-76]. PI3K (phosphatidylinositol-3-OH kinase) is also recruited to the SLP-76/LAT adapter complex [77] and subsequently leads to the activation of Akt1 (thymoma viral proto-oncogene 1), Akt2, and Akt3 resulting in β-selection induced survival and proliferation signals [78]. The Rho GTPase is activated downstream of the pre-TCR and is required for p53-dependent survival [79-81]. PLCγ (phospholipase C-γ1) also becomes phosphorylated and activated downstream of the pre-TCR signal [65, 82]. PLCγ hydrolyzes phosphatidylinositol (4,5) bisphosphate (PIP_2) generating inositol (1,4,5)triphosphate (IP_3) and diacylglycerol (DAG) [83]. IP_3 and store-operated plasma membrane Ca^{2+} channels contribute to the biphasic rise of Ca^{2+} [65]. Ca^{2+} and DAG activate protein kinase C (PKC) [84] which induces signals for allelic exclusion and activates transcription factors nuclear factor of activated T cells (NFAT) and nuclear factor κB (NFκB) family members (p50-p65 heterodimers) [85] to mediate survival and differentiation [65, 85-87]. Many of these downstream signaling pathways mediate more than one downstream functional outcome of β-selection suggesting that the β-selection signals are not exclusive. How these signaling pathways directly mediate

survival, proliferation, differentiation or allelic exclusion at the *Tcrb* locus is just beginning to be unraveled.

Pre-TCR Mediated Proliferation. Early studies demonstrated that DN3 thymocytes that received proliferation signals to become DN3L thymocytes contain hyperphosphorylated retinoblastoma protein (Rb) as compared to DN3E thymocytes [2]. Rb enforces the G1 checkpoint during the cell cycle by binding and sequestering E2F transcription factors to inhibit transcription of genes required for S-phase [88]. Hyperphosphorylation of Rb is mediated by the D cyclins complexed with cyclin-dependent-kinase (cdk4) or cdk6 early in G1 and by cyclin E and cyclin A complexed with cdk2 during middle to late G1 [89] (Figure 3). Despite the fact that DN3L thymocytes contain hyperphosphorylated Rb, it is not known if hyperphosphorylation of Rb is absolutely required to traverse the β-selection checkpoint [12]. Interestingly, thymi of *ccnd3*$^{-/-}$ mice but not *ccnd2*$^{-/-}$ or *ccnd1*$^{-/-}$ mice contain greatly reduced numbers of total and DP thymocytes and differentiation beyond the DN stage is severely compromised [1, 90]. *Cyclin D3*$^{-/-}$ thymocytes have a reduction in the proportion of DN4 and ISP thymocytes in S-phase and anti-CD3ε treatment of *Rag2*$^{-/-}$*cyclin D3*$^{-/-}$ mice does not increase thymocyte cellularity [1]. Cyclin D3 is expressed downstream of the pre-TCR through activation of Lck and is the only D cyclin expressed in DN4 thymocytes undergoing β-selection prior to down-regulated in DP thymocytes [1]. Thus, cyclin D3 is required for proliferation and/or survival of DN4 and ISP thymocytes in response to pre-TCR signaling.

Figure 3. Pre-TCR Mediated Proliferation. Cyclin D3 mRNA and protein expression are induced downstream of pre-TCR signaling and is dependent on activation of Lck [1]. Early in the G1 phase, Cyclin D3 forms complexes with cyclin dependent kinase 4 (cdk4) or cdk6 to induce phosphorylation of the retinoblastoma (Rb) protein. Cyclin E forms complexes with cdk2 to induce phosphorylation of Rb during middle to late G1 phase. Hyperphosphorylation of Rb releases transcription factor E2F to transcribe genes required for S-phase. Cyclin A forms a complex with cdk2 in S-phase and with cdk1 during G2 phase and cyclin B forms a complex with cdk1 during G2/M phase. Cyclin dependent kinase inhibitors p15, p16, and p17 inhibit D cyclin complexes and p27 and p21 inhibit all other cyclin complexes. (Adapted from [10]).

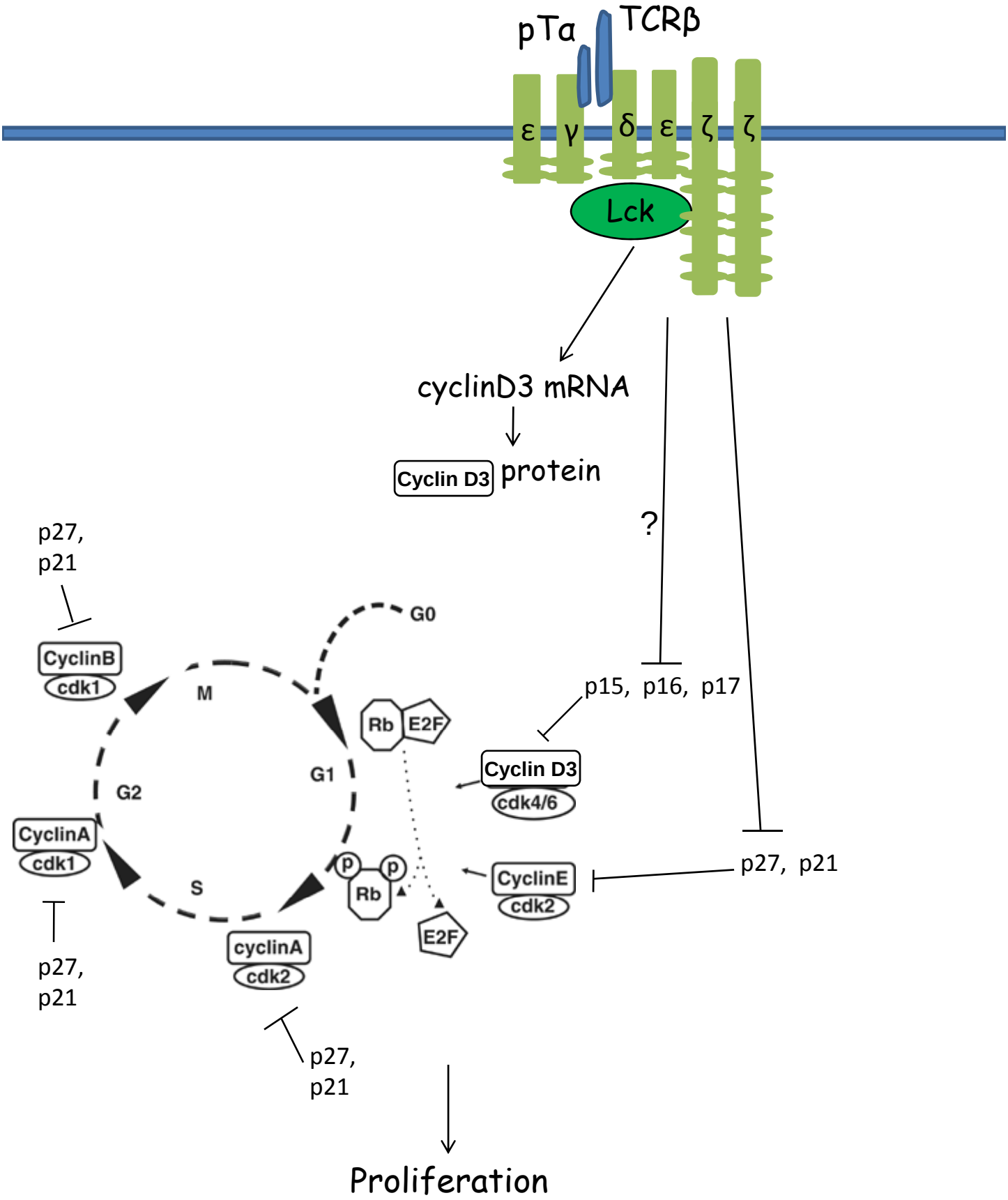
pTα
TCRβ
ε
γ
δ
ε
ζ
ζ
Lck
cyclinD3 mRNA
Cyclin D3 protein
?
p15, p16, p17
p27, p21
p27, p21
p27, p21
p27, p21
p27, p21
CyclinB
cdk1
CyclinA
cdk1
cyclinA
cdk2
Cyclin D3
cdk4/6
CyclinE
cdk2
Rb
E2F
Rb
E2F
G0
G1
S
G2
M
Proliferation

The cell cycle is negatively regulated by cdk inhibitors that function by inactivating cyclin-dependent-kinase complexes. The cdk inhibitors p15, p16, and p17 inhibit cyclin D/cdk complexes and p27 and p21 inhibit all other cyclin/cdk complexes [10]. Expression of p27 protein decreases as cells transit from the DN3E to DN3L stage suggesting that the pre-TCR induces down regulation of p27 [2]. Expression of a $p16^{Ink4\alpha}$ transgene or a $p27^{Kip1}$ transgene in thymocytes blocked differentiation at the DN3 stage [91, 92]. Furthermore, expression of a $p16^{Ink4\alpha}$ transgene in thymocytes, also resulted in apoptosis in thymocytes attempting to undergo β-selection [91] demonstrating that β-selection proliferation and survival signals may not be exclusive.

Pre-TCR Mediated Survival. In the absence of a pre-TCR signal, DN3 thymocytes activate caspase-3 and undergo apoptosis [53, 86, 93]. There are two pathways (extrinsic and intrinsic) that result in caspase-3 activation and apoptosis (Figure 4) and both pathways appear to induce apoptosis in the absence of a pre-TCR signal [86, 94, 95]. The extrinsic pathway involves ligand induced activation of a cell surface death receptor (members of the Tumor Necrosis Factor Receptor Superfamily [TNFRSF]) which signals formation of the death-inducing signaling complex (DISC), and activation of initiator caspases 8 and 10. The initiator caspases cleave and activate effector caspases 3, 6, and 7 which in turn cleave intracellular substrates that leads to cellular destruction. The intrinsic pathway is triggered by DNA damage or cellular stress and signals the formation of an apoptosome, activation of initiator caspases 2 and 9 which activate the

Figure 4. Schematic of the Extrinsic and Intrinsic Apoptotic Pathways. On the left side is the Extrinsic apoptotic pathway which signals formation of the death-inducing signaling complex (DISC) and on the right side is the Intrinsic apoptotic pathway which signals formation of the apoptosome. Molecular components of the DISC and apoptosome are highlighted. Both apoptotic pathways activate effector caspases resulting in apoptosis. (Adapted from [9]).

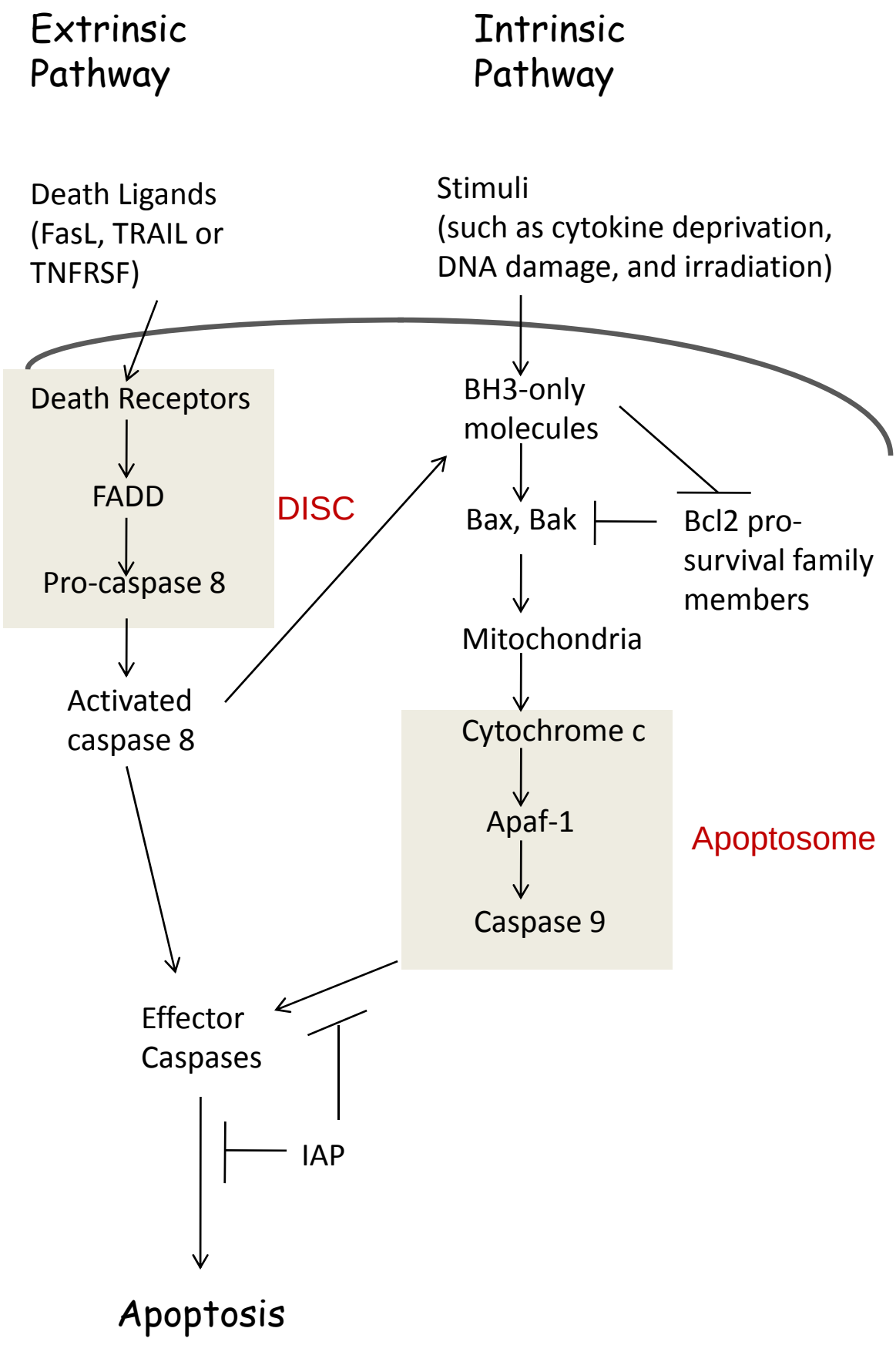
Extrinsic Pathway
Intrinsic Pathway
Death Ligands (FasL, TRAIL or TNFRSF)
Stimuli (such as cytokine deprivation, DNA damage, and irradiation)
Death Receptors
FADD
Pro-caspase 8
DISC
Activated caspase 8
BH3-only molecules
Bax, Bak
Bcl2 pro-survival family members
Mitochondria
Cytochrome c
Apaf-1
Caspase 9
Apoptosome
Effector Caspases
IAP
Apoptosis

effector caspases and the release of mitochondrial factors. Release of mitochondrial factors is determined by the Bcl-2 family members that include proapoptotic and prosurvival members. The ratio of proapoptotic family members (Bax, Bak, Bok, Bcl-x, Bcl-G_L, Bmf, Bid, Bim, Hrk, Noxa, Puma, Bcl-Gs, Blk, Bik and Bad) to prosurvival family members (Bcl-2, Bcl-xl, Mcl-1, A1, Bcl-b and Bcl-w) determines cell fate outcome (Figure 5) [11]. Once the mitochondrial membrane integrity is destroyed, there is no turning back for the cell. In addition to the prosurvival Bcl-2 family members, another prosurvival family of proteins, the inhibitors of apoptosis (IAP), bind to caspases 3, 7 and 9 and block their activity [96, 97].

Evidence suggests that the pre-TCR induces the expression of pro-survival molecules and the down-modulation of pro-apoptotic molecules to ensure survival [53, 86, 94, 95]. One way in which the pre-TCR signals survival is through the activation of NFkB family members [65, 85] and increased transcription of the pro-survival protein Bcl2a1 in DN4 thymocytes [86]. Interestingly, exogenous expression of Bcl2a1 in *Rag1*$^{-/-}$ thymocytes rescued survival and differentiation to the DP stage coupling survival signals and the ability to differentiate [86]. Knockdown of Bcl2a1 by siRNAs in a pre-TCR+ cell line resulted in impaired survival but did not affect survival of a pre-TCR- cell line demonstrating the requirement for Bcl2a1 in response to pre-TCR signals [86]. Bcl2a1 appears to be the only known Bcl-2 pro-survival family member induced downstream of pre-TCR signaling to mediate survival of pre-TCR+ thymocytes [86]. In fact, in the absence of pro-survival family members Bcl-2 and Bcl-xl, β-selection proceeds normally

Figure 5. The ratio of pro-survival Bcl2 family members to pro-apoptotic Bcl2 family members determines cell fate outcome following an apoptotic stimulus. When Bcl2 is in excess, Bcl2 can exist as a monomer or it can homodimerize which results in cell survival. In the presence of Bax, Bcl2 and Bax will form heterodimers and if Bax is in excess, Bax will form homodimers which results in apotosis. (Adapted from [11]).

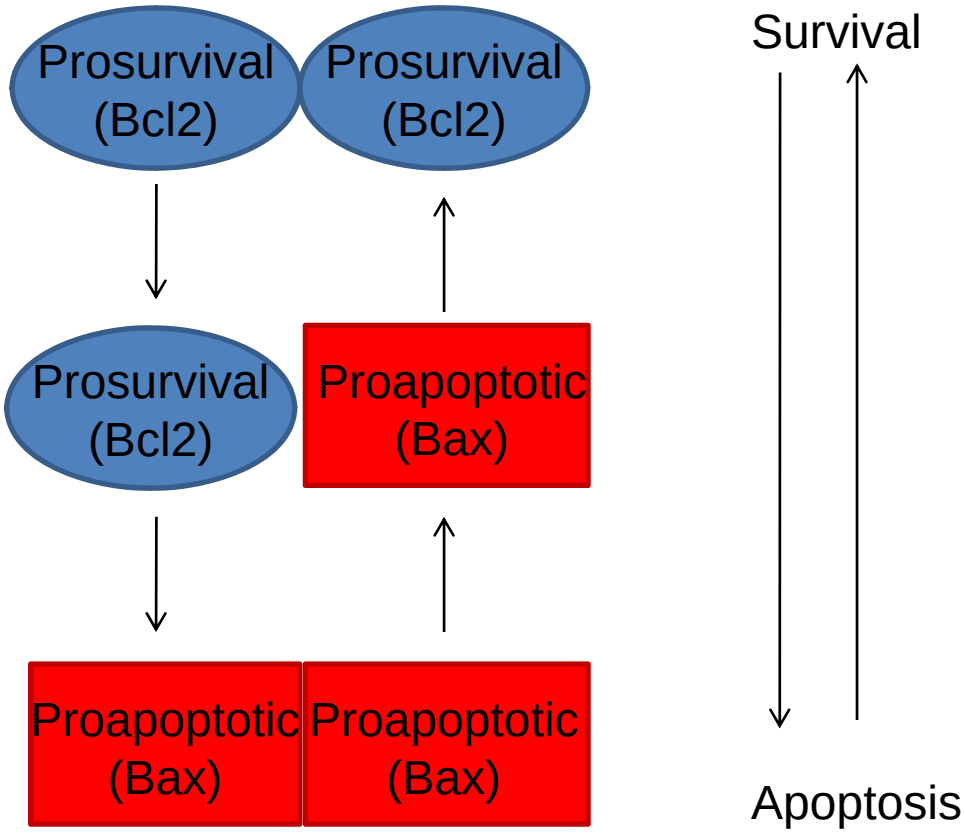
Prosurvival (Bcl2)
Prosurvival (Bcl2)
Prosurvival (Bcl2)
Proapoptotic (Bax)
Proapoptotic (Bax)
Proapoptotic (Bax)
Survival
Apoptosis

[98, 99] and exogenous expression of Bcl-2 and Bcl-xl cannot rescue survival of pre-TCR-deficient thymocytes [100-102]. The pro-survival Bcl-2 family member Mcl-1 does not appear to be induced downstream of the pre-TCR but it is required for survival of early cytokine-dependent DN thymocytes [103, 104]. T cell-specific deletion of Mcl-1 resulted in a partial block in DN2 to DN3 differentiation and decreased differentiation beyond the DN3 stage resulting in severely reduced numbers of DN3 and DN4 thymocytes [103, 104]. The defect in DN3 differentiation and the decrease in DN3 and DN4 cellularity suggest that Mcl-1 may play a role in β-selection survival. However, it is difficult to confirm this since Mcl-1 is required for survival of early DN thymocytes that do not yet express a TCRβ-chain. In addition, expression of the IAP family member, Birc5 (survivin), is increased in DN3L thymocytes as compared to DN3E thymocytes suggesting that it may be induced downstream of pre-TCR signaling to mediate survival [105]. T-cell specific deletion of Birc5 resulted in cell cycle arrest of DN3L and DN4 thymocytes due to impaired spindle formation during cytokinesis [105, 106] and cell death [105]. However, it is not understood if cell survival is a direct function of Birc5 since a role for Birc5 in cell survival is unclear or if cells simply die due to impaired cell division. Consequently, Bcl2a1 is the only known pro-survival member induced downstream of pre-TCR signaling to mediate survival.

Pre-TCR signaling also induces the down-regulation of pro-apoptotic molecules. Expression of the tumor suppressor protein p53 is reduced in DN4 thymocytes compared to DN3 thymocytes undergoing V(D)J recombination [95] and introduction of

a p53 deficiency in *SCID* mice allowed for the generation of some DP thymocytes [53, 107-110]. p53 induces apoptosis in cells with double-strand DNA breaks which occur during V(D)J recombination[108, 110]. In pre-TCR-negative thymocytes, p53 induces apoptosis through direct transcriptional induction of Bid [95]. Mice that do not express a pre-TCR and lack Bid contain thymi with an increased number of progenitor cells and DN3 thymocytes that survive longer than pre-TCR-negative thymocytes that express Bid [95]. Interestingly, expression of Bim is also decreased in response to pre-TCR signals [95]. In DN thymocytes, expression of Bim is regulated by the FoxO3a transcription factor [95]. Expression of FoxO3a protein is decreased in DN4 thymocytes by Akt in response to pre-TCR signaling, which results in decreased amounts of Bim mRNA and protein [95]. Introduction of a Bim deficiency in pre-TCR^{-} mice enhanced the survival of DN3 thymocytes and increased the number of progenitor cells [95]. Together this data demonstrates that Bim and Bid induce apoptosis in DN3 thymocytes lacking a pre-TCR [95]. The absence of Bim or Bid does not induce differentiation in thymocytes lacking a pre-TCR suggesting that these proteins exclusively control survival [95].

Recent studies suggest that pre-TCR signaling may override death receptor mediated apoptosis. SCID mice that carry a defective allele for the TNFRSF member Fas (*Fas*^{lpr}) contained thymi with DP thymocytes suggesting that TNFRSF signaling mediates death in the absence of a pre-TCR [111]. In addition, transgenic expression of a dominant negative form of the universal adapter used by death receptors, FADD (Fas associated death domain), in *Rag1*$^{-/-}$ mice generated thymi with DP thymocytes but not

a concomitant increase in thymic cellularity [94]. T-cell specific deletion of FADD generated a block in DN3 to DN4 differentiation and reduced thymic cellularity [94, 112]. The failure to increase cellularity in these FADD mutant mice has been attributed to a failure to proliferate which further complicates understanding the role of death receptor mediated apoptosis in the survival of thymocytes performing β-selection [94, 112, 113]. Thus, we are still in the process of understanding how β-selection signals mediate proliferation and survival signals to contribute to proliferative expansion.

It is also possible that the pre-TCR overrides apoptotic signals independent of caspase-3. The generation of DP and SP thymocytes occurred normally in the absence of caspase-3 in two week old mice [114] suggesting that a caspase-3 independent pathway can mediate death in the absence of a pre-TCR. Thus, this leaves open the possibility that death of pre-TCR-deficient thymocytes involves caspase 3-independent and caspase 3-dependent cell death.

Thymocyte:Stromal Cell Interactions Required for β-selection. In addition to signals generated by the pre-TCR, additional interactions between developing thymocytes and stromal cells are required for normal β-selection [32, 115]. One such interaction is that of Notch receptors (Notch1-Notch4) with their ligands Delta-like1 (DL1), DL3, DL4, Jagged1, Jagged2. Ligand binding to Notch receptors results in proteolytic cleavage of Notch receptors, which generates an intracellular Notch (ICN) that translocates to the nucleus to form a heterodimer with RBP-J (recombination signal

binding protein for immunoglobulin kappa J region) which recruits transcriptional coactivator Mastermind (MAM) to activate transcription (Figure 6). DL3 [116] and DL1 [117] are not expressed by thymic epithelial cells and deletion of *Jagged1*$^{-/-}$ [118] and *Jagged2*$^{-/-}$ [119] did not affect T cell development. However, deletion of DL4 in thymic epithelial cells blocked differentiation at the DN1 stage and supported aberrant B cell development in the thymus [33, 117]. Early studies demonstrated that Notch signaling played an essential role in T-cell lineage commitment by inducing the expression of T-lineage specific genes and suppressing the expression of non-T-lineage genes [120, 121].

More recent studies demonstrate that Notch signaling in combination with pre-TCR signaling is required during β-selection signaling [32, 115]. Thymocyte-specific deletion of *Notch1* beginning in DN2 thymocytes resulted in a block in differentiation of DN3 thymocytes and a reduction in the number of DP thymocytes which was attributed to impaired Vβ-DJβ recombination [32]. It has since been reported that Notch-DL1 signaling provides survival signals in *Rag2*$^{-/-}$ DN3E thymocytes by regulating glucose metabolism and *Glut1* transcription [115]. However, the dependence on Notch signaling decreases as cells differentiate from the DN3E to DN3L stage concomitant with decreased transcription of Notch receptors and Notch target genes [12, 122, 123]. DN3L thymocytes differentiated to the DP stage but with reduced proliferation on stromal cells that do not express a Notch ligand [122]. Thus, Notch-DL1 signaling is required to jumpstart β-selection signaling events and appears to enhance proliferation of thymocytes undergoing β-selection.

Figure 6. A schematic overview of Notch Signaling. Notch signaling initiates when delta-like or Jagged ligands on stromal cells bind to Notch receptors on the surface of the thymocyte. Presenilin-dependent γ-secretase cleaves the Notch receptor generating an intracellular Notch (ICN). ICN translocates to the nucleus where it interacts with co-activator mastermind (MAM) and RBP-J (recombination signal binding protein for immunoglobulin kappa J region) to displace the co-repressor to activate transcription. (Adapted from [8]).

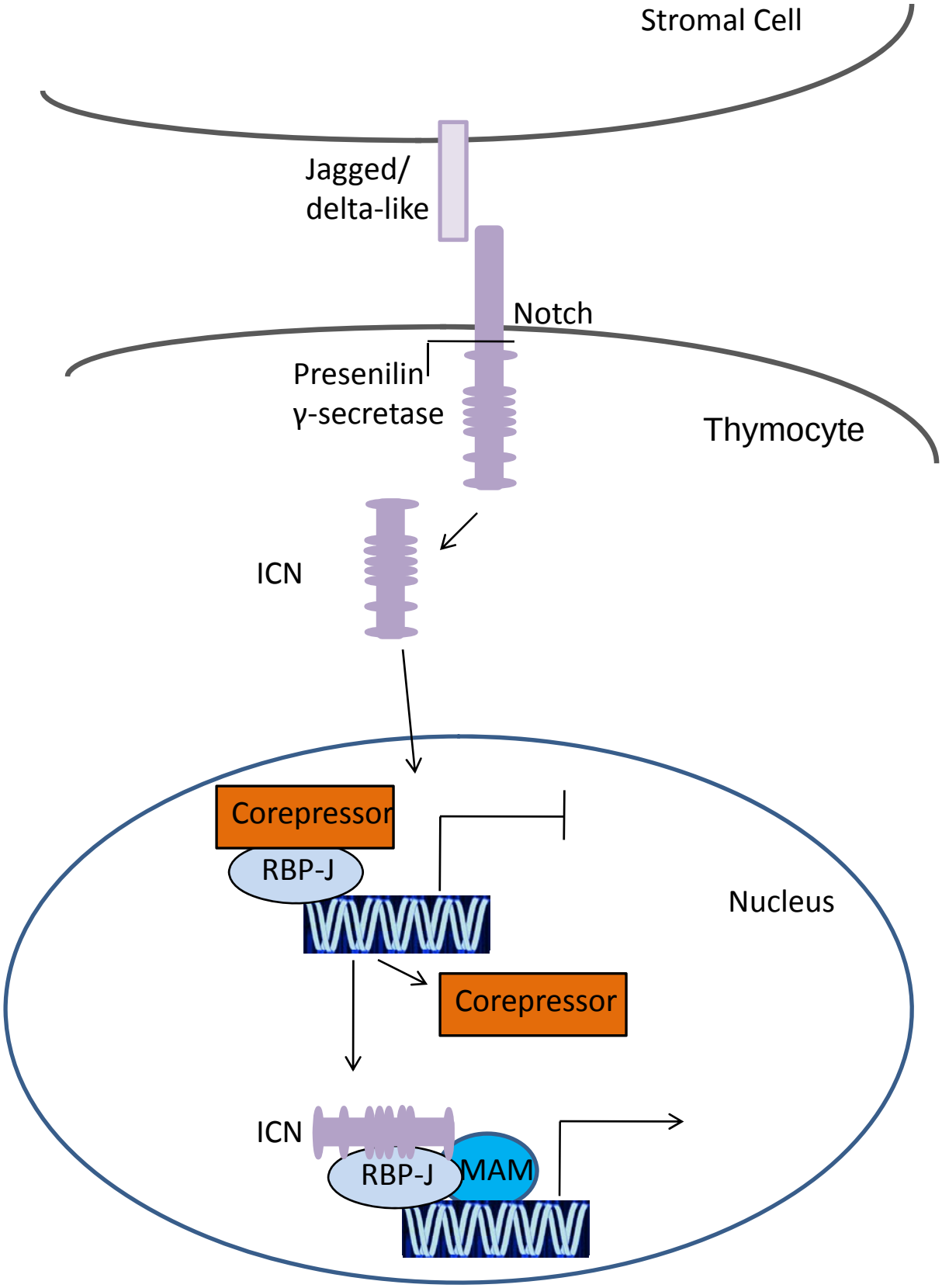
Stromal Cell
Jagged/
delta-like
Notch
Presenilin
γ-secretase
Thymocyte
ICN
Corepressor
RBP-J
Nucleus
Corepressor
ICN
RBP-J
MAM

In addition to Notch mediated signaling, the Wnt signaling pathway is also required for DN differentiation [35-39]. The canonical Wnt signaling pathway is initiated when soluble Wnt proteins bind to a member of the frizzled (FZ) family of receptors and a member of the low-density-lipoprotein-receptor-related-protein family (LPR5 or LPR6). Ligand binding triggers stabilization of β-catenin which then migrates to the nucleus where it binds to T-cell factor-1 (TCF1) and lymphocyte-enhancer-binding factor-1 (LEF1) transcription factors to activate target genes (Figure 7) [13]. In the absence of Wnt signaling, β-catenin is phosphorylated and targeted for proteasomal degradation by casein kinase 1 (CK1) and by glycogen-synthase kinase 3β which is in a multiprotein destruction complex that contains axis inhibitor (AXIN) and adenomatous polyposis coli (APC).

Numerous studies suggest that Wnt/β-catenin/TCF signaling is required during β-selection. Expression of soluble Wnt receptor mutants to block Wnt binding to frizzled receptors resulted in reduced proliferation of DN and ISP thymocytes [38]. Additionally, deletion of *Tcf1* resulted in a partial block in differentiation of DN3 and ISP thymocytes which was attributed to a reduction in proliferation [35] and impaired survival of DN3 and DN4 thymocytes [124]. There is a currently a great deal of controversy regarding the role of β-catenin during thymopoiesis. In one study, T-cell specific Cre-loxP mediated deletion of β-catenin resulted in a block in DN3 to DN4 differentiation associated with impaired proliferation of DN4 thymocytes [125]. However, another group generated inducible Cre-loxP deletion of β-catenin in bone marrow progenitor

Figure 7. A schematic overview of Wnt-signaling. The canonical Wnt signaling pathway is initiated when soluble Wnt proteins bind to a member of the frizzled (FZ) family of receptors and a member of the low-density-lipoprotein-receptor-related-protein family (LPR5 or LPR6). Ligand binding inhibits phosphorylation of β-catenin by casein kinase 1 (CK1) and by glycogen-synthase kinase 3β which is part of a multiprotein destruction complex that contains axis inhibitor (AXIN) and adenomatous polyposis coli (APC). By preventing phosphorylation of β-catenin, β-catenin is not targeted for proteasomal degradation and it is able to migrate to the nucleus where it displaces a co-repressor and binds to T-cell factor-1 (TCF1) and lymphocyte-enhancer-binding factor-1 (LEF1) transcription factors to activate transcription of target genes (Adapted from [13]).

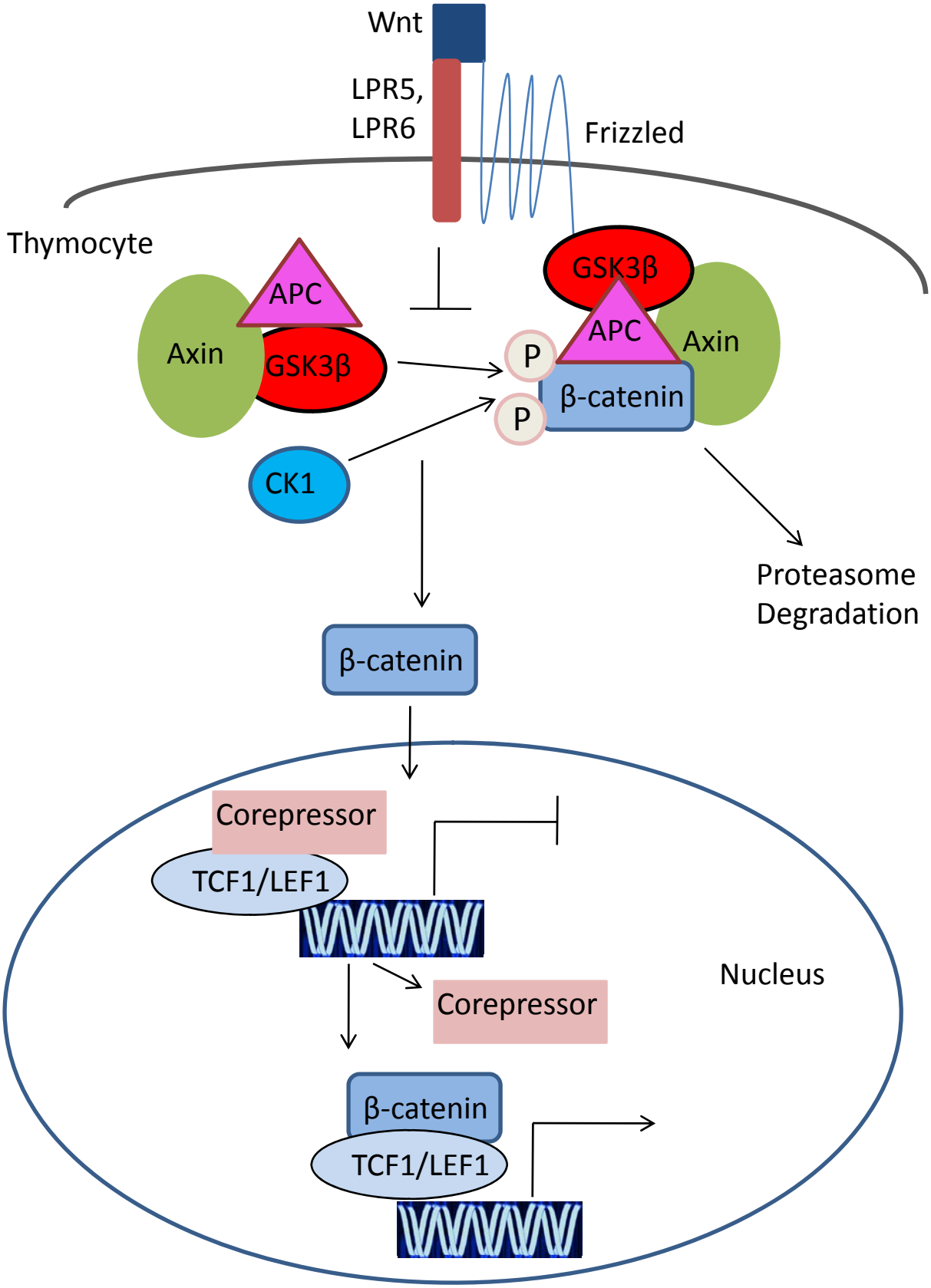
Wnt
LPR5,
LPR6
Frizzled
Thymocyte
APC
Axin
GSK3β
GSK3β
APC
Axin
P
β-catenin
P
CK1
Proteasome
Degradation
β-catenin
Corepressor
TCF1/LEF1
Nucleus
Corepressor
β-catenin
TCF1/LEF1

cells that had no effect on thymopoiesis thus questioning the role of β-catenin during thymopoiesis [126]. The floxed targeting stategy of the latter group could theoretically produce a truncated β-catenin protein lacking the amino terminus. However, they did not detect any β-catenin protein by western blotting so the role of β-catenin remains unclear. Interestingly, another report did not detect any change in β-catenin protein stability in response to anti-CD3ε treatment and instead detected an increase in TCF1 expression downstream of pre-TCR signaling [124]. This group also demonstrated that TCF1 is required for survival of pre-TCR+ DN3 thymocytes but not for their proliferation [124]. These results suggest that the pre-TCR may control Wnt signaling by regulating expression of TCF1 in a β-catenin independent manner and that TCF1 is required for survival of pre-TCR+ thymocytes [124].

Thymocytes express chemokine receptors and integrins allowing them to interact with the thymic microenvironment. The contribution of these interactions to β-selection events is just beginning to be addressed. As DN3E thymocytes differentiate to DN3L thymocytes, they move from the outer cortex to the outer portion of the outer cortex of the thymus termed the subcapsular zone. As they differentiate into DP thymocytes, they move away from the subcapsular zone back to the outer cortex [17]. This migration is thought to be mediated by chemokine and chemokine receptor interactions. DN3 thymocytes express chemokine receptors CXCR4 and CCR9 and cortical thymic epithelial cells express their respective ligands, CXCL12 (SDF-1α) and CCL25 [127]. Thymus specific deletion of CXCR4 resulted in a block beyond DN1

differentiation [34]. Deletion of CXCR4 in DN3 thymocytes resulted in a block in DN3 differentiation and impaired survival of DN3L thymocytes demonstrating a role for CXCR4 signaling during β-selection (Paul Trampont and Kodi Ravichandran personal communication). Interestingly, CCR9-deficient DN thymocytes failed to accumulate in the subcapsular zone although their differentiation did not appear to be impaired [128, 129]. DN thymocytes also express integrins $\alpha4\beta1^{hi}$, $\alpha5\beta1^{hi}$, $\alpha6\beta1^{int}$ [127], α6β4 [130]. Differential integrin expression allows thymocytes to bind to different extracellular matrix (ECM) proteins such as fibronectin, laminins, or VCAM1 (vascular cell adhesion molecule 1). Laminin 11, a ligand for β1 integrins, is expressed in the subcapsular zone of the thymus and increases the ability of DN3 thymocytes to migrate to CXCL12 in an *in vitro* chemotaxis assay (Paul Trampont and Kodi Ravichandran personal communication). DN thymocytes that lack laminin-2 are severely reduced in number and undergo apoptosis [131] and blocking laminin-5 interactions with monoclonal antibodies also blocked differentiation of DN thymocytes to the DP stage with an increased proportion of apoptotic DN thymocytes [132] demonstrating that laminin/integrin mediated interactions are required during β-selection. The contribution of additional receptor/ligand interactions during β-selection is not completely understood but current work suggests a complex crosstalk between cell adhesion molecules, chemokines and the pre-TCR.

c-Myb

The *Myb* proto-oncogene was first identified as the cellular homolog of the transforming v-*Myb* oncogene isolated from Avian myeloblastosis virus (AMV) and avian leukemia virus E26 which induce myeloblastic and erythroblastic leukemias, respectively [133]. The v-*Myb* and *Myb* genes encode nuclear DNA binding proteins that function as both transcriptional activators and repressors [134-136]. c-Myb is highly evolutionarily conserved and is found in all vertebrates examined [137]. Compared to c-Myb, AMV v-Myb is truncated at both the N-terminal and carboxyl-terminal regions and contains 10 point mutations which enables it to induce acute myeloblastic leukemia in animals and transform immature hematopoietic cells in culture [138] (Figure 8). In addition to truncations and mutations, AMV v-Myb is fused to part of the gag gene and E26 v-Myb is fused to both gag and Ets-1 genes. AMV v-Myb encodes a 45-kDa protein and E26 v-Myb encodes a 135-kDa protein. The major translational product encoded at the *Myb* locus is a 636 amino acid, 75-kDa protein but an alternatively spliced form of *Myb* produces an 89kDa protein [139, 140].

Structure and Function of c-Myb. c-Myb contains three structural domains: an amino-terminal DNA binding domain (DBD), a central transactivation domain (TAD) and a carboxyl-terminal negative regulatory domain (NRD) (Figure 8). The DBD consists of three tandem repeats (R1-R3) of 50-52 amino acids each [135, 141, 142] with each

Figure 8. Vertebrate Myb proteins. The conserved functional domains of c-Myb are indicated by shaded and colored boxes. The DNA binding domain (DBD) is represented by blue boxes and R1, R2, and R3 refer to the three repeats of the DBD. The transcriptional activation domain (TAD) is represented by a red box. The Negative regulatory domain (NRD) and the amino terminal region containing R1 of the DBD are lacking in the transforming v-Myb proteins from Avian myeloblastosis virus (AMV) and E26. LR stands for the highly conserved leucine repeat and EVES refers to a highly conserved motif in the NRD. P indicates sites of amino acid phosphorylation, S indicates sites of sumoylation, and Ac indicates sites of acetylation. Blue dots indicate point mutations in the AMV v-Myb protein (adapted from [3, 4]).

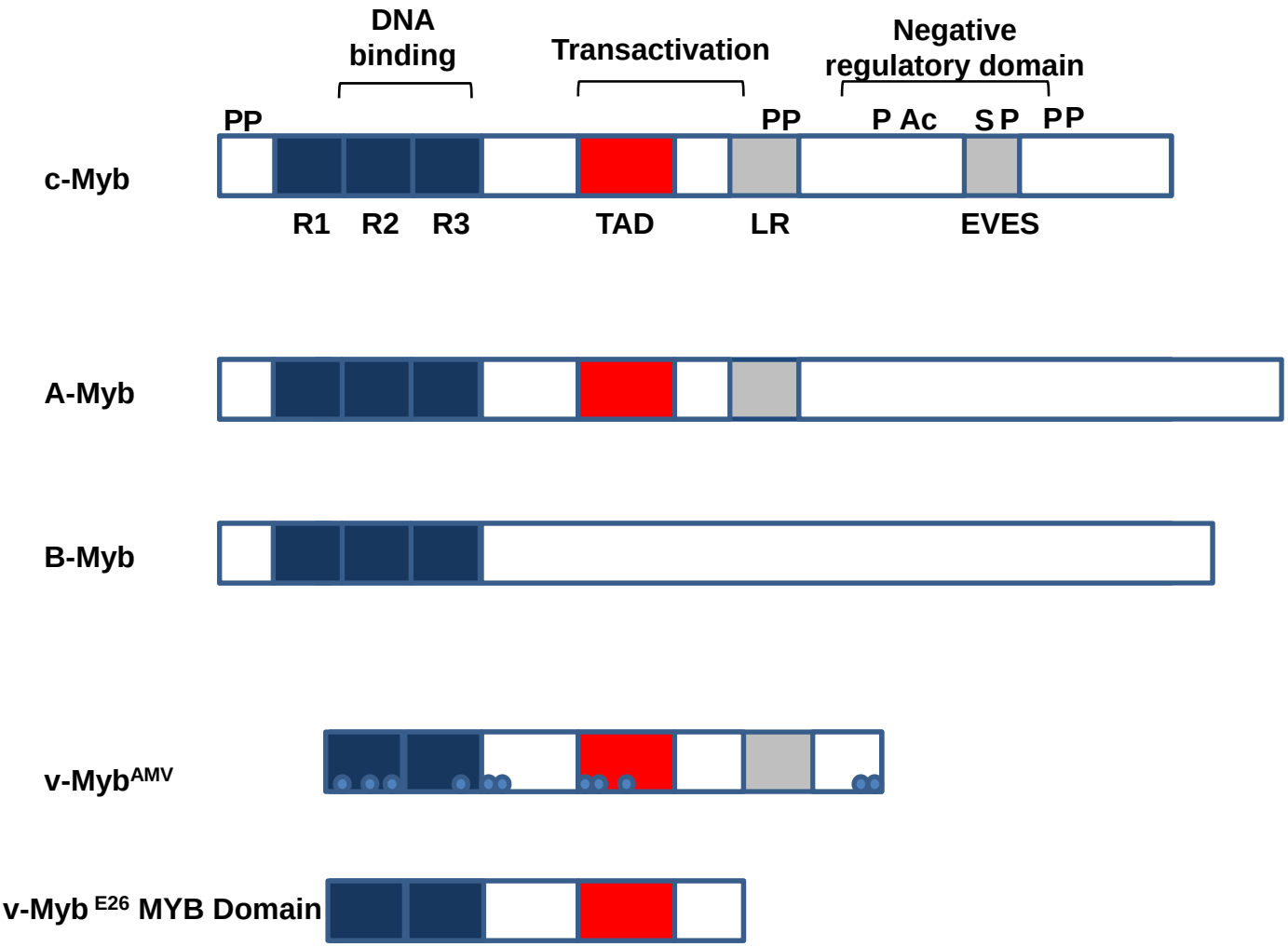
DNA binding
Transactivation
Negative regulatory domain
PP
PP
P Ac
S P
PP
c-Myb
R1
R2
R3
TAD
LR
EVES
A-Myb
B-Myb
v-Myb AMV
v-Myb E26 MYB Domain

repeat forming three alpha helices in a helix-turn-helix variant motif [143, 144]. Each repeat also contains a SANT domain that serves as a protein interaction domain that binds proteins involved in histone modifications [145]. There are three conserved tryptophan residues separated by 18-19 amino acids in each repeat to allow for packing of a hydrophobic core [146]. R1 does not bind to DNA but appears to be involved in stabilization of the c-Myb:DNA complex while R2 and R3 physically bind to the major groove of DNA [147, 148]. R2 and R3 exhibit a positively charged surface to facilitate binding to negatively charged DNA [142, 144, 147, 149] and cover one face of the DNA, possibly allowing room for accessory proteins [150]. The Myb consensus binding site PyAACG/TG is referred to as Myb binding sequence (MBS) or Myb responsive element (MRE) [148]. Myb proteins have shown flexibility in sequence recognition with ranging binding affinities for sequence variants of the Myb binding site [151]. In addition, there is preferential binding for certain nucleotides flanking the Myb consensus sequence [152].

The DBD alone is not sufficient to activate transcription of test constructs and requires the centrally located acidic transactivation domain to activate transcription. The TAD is composed of approximately 85 amino acids [136, 141, 153]. The TAD was identified by fusing a Gal4 DBD with portions of c-Myb and testing the ability of the fusion protein to activate a promoter with a Gal4 binding site linked to a reporter gene [135, 153]. Little is known about the requirements of this domain but point mutations suggest that acidity of the residues is not essential and conformation is of critical

importance [135]. In addition, recent studies demonstrated that undefined regulatory elements within the transactivation domain control promoter specific target gene expression [154].

The carboxyl-terminal negative regulatory domain was identified as a portion of the carboxyl-terminal sequences that are absent in the transforming v-*Myb* [155, 156]. This suggested that c-Myb auto-regulates its activity or that the NRD provides surfaces for protein-protein interactions that negatively regulate c-Myb. Deletion of carboxyl-terminal regions from c-Myb and testing the transactivation activity in transient DNA transfection assays resulted in a ten-fold increase in transcriptional transactivation activity [135, 141]. Interestingly, yeast two-hybrid studies revealed that the amino and carboxyl-termini of c-Myb interact with one another via the first 192 amino acids of the amino-terminal portion of c-Myb containing the DBD and a highly conserved carboxyl terminal region referred to as the EVES motif [157]. Since the EVES motif is absent in the transforming non-regulated v-Myb, this lead to the suggestion that c-Myb domains interact to auto-regulate activity. The NRD is also composed of a leucine zipper like motif that lies upstream of the EVES motif and contains one isoleucine and three leucine residues [148]. The leucine zipper motif functions as a protein interaction domain [4]. Mutagenesis of leucines at positions 3 and 4 to proline (L34P) of the leucine zipper motif resulted in increased c-Myb transcriptional transactivation activity of promoter-reporter gene constructs [158]. However, the increased transcription transactivating activity depended on the promoter and the particular Myb-binding sites within the promoter of

the promoter-reporter gene construct [159]. Interestingly, the alternatively spliced p89 c-Myb lacks the putative leucine zipper motif and has been reported to exhibit greater transcriptional transactivation activity than p75 c-Myb [160]. It has been suggested that regulation of c-Myb transcriptional transactivational activity may result from c-Myb homodimers formed through the leucine zipper motif [161]. However, this has not been shown to occur *in vivo*. Instead, many proteins have been identified that bind to the leucine zipper like motif of c-Myb to negatively regulate c-Myb transcriptional transactivation activity [162, 163].

Regulation of c-Myb Transcription Activating Activity. c-Myb activity can be modulated a number of ways including protein/protein interactions and post translational modifications. c-Myb interacts with a number of proteins that mediate its transcriptional transactivation activity that include Ets-family members Ets-1 and Ets-2 [164, 165], Runx1 [166, 167] Pax5 [168, 169], Lef1 [169], PU.1 [170], C/EBPβ (CCAAT/enhancer binding protein beta) [149, 170, 171], and p100 [157]. p100 contains an EVES motif and interacts with the c-Myb DBD [157]. A model proposed for c-Myb regulation is based on competition for binding the c-Myb DBD between p100 and the c-Myb EVES domain, which activates or represses c-Myb transcriptional transactivation activity, respectively [4]. Interestingly, p100 is phosphorylated by the Pim1 serine/threonine protein kinase which resulted in a stable complex between p100 and Pim1 and enhanced c-Myb transcriptional transactivating activity connecting c-Myb activity to a signaling cascade [172]. c-Myb also interacts with complexes that contain

histone acetylases [173, 174] and histone deacetylases [162] and c-Myb has the potential to affect gene expression based on the complex it interacts with. CREB-binding protein (CBP) and the related protein p300 are ubiquitously expressed histone acetyltransferases that bind to and acetylate c-Myb which increases its transcription transactivation activity [173-175]. CBP and p300 interact with RNA polymerase II and serve as a bridge between c-Myb and the basal transcriptional machinery to enhance the transcriptional activity of c-Myb [4, 174, 176].

c-Myb is also regulated by post-transcriptional modifications including sumoylation, phosphorylation, ubiquitination, and acetylation [177-183]. These modifications lead to changes in c-Myb stability, DNA-binding activity and transcriptional transactivating activity. c-Myb is negatively regulated by sumoylation at K523 by SUMO-1 (SMT3 suppressor of mif two 3 homolog 1) which decreases c-Myb stability and negatively regulates c-Myb transcriptional transactivation activity [181]. Pharmacological inhibition of cellular serine/threonine protein phosphatases by okadaic acid resulted in hyperphosphorylation and degradation of c-Myb in hematopoietic cells by the 26S proteasome suggesting that some phosphorylation events destabilize c-Myb protein [184]. In addition, it was recently reported that phosphorylation of Thr354, Thr486, Ser556, and Thr572 in the NRD by p38MAPK in response to stress led to proteasomal degradation of c-Myb [183]. The proteasome is targeted to the NRD, through ubiquitination which occurs at an undefined lysine residue(s) in the NRD [180, 185]. Thr572 is also targeted for phosphorylation by glycogen synthase kinase 3 (GSK3)

which recruits E3 ubiquitin ligase Fbw7 leading to degradation of c-Myb [186]. Moreover, there are also phosphorylation sites in the DBD that affect c-Myb stability. HIPK2 (homeodomain-interacting protein kinase 2), and NLK (Nemo-like kinase) bind to the DBD and phosphorylate c-Myb at multiple serine and threonine residues resulting in degradation of c-Myb downstream of Wnt-1 signaling [182]. The NRD also contains multiple phosphorylation sites which modulate c-Myb transcriptional transactivation activity one of which lies in the EVES motif, serine 528 (S528). S528 is phosphorylated *in vivo* and is targeted for phosphorylation by p41MAPK (42-kD mitogen activated protein kinase) *in vitro* [187]. Mutation of the S528 to alanine (S528A), resulted in a two-seven-fold increase in transcriptional transactivation activity [178] but did not affect the ability of c-Myb to bind DNA [188]. There was an increase in transcription at the CD34 promoter with the S528A mutation but transcription was not affected at the chicken mim-1 promoter suggesting that phosphorylation may differentially regulate c-Myb activity at different promoters [188]. Pim-1 can also phosphorylate undefined residues within the first 200 amino acids of c-Myb encompassing the DBD [189] to increase c-Myb transcriptional transactivation activity [172]. c-Myb is acetylated in the conserved carboxyl-terminal lysine residues by p300 and CBP which increases DNA binding, transactivational activity, and affinity between c-Myb and CBP/p300 [173, 179, 190].

Myb Family Members. The c-Myb DBD defines a family of evolutionarily conserved proteins in vertebrates that includes A-Myb and B-Myb [137, 191]. A-Myb,

encoded by the *Mybl1* locus*,* is expressed in male germ cells, breast epithelial cells [192], and germinal center B cells [193] where as B-Myb, encoded by the *Mybl2* locus*,* is ubiquitously expressed [191]. c-Myb is primarily expressed in hematopoietic lineages although it is expressed in other cell types (see below) [194]. The expression patterns of the Myb family proteins suggest that they do not share completely redundant functions and this is reflected in the phenotypes of *Myb, Mybl1* and *Mybl2* null mice. *Myb* null mice die during embryogenesis due to severe anemia [195], whereas *Mybl1* null mice are viable but unable to undergo spermatogenesis and mammary gland genesis [192] and *Mybl2* null mice die pre-implantation during embryogenesis [196]. Additionally, ectopic expression of *Mybl1, Mybl2* or *Myb* in human tissue cell lines resulted in activation of a unique set of genes [197, 198]. Thus, despite the fact that all three Myb proteins share a DNA binding domain they have unique physiological functions.

Expression and Function of Myb During Hematopoiesis. *Myb* mRNA is primarily expressed in immature cells of each hematopoietic lineage [194]. However, expression is also detected in smooth muscle cells [199], gut epithelium [200], hair follicles [201] and several non-hematopoietic carcinomas such as small cell lung carcinoma [202], colon carcinoma [203], breast carcinoma [204], and neuroblastoma [205], as well as T-cell acute lymphoblastic leukemia [206, 207]. Interestingly, expression of *Myb* mRNA is abundantly expressed in hematopoietic progenitor cells and expression decreases as cells approach terminal differentiation [194, 208-210]. The intriguing pattern of *Myb* mRNA expression led to the notion that c-Myb plays a crucial role during differentiation

of each hematopoietic lineage. Early studies demonstrated that forced expression of c-Myb blocked differentiation of murine erythroleukemia and myelomonocytic leukemia cell lines that could be chemically induced to differentiate [211-213]. Tetracycline-inducible over-expression of c-Myb in *c-Myb*$^{-/-}$ embryonic stem cells blocked differentiation of erythrocytes, megakaryocytes and B-lymphocytes [214]. These experiments support the notion that c-Myb levels need to decrease for hematopoietic lineages to differentiate.

Expression of c-Myb is controlled at the transcriptional and post-translational levels [177, 180-184, 189, 215, 216]. *Myb* mRNA expression appears to be primarily regulated at the level of transcription by a conditional block to transcription elongation within the first intron [215]. Other mechanisms that appear to contribute to the regulation of steady state *Myb* mRNA levels include rates of transcription initiation and changes in mRNA stability [216]. Transcription factors NFkB [217], WT-1 [218], Ets-1 [219] are thought to bind to *cis* regulatory elements to regulate transcription of *Myb* mRNA in a lineage specific fashion. However, signaling pathways and mechanisms that regulate transcription at the *Myb* locus remain poorly defined. Two recent reports demonstrated that *Myb* mRNA is a target of microRNA miR-150 [220], which is expressed in mature resting lymphocytes [221], and miR-15a [222]. The c-Myb protein also has a short half-life of approximately 20-30 minutes *in vivo* [180, 185, 223]. As discussed in the previous section, c-Myb is a target for many forms of post-translational protein modifications including phosphorylation, sumoylation and ubiquitination which

target it for proteosomal degradation [177, 180-184, 189]. Thus, multiple mechanisms exist to control steady state levels of c-Myb expression.

In order to study c-Myb function during hematopoiesis, a *Myb*-null allele was generated which resulted in death at embryonic day 15 due to the inability to switch from embryonic to adult erythropoiesis [195]. *Myb*$^{-/-}$ embryonic stem cells are found in the fetal liver but they fail to increase in number and their differentiation is impaired [224]. This study provided the first definitive evidence that c-Myb is required for hematopoiesis. However, the embryonic lethality has hampered the ability to further study c-Myb function during hematopoiesis since developing embryos die before lymphopoiesis occurs [195]. *Myb*-null embryonic stem cells were used to generate chimeric mice homozygous null for *Myb/Rag1* such that all T and B cells that developed were of the *Myb*$^{-/-}$ genotype whereas other tissues were chimeric [225]. Interestingly, while mature lymphoid and macrophage *Myb*$^{-/-}$ cells were not detected, this study did detect *Myb*$^{-/-}$ CD44^{lo}CD25- DN1 precursor cells in the thymus [225]. Thus, c-Myb is not required for stem cell function per se.

Many mutant alleles have since been generated to study c-Myb function during hematopoiesis. A dominant interfering *Myb* allele, which interferes with each vertebrate member of the Myb family of proteins, was generating by fusing the c-Myb DBD to the engrailed repressor to suppress the activities of Myb proteins [226]. Inducible expression of the dominant interfering *Myb* allele in a hematopoietic cell line

reduced cellular proliferation and survival [227]. During the generation of a LoxP targeted *Myb* allele to target *Myb* for conditional deletion using the Cre-LoxP recombination system, a knock down allele of c-Myb, *c-myb*^{loxP}, which carries the neo^{R} cassette was generated resulting in a 90% decrease in c-Myb protein expression [228]. This model demonstrated that cells expressing low levels of c-Myb greatly enhanced differentiation down the megakaryocyte lineage while erythroid and lymphoid differentiation is severely impaired [228]. In addition, hypomorphic alleles of c-Myb that contain point mutations in the DBD (Plt3), TAD (M303V) and NRD (Plt4), enhanced differentiation of megakaryocytes but production of erythroid and lymphoid lineages was diminished [229, 230]. Interestingly, the number of progenitor cells generated in the hypomorphic allele models is greatly increased [228-230]. Together this data demonstrates that c-Myb regulates hematopoiesis at critical points where cells receive and respond to signals to proliferate, differentiate and survive. However, these model systems are not able to differentiate between a defect in progenitor cells versus a defect due to events that take place at a later stage of differentiation.

The identification of direct c-Myb targets is crucial to understand how c-Myb mediates effects on proliferation, differentiation and survival. Interestingly, potential c-Myb transcriptional targets include Ptcra [231], Bcl-2 [232-235], Ada (Adenosine deaminase) [236, 237], H2A.Z (H2A histone Z) [238], c-Myc [236, 239-242], Mat2a (Methionine adenyl-transferase II, alpha) [236, 243, 244], Gata-3 [245], Rag-2 [168, 169, 246], c-kit [247-249], CD4 [245, 250, 251], and cyclin B1 [252]. However, many of these

genes were identified by testing the ability of exogenously expressed c-Myb to activate promoter-reporter gene constructs in cells that do not normally express c-Myb [138, 253] and it has recently been reported that the ability of Myb proteins to activate test constructs varied greatly from their ability to activate endogenous genes [154]. Moreover, some genes were identified using the dominant interfering Myb allele in leukemic cell lines [245, 254-256] which is not able to discriminate between activity of Myb family members. None of the genes on this list have been tested for their ability to mediate c-Myb activity. Thus, there is very little known about the mechanisms and transcriptional targets of c-Myb that mediate proliferation, survival or differentiation.

c-Myb and Thymopoiesis. c-Myb has long been thought to play a role during thymopoiesis based on the large amount of *Myb* mRNA that is detected in developing thymocytes [216, 257]. In the thymus, *Myb* mRNA expression is greatest in cortical DN and DP thymocytes where expression is increased during the DN to DP transition and is severely reduced during the DP to SP transition [14, 201]. Proper expression of c-Myb appears to be critical for normal thymopoiesis. Gene duplication of *Myb* or translocation of the *Myb* locus into the *Tcrb* locus is detected in patients with T-cell acute lymphoblastic leukemia (T-ALL), a neoplastic disorder of progenitor T cells [206, 207]. The *Myb-Tcrb* translocation, which defines a new subset of T-ALL, places *Myb* expression under the control of *Tcrb* regulatory elements suggesting that continuous expression of c-Myb during thymopoiesis had an adverse effect characterized by

increased expression of genes involved in cellular proliferation [206]. Together this data demonstrated that regulation of *Myb* expression is crucial during thymopoiesis; however, understanding c-Myb function during thymopoiesis has been hampered due to the lack of a tractable genetic system.

The mechanisms underlying c-Myb function during thymopoiesis are not well characterized. Attention has been focused on a role for c-Myb in proliferation since early studies detected expression of *Myb* mRNA in peripheral T cells that had entered the G1 phase in response to IL-2 [258]. Other studies had also demonstrated that in mature lymphocytes, expression of *Myb* mRNA was dependent on the cell-cycle and peaked mid to late G1 phase or in S-phase [216, 259, 260]. Expression of antisense c-Myb oligodeoxynucleotides to test c-Myb function during hematopoiesis inhibited proliferation of myeloid leukemia cell lines and T lymphocytes further confirming a role for c-Myb in lymphocyte proliferation [261, 262]. However, these results have been severely questioned because the antisense oligodeoxynucleotides used in these studies exhibited non-specific anti-proliferative effects [263]. Moreover, our lab demonstrated that *Myb*-deficient mature splenic B-cells are able to proliferate in the absence of c-Myb suggesting that c-Myb is not necessarily required for proliferation [264]. Thus, the role of c-Myb during proliferation remains in question.

The mutant Myb allele models have been useful in studying c-Myb function at different stages of thymopoiesis. Expression of the dominant interfering Myb allele as a

transgene in developing thymocytes resulted in reduced thymic cellularity, a partial block in DN3 to DN4 differentiation, an increased proportion of CD4-CD8+ thymocytes, and diminished proliferation of DN3, DN4 and peripheral T-cells [226, 265]. Furthermore, expression of the dominant interfering Myb allele in a thymoma cell line resulted in apoptosis with decreased expression of *Bcl2* mRNA [232]. However, data obtained with the dnMyb protein is difficult to interpret because it does not discriminate between effects of c-Myb, B-Myb or A-Myb. Expression of the hypomorphic *c-myb*^{loxP} allele severely reduced thymic cellularity and resulted in a block in differentiation at the DN1 and DN2 stages with very few cells making it to the DP stage suggesting that c-Myb is required for differentiation during thymopoiesis beyond the DN1 stage [228]. However, the hypomorphic allele is expressed in progenitor cells and the failure to differentiate beyond the DN1 stage may be due to a defect in progenitor cells and not due to a defect in thymopoiesis. We and others used tissue specific conditional mutagenesis using the Cre-LoxP system to study c-Myb function during thymopoiesis [14, 266]. Our lab targeted exon II of *Myb* with loxP sites (Figure 9) for Cre recombinase mediated deletion using two strains of mice that express Cre under the proximal Lck promoter to examine c-Myb function at multiple stages of thymopoiesis [14]. We determined that c-Myb is required for DN3 to DN4 differentiation, survival of pre-selection DP thymocytes, and differentiation of CD4 lineage thymocytes demonstrating for the first time that c-Myb is required during thymopoiesis [14]. Cellularity of *Myb*-deficient DN thymocytes was decreased two-fold and expression of TCRβ is decreased. Examination of V(D)J recombination of the *Tcrb*

locus revealed that Vβ to DJβ recombination is severely reduced in DN3 thymocytes lacking c-Myb yet survival and proliferation of DN3 thymocytes did not appear to be altered [14]. Deletion of *Myb* in DN4 thymocytes not only resulted in decreased survival of pre-selection DP thymocytes but impaired CD4 differentiation which could not be rescued by expression of the OT-II TCR transgene [14] which is restricted to MHC-class II selection [267]. These findings were confirmed by Reddy and colleagues [266] using a different LoxP targeted *Myb* allele using two mouse strains that express Cre under the proximal Lck promoter and the CD4 promoter. Together, this data demonstrates that c-Myb is required for thymocyte survival, proliferation and differentiation at multiple stages of thymopoiesis where cells are at a crossroad to proliferate, differentiate or die. However, while we demonstrated that c-Myb is required for efficient Vβ to DJβ recombination in DN3 thymocytes, it is not known if c-Myb plays an additional role(s) in DN3 differentiation and how c-Myb mediates these roles.

Project Rationale.

Efforts to elucidate the roles of c-Myb during hematopoiesis have been hampered by the embryonic lethality of the homozygous *Myb* null mutants [195] and understanding the role(s) of c-Myb during hematopoiesis has been greatly impeded due to the lack of a tractable genetic system. We have constructed mice carrying loxP sites that target the *Myb* locus for deletion by the Cre recombinase. By mating these mice

with mice that express Cre under the control of the lck proximal promoter, we were able to delete *Myb* early in T cell development during the DN2 stage [14]. At the start of this project, our lab had recently characterized T cell development in mice that expressed Cre under the proximal *lck* promoter (cwlckCre) [14]. We demonstrated efficient Cre mediated deletion of the targeted *Myb* locus by the DN3 stage which resulted in a strong developmental block in DN3 to DN4 differentiation concomitant with severely impaired Vβ to DJβ recombination of the *Tcrb* locus [14]. Survival of DN3 thymocytes cultured in suspension without exogenous cytokines was not impaired in the absence of c-Myb. In addition, proliferation of c-Myb-deficient DN3 thymocytes was not altered. This suggested that the impairment in Vβ to DJβ recombination was the cause of the block in DN3 differentiation. However, a small proportion of DN3 thymocytes expressed a TCRβ protein yet we did not detect any DN4 thymocytes in the absence of c-Myb which suggested that c-Myb is required for DN3 differentiation independent of V(D)J recombination. Thus, the goal of this project was to determine if the impaired Vβ to DJβ recombination observed in the absence of c-Myb was the sole cause for the block in DN3 differentiation or if c-Myb was required for differentiation of DN3 thymocytes independent of V(D)J recombination. To determine if c-Myb is required for maintenance of DN3E thymocytes prior to V(D)J recombination, which might be expected to affect the efficiency of V(D)J recombination we crossed our $Myb^{f/f}$ *cwlckCre* mice with $Rag2^{-/-}$ mice. Thymocytes from $Rag2^{-/-}$ mice are unable to perform V(D)J recombination of the *Tcrb* locus and are blocked at the DN3E stage [24]. Since it is possible that the defect in V(D)J recombination in $Myb^{f/f}$ *cwlckCre* thymocytes is simply

a consequence of reduced survival and the inability to complete V(D)J recombination, we can examine survival of *Rag2*$^{-/-}$ DN3E thymocytes that lack c-Myb. A second possibility is that c-Myb is required to keep thymocytes at the DN3E stage to complete V(D)J recombination and that in the absence of c-Myb, DN3E thymocytes spontaneously differentiate in the absence of pre-TCR signals. The *Myb*$^{f/f}$ *cwlckCre Rag2*$^{-/-}$ mice will enable us to examine if c-Myb is required to keep thymocytes at the DN3E stage to perform V(D)J recombination by testing for the presence of DP thymocytes in *Myb*$^{f/f}$ *cwlckCre Rag2*$^{-/-}$ mice. A third possibility is that c-Myb is directly required during the process of V(D)J recombination in DN3E thymocytes and that we will not detect altered differentiation of *Rag2*$^{-/-}$ thymocytes or a decrease in their survival in the absence of c-Myb. When we initially examined Vβ to DJβ recombination, the amount of DNA in the germline configuration at the *Tcrb* locus was severely reduced which suggested that Vβ to DJβ recombination was not successful on either allele leaving very little DNA in the germline configuration. This suggested that the process of V(D)J recombination was somehow impaired in the absence of c-Myb. Therefore, we predict that c-Myb is not required for maintenance of DN3E thymocytes and that c-Myb is directly required during the process of V(D)J recombination.

We also crossed our *Myb*$^{f/f}$ *cwlckCre* mice with *Tcrb* transgenic mice to determine if expression of a *Tcrb*-transgene (Tg) could rescue DN3 to DN4 differentiation. A *Tcrb* transgene is able to rescue differentiation of *Rag2*-deficient DN3E thymocytes to the DP stage and results in a total thymic cellularity that is several

fold greater than a normal thymus [268]. If defective V(D)J recombination is the sole cause for the block in DN3 to DN4 differentiation in the absence of c-Myb, then the presence of a *Tcrb*-Tg will rescue DN3 to DN4 differentiation and cellularity of DN thymocytes. However, it is also possible that c-Myb is required for survival, proliferation, and/or differentiation of DN3 *Tcrb*-Tg+ thymocytes during β-selection. When we initially characterized the *Myb*$^{f/f}$ *cwlckCre* mice, we detected a small proportion of DN3 thymocytes that express a TCRβ chain but we detected very few DN4 thymocytes suggesting a role(s) for c-Myb during β-selection events. Therefore, we predict that c-Myb is required for DN3 differentiation independent of V(D)J recombination and that the presence of a *Tcrb*-Tg will not rescue DN3 differentiation. Since we previously reported a role for c-Myb in survival but not proliferation of peripheral B-cells [264], we predict that c-Myb is not required for proliferation but it is required for survival and/or differentiation of DN3 pre-TCR+ thymocytes during β-selection.

Chapter II. Materials and Methods

Mice. Generation of *Myb*$^{f/f}$, *Myb*$^{w/f}$, *Myb*$^{f/d}$, *Myb*$^{w/d}$ *cwlckCre* mice were previously described [14]. Briefly, *Myb*$^{f/f}$ mice were generated by flanking exon II of the *Myb* locus with *loxP* sites (Figure 9). Expression of the Cre recombinase leads to recognition of the loxP sites and excision of the intervening DNA resulting in deletion of exon II. Deletion of exon II results in out-of-frame splicing and the inability to generate any c-Myb protein due to the lack of a methionine residue. *Myb*$^{f/d}$ mice were generated by crossing *Myb*$^{w/f}$ mice with hCMV/Cre mice which express Cre in all tissues including the germline. The *Myb*$^{f/f}$, *Myb*$^{w/f}$, *Myb*$^{f/d}$, *Myb*$^{w/d}$ mice were crossed with mice expressing Cre under the transcriptional control of the proximal lck promoter, cwlckCre mice, to generate *Myb*$^{f/f}$*cwlckCre,* *Myb*$^{w/f}$ *cwlckCre,* *Myb*$^{f/d}$ *cwlckCre,* and *Myb*$^{w/d}$ *cwlckCre* mice. These mice were crossed with *Rag2*$^{-/-}$ *Tcrb*-Tg+ mice from Taconic (Albany, NY) to generate *Myb*$^{f/f}$*cwlckCre Rag2*$^{-/-}$ *Tcrb*-Tg+, *Myb*$^{w/f}$ *cwlckCre Rag2*$^{-/-}$ *Tcrb*-Tg+, *Myb*$^{f/d}$ *cwlckCre Rag2*$^{-/-}$ *Tcrb*-Tg+, *Myb*$^{w/d}$ *cwlckCre Rag2*$^{-/-}$ *Tcrb*-Tg+ mice and *Myb*$^{f/f}$ *cwlckCre Rag2*$^{-/-}$, *Myb*$^{w/f}$ *cwlckCre Rag2*$^{-/-}$, *Myb*$^{f/d}$ *cwlckCre Rag2*$^{-/-}$, *Myb*$^{w/d}$ *cwlckCre Rag2*$^{-/-}$ mice. The *Myb*$^{f/f}$*cwlckCre, Myb*$^{w/f}$ *cwlckCre, Myb*$^{f/d}$ *cwlckCre,* and *Myb*$^{w/d}$ *cwlckCre* mice were also crossed with *p53*$^{-/-}$ mice a gift from Heidi Scrable (The University of Virginia, Department of Neuroscience) and Eμ-bcl-2 (strain Bcl-2-25) mice were a gift from Ellen Rothenberg (California Institute of Technology, Pasadena, CA) to generate *Myb*$^{f/f}$*cwlckCre p53*$^{-/-}$, *Myb*$^{w/f}$ *cwlckCre p53*$^{-/-}$, *Myb*$^{f/d}$ *cwlckCre p53*$^{-/-}$, and *Myb*$^{w/d}$ *cwlckCre p53*$^{-/-}$ mice and *Myb*$^{f/f}$*cwlckCre Bcl2-Tg+, Myb*$^{w/f}$ *cwlckCre Bcl2-Tg+,*

Figure 9. Targeting Strategy for Cre recombinase mediated deletion at the *Myb* locus. The blue filled boxes represent exons I-IX of the *Myb* locus and the blue filled triangles represent loxP sites. Representation of exons I-IX at the *Myb* locus in the wildtype allele (1), the targeted allele after homologous recombination (2), and the floxed allele after Cre mediated deletion of the neomycin resistant cassette (3). Exon II is removed from the floxed allele by the addition of Cre to generate the deleted allele (4) (adapted from [14]).

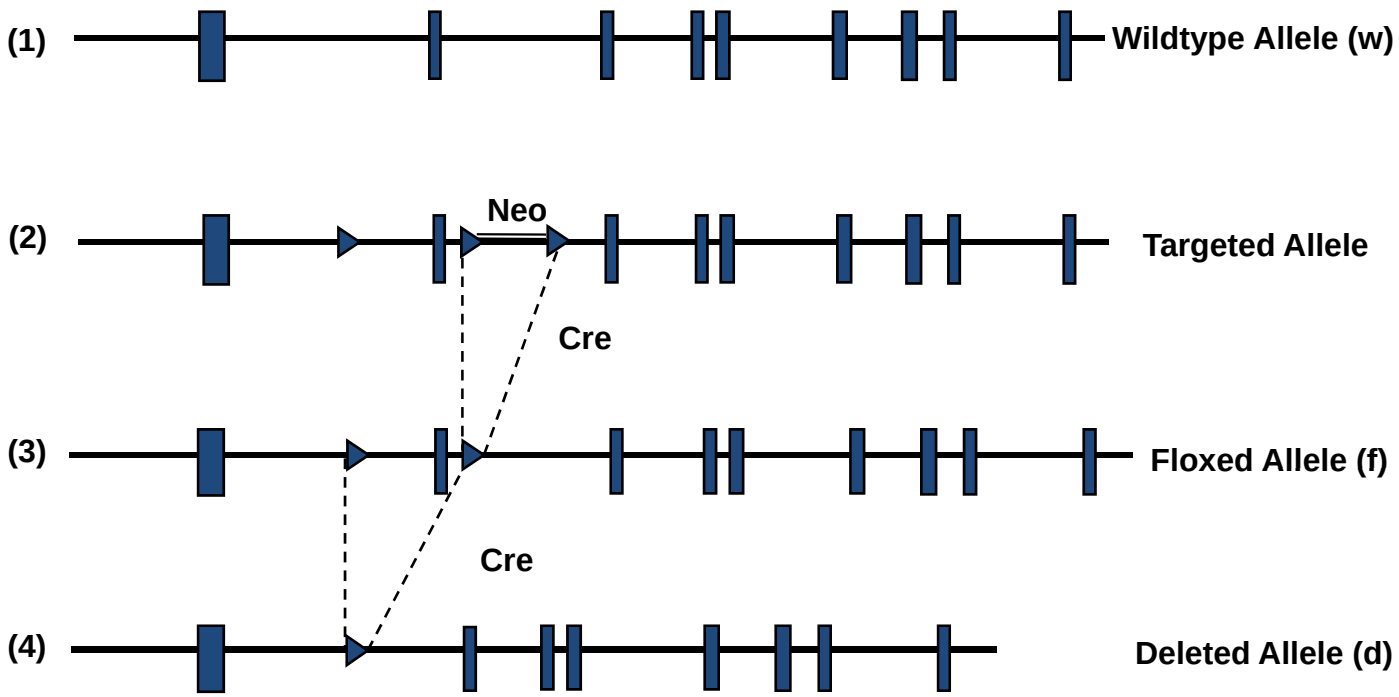
(1)
Wildtype Allele (w)
(2)
Neo
Targeted Allele
Cre
(3)
Floxed Allele (f)
Cre
(4)
Deleted Allele (d)

Myb$^{f/d}$ *cwlckCre Bcl2-Tg+,* and *Myb*$^{w/d}$ *cwlckCre Bcl2-Tg+* mice. All mice were maintained in accordance with the University of Virginia Animal Care and Use Committee guidelines.

All mice were genotyped using a polymerase chain reaction (PCR) assay. Table I lists all primers used for genotyping. *Myb*^{f} *Myb*^{d} and *Myb*^{w} alleles were identified using 3 PCR primers [14]: N2 (forward) located 5' of exon II and upstream of the 5' loxP site, N4 (reverse) located 5' of exon II and downstream of the 5' loxP site, and N6 (reverse) located 3' of exon II and downstream of the 3' loxP site. On the *Myb*^{w} allele, the N2 and N4 primers generated a 161bp fragment. The addition of the loxP site on the *Myb*^{f} allele increased the N2 to N4 fragment to 194bp which is easily distinguished from the 161bp product on a 3% agarose gel. The *Myb*^{d} allele does not contain exon II and no longer contains the sequence specific for the N4 primer which allows for N2 and N6 primers to be in close proximity to generate a 267bp product. Mice were genotyped for *Cre* expression using two primers Cre819 and Cre531 that generated a 250bp product; and for *Tcrb-Tg* expression using two primers Vb01 and Vb02 that generated a ~250bp product. For *Rag2* expression three primers RagA, RagB and NeoA were used to generate a ~400bp product for the *Rag2-null* allele and a ~250bp product for the *Rag2* allele. Expression of the *Bcl2-Tg* was detected using four primers IMR0042 and IMR0043 were specific for sequences encoded at the *Il2* locus and generated a 324bp product that served as an internal control for the PCR reaction. IMR0550 and IMR0551 which were specific for the *Bcl2-Tg* and generated a 170bp product. For expression of p53, two PCR reactions were performed one to amplify the Neo cassette of the *p53-null*

Table I. ***Primer Sequences for genotyping and RT-PCR***

Primer Name for genotyping	Primer Sequence (5' to 3')
N2	GCATGCCTCTGGAAAGTACCTTAAAC
N4	GTCTAGGAGCAAAGTTCTAACAGC
N6	CAGACAGACAGAACGTGCATTC
Cre531	CGATGCAACGAGTGATGAGG
Cre819	GCATTGCTGTCACTTGGTCCT
VbDO1	ATGTACTGGTATCGGCAGGACACGG
VbDO2	CAACTGTGAGTCTGGTTCCTTTACCA
Bcl2 imr0550	TGGATCCAGGATAACGGAGG
Bcl2 imr0551	TGTTGACTTCACTTGTGGCC
Imr0042	CTAGGCCACAGAATTGAAAGATCT
Imr0043	GTAGGTGGAAATTCTAGCATCATCC
RagA	GGGAGGACACTCACTTGCCAGTA
RagB	AGTCAGGAGTCTCCATCTCACTGA
NeoA	CGGCCGGAGAACCTGCGTGCAA
pMC1Neo Fw	CCATCATGGCTGATGCAATGCG
pMC1Neo Rev	GATGCGCTGCGAATCGGGAGCG
p53F	AAAGGTCCCAGTCCTCTCTTTGCT
p53R	CCGTCATGTGCTGTGACTTCTTGT

allele and one to amplify sequences encoded at the endogenous *p53* locus. The Neo cassette reaction generated a ~500bp product through the use of pMCLNeoFw and pMCLNeoRv primers and the p53 reaction generated a 285bp product through the use of p53F and p53R primers.

Antibodies and Flow Cytometry. Single-cell suspensions from 4 to 6 week old mice were prepared and stained with fluorochrome- or biotin-conjugated antibodies as previously described [14]. Briefly, to generate single-cell suspension, thymi were harvested and pushed through a 100 micron nylon mesh cell strainer (BD Falcon, Franklin Lakes, NJ) in cold DMEM (Dulbecco's Modified Eagle Medium Invitrogen, Carlsbad, CA) with 5% FBS (Fetal Bovine Serum) from (Invitrogen, Carlsbad, CA), 2 mM L-glutamine (Invitrogen, Carlsbad, CA), and 100 U/100ug Penicillin/Streptomycin (Invitrogen, Carlsbad, CA) (referred to herein as DMEM). The cells were then gently pushed through a 21 gauge needle syringe and then the cells were isolated by centrifugation. All centrifugation steps in this procedure were performed at 1800 rpm at 4^{o}C for 5 minutes Sorvall Legend RT+ Centrifuge (Thermo Scientific, Hudson, NH). After centrifugation, cells were resuspended in 2 to 4ml of AKC lysis buffer (0.15M NH_4Cl, 10mM $KHCO_3$, 0.1 mM Na_2EDTA [pH 7.2]) for 5 minutes on ice to lyse the red blood cells unless otherwise stated. After the 5 minute incubation, an equal volume of DMEM was added to the reaction to stop the lysis. The cells were centrifuged and resuspended in either DMEM, PBS (Phosphate Buffered Saline) (Invitrogen, Carlsbad, CA) or PBA (PBS + 0.01% NaN_3 + 0.5% BSA [Bovine Serum Albumin] Roche, Indianapolis,

IN). To obtain absolute cell numbers, thymocytes were counted on a hemacytometer and to assess whether cellularity is statistically significantly different, a Student's T-test with 2 tails type 3 was performed in Microsoft Excel. For flow cytometry, the cells were resuspended in DMEM and counted on a hemacytometer. Two million or fewer cells were surface stained with cell surface marker antibodies. In all cases, the amount of antibody used in each staining reaction was predetermined by titration. All surface staining reactions were performed in 50 ul of PBA for 15 minutes on ice in the dark. After the incubation, the cells were washed with 200 ul PBA, centrifuged and resuspended in 50 ul of PBA plus a streptavidin antibody and stained for 15 minutes on ice in the dark. The cells were then washed with 200 ul PBA, centrifuged and resuspended in 300 ul of PBA for acquisition. In some cases where a live/dead indicator is necessary, a final concentration of 1 ug/ml of 7-aminoacetomycin D (7AAD) (Invitrogen, Carlsbad, CA) or 0.5 ug/ml of 4',6-diamidino-2-phenylindole (DAPI) (Sigma-Aldrich, St. Louis, MO) was added to each sample and incubated at room temperature (RT) for 10 minutes prior to acquisition. Acquisition of data was performed on a FACSCalibur dual laser Flow Cytometer (BD Biosciences, Franklin Lakes, NJ), or a Cyan ADP LX 9 Color (Dako, Fort Collins, CO). The flow cytometry data was analyzed using FlowJo software (Tree Star, Inc. Ashland, OR).

Antibodies and reagents were purchased as follows Caltag (Burlingame, CA): CD25 (Pc61) PE; CD8 (5h10) APC-Alexa 750, Streptavidin-PE-Texas Red. eBioscience (San Diego, CA): CXCR4 (2B11) PE, CD18 (M18/2) PE; Integrin β1 (HMb1-1) PECy7; CD49d (R1-

2) PE; Integrin α5 (HMa5-1) PE; CD2 (RM2-5) PE; CD44 (1M7) FITC, PECy7, APC, biotin; CD25 (PC61) PECy7, APC; CD117 (2B8) APC; CD4 (GK1.5) biotin, PE, PECy7; CD8a (53-6.7) biotin, APC; Thy1.2 (53 2.1) biotin, PE; Streptavidin-APC, APC-Cy7; anti-rat IgM (HIS40) PE; CD90L (MFL3) PE; CD27 (LG.7F9) APC. BD Pharmingen (San Diego, CA): Streptavidin-FITC; CD5 (53-7.3) PE, TCRβ (H57-597) FITC, PE; Integrin β7 (FIB504) complex PE ;CD95 (Jo2) PE; CD53 (OX-79); Vβ8.1, 8.2 (MR5-2) FITC, PE; Vβ8.3 (1B3.3) FITC; Vβ4 (KT4) FITC; Vβ9 (MR10-2) FITC; Vβ7 (TR310) FITC; Vβ5.1, 5.2 (MR9-4) biotin; Integrin α4 (R1-2) FITC; Integrin α6 (GoH3) FITC; BD Cytofix/Cytoperm, BD Perm/Wash, Intracellular active caspase-3-PE, Mouse Lineage Panel (CD3ε-biotin, Gr-1-biotin, Mac-1-biotin, Ter119/Ly-76-biotin, CD45R/B220-biotin), anti-Bcl-2-FITC (3F11).

Isolation of Total DN Thymocytes. For depletion of CD4+CD8+ DP thymocytes or all CD4+ thymocytes, thymi were harvested and single cell suspensions were prepared as described above. The thymi from control mice were divided into two samples per thymi and *Myb*$^{f/f}$ *C* or *Myb*$^{f/d}$ *C* mutant thymi from multiple mice (3 to 6 mice) were combined into one sample. The cells were centrifuged and resuspended in 800 ul of sterile filtered degassed Macs Buffer (PBS+ 2mM (EDTA) [ethylenediaminetetraacetic acid] + 0.5% BSA) per control sample and 80 ul of Macs Buffer per mutant pooled sample. Macs MicroBeads conjugated with CD4 (L3T4) and CD8 (Ly-2) monoclonal antibodies (Miltenyi Biotec, Auburn, CA) were vortexed on high and 80-100 ul and 10 ul of each bead was added to control and mutant samples, respectively. Only CD4 beads were added when CD8 ISP thymocytes were isolated by electronic cell sorting. The cells

were incubated with microbeads for 15 minutes at 4^{o}C with gentle agitation every 5 minutes. The samples were washed with 10 ml of Macs Buffer, centrifuged and resuspended in 5 ml of Macs Buffer. Macs LS separation columns (Miltenyi Biotec, Auburn, CA) were placed on MidiMacs Separator magnets (Miltenyi Biotec, Auburn, CA) and prepared with 3 ml of Macs Buffer which flowed through the column and was not saved. Samples were immediately applied to the columns followed by 2 x 3 ml washes with Macs Buffer. Sample flow through and all washes were collected and saved. The cells were then collected by centrifugation and resuspended in 5 ml of Macs Buffer. If the cells were used for cell culture, the entire procedure post thymi removal from the mouse was performed under a laminar flow hood with sterile solutions. If cells were depleted for sorting, only control cells were depleted of DP thymocytes prior to electronic sorting.

Fluorescence Activated Cell Sorting. To sort DN subsets, thymocytes from control mice were first depleted of CD4+ and CD8+ cells as described above. The thymocytes were surface stained with the Mouse Lineage Panel (MLP) antibodies (CD3ε-biotin, Gr-1-biotin, Mac-1-biotin, Ter119/Ly-76-biotin, CD45R/B220-biotin), CD25-PE, CD44-FITC, CD4-biotin, CD8-biotin, CD117-APC, and SA-APCCY7. To sort CD8 ISP thymocytes, cells were first depleted of CD4+ cells as described above and then surface stained for MLP, CD25-PE, CD44-APC, CD4-biotin, and CD8-APC-Alexa750. DN1 thymocytes were identified as CD4-CD8-MLP-CD117+CD44+CD25-, DN2 thymocytes were identified as CD4-CD8-MLP-CD117+CD44+CD25+, DN3 thymocytes were identified

as CD4-CD8-MLP-CD117-CD44-CD25+, DN4 thymocytes were identified as CD4-CD8-MLP-CD117-CD44-CD25-, and CD8 ISP thymocytes were identified as CD4-MLP-CD8+. The electronic cell sorting was performed on a FACSVantage SE Turbo Sorter fitted with the DIVA Option (BD Biosciences, Franklin Lakes, NJ). The thymocytes were sorted into either αMEM (alpha-Minimum Essential Medium) (Invitrogen, Carlsbad, CA) + 20% FBS or Macs Buffer.

5-bromo-2'-deoxyuridine (BrdU) Incorporation and 7AAD (7-aminoacetomycin D) Staining. For BrdU incorporation in thymocytes, mice were injected intraperitoneally once with 150 ug of BrdU (Sigma-Aldrich, St. Louis, MO) and harvested 2 hours post injection unless otherwise indicated. Thymocytes were then surfaced stained with CD8-APC-Alexa 750, CD3ε-PE, CD25-PeCy7, CD44-APC, CD4-biotin, MLP (minus CD3ε), and SA-PE-Texas Red. After surface staining, the thymocytes were transferred to 5 ml polystyrene round-bottom tubes and stained for BrdU and 7AAD according to the BrdU Flow Kit staining protocol (BD Biosciences, San Diego, CA) with some modifications. After surface staining, cells were resuspended in 100 ul of Cytofix/Cytoperm from the kit for 20 minutes at RT in the dark. After the incubation, the cells were washed with 1X Perm/Wash from the kit, centrifuged, and resuspended in 100 ul of Cytoperm Plus Buffer from the kit for 10 minutes on ice. The cells were then washed with 1X Perm/Wash, centrifuged and resuspended in 100ul Cytofix/Cytoperm for 5 minutes at RT. After the incubation, the cells were washed with 1X Perm/Wash, centrifuged and resuspended in 1 ml of freshly made DNase solution (0.15M NaCl, 4.2mM $MgCl_2$, 225

ug/mL of DNase-1 [Sigma-Aldrich, St. Louis, MO]) for 30 minutes at RT. The cells were then washed with 2 ml of 1X Perm/Wash, centrifuged and resuspended in 50 ul of PBA with a FITC conjugated anti-BrdU (BD Pharmingen, San Diego, CA) for 30 minutes at RT. After the incubation, the cells were washed with 1ml of 1X Perm/Wash, centrifuged and resuspended in 20 ul of 7AAD solution. Just prior to putting the sample on the flow cytometer, 300 ul of PBA was added to the sample with the 20 ul of 7AAD solution.

For *in vitro* incorporation of BrdU, 750,000 total thymocytes were added to each well of a 24 well plate with OP9-DL1 stromal cells (described below) [269] 12 hours prior to adding 10 uM of BrdU (BD Pharmingen, San Diego, CA). Two hours post BrdU addition, thymi were harvested and thymocytes were stained for surface markers and BrdU and 7AAD as above.

Intracellular Staining for Flow Cytometry. For intracellular staining to identify active caspase-3 and TCRβ, thymocytes were first surface stained with antibodies as described above. After the final wash, cells were resuspended in 100 ul of Cytofix/Cytoperm (BD Pharmingen, San Diego, CA) at RT for 15 minutes in 96 well v-bottom plates in the dark. After the incubation, the cells were centrifuged, washed with 200ul of 1X Perm/Wash (BD Pharmingen, San Diego, CA), centrifuged and resuspended in the following staining reactions:

For intracellular active caspase-3 staining (BD Pharmingen, San Diego, CA), the cells were resuspended in 50 ul 1X Perm/Wash with 10 ul of PE conjugated anti-active caspase-3-PE mAb per test sample. After 30 minutes at RT in the dark, the cells were washed with 200 ul of 1X Perm/Wash, and resuspended in 300 ul of 1X Perm/Wash for acquisition.

For intracellular TCRβ staining or anti-Bcl2 staining, the cells were resuspended in 50ul of Perm/Wash with a pre-titrated TCRβ conjugated antibody or anti-Bcl2-FITC (3F11) antibody and incubated on ice in the dark for 15 minutes. The cells were washed in PBA, centrifuged and resuspended in PBA for acquisition.

Measurement of Apoptotic Cell Death. As a positive control for cell death, thymocytes were harvested directly *ex vivo*, treated with AKC lysis buffer as described above, and 2,000,000 thymocytes were treated with 1 uM of dexamethasone (Sigma-Aldrich, St. Louis, MO) in 1 ml of 5% FBS RPMI medium for 3 hours in a water-bath at 37^{o}C. All cells (dexamethasone treated and untreated) were stained with surface antibodies prior to staining for AnnexinV/7AAD, active caspase-3 or the TUNEL assay.

For AnnexinV/7AAD staining [270], cells were surface stained and resuspended in 48 ul of 1X Annexin V Binding Buffer (BD Pharmingen, San Diego, CA) plus 2ul FITC-conjugated Annexin V (BD Biosciences, San Diego, CA) and kept in the dark at RT for 30 minutes. After incubation, 225 ul of 1X Annexin V Binding Buffer was added plus a 1

ug/ml of 7AAD (Molecular Probes Invitrogen). The percentage of surviving cells was measured by flow cytometry as the Annexin V− and 7AAD− population and the percentage of apoptotic cells as the Annexin V+ and 7AAD− population.

For the TUNEL assay, total thymocytes were surfaced stained and then fixed in 250 ul of Cytofix/Cytoperm (BD Pharmingen, San Diego, CA) for 30 minutes on ice in the dark. The cells were centrifuged, resuspended in 250 ul of 1X Perm/Wash (BD Pharmingen, San Diego, CA), centrifuged, and resuspended in 25 ul of TMR red Tdt-incorporation solution from the In Situ Cell Death Detection Kit (Roche, Indianapolis, IN). The cells were incubated for 1 hour at 37^{O}C in a humidified incubator with a 5% CO_2 atmosphere, washed with PBA and resuspended in PBA for acquisition.

Measurement of DNA content. For Draq5 DNA staining, cells harvested from co-coultures were first stained with fluorescent tagged antibodies. The cells were then resuspended in 300 ul of PBA with 5 ul of Draq5 (Alexis Biochemcials, Leicestershire, UK) for 2,000,000 cells or 3 ul of Draq5 for <500,000 cells. The cells were incubated in a water-bath at 37^{O}C for 20 minutes prior to acquisition.

αCD3ε Treatment. Anti-CD3ε mAb (145-2C11) was purified from cell culture supernatant fluid by the University of Virginia Lymphocyte Core Facility (Charlottesville, VA) as described previously [14]. Mice were injected once intraperitoneally with 150 ug of αCD3ε in 300 ul of PBS and were euthanized at indicated timepoints post injection. Thymi were either: 1) stained with fluorescent tagged antibodies for flow cytometry as

described above or 2) used to obtain protein lysate for Western blotting. For protein lysate, blood was gently removed from the thymi with forceps and no red blood cell AKC lysis was performed. Thymi were then pushed through the 100 micron cell strainers to obtain single-cell suspensions and kept on ice. The cells were washed in PBS + protease inhibitors, briefly centrifuged at 10,000 rpm and lysed in 0.1% NP40 buffer as described in immunoblotting section of this chapter.

OP9 Cell Co-cultures. For co-culture on OP9-DL1 or OP9-control stromal cells (a kind gift of Dr. Juan Carlos Zuniga-Pflucker, University of Toronto) [269], *Myb$^{f/f}$ cwlckCre* and *Myb$^{f/f}$ cwlckCre Rag2$^{-/-}$ Tcrb-Tg+* thymocytes were either electronically sorted prior to co-culture or they were depleted of CD4+CD8+ DP thymocytes to obtain a total DN population. Total thymocytes from *Rag2$^{-/-}$* mice were added to cultures. All thymocyte co-cultures were performed with 20% FBS αMEM with 2 mM L-glutamine, 100 U/100 ug Penicillin-Streptomycin liquid (P/S) in the presence of 5 ng/ml of mouse recombinant IL-7 and Flt3L from (Peprotech, Rocky Hill, NJ) as described elsewhere [269].

To inhibit caspase activation, sorted DN3 thymocytes were added to OP9-DL1 stromal cells in the presence of 40uM of Z-VAD(OMe)-FMK (ICN Pharmaceuticals , Aurora, OH). Co-cultures were harvested and stained with cell surface marker antibodies and intracellular caspase-3 activation as described above.

Immunoblotting. Total thymocytes from *Rag2$^{-/-}$* mice or sorted DN3 and ISP thymocyte subsets from *Rag2$^{-/-}$ Tcrb-Tg+* mice were washed in 100 ul of PBS containing

a cocktail of protease inhibitors: AEBSF (4-(2-Aminoethyl) benzenesulfonyl fluoride hydrochloride), Aprotinin, E-64, and Leupeptin from (Calbiochem, Gibbstown, NJ) plus 1 mM phenylmethylsulfonyl fluoride (PMSF), 50 mM NaF and 1 mM Na_3VO_4. The cells were centrifuged for 5 seconds at 10,000 rpm and resuspended in lysis buffer (0.1% NP-40, 150mM NaCl, 5mM EDTA, 50mM Tris pH 7.4) for 30 minutes on ice. The samples were centrifuged for 15 minutes at 4^{o}C and lysate was transferred to a new tube and stored at -20^{o}C until used for immunoblotting. The protein concentrations were determined by the bicinchoninic acid (BCA) Protein Assay (Pierce, Rockford, IL). Ten micrograms of protein per lane were either fractionated on 10% (for the cyclin D3 immunoblot) or 6% (for the Rb immunoblot) sodium dodecyl sulfate polyacrylamide gel electrophoresis (SDS-PAGE), transferred to nitrocellulose and incubated with either anti-cyclin D3 (DCS22) (Cell Signaling Technology, Beverly, MA), anti-Rb (G3-245) (BD Pharmingen, San Diego, CA), anti-ERK1/2 (Cell Signaling Technology, Beverly, MA) and anti-β-actin-peroxidase (Sigma-Aldrich, St. Louis, MO). Immunoblots needing secondary antibody peroxidase were incubated with appropriate mouse or rabbit peroxidase-conjugated IgG (Amersham GE Healthcare, Pittsburgh, PA) followed by enhanced chemiluminescence (ECL) detection (PerkinElmer, Waltham, MA).

Semi-quantitative Reverse Transcriptase Polymerase Chain Reaction (RT-PCR) and Quantitative Real Time Polymerase Chain Reaction (qPCR). Total cellular RNA was isolated from thymocytes using the PicoPure RNA Isolation Kit (Arcturus, Sunnyvale, CA) or using RNeasy Kit (QIAGEN Sciences, Germantown, MD). Samples were treated with

DNase I (QIAGEN Sciences, Germantown, MD) while on the purification columns according to the manufacturer's directions. First-stand cDNA synthesis was performed using Superscript II according to the random priming kit protocol (Invitrogen, Carlsbad, CA). For semi-quantitative RT-PCR, cDNA was first diluted 1:3 and further 1:3 serial dilutions were amplified by PCR with the following primers: *Ccnd3* (67^{o}C), forward 5'-GCGTCCCCACCCGAAAGGCG-3', and reverse, 5'-CCAGGAAGTCGTGCGCAATC-3'; *Actb* (60^{o}C), forward 5'-CCTAAGGCCAACCGTGAAAAG-3', and reverse 5'-TCTTCATGGTGCTAGGAGCCA-3'; Hes1 (56^{o}C), forward 5'-AACACGACACCGGACAAAC-3', and reverse 5'-GAATGCCGGGAGCTATCTT-3'; pTα (59^{o}C), forward 5'-CACACTGCTGGTAGATGGAAGGC-3', and reverse 5'-GTCAGGAGCACATCGAGCAGAAG-3'. For qPCR, cDNA was diluted 1:10 and 2 ul of diluted cDNA was added to each well. Reactions were performed in duplicate. For validation of the gene expression microarray experiments, qPCR reactions were performed using Titanium Taq DNA polymerase (Clonetech, Mountain View, CA) and SYBR Green (Invitrogen, Carlsbad, CA) in an Opticon DNA engine (MJ Research, Waltham, MA). Reaction conditions were 3 minutes at 95^{o}C, 40 cycles of: 95^{o}C for 40 seconds, 66^{o}C for 20 seconds, 72^{o}C for 30 seconds; 72^{o}C for 1 minute followed by a melting curve analysis. Gene primers for microarray confirmation are listed in Table II.

Migration Assay. Thymi from *Myb*$^{w/f}$ and *Myb*$^{f/f}$ *cwlckCre* mice were harvested, the blood was gently removed with forceps, and red blood cell AKC lysis was not performed. Thymocytes were pooled from 4 *Myb*$^{w/f}$ and pooled from 5 *Myb*$^{f/f}$ *cwlckCre*

Table II. ***List of gene primer sequences for qPCR validation of microarrays.***

Gene	5' →3' Forward Primer Sequence	5' →3' Reverse Primer Sequence
Bcl2	CTCGTCGCTACCGTCGTGACTTCG	CAGATGCCGGTTCAGGTACTCAGTC
Bmf	GAGGTGCAGATCGCCAGAAA	TGTTCAGGGCGAGGTTTTGA
Btg1	GCGGTGTCCTTCATCTCCAA	CGGCTTTTCTGGGAACCAGT
Camk4	TATGCAACTCCAGCCCCTGA	TAGGCACAGCCTCGGAGAAT
Ctss	GCAATGGAGCAACTGCAGAG	TTCCCAGATGAGACGCCGTA
Dtx1	ATGCATCAGTTCCGGCAAGA	TCTCCCATTCCCACACGATG
Edem1	GGGAAGCCTGCAATGAAGGAGA	TGGCATCTTCCACATCCCCTA
Egr1	CAGCGCCTTCAATCCTCAAG	TCTCCACCATCGCCTTCTCA
Fos	TGGTGAAGACCGTGTCAGGA	CCCTTCGGATTCTCCGTTTC
Gata3	CCTACCGGGTTCGGATGTAA	CGCAGGCATTGCAAAGGTAG
Gfi1	ACTTTTGGAGGCCCCCTTCT	GGCTTGAAAGGCAGCGTGTA
Hprt	TGCCGAGGATTTGGAAAAAGTG	CACAGAGGGCCACAATGTGATG
Hspa1b	TCGTCCATGGTGCTGACGAA	TGCCGCTGAGAGTCGTTGAA
Ikaros	GATCATTCTTGGCCCCCAAA	TGGGACATGTCTTGACCCTCA
Irf4	TGTGCTTTGGTGAGGAGTTTCC	TCGTAGCCCCTCAGGAAATGT
Jun	ACCGGTATTTTGGGGAGCAT	AAGGCGCAGAAGAGATTTGC
Lnx2	TCATCGCCAGAGATGGAAGG	TGTGGGACACGTTGCTGATG
Mtf2	GGCAGAAAGGCATCCAAACC	TATATGGGCCAGGAGGACGA
Nrdg1	TTTGTGCAGGGCATGGGATA	ATCAGGCGAGTCATGCTG
Ptprf	CGGCCCAGGTCACAGTAAAA	AACACTGGTGGCGGTTGTCT
Runx1	AAGACCCTGCCCATCGCTTT	CCGCGGTAGCATTTCTCAGTT
Sh2d1a	TGGAAGCTATCTGCTGCGAGAC	CGGCACTCCAAGAACCTGTTT
Smo	TGGCCTGACTTTCTGCGTTG	GGGTTGTCTGTTCGCACCAA
Smyd3	TACACTGTGTGCAAGGGGAGTC	GGCAATTCGGCATTGAGAAC
Socs3	AAGGCCGGAGATTTCGCTTC	GGGAAACTTGCTGTGGGTGA
Sox4	GCGCAAGATCATGGAGCAGT	GCCTCCTGGATGAACGGAAT
Spib	ATGGTCCTAACCCCTCCACCTA	ACGGAGCATAAGCCAAGGAG
Tnfaip3	TCCCTGGAAAGCCAGAAGAA	GCATGCATGAGGCAGTTTCC
Zfp36l2	TCCACGCTTGCAATTTCGAC	CGCCTTCTTGTCCAGCATGT

mice and resuspended at a concentration of $1x10^7$ cells/ml in RPMI medium supplemented with 0.5% BSA, 25 mM Hepes, and 2 mM L-glutamine. Transwell plates with 5 um pore-size inserts (Corning Costar, Lowell, MA) were coated with extracellular matrix proteins as follows. Both the upper (100 ul volume) and lower (600 ul volume) side of the transwell were coated with 10 ug/ml of BSA, fibronectin or laminin. The transwell plates were incubated for 1 hour at 37^{o}C. The transwells were dried by gently removing the transwell and gently aspirating the extracellular matrix without touching the filter. The transwells were placed into a new 6-well plate to dry under a laminar flow hood for 30 minutes. One million thymocytes in 100 ul were added to the upper chamber while 600 ul of DMEM supplemented with 1% BSA and 10 uM of CXCL12 (PeproTech, Rocky Hill, NJ) was added to the lower well. The plates were incubated at 37^{o}C in a humidified incubator with a 5% CO_2 atmosphere for 90 minutes. The thymocytes that migrated to the lower wells were collected and the cells were surface stained for surface markers CD3ε-PeCy5.5, CD4-PE, CD8-APC-Alexa 750, CD44-APC and CD25-FITC.

Retroviral Infections. pMIGR1 was a gift from Dr. Warren Pear (University of Pennsylvania, Philadelphia, PA) [271] and pBSKS-wtcycD3 and pBSKS-T3cycD3 (T283AcyclinD3) were gifts from Dr. Maurizia Caruso (Via Fosso di Fiorano, Roma, Italy) [272]. pMIGR1/c-Myb was generated by first subcloning a c-Myb encoding cDNA fragment from pLitmus28-c-Myb into HA-pEBB (gift from Dr. Kodi Ravichandran, University of Virginia, Charlottesville, VA) to produce a c-Myb cDNA that encoded the

triple HA-tag at the amino terminal end. The HA-c-Myb was cloned into the pMIGR1 vector at the BamHI/BglII site (Yuan et al. in progress). WtcycD3 and T3cycD3 encoding cDNA fragments from pBSKS-wtcycD3 and pBSKS-T3cycD3 were cloned into the EcoRI site in pMIGR1 to generate pMIGR1/wtCycD3 and pMIGR1/T283ACycD3.

Retroviral supernantants were generated by transient $CaPO_4$ mediated co-transfection of 293T cells [273] with RetroMax packaging vector pCL-Eco (Imgenex, San Diego, CA) and a pMIGR1 based retrovirus construct (pMIGR1, pMIGR1/HA-c-Myb, pMIGR1/T283ACycD3, or pMIGR1/ WtCycD3) [273]. The retrovirus containing supernatants were harvested at 48 and 72 hours post transfection. The number of infectious particles was determined by titrating the retroviral supernatant on 3T3 cells. The day before infection 200,000 3T3 were plated in 6-well plates (Day -1). The following day (Day 0) 1 ul, 10 ul or 100 ul of viral supernatant was added to 2 ml of 10% FBS, 2mM L-glutamine, 100 U/100ug Penicillin/Streptomycin, Iscove's Modified Dulbecco's Medium (IMDM) plus 8 ug/ml of polybrene for a total of 4 ml. The cells were transduced by "spinfection" [274]. Briefly after adding retrovirus containing supernate, the plates were centrifuged at 2000 rpm at RT for 90 minutes with no brake. The cells were harvested the following day (Day 1) and the percentage of infected cells measured as GFP+ by flow cytometry. The titers were obtained by the following equation where $8x10^5$ is the number of 3T3 cells at time of harvest if 200,000 3T3 were plated at Day-1: (%GFP+ x $8x10^5$)/dilution in mls [275].

Electronically sorted DN3E or DN1/2 thymocytes were split into 4 aliquots (4 infection conditions: MIGR1, MIGR1-c-Myb, MIGR1-wtcycD3, MIGR1-T283AcycD3) according to the lowest number of cells sorted. The thymocytes were resuspended in 50 ul of alpha-MEM with 5 ng/ml of IL-7 and Flt3L as described in 'OP9 Cell Co-cultures' section. The following was added to one well of a 24 well plate: 50 ul volume of thymocytes, 8 ug/ml of polybrene , a 4:1 ratio of infectious particles:cell, and supplemented alpha-MEM medium as described above with cytokines for a total volume of 1 ml. The cells were transduced by "spinfection" as described above. The wells were harvested by pipeting up and down and transferred to an eppendorf tube before being equally aliquoted (duplicate wells per time point) to wells containing OP9-DL1 cells. The thymocytes were transferred to fresh OP9-DL1 monolayers every 4 days by gently pipeting up and down to harvest thymocytes while avoiding harvesting the OP9 layer. At the indicated timepoints, thymocytes were harvested with more forceful pipetting and stained for CD4-PE, Thy1.2-biotin, CD25-PeCy7, CD44-APC, CD8-APCALEXA750, SA-PeTexRed and DAPI.

Gene Expression Microarray Preparation and Analysis. Thymocytes were harvested from mice and depleted of DP cells as described in 'Isolation of total DN cells' section of this chapter. DN2 and DN3 thymocytes from *Myb*$^{w/f}$ *cwlckCre and Myb*$^{f/f}$ *cwlckCre* mice and DN3 thymocytes from *Myb*$^{w/f}$ *cwlckCre Rag2*$^{-/-}$ *Tcrb-Tg+* and *Myb*$^{f/f}$ *cwlckCre Rag2*$^{-/-}$ *Tcrb-Tg+* mice were electronically sorted as described in 'Fluorescence Activated Cell Sorting' section of this chapter. RNA from DN2, DN3, DN3 *Tcrb-Tg+*

thymocytes was isolated from each sample using the PicoPure RNA Isolation Kit (Arcturus, Sunnyvale, CA). RNA from each sorted sample was amplified using the RiboAmp OA Amplification Kit (Arcturus, Sunnyvale, CA). Preparation of total cellular RNA subsequent amplification was carried out in collaboration with Dr. David Mullins (Department of Microbiology, University of Virginia). Amplified RNA was sent to the Gene Chip Analysis Core Facility (University of Virginia) to generate cRNA. cRNA was fluorescently labeled and hybridized to GeneChip Mouse Genome 430 2.0 Array (Affymetrix, Santa Clara, CA) chips. Data was acquired in the Gene Chip Analysis Core Facility (University of Virginia).

Statistical analysis was performed in collaboration with Dr. Stefan Bekiranov (Department of Biochemistry and Molecular Genetics, University of Virginia) . Relative RNA abundance from the Affymetrix arrays was calculated by quantile normalizing[276] all arrays using GCRMA (GC Robust Multi-array Average)[277]. The CEL files were processed using the Affymetrix MAS5 algorithm (Affymetrix Whitepaper. Statistical Algorithms Description Document. Affymetrix 2002. http://www.affymetrix.com/support/technical/whitepapers/sadd_whitepaper.pdf) to obtain presence/absence calls for each array. All possible pairwise comparisons between control and *Myb*-deficient DN2, DN3 and DN3 Tcrb-Tg+ samples were performed. Probe sets were eliminated if there was a majority of absence calls made in both pairwise samples being compared indicating a strong likelihood that the transcript could not be detected in either sample. T-tests were performed on the log transformed

values to estimate p-values for every probe. These p-values were used to estimate the false discovery rate (FDR) for every probe set [278]. The values listed were log2 transformed. Gene lists of differentially expressed genes were generated by applying a 20% FDR cutoff and requiring the estimated fold change to be greater than 1.1. Gene ontology functional categories were identified using Onto-Express and metabolic pathways were identified using Pathway-Express[279].

Chapter III. c-Myb is Required for β-selection Survival and Proliferation.

Introduction

Thymocyte development can be subdivided into cellular subsets based on expression of the CD4 and CD8 coreceptors, rearrangement status of TCR genes and expression of the TCR. The most immature subset is referred to as double-negative (DN) and lacks expression of the CD4 and CD8 coreceptors. The DN compartment can be further subdivided based on expression of CD25, CD44 and CD117. DN thymocytes progress sequentially through DN1 (CD44+CD25-CD117+), DN2 (CD44+CD25+CD117+), DN3 (CD44-CD25+CD117-), and DN4 (CD44-CD25-CD117-) [15]. Rearrangement of the *Tcrb* gene segments *Dβ* to *Jβ* initiates during the DN2 stage and developing thymocytes complete rearrangement at the *Tcrb* locus by joining *Vβ* to *DJβ* at the DN3 stage [26]. Nascent TCRβ protein pairs with the preTα to form the pre-TCR in a complex with the CD3ε, γ, η/ζ signaling molecules [31]. Signals generated by the pre-TCR drive a series of events referred to as β-selection and provide cues for survival, proliferation, allelic exclusion at the *Tcrb* locus, down regulation of CD25, and differentiation to the CD4+CD8+ double positive (DP) stage [40, 42, 55, 280]. Thymocytes unable to generate a functional TCRβ chain do not receive signals to advance beyond the DN3 stage of development. In addition to signals from the pre-TCR, thymocyte:stromal cell interactions including Notch, Wnt, and CXCR4 receptor interactions are required to traverse the β-selection checkpoint [32-39].

Both proliferation and survival signals contribute to the proliferative expansion of β-selecting thymocytes. One mechanism by which the pre-TCR signals proliferation is through activation of Lck and the induction of cyclin D3 [1, 12]. D cyclins are the first cyclins expressed during the cell cycle early in G1. D cyclins form complexes with cdk4 or cdk6 and contribute to the hyperphosphorylation of the retinoblastoma protein and release of E2F transcription factors to transcribe genes required for S-phase [88, 89]. Cyclin D3 is the only D cyclin expressed in DN4 and ISP thymocytes before it is then down-regulated in DP thymocytes [1]. *Ccnd3*$^{-/-}$ mice contain thymi with severely reduced numbers of DP thymocytes and a reduced percentage of DN4 and ISP cells in S-phase [1]. Proliferation during β-selection is also regulated by cdk inhibitors p16 and p27 and expression of a p16$^{Ink4\alpha}$ transgene or a p27^{Kip1} transgene in thymocytes blocked differentiation at the DN3 stage [91, 92]. Moreover, expression of p27 protein decreases as cells transit from the DN3E to DN3L stage suggesting pre-TCR control over expression of p27 [2]. In the absence of a survival signal generated by pre-TCR signaling, thymocytes undergo apoptosis [53, 86, 93]. The pre-TCR signals survival through activation of transcription factor NFκB and pre-TCR signals resulting in increased expression of the antiapoptotic Bcl-2 family member Bcl2a1 [86]. However, suppression of Bcl2a1 expression using shRNA did not affect survival during β-selection [221]. The pre-TCR also signals survival through down-regulation of pro-apoptotic molecules Bim by inhibiting expression of the FOXO3a transcription factor and Bid through down-regulation of p53 in DN4 thymocytes [95]. It has also speculated that pre-TCR signaling

may override death receptor mediated apoptosis. Early studies demonstrated that transgenic expression of a dominant negative form of the universal death adapter, FADD, in *Rag1*$^{-/-}$ mice generated thymi with DP thymocytes without a concomitant increase in thymic cellularity [94]. In addition, thymocyte specific deletion of FADD generated a partial block in DN3 differentiation with reduced thymic cellularity [94, 112]. The failure to increase cellularity in these FADD mutant mice has been attributed to a failure to proliferate which further complicates understanding the role of death receptor mediated apoptosis in the survival of β-selecting thymocytes [94, 112, 113]. Thus, mechanisms that control survival during β-selection remain unclear.

c-Myb is expressed throughout thymopoiesis indicating that it may play specific roles at multiple stages throughout the development of a thymocyte [14, 216, 257]. Null and hypomorphic *Myb* alleles suggested a role for c-Myb during thymocyte development but were not able to discriminate between a requirement for c-Myb in early progenitor cells versus a requirement for c-Myb during thymopoiesis [195, 225, 228]. We and others used tissue specific Cre/loxP mediated mutagenesis to specifically delete the *Myb* locus during thymopoiesis [14, 266]. Thymocyte specific deletion of *Myb* demonstrated that c-Myb is required for efficient differentiation of thymocytes beyond the DN3 stage, for the survival of pre-selection DP thymocytes, and for differentiation of CD4 lineage thymocytes [14]. We demonstrated that expression of a TCRβ protein is diminished and Vβ to DJβ recombination of the *Tcrb* locus is severely impaired in the absence of c-Myb [14]. However, a small percentage of DN3 thymocytes

expressed a TCRβ protein yet failed to efficiently differentiate suggesting that c-Myb may also be required during β-selection. To determine if c-Myb is required for differentiation of DN3 thymocytes independent of V(D)J recombination, we crossed our *Myb*$^{f/f}$ *cwlckCre* mice with *Rag2*$^{-/-}$ and *Tcrb* transgenic mice. These crosses enabled us to measure cell death in the absence of V(D)J recombination. We demonstrate that c-Myb is not required for the intrinsic survival of DN3 thymocytes that lack a pre-TCR but that c-Myb is crucial for the survival and proliferative expansion of thyomcytes during β-selection. Survival and proliferative expansion could not be rescued by breeding a *p53* null mutation or a Bcl-2 producing transgene onto the c-Myb deficient background. Surprisingly, c-Myb deficient thymocytes fail induce expression of cyclin D3 protein during β-selection.

Results

c-Myb is required for normal β-selection. *Myb*$^{f/f}$ *cwlckCre (C)* mice have a severe block during thymocyte development beyond the DN3 stage with a concomitant defect in Vβ to DJβ recombination [14]. To determine if c-Myb is required for survival of DN3 thymocytes prior to V(D)J recombination, which might be expected to affect the efficiency of V(D)J recombination, we crossed the *Myb*$^{f/d}$ *C* and *Myb*$^{f/f}$ *C* mice onto the *Rag2*$^{-/-}$ background to generate *Myb*$^{f/f}$ and *Myb*$^{f/d}$ *cwlckCre Rag2*$^{-/-}$ *(CR)* mice as well as littermate controls (LMC) (Table III). We did not detect a difference in total thymic

cellularity or in the absolute number of DN3 or DN4 thymocytes between *Myb*$^{f/f}$ *CR* and LMC mice (Figure 10A). Deletion of the *Myb* locus in *Myb*$^{f/f}$ *CR* DN3 cells was approximately 64% (Figure 10B). Analysis of CD25 and CD44 as well as CD4 and CD8 surface expression on *Myb*$^{f/f}$ *CR* thymocytes demonstrated that differentiation remained blocked at the DN3 stage and that c-Myb deficient DN3 thymocytes do not spontaneously differentiate in the absence of c-Myb (Figure 10C). We also measured the ability of *Myb*$^{f/f}$ *CR* thymocytes to survive in liquid culture without a source of exogenous cytokines and detected no difference in the percentage of live cells recovered after culture for 18 or 34 hours between *Myb*$^{f/f}$ *CR* and LMC mice (Figure 10D). Thus, c-Myb does not appear to be required for the survival of DN3 thymocytes that lack a pre-TCR.

When we initially characterized the phenotype of *Myb*$^{f/f}$ *C* DN thymocytes, we examined intracellular expression of TCRβ to determine if DN3 thymocytes expressed a TCRβ protein to form the pre-TCR to signal differentiation beyond the DN3 stage [14]. We detected a decrease in the proportion of DN3 thymocytes that express a TCRβ protein but a small proportion of them did express a TCRβ protein yet we detected very few thymocytes in the DN4 stage suggesting that c-Myb may also be required for β-selection. To test if c-Myb is required for β-selection, we crossed the *Myb*$^{f/f}$ and *Myb*$^{f/d}$ *CR* mice with mice that express a *Tcrb*-Tg to generate *Myb*$^{f/f}$ and *Myb*$^{f/d}$ *cwlckCre Rag2*$^{-/-}$

Table III. ***List of mice genotypes and abbreviations***

Full mouse genotype	Abbreviation
Myb$^{f/f}$ cwlckCre	*Myb$^{f/f}$ C*
Myb$^{f/f}$ cwlckCre Rag2$^{-/-}$	*Myb$^{f/f}$ CR*
Myb$^{f/f}$ cwlckCre Rag2$^{-/-}$ Tcrb-Tg+	*Myb$^{f/f}$ CRT*
Myb$^{f/f}$ cwlckCre p53$^{-/-}$	*Myb$^{f/f}$ PC*
Myb$^{f/f}$ cwlckCre Bcl2-Tg+	*Myb$^{f/f}$ BC*

Tcrb-Tg+ (*CRT)* mice (Table III) to determine if expression of a *Tcrb*-Tg could rescue DN3 to DN4 differentiation. A *Tcrb* transgene is able to rescue differentiation of *Rag2*-deficient thymocytes to the DP stage and results in a total thymic cellularity that is several fold greater than a normal thymus [268] (Figure 11A and 11B). In contrast, while the *Tcrb* transgene does result in the production of some DP thymocytes in *Myb*- and Rag2-doubly-deficient thymocytes, the total thymic cellularity is not increased and the majority of thymocytes remain in the DN compartment. Inspection of the DN compartment also demonstrates that thymocyte development in $Myb^{f/f}$ and $Myb^{f/d}$ *CRT* mice remains profoundly blocked to differentiation beyond the DN3 stage (Figure 11B). Cre mediated deletion of the *Myb* locus in DN3 and DN4 sorted subsets from $Myb^{f/f}$ *CRT* mice is quite efficient while deletion in the ISP subset is decreased (Figure 11C), suggesting that most of the thymocytes that differentiate beyond the DN stage retained a functional c-Myb allele. The *Tcrb*-Tg is under the transcriptional control of the Vβ8.2 promoter that contains multiple Myb binding sites [281]. However, examination of TCRβ expression by intracellular staining demonstrates that the *Tcrb*-Tg is expressed in DN3 (CD25+) thymocytes from $Myb^{f/f}$ *CRT* mice (Figure 11D). Thus, expression of c-Myb is crucial for normal β-selection independent of the previously reported defect in V(D)J recombination at the *Tcrb* locus.

c-Myb deficient thymocytes differentiate but fail to undergo proliferative expansion during β-selection. Since c-Myb is required for β-selection independent of V(D)J recombination, we determined whether cells lacking c-Myb can initiate events

Figure 10. A reduction in c-Myb does not affect survival of *Rag2*$^{-/-}$ thymocytes. (A) The absolute number of Total, DN3 and DN4 thymocytes between *Myb*$^{w/f}$ and *Myb*$^{f/f}$ *cwlckCre Rag2*$^{-/-}$ (*CR*) mice is not changed. To obtain DN3 and DN4 numbers, cells were stained for flow cytometry with monoclonal antibodies for CD44, CD25, and the DN lineage markers (B220, CD3ε, Mac1, Ter119, Gr-1, CD4 and CD8) which served as the DN lineage− gate. Error bars represent the standard deviation of the mean of at least 8 mice per genotype over 3 independent experiments. **(B)** Cre mediated deletion of the loxP targeted *Myb* allele in sorted DN3 thymocytes from 2 *Myb*$^{f/f}$ *CR* mice. DNA was isolated and analyzed by a PCR assay. Serial 1:3 dilutions of *Myb*$^{f/d}$ tail DNA serve as a control to demonstrate equal ratios of the floxed and deleted *Myb* alleles in the PCR assay. The percentage of the deleted allele was determined by densitometry and is listed below the gel picture. **(C)** Contour plots of different thymocyte populations of *Myb*$^{w/f}$ *CR* and *Myb*$^{f/f}$ *CR* mice did not detect any abnormal populations. For CD4 and CD8 expression, cells were stained with monoclonal antibodies for CD4, CD8 and a lineage panel of B220, Mac1, Ter119, and Gr-1 which served as the lineage− gate. To assess the DN compartment, thymocytes were stained as mentioned in (A). The percentage of cells in each quadrant is listed. Data are representative of 8 mice. **(D**) The percentage of *Myb*$^{w/f}$ and *Myb*$^{f/f}$ *CR* thymocytes recovered after culture in suspension for 18 and 34 hrs. Total single cell suspended thymocytes from 3 LMC and 3 *Myb*$^{f/f}$ *CR* mice were placed in culture for 18 and 34 hrs, harvested and counted on a hemacytometer to obtain the number of cells recovered which was compared to the number of input cells as the percentage of cells recovered.

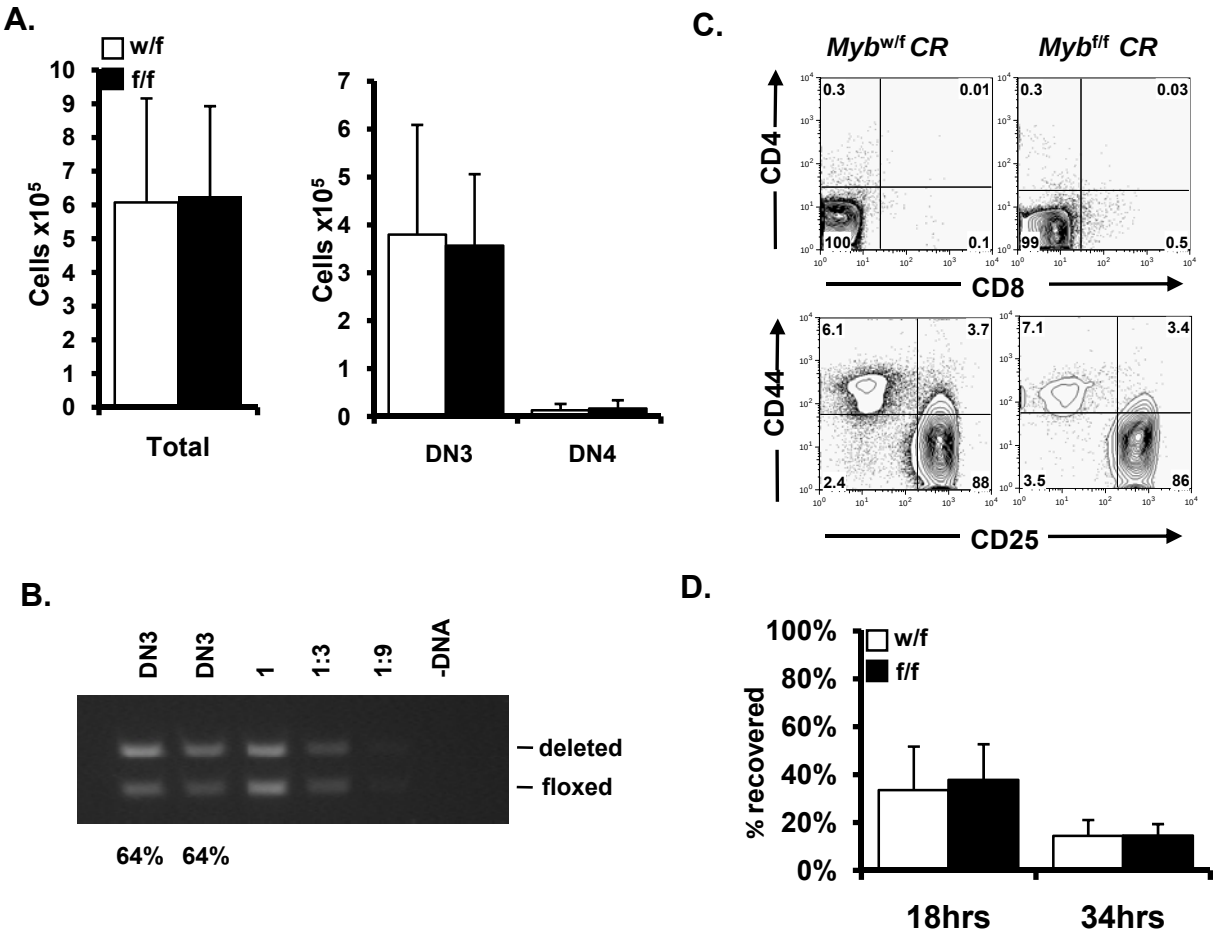
A.
w/f
f/f
Cells x10^5
Total
DN3
DN4
B.
DN3
DN3
1
1:3
1:9
-DNA
deleted
floxed
64%
64%
C.
Myb^w/f CR
Myb^f/f CR
CD4
CD8
CD44
CD25
0.3
0.01
100
0.1
0.3
0.03
99
0.5
6.1
3.7
2.4
88
7.1
3.4
3.5
86
D.
% recovered
w/f
f/f
18hrs
34hrs

associated with pre-TCR signaling by examining CD5, CD2, CD27 and CD25 surface marker expression. Expression of CD5 on DN thymocytes is dependent on pre-TCR and Lck activation [282], expression of CD2 is detected on TCRβ expressing DN thymocytes [283], and expression of CD27 is detected on large DN3 (DN3L) thymocytes that have initiated β-selection signaling. Whereas, a $CD25^{bright}$ population of DN3 thymocytes [32] and CD25 expression on DP thymocytes [53, 284-287] have both been reported to occur in mice with impaired pre-TCR signaling. Expression of CD2 and CD5 in *Myb*$^{f/f}$ *C* DN3 thymocytes is decreased as compared to LMC whereas expression of CD2 and CD5 in *Myb*$^{f/f}$ *CRT* DN3 thymocytes is equivalent to that detected in LMCs (Figure 12). The reduced expression of CD2 and CD5 in *Myb*$^{f/f}$ *C* DN3 but not in *Myb*$^{f/f}$ *CRT* DN3 thymocytes is probably due to the fact that *Myb*$^{f/f}$ *C* DN3 thymocytes have a reduced proportion of cells that produce a TCRβ protein, likely due to inefficient V(D)J recombination at the *Tcrb* locus [14]. However, in CRT mice essentially all of the DN3 thymocytes produced express a TCRβ protein and have a pre-TCR (Figure 11D) and expression of CD2 and CD5 indicate that the pre-TCR delivers signals to initiate β-selection in *Myb*-deficient thymocytes. The DN3 thymocytes that do initiate pre-TCR signaling to become DN3L thymocytes [2] express CD27 in *Myb*$^{f/f}$ *C* and *Myb*$^{f/f}$ *CRT* mice similar to the controls (Figure 12). Examination of CD25 expression in DN thymocytes demonstrates that *Myb*$^{f/f}$ *C* and *Myb*$^{f/f}$ *CRT* contain $CD25^{bright}$ thymocytes as compared to controls. We gated on the CD25+ population to obtain the mean fluorescence intensity (MFI). The MFI is statistically significantly increased in *Myb*$^{f/f}$ *C* and *Myb*$^{f/f}$ *CRT* as compared to control mice demonstrating that *Myb*$^{f/f}$ *C* and *Myb*$^{f/f}$ *CRT* contain $CD25^{bright}$

Figure 11. A rearranged *Tcrb* Tg fails to rescue differentiation from the DN3 to the DN4 stage of thymocyte development. **(A)** The absolute number of Total, DN3 and DN4 thymocytes from *Myb*$^{f/f}$ *cwlckCre Rag2*$^{-/-}$ *Tcrb Tg+* (*CRT*) mice is severely reduced as compared to *Myb*$^{w/f}$ *CRT* mice. Error bars represent standard deviation of the mean for at least 10 mice per genotype. * $p \leq 0.001$ **(B)** Contour plots of different thymocyte populations of *Myb*$^{w/f}$ and *Myb*$^{f/f}$ *CRT* mice reveal a block in DN3 differentiation. Thymocytes were surface stained and gated through the lineage− gate to examine CD4 and CD8 expression and through the DN lineage− gate to examine CD25 and CD44 expression. Data are representative of 10 mice. **(C)** Cre mediated deletion of the loxP targeted *Myb* allele in sorted DN3, DN4, and ISP (CD3-CD8+) thymocytes from *Myb*$^{f/f}$ *CRT* mice. DNA was analyzed by a PCR assay. Serial 1:3 dilutions of *Myb*$^{f/d}$ tail DNA serve as a control for the PCR assay. **(D)** The *Tcrb*-Tg is expressed in c-Myb deficient thymocytes. Thymocytes from *Myb*$^{w/f}$ and *Myb*$^{f/f}$ *CRT* mice were analyzed by gating through the DN lineage−CD44− gate to examine intracellular expression of TCRβ by flow cytometry. Data are representative of 3 mice.

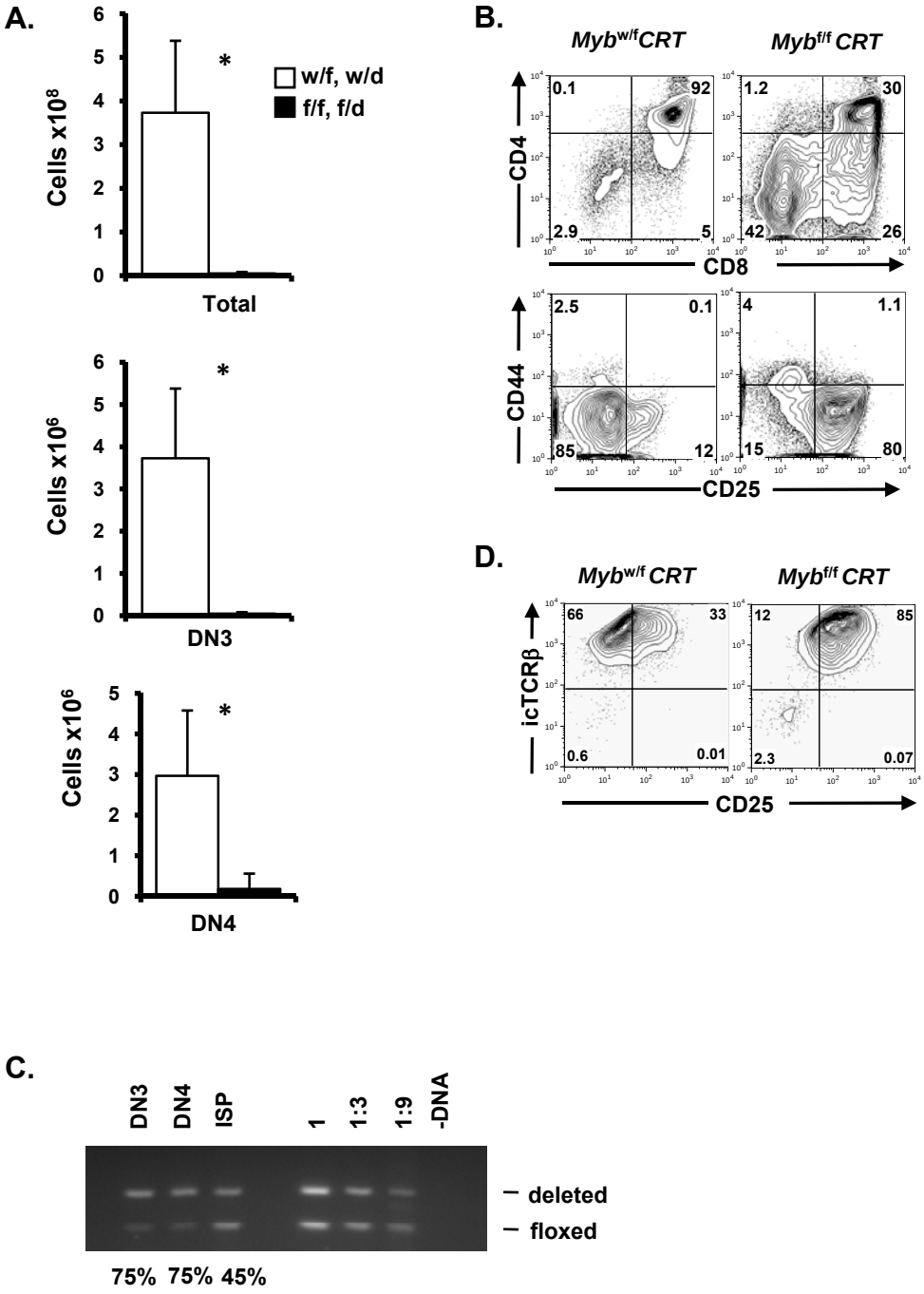
A.
Cells x10^8
w/f, w/d
f/f, f/d
Total
Cells x10^6
DN3
Cells x10^6
DN4
B.
Myb^w/f CRT
Myb^f/f CRT
CD4
CD8
CD44
CD25
D.
Myb^w/f CRT
Myb^f/f CRT
icTCRβ
CD25
C.
DN3
DN4
ISP
1
1:3
1:9
-DNA
deleted
floxed
75% 75% 45%

DN3 thymocytes. In addition, DP thymocytes abnormally express CD25 in *Myb*$^{f/f}$ *C* and *CRT* mice (Figure 12) suggesting that pre-TCR signaling is somewhat impaired. Thus, *Myb*-deficient thymocytes are able to initiate some but not all aspects of pre-TCR signaling.

Injection of Rag-1 or Rag-2-deficient mice with anti-CD3ε antibody is thought to mimic pre-TCR signaling and provides a sufficient signal to drive DN3 thymocytes to proliferate and differentiate to the DP stage [63]. We have previously reported that *Myb*$^{f/f}$ *C* DN3 thymocytes treated with anti-CD3ε differentiated to the DN4 stage [14]. However, because *Myb*$^{f/f}$ *C* mice contain DP cells that produce an αβ-TCR, it was difficult to determine if the DN3 cells proliferated due to the massive amount of cell death caused by crosslinking CD3ε on the DP cells. To further address the outcome of pre-TCR signaling in c-Myb deficient thymocytes, we injected *Myb*$^{f/f}$ *CR* and LMC mice with a single dose of anti-CD3ε monoclonal antibody and examined the distribution of DN thymocytes in the CD25+ DN3 and CD25- DN4 compartments as well as the distribution of total thymocytes in the CD4 and CD8 subsets over a five day time course. One day after anti-CD3ε injection, *Myb*$^{f/f}$ *CR* thymi contained a greater proportion of cells in the CD25- DN4 compartment than controls (Figure 13A). However, from 2 to 5 days after injection, the proportion of cells in the DN3 and DN4 compartments was comparable between *Myb*$^{f/f}$ and *Myb*$^{w/f}$ *CR* mice. In contrast, the percentage of ISP thymocytes in *Myb*$^{f/f}$ *CR* mice was increased 1 day after injection compared to control mice and this increased proportion of ISP thymocytes in *Myb*$^{f/f}$ *CR* thymi was sustained throughout the

Figure 12. Surface marker expression of CD5, CD2, CD27 and CD25. Flow cytometric analysis of CD5, CD2, CD27, and CD25 expression on thymocyte subsets from *Myb*$^{w/f}$ and *Myb*$^{f/f}$ *C* and *CRT* mice. DN3 thymocytes were gated through the DN lineage− gate to examine CD2 and CD5 expression. The DN3 population was further gated on large (DN3L) thymocytes based on size by forward light scatter (FSC) and side light scatter (SSC) flow cytometry as previously described [2] to examine CD27 expression. DN and DP cells were gated through the lineage− gate to examine CD25 expression. CD25+ DN thymocytes were gated to obtain the mean fluorescence intensity (MFI) of the CD25+ population. Data is representative of 5 mice per genotype. ** $p \leq 0.001$ * $p \leq 0.05$

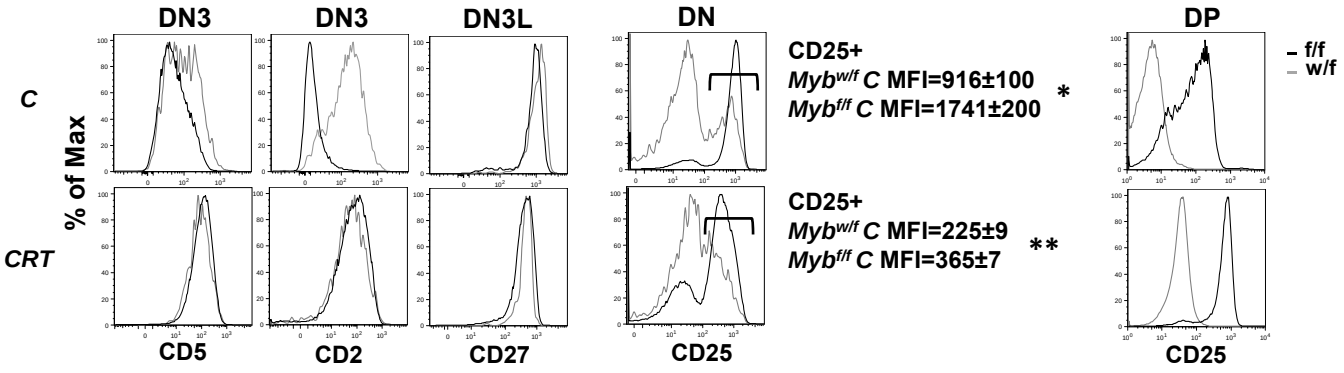
DN3
DN3
DN3L
DN
DP
C
CRT
% of Max
CD5
CD2
CD27
CD25
CD25+
Myb^w/f C MFI=916±100
Myb^f/f C MFI=1741±200
*
CD25+
Myb^w/f C MFI=225±9
Myb^f/f C MFI=365±7
**
CD25
f/f
w/f

time course of the experiment. Three days after injection, both *Myb*$^{f/f}$ *CR* and control mice had a small proportion of cells in the DP compartment. However, by 4 and 5 days after injection the vast majority of cells in control mice were in the DP compartment while only a small proportion of *Myb*$^{f/f}$ *CR* thymocytes were DP. These results demonstrate that *Myb*$^{f/f}$ *CR* DN3 thymocytes can respond to pre-TCR signals to down-regulate CD25 and differentiate. However, c-Myb deficient thymocytes appear to move more quickly from the DN3 to the DN4 and ISP compartments than control thymocytes but fail to efficiently differentiate or accumulate in the DP compartment. Total thymic cellularity did not appreciably increase in *Myb*$^{f/f}$ *CR* thymi in response to anti-CD3ε over the time course of the experiment compared with the large increase in thymic cellularity that takes place in control mice (Figure 13B). The number of c-Myb deficient DN3, DN4 and ISP thymocytes undergoes a minimal increase in number over time. In the first day after injection with anti-CD3ε, we detect a small number of ISP cells in *Myb*$^{f/f}$ *CR* mice but we do not detect any number of ISP from LMC mice, which appears to be due to the accelerated differentiation of *Myb*$^{f/f}$ *CR* DN3 thymocytes to the ISP stage. Importantly, the CD25-DN4 and ISP thymocytes from *Myb*$^{f/f}$ *CR* mice generated at Day 1, 2 and 3 efficiently deleted *Myb* demonstrating that *Myb*-deficient thymocytes respond to β-selection signals to down-regulate CD25 and up-regulate CD8 expression (Figure 13C). Thus, *Myb*-deficient thymocytes receive signals to differentiate but fail to undergo proliferative expansion.

Figure 13. Anti-CD3ε treated *Myb*$^{f/f}$ *CR* DN3 thymocytes respond to signals to down-regulate CD25 and up-regulate CD8 but fail to increase in number. **(A)** Anti-CD3ε treated *Myb*$^{f/f}$ *CR* DN3 thymocytes differentiate at an accelerated rate. *Myb*$^{w/f}$ and *Myb*$^{f/f}$ *CR* mice were injected once with anti-CD3ε and harvested over a period of 5 days. Examination of CD4 and CD8 expression was through the lineage− gate and CD25 expression was analyzed by gating through a DN lineage−CD44− gate. Data is representative of 2-5 experiments for each time point containing at least 2 mice per genotype for each time point. **(B)** The absolute number of Total, DN3, DN4, and ISP thymocytes from *Myb*$^{w/f}$ *CR,* but not *Myb*$^{f/f}$ *CR* mice, increases in response to anti-CD3ε treatment. Absolute cell numbers from one experiment is shown and the trend is representative of data obtained from 2-5 experiments. **(C)** Cre mediated deletion of the loxP targeted *Myb* allele in sorted DN3, DN4 and ISP thymocytes from anti-CD3ε treated *Myb*$^{f/f}$ *CR* mice at Day1, 2, and 3 post injection. *Myb* deletion was analyzed by a PCR assay. Data is representative of 2 independent experiments each containing 2 mice per condition.

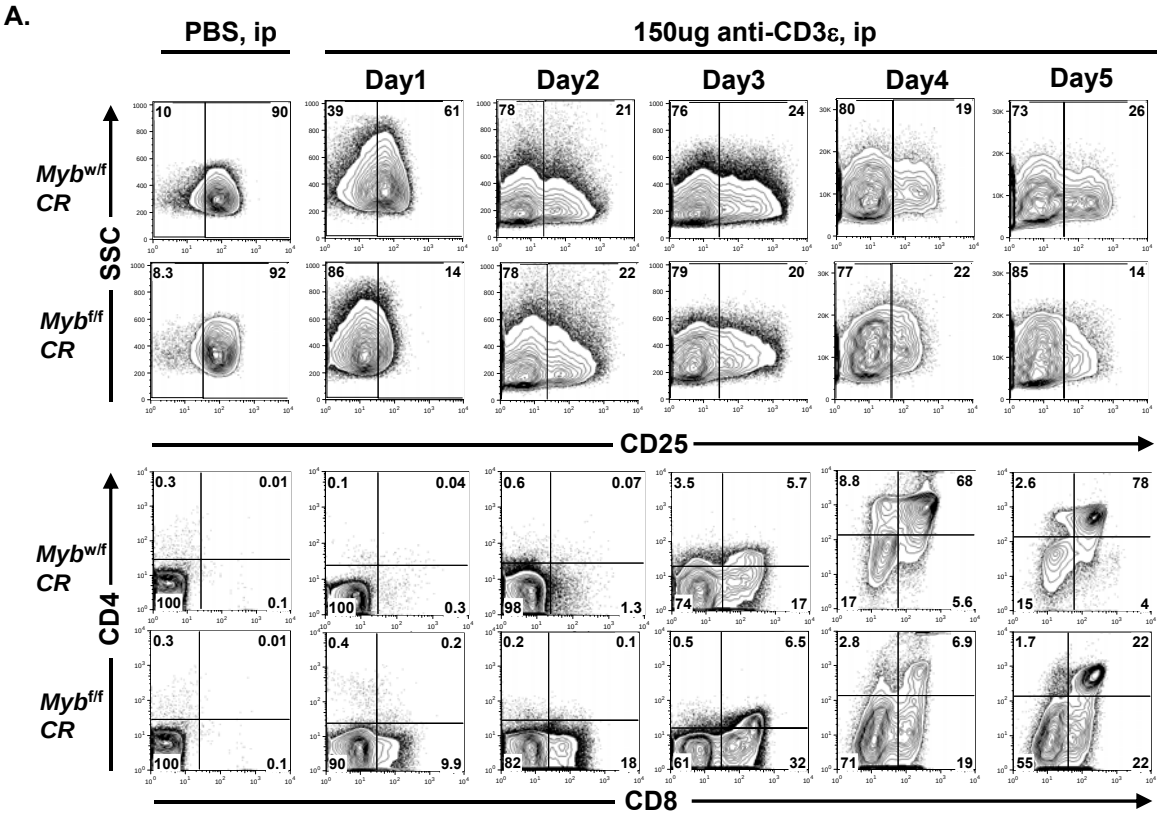
A.
PBS, ip
150ug anti-CD3ε, ip
Day1
Day2
Day3
Day4
Day5
Myb w/f CR
Myb f/f CR
SSC
CD25
CD4
CD8
10
90
39
61
78
21
76
24
80
19
73
26
8.3
92
86
14
78
22
79
20
77
22
85
14
0.3
0.01
100
0.1
0.1
0.04
100
0.3
0.6
0.07
98
1.3
3.5
5.7
74
17
8.8
68
17
5.6
2.6
78
15
4
0.3
0.01
100
0.1
0.4
0.2
90
9.9
0.2
0.1
82
18
0.5
6.5
61
32
2.8
6.9
71
19
1.7
22
55
22

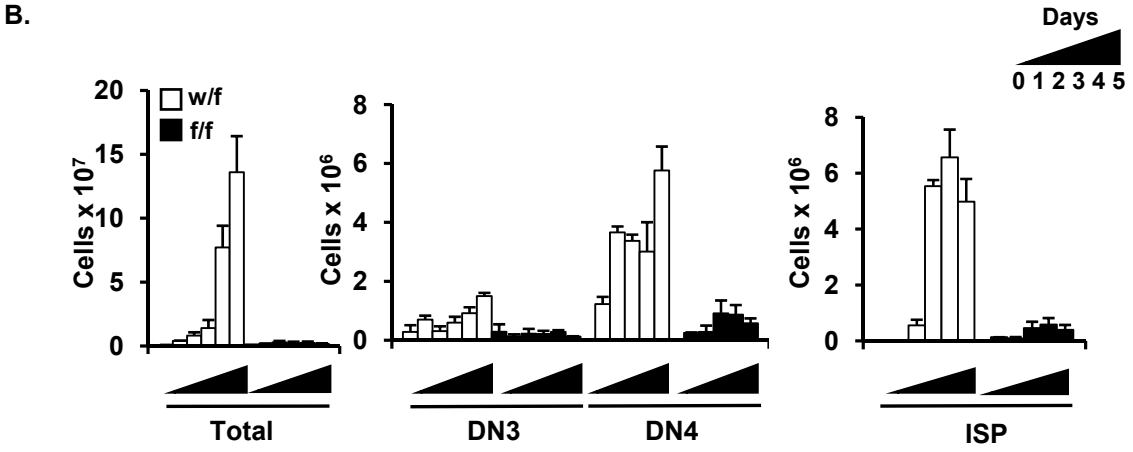
B.
Days
0 1 2 3 4 5
w/f
f/f
Cells x 10^7
Cells x 10^6
Cells x 10^6
Total
DN3
DN4
ISP

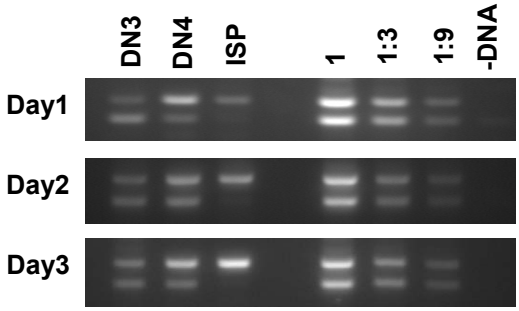
C.
DN3
DN4
ISP
1
1:3
1:9
-DNA
Day1
Day2
Day3

Increased cell death in c-Myb deficient thymocytes during β-selection. *Myb*$^{f/f}$ *CR* DN3 thymocytes treated with anti-CD3ε are able to respond to signals to differentiate to the DN4 stage yet they fail to increase in cell number. This could be due to a failure to proliferate, survive or both. To measure the ability of anti-CD3ε treated thymocytes to proliferate, we examined new DNA synthesis and DNA content by simultaneously measuring BromodeoxyUridine (BrdU) incorporation and DNA content (Figure 14). *Myb*$^{f/f}$ *CR* and control mice treated with anti-CD3ε were injected with BrdU two hours prior to harvest to allow for incorporation of BrdU, a thymidine analog, into the DNA as the cells initiate DNA synthesis during the cell cycle. The amount of BrdU that was incorporated into the DNA was measured by flow cytometry in conjunction with a DNA stain to be able to identify the G1, S and G2/M phases of the cell cycle and to identify cells with <2n DNA content. Interestingly, at Day 1 post anti-CD3ε treatment, the proportion of thymocytes in S phase is similar in *Myb*$^{f/f}$ and LMCs and this remains constant over the time course of the experiment. However, by 2 and 3 days after injection, the proportion of DN4 and ISP thymocytes in S-phase is decreased and the proportion of cells with <2n DNA content is greatly increased in *Myb*$^{f/f}$ *CR* mice compared to controls. This data suggests that anti-CD3ε treated *Myb*$^{f/f}$ *CR* DN3 thymocytes receive signals to proliferate as they initiate β-selection but fail to survive as they differentiate from DN3 to DN4 to ISP thymocytes.

Anti-CD3ε treatment may provide a different stimulus to DN3 thymocytes than signals generated by the pre-TCR during β-selection. DN3 thymocytes that receive

Figure 14. Anti-CD3ε treated *Myb*$^{f/f}$ *CR* DN3 thymocytes respond to signals to proliferate but they fail to survive. Anti-CD3ε treated *Myb*$^{w/f}$ and *Myb*$^{f/f}$ *CR* mice were injected with 150 ug of BrdU 2 hours prior to harvest to examine surface expression of CD4, CD8, CD25, and CD44 and BrdU incorporation in conjunction with 7AAD DNA staining. BrdU incorporation and 7AAD staining are shown for DN3, DN4 and ISP thymocytes at Day 1, 2 and 3 post-treatment with anti-CD3ε. DN3 and DN4 thymocytes were gated through the DN lineage− gate and ISP were gated through a CD4−lineage− gate. Data is representative of 2 independent experiments for each time point containing 2 mice per condition.

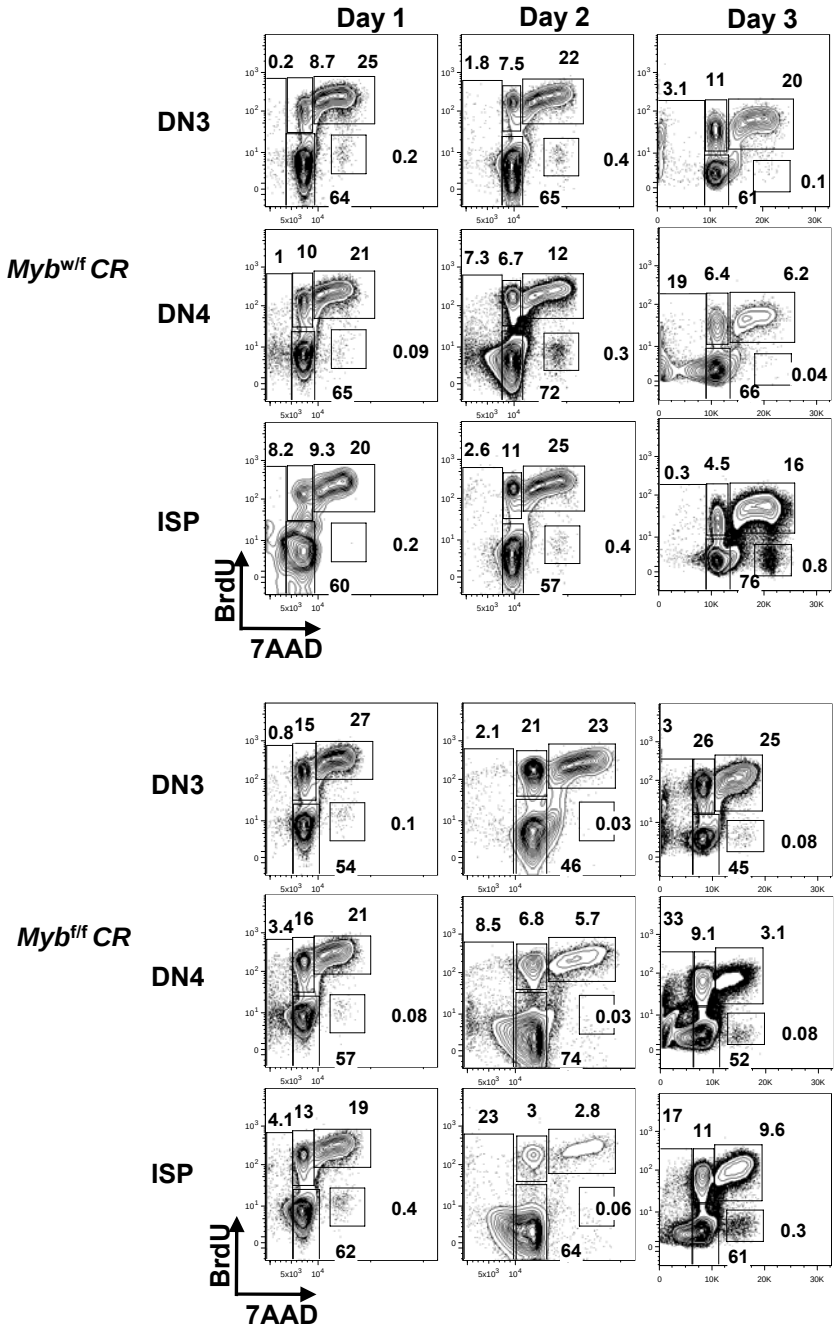
Day 1
Day 2
Day 3
DN3
DN4
ISP
Mybw/f CR
0.2 8.7 25
0.2
64
1.8 7.5 22
0.4
65
3.1 11 20
0.1
61
1 10 21
0.09
65
7.3 6.7 12
0.3
72
19 6.4 6.2
0.04
66
8.2 9.3 20
0.2
60
2.6 11 25
0.4
57
0.3 4.5 16
0.8
76
BrdU
7AAD
Mybf/f CR
0.8 15 27
0.1
54
2.1 21 23
0.03
46
3 26 25
0.08
45
3.4 16 21
0.08
57
8.5 6.8 5.7
0.03
74
33 9.1 3.1
0.08
52
4.1 13 19
0.4
62
23 3 2.8
0.06
64
17 11 9.6
0.3
61
BrdU
7AAD

normal pre-TCR signals to proliferate *in vivo*, increase in cell size and increase DNA content. We measured the size of DN3E, DN3L and DN4 thymocytes in *Myb*$^{f/f}$ *C* and *Myb*$^{f/f}$ *CRT* mice receiving normal pre-TCR signals *in vivo*. Small DN3E and large DN3L thymocytes are of similar size in *Myb*$^{f/f}$ *C* and *Myb*$^{f/f}$ *CRT* mice as compared to LMC (Figure 15A), consistent with the observation that DN3 thymocytes from *Myb*$^{f/f}$ *CRT* mice express surface markers associated with β-selection. However, *Myb*$^{f/f}$ *C* and *Myb*$^{f/f}$ *CRT* DN4 thymocytes are much smaller than control DN4 thymocytes, which is consistent with the notion that the c-Myb deficient DN4 thymocyte population contains a high proportion of dying cells. We then examined new DNA synthesis and DNA content in *Myb*$^{f/f}$ *C* and *Myb*$^{f/f}$ *CRT* directly *ex vivo*. DN3E thymocytes are mostly non-proliferating cells, the majority of which are in the G1 phase in all mice (Figure 15B). The majority of DN3L cells are in S-phase but there is a reduction in the percentage of cells in S-phase in *Myb*$^{f/f}$ *C* and *CRT* mice. Interestingly, *Myb*$^{f/f}$ *C* and *CRT* DN4 and ISP thymocytes have a reduced proportion of cells in S-phase and an increase in the proportion of cells with <2n DNA content compared to controls. Thus, c-Myb deficient DN3L thymocytes receive β-selection signals to increase in size, synthesize new DNA and proliferate but they die as they move into the DN4 and ISP compartments.

Activation of caspase-3 in c-Myb deficient thymocytes. To better understand the cell death and impaired proliferation of thymocytes performing β-selection in the absence of c-Myb, we examined DNA content and new DNA synthesis in thymocytes from *Myb*$^{f/f}$ *C* and control mice on OP9 stromal cells which express the Notch ligand

Figure 15. DN4 and ISP thymocytes fail to proliferate and die. (A) Cell size was compared using FSC flow cytometry in DN3E, DN3L and DN4 thymocytes from *Myb*$^{w/f}$ and *Myb*$^{f/f}$ *C* and *CRT* mice. Data is representative of 10 mice. **(B)** DN4 and ISP thymocytes fail to enter S-phase and have an increase in the proportion of cells with <2n DNA content. *Myb*$^{w/f}$ and *Myb*$^{f/f}$ *C* and *CRT* mice were injected with 150 ug of BrdU and were harvested 2 hours post injection to examine surface expression of CD4, CD8, CD25, and CD44 and BrdU incorporation in conjunction with 7AAD DNA staining. BrdU incorporation and 7AAD staining are shown for DN3E, DN3L, and DN4 thymocytes that were gated through the DN lineage− gate and ISP thymocytes were gated through the lineage− gate. Data is representative of 2 independent experiments each containing 3 mice.

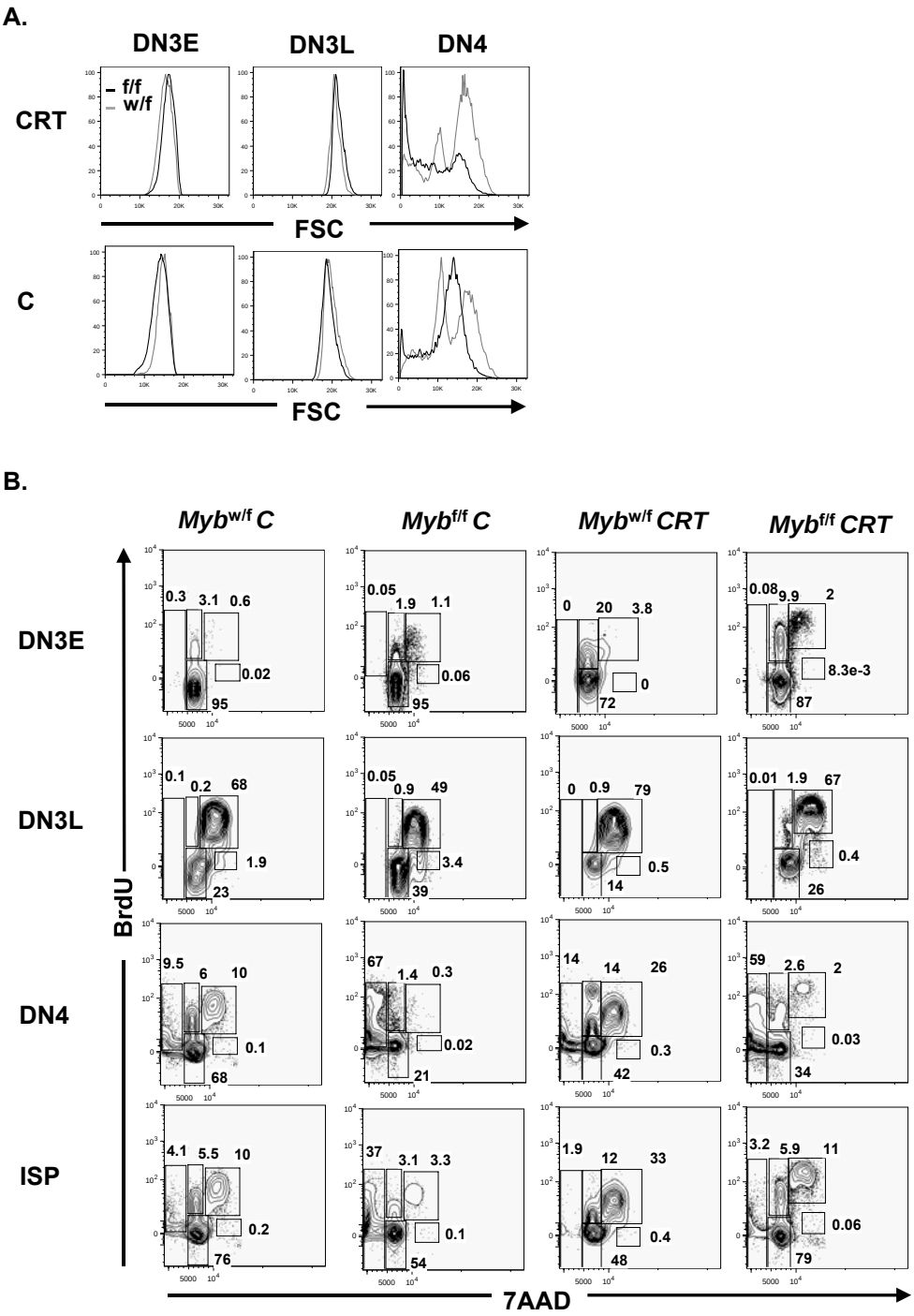
A.
DN3E
DN3L
DN4
CRT
f/f
w/f
FSC
C
FSC
B.
Myb^w/f C
Myb^f/f C
Myb^w/f CRT
Myb^f/f CRT
DN3E
DN3L
DN4
ISP
BrdU
7AAD
0.3 3.1 0.6 0.02 95
0.05 1.9 1.1 0.06 95
0 20 3.8 0 72
0.08 9.9 2 8.3e-3 87
0.1 0.2 68 1.9 23
0.05 0.9 49 3.4 39
0 0.9 79 0.5 14
0.01 1.9 67 0.4 26
9.5 6 10 0.1 68
67 1.4 0.3 0.02 21
14 14 26 0.3 42
59 2.6 2 0.03 34
4.1 5.5 10 0.2 76
37 3.1 3.3 0.1 54
1.9 12 33 0.4 48
3.2 5.9 11 0.06 79

delta-like 1 (DL1) [269]. The OP9-DL1 culture system provides differentiation signals to thymocytes and allows us to examine the cell cycle and <2n DNA content in an environment where dying cells are not readily cleared. We performed one experiment where we plated total thymocytes from *Myb*$^{f/f}$ *C* and *Myb*$^{w/f}$ *C* mice on OP9-DL1 stromal cells for 12 hrs before adding BrdU to the co-cultures for 2 hrs prior to harvest. DN3 thymocytes from the *Myb*$^{f/f}$ *C* mice have a decreased proportion of cells in S-phase and an increased proportion of cells with <2n DNA content as compared to the control (Figure 16). The majority of the <2n population is BrdU-negative suggesting that cells do not enter the DNA replication phase of the cell cycle and then die. This data obtained by examining BrdU incorporation *in vitro* suggests that it is at the DN3 stage where thymocytes are impaired in survival where as the data obtained by examining BrdU incorporation *in vivo* did not detect impaired survival of DN thymocytes until the DN4 stage.

Thymocytes cultured in suspension *in vitro* that lack a pre-TCR like *Rag1*$^{-/-}$ and *Ptcra*$^{-/-}$ activate caspase-3 indicative of apoptotic cell death [86]. To gain insight into the mechanism of cell death in the absence of c-Myb, we examined caspase-3 activation in co-cultures on OP9-DL1 stromal cells containing total thymocytes from *Myb*$^{w/f}$ *CR* and *Myb*$^{f/f}$ *CR* mice or sorted DN3 thymocytes from *Myb*$^{f/f}$ *C* and *Myb*$^{f/f}$ *CRT* and control mice. The percentage of the initial number of cells plated that are recovered from the co-cultures is not statistically different at 18 hrs yet at 34 hrs it is severely reduced in *Myb*$^{f/f}$ *C* and *CRT* thymocytes compared to LMCs but no difference was detected in *CR*

Figure 16. DN3 thymocytes undergoing β-selection *in vitro* fail to enter S-phase and die. Total thymocytes from *Myb*$^{w/f}$ and *Myb*$^{f/f}$ *C* mice were co-cultured on OP9-DL1 cells for 12 hours before a 2 hour pulse with BrdU. Co-cultures were harvested to examine BrdU incorporation in conjunction with 7AAD DNA staining of DN3 and DN4 thymocytes. Thymocytes shown were gated through a Thy1.2+ DN lineage− gate. Data is representative of 2 independent experiments each containing 2 mice.

DN3

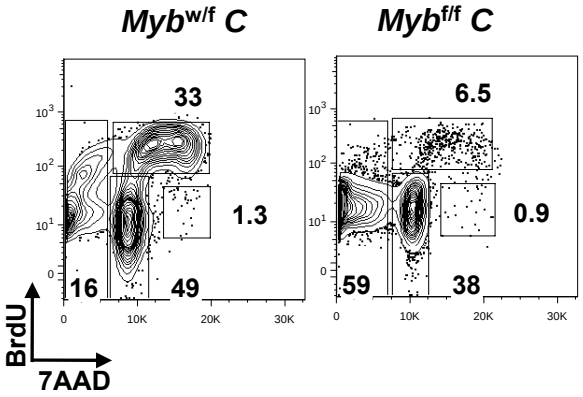

thymocytes (Figure 17A). At 18 and 34 hrs of co-culture, we detected greater caspase-3 activation in CD25+ DN3 thymocytes from *Myb*$^{f/f}$ *C* and *CRT* mice as compared to LMCs correlating with impaired survival of DN3 thymocytes performing β-selection (Figure 17B). The *Myb*$^{w/f}$ *CR* mice that do not express a pre-TCR have greater activation of caspase-3 than *Myb*$^{w/f}$ *C* or *CRT* mice that express a pre-TCR. However, there is no difference in caspase-3 activation between *Myb*$^{f/f}$ *CR* and LMC thymocytes suggesting that impaired survival in the absence of c-Myb occurs upon acquisition of a pre-TCR. Analysis of DNA content at 18 and 34 hrs reveals a reduction in the percentage of cells in G2-M-S phase and an increase in the percentage of cells with <2n DNA content in *Myb*$^{f/f}$ *C* and *CRT* mice as compared to LMCs demonstrating that thymocytes performing β-selection fail to proliferate and die (Figure 17C). However, there is no difference in DNA content between *Myb*$^{f/f}$ *CR* and LMC thymocytes, which is consistent with caspase-3 activation and supports the notion that cell death in c-Myb deficient thymocytes is associated with acquisition of a pre-TCR and events during β-selection.

Caspase-3 activation of DN3 thymocytes was reduced at 18 hrs of co-culture in the presence of the general caspase inhibitor ZVADfmk (Figure 18A). However, we also detected a reduction in cellularity of control thymocytes co-cultured with ZVADfmk after 18 hrs (Figure 18B) due to its ability to inhibit proliferation of DN4 thymocytes (Figure 18C) [288]. However, since ZVAD inhibits proliferation, we are unable to inhibit caspase-3 activation and then measure the ability of thymocytes to proliferate. In addition, we also measured apoptosis by staining cells harvested from the co-cultures

Figure 17. DN3 thymocytes undergoing β-selection *in vitro* activate caspase-3. (A) Sorted DN3 thymocytes from *Myb*$^{w/f}$ and *Myb*$^{f/f}$ *C* and *CRT* or total thymocytes from *CR* mice were co-cultured on OP9-DL1 cells for 18 and 34 hrs. The percentage of Thy1.2+ cells recovered was determined by comparing the number of cells recovered with the number of input cells at 18 and 34 hrs of co-culture and is reduced in *Myb*$^{f/f}$ *C* and *CRT* mice but not in *CR* mice. Data is representative of 3 independent experiments of at least 6 mice per genotype. * $p \leq 0.002$ **(B)** Intracellular caspase-3 activation was measured by flow cytometry at 18 and 34hrs of co-culture. Cells shown were gated through a Thy1.2+CD25+ gate. RCN stands for relative cell number. Data is representative of 3 independent experiments of at least 6 mice per genotype. **(C)** DNA content was measured at 18 and 34hrs of co-culture by Draq5 staining. Cells shown were gated through a Thy1.2+CD25+ gate. Data is representative of 2 independent experiments of at least 2 mice per genotype.

A.

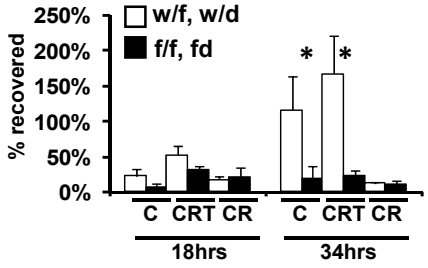
w/f, w/d
f/f, fd
% recovered
250%
200%
150%
100%
50%
0%
*
*
C
CRT
CR
C
CRT
CR
18hrs
34hrs

B.

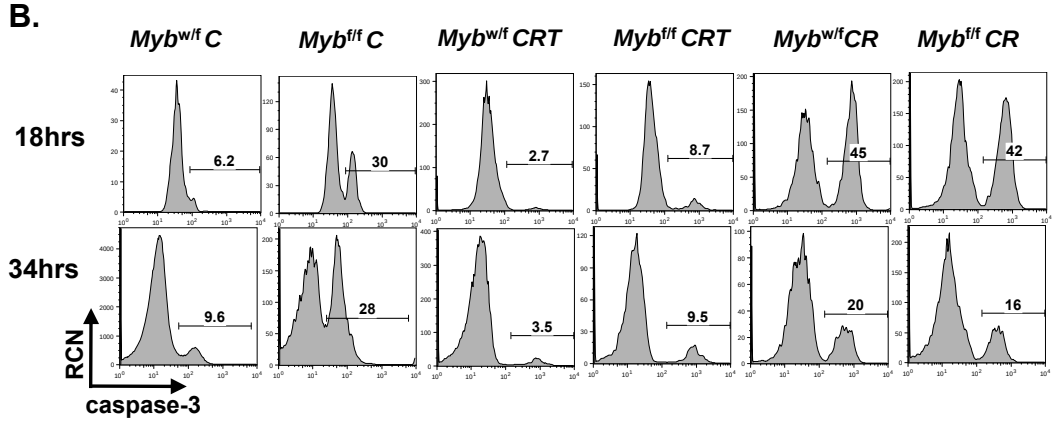
Myb w/f C
Myb f/f C
Myb w/f CRT
Myb f/f CRT
Myb w/f CR
Myb f/f CR
18hrs
34hrs
6.2
30
2.7
8.7
45
42
9.6
28
3.5
9.5
20
16
RCN
caspase-3

C.

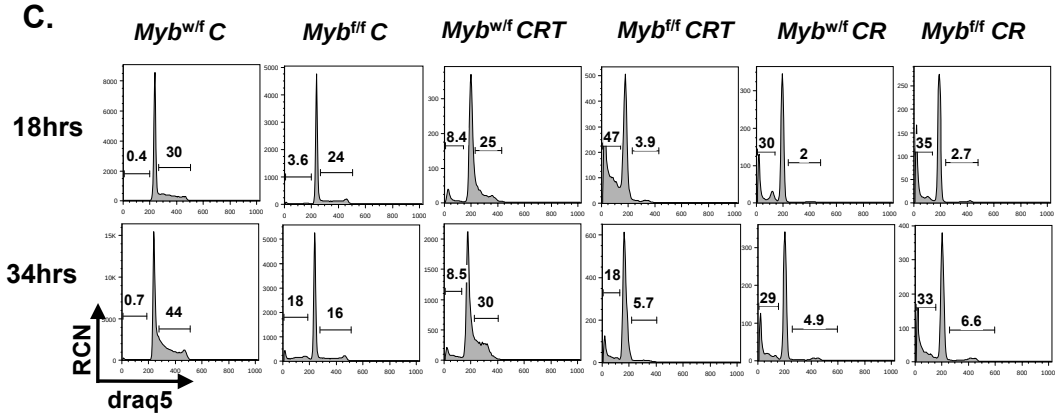
Myb w/f C
Myb f/f C
Myb w/f CRT
Myb f/f CRT
Myb w/f CR
Myb f/f CR
18hrs
34hrs
0.4
30
3.6
24
8.4
25
47
3.9
30
2
35
2.7
0.7
44
18
16
8.5
30
18
5.7
29
4.9
33
6.6
RCN
draq5

Figure 18. ZVADfmk caspase inhibitor suppresses caspase-3 activation but it impairs DN4 proliferation. (A) Sorted DN3 thymocytes from *Myb*$^{w/f}$ and *Myb*$^{f/f}$ *CRT* mice were co-cultured with OP9-DL1 cells with 40 uM of Z-VAD(OMe)fmk for 18 hrs. Intracellular caspase-3 activation was measured by flow cytometry. Cells shown were gated through a Thy1.2+CD25+ gate. Data is representative of 2 independent experiments containing 2 mice. **(B)** The percentage of Thy1.2+ cells recovered was determined by comparing the number of cells recovered with the number of input cells at 18 hrs of co-culture and is reduced in the presence of ZVAD. **(C)** Proliferation of control *Myb*$^{w/f}$ *CRT* DN4 thymocytes is impaired in the presence of ZVAD at 18 hrs. Sorted DN3 thymocytes from *Myb*$^{w/f}$ *CRT* mice were co-cultured with OP9-DL1 cells to examine DNA content by Draq5 staining by flow cytometry. Cells shown were gated through a Thy1.2+CD25+ gate. n=2

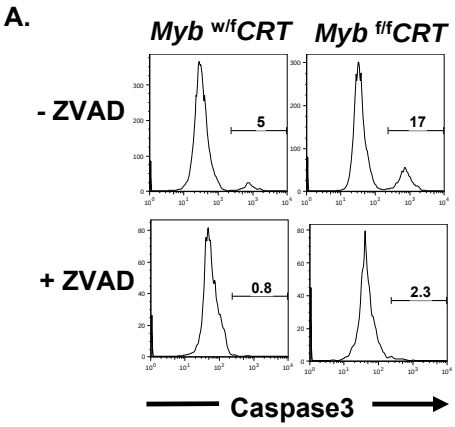
A.
Myb w/fCRT
Myb f/fCRT
- ZVAD
+ ZVAD
5
17
0.8
2.3
Caspase3

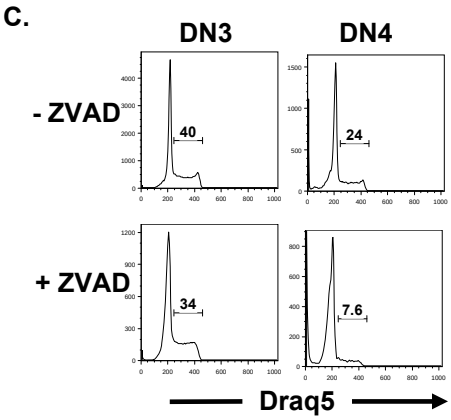
C.
DN3
DN4
- ZVAD
+ ZVAD
40
24
34
7.6
Draq5

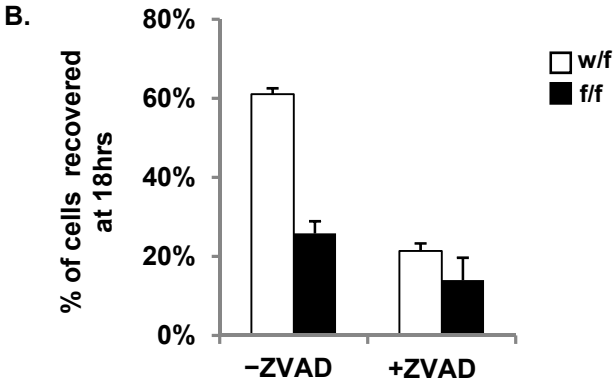
B.
% of cells recovered at 18hrs
80%
60%
40%
20%
0%
−ZVAD
+ZVAD
w/f
f/f

with Annexin V-FITC and 7AAD. Cells in early stages of apoptosis expose the phosphatidylserine (PS) of their plasma membrane which is specifically recognized by Annexin V. 7AAD is a DNA intercalating dye which is not cell permeable and can only enter cells with holes in their membrane as a result of cell death. Apoptotic cells are Annexin V+7AAD− and after 18 hrs of co-culture, we detected an increase in AnnexinV+7AAD− apoptotic DN3 thymocytes and a decrease in Annexin V−7AAD− surviving DN3 thymocytes from co-cultures with *Myb*$^{f/f}$ *C* thymocytes as compared to control (Figure 19). Together this data demonstrates that c-Myb deficient DN3 thymocytes undergo apoptotic death during β-selection.

Notch signaling in c-Myb deficient thymocytes. Notch-DL1 signaling is required to jumpstart β-selection and appears to be required for the continued proliferation but not survival or differentiation of thymocytes during β-selection [12, 32, 115, 122, 123]. Notch-DL1 signaling is able to provide survival signals to *Rag2*$^{-/-}$ DN3E thymocytes in OP9-DL1 co-cultures by regulating glucose metabolism and *Glut1* expression [115, 289]. We determined if thymocytes from *Myb*$^{f/f}$ *CR* mice could respond to Notch1 signals by measuring the survival of *Rag2*$^{-/-}$ DN3E thymocytes co-cultured on OP9-DL1 cells and OP9-control cells [289]. *Myb*$^{f/f}$ *CR* thymocytes responded to the survival advantage provided by OP9-DL1 cells and caspase-3 activation is reduced in thymocytes co-cultured on OP9-DL1 cells as compared to OP9-control cells (Figure 20A). Furthermore, we examined expression of Notch1 transcriptional targets Ptcra and Hes1 in sorted *Myb*$^{f/f}$ *C* DN3 thymocytes and they are expressed in the absence of c-Myb suggesting

Figure 19. *Myb*-deficient DN3 thymocytes undergoing β-selection *in vitro* are AnnexinV+7AAD-. Sorted DN3 thymocytes from *Myb*$^{w/f}$ and *Myb*$^{f/f}$ *C* mice were co-cultured on OP9-DL1 cells and were harvested at 18 hrs to measure apoptosis by examining Annexin V and 7AAD staining. Thy1.2+CD25+ cells are shown. The percentage of apoptotic Thy1.2+CD25+ thymocytes is defined as AnnexinV+7AAD-. Data is representative of 2 independent experiments each containing 2 mice. * $p \leq 0.05$

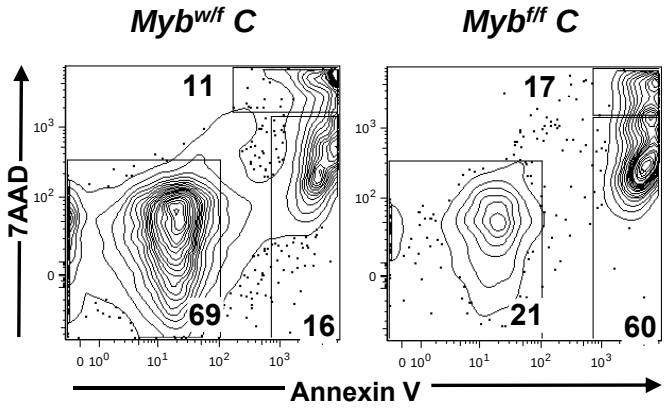
Myb^w/f C
Myb^f/f C
11
69
16
17
21
60
7AAD
Annexin V
0 10^0 10^1 10^2 10^3
10^3
10^2
0

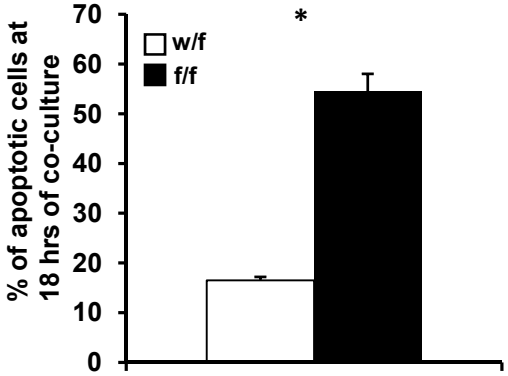
% of apoptotic cells at 18 hrs of co-culture
w/f
f/f
*
70
60
50
40
30
20
10
0

Figure 20. DN3 thymocytes respond to Notch1/DL1 mediated survival signals. (A) Total *Myb*$^{w/f}$ and *Myb*$^{f/f}$ *CR* thymocytes were co-cultured on OP9-DL1 or OP9-control cells for 18 hrs to measure active caspase-3 staining. Thymocytes are gated through a Thy1.2+CD25+ gate. Data is representative of 2 independent experiments each containing 2 mice. **(B)** Semi-quantitative RT-PCR of Notch1 targets, Ptcra and Hes1, and a loading control, Actb, in sorted DN3 thymocytes from *C* mice. Triangles represent concentration of template of 1:3 serial dilutions. Data is representative of 2 independent experiments of 4 mice. **(C)** Sorted DN3 thymocytes from *CRT* mice in co-cultures with OP9-DL1 cells were harvested at 18 hrs. The cells were identified through a Thy1.2+CD25+ gate prior to examining FSC versus SSC to identify DN3E and DN3L cells to measure active caspase-3 staining. Data is representative of 3 independent experiments of 6 mice.

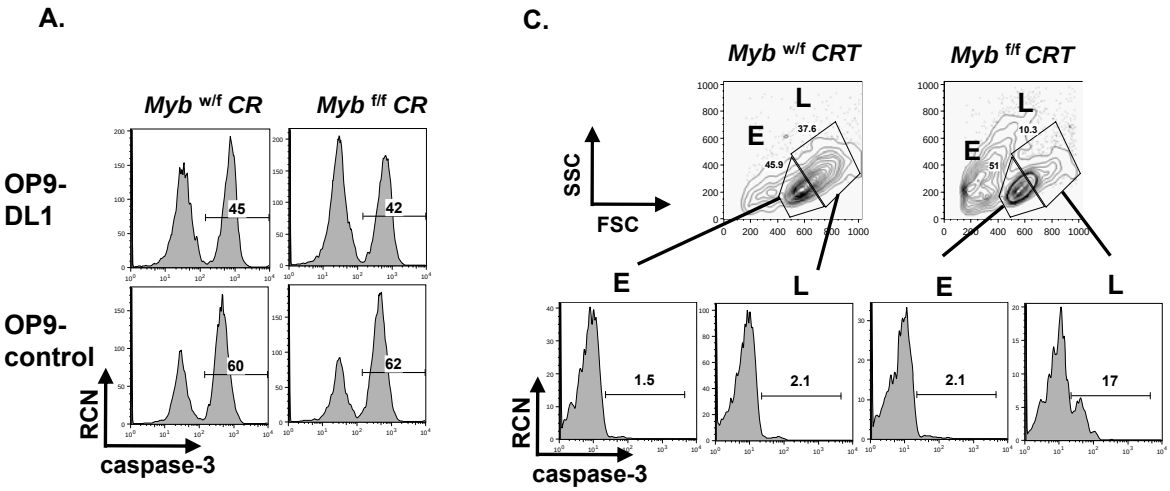
A.
Myb w/f CR
Myb f/f CR
OP9-DL1
OP9-control
45
42
60
62
RCN
caspase-3
C.
Myb w/f CRT
Myb f/f CRT
SSC
FSC
L
E
37.6
45.9
10.3
51
1.5
2.1
2.1
17
RCN
caspase-3

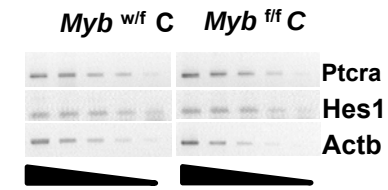
B.
Myb w/f C
Myb f/f C
Ptcra
Hes1
Actb

that c-Myb deficient thymocytes respond to Notch1 signaling (Figure 20B). As DN3E thymocytes respond to β-selection signals they increase in size to become DN3L cells and are able to differentiate to the DP stage without Notch-DL1 interaction [122]. The proportion of DN3L thymocytes is reduced in *Myb*$^{f/f}$ *CRT* mice (Figure 20C). Compared to LMC, *Myb*-deficient DN3L thymocytes activate caspase-3 whereas DN3E thymocytes do not (Figure 20C). Since Notch-DL1 interaction is required for the survival of DN3E thymocytes and does not appear to be required for the survival of DN3L thymocytes [122], our data suggests that *Myb*$^{f/f}$ DN3E thymocytes survive and respond to Notch survival signals whereas *Myb*$^{f/f}$ DN3L thymocytes die independently of Notch signaling.

Death of c-Myb deficient pre-TCR+ thymocytes is independent of p53 and Bcl2.

A major function of the pre-TCR is to suppress cell death during the process of β-selection [50]. However, little is actually understood about mechanisms that suppress or enforce cell death downstream of the pre-TCR but the balance of pro-apoptotic and anti-apoptotic Bcl-2 family members appears to play a significant role during β-selection [86, 95, 103, 104]. In particular, repression of Bid and Bim expression has recently been reported to be important for survival during β-selection [95] and Bcl2A1 expression is increased during β-selection [86]. To gain further insight into the survival defect in DN3 thymocytes performing β-selection, we tested if crossing our *Myb*$^{f/f}$ *C* mice onto a *p53*$^{-/-}$ background (*Myb*$^{f/f}$ *cwlckCre p53*$^{-/-}$ *(PC))* could rescue the block in DN3 differentiation. p53 mediates apoptosis of pre-TCR^{-} thymocytes by inducing expression of pro-apoptotic molecule Bid [95] and introduction of a p53 deficiency in pre-TCR^{-} thymocytes allowed

for the generation of some DP thymocytes [53, 107-110]. In addition, we also crossed our *Myb*$^{f/f}$ *C* mice to mice expressing a *Bcl-2*-Tg+ (*Myb*$^{f/f}$ *cwlckCre Bcl-2-Tg+ (BC))* to test if expression of a pro-survival Bcl2 family member could rescue apoptosis. Bcl2 is involved in survival of early DN thymocytes prior to the generation of a pre-TCR [101, 290, 291]. Bcl-2 protein expression is reduced in IL-7 deficient mice and DN thymocytes undergo apoptosis but addition of rIL-7 induced Bcl-2 expression in DN thymocytes from IL-7 deficient mice *in vitro* [290]. Moreover, expression of a Bcl2-Transgene in IL7-deficient mice can rescue thymopoiesis [101]. However, there is no direct evidence from Bcl2 knockout mice that Bcl-2 is required for survival of DN thymocytes [98]. Bcl2 has previously been proposed to be a transcriptional target of c-Myb [232-235] but, we did not detect a decrease in Bcl-2 protein expression in DN3 or DN4 thymocytes from *Myb*$^{f/f}$ *C* and *CRT* mice as compared to LMCs (Figure 21). However, we hypothesized that over-expression of a pro-survival Bcl-2 family member may enhance survival if there is an over-expression of a pro-apoptotic Bcl-2 family member or a reduced expression of a pro-survival Bcl-2 family member in the absence of c-Myb. In *Myb*-deficient thymocytes, expression of a Bcl2-Tg and loss of p53 did not rescue thymic cellularity (Figure 22A). The absolute number of Total, DN3 and DN4 thymocytes from *Myb*$^{f/f}$ *BC* and *Myb*$^{f/f}$ *PC* mice is not increased as compared to *Myb*$^{f/f}$ *C* mice demonstrating that gain of a Bcl2-transgene and loss of p53 did not rescue cellularity in the absence of c-Myb (Figure 22A). In addition, differentiation remains blocked at the DN3 stage (Figure 22B). Thus, c-Myb appears to be required for survival of DN3 thymocytes during β-selection independent of p53 and Bcl2.

Figure 21. Intracellular expression of Bcl2 is not decreased in DN3 and DN4 thymocytes. Flow cytometric analysis of intracellular Bcl2 protein expression in DN3 and DN4 thymocytes from *Myb*$^{w/f}$ and *Myb*$^{f/f}$ *C* and *CRT* mice. DN3 and DN4 thymocytes were gated through the DN lineage− gate to examine Bcl2 expression. FMO represents a stain that did not include Bcl2-FITC. Data is representative of 2 mice per genotype.

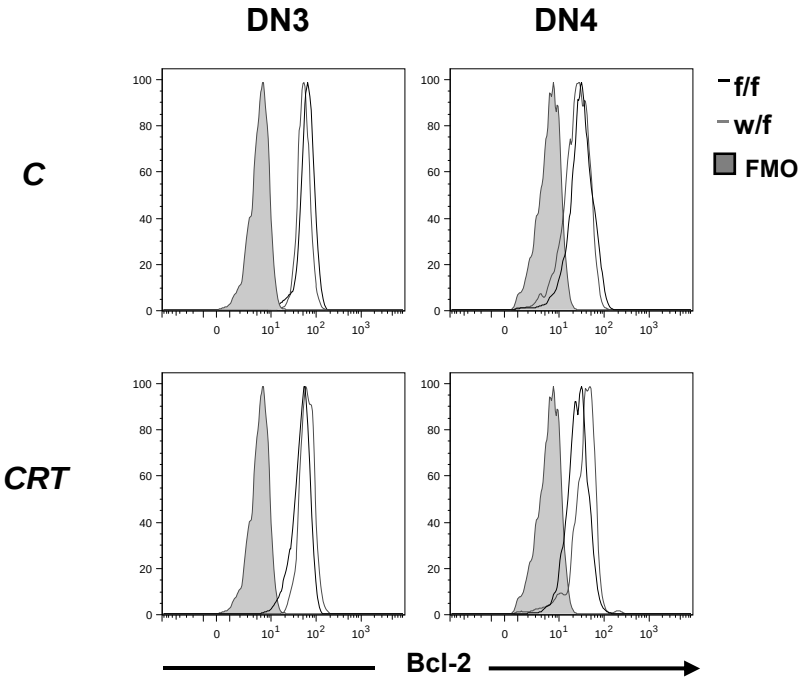
DN3
DN4
C
CRT
f/f
w/f
FMO
Bcl-2

Figure 22. Loss of p53 or gain of a Bcl2-transgene does not rescue thymic cellularity or DN3 differentiation. (A) The absolute number of Total, DN3 and DN4 thymocytes from *Myb$^{f/f}$ cwlckCre Bcl2-Tg+ (BC*) or from *Myb$^{f/f}$ cwlckCre p53-/- (PC)* mice is still severely reduced as compared to *Myb$^{f/f}$ C* mice. Data is representative of 3 independent experiments of at least 5 mice per genotype. * p≤0.01 **(B)** Flow cytometric analysis of different thymocyte populations from *Myb$^{w/f}$* and *Myb$^{f/f}$ BC* and *PC* mice reveal a block in DN3 differentiation in the absence of c-Myb. Thymocytes were gated through the DN lineage− gate to examine CD25 and CD44 expression. Data is representative of 3 independent experiments of at least 5 mice per genotype.

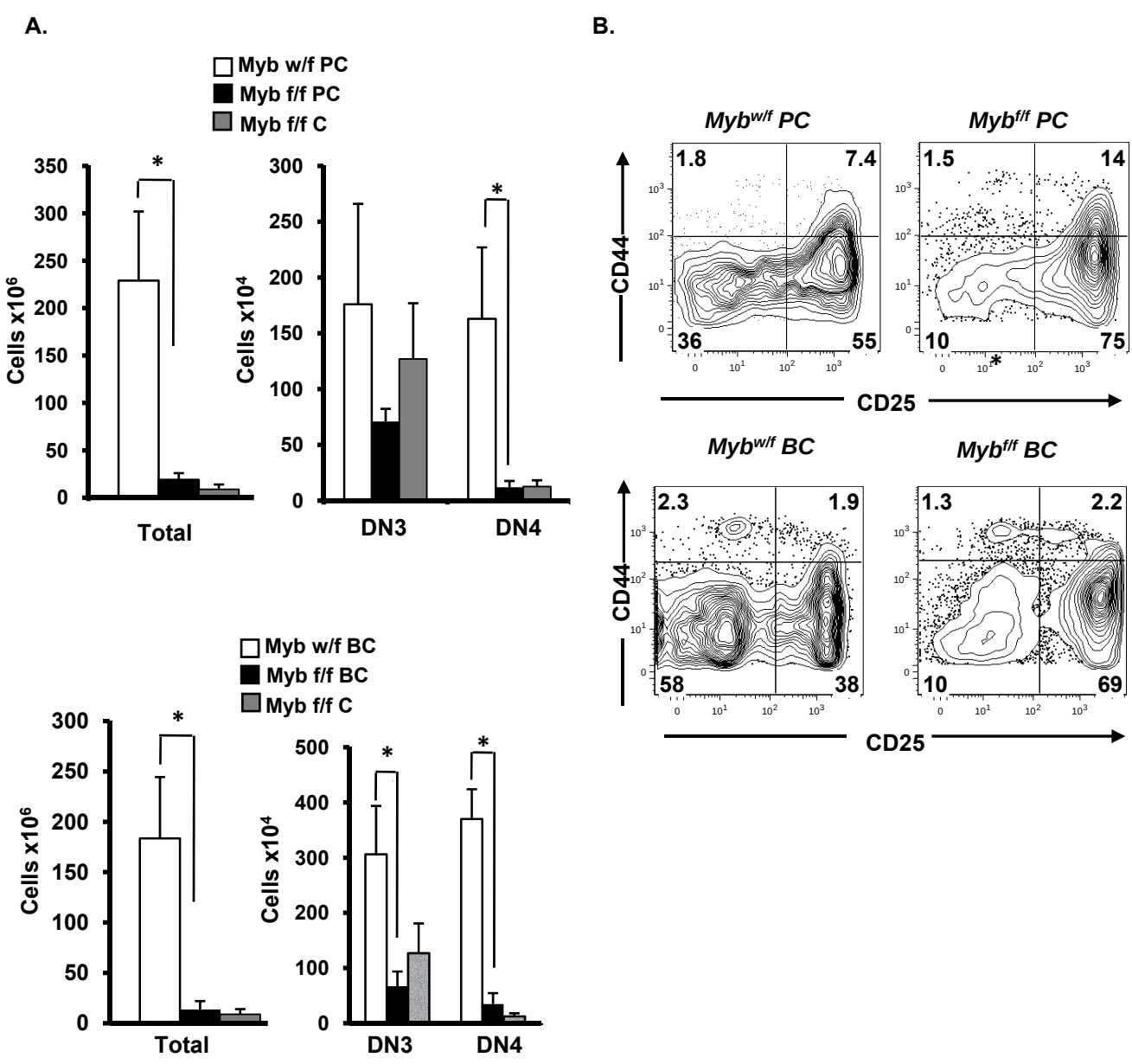
A.
Myb w/f PC
Myb f/f PC
Myb f/f C
Cells x10^6
Total
Cells x10^4
DN3
DN4
Myb w/f BC
Myb f/f BC
Myb f/f C
B.
Myb^w/f PC
Myb^f/f PC
CD44
CD25
1.8
7.4
36
55
1.5
14
10
75
Myb^w/f BC
Myb^f/f BC
2.3
1.9
58
38
1.3
2.2
10
69

Since expression of pro-survival Bcl2 family member Bcl2 is unable to rescue survival, we also examined expression of Bcl2a1 since it is up-regulated in response to pre-TCR signaling and exogenous expression of Bcl2a1 can rescue survival of *Rag1*$^{-/-}$ thymocytes [86]. We performed three independent experiments to address Bcl2a1 expression (Figure 23). First we examined expression in sorted DN3 and DN4 subsets from *Myb*$^{f/f}$ CRT and control mice (Figure 23 Experiment 1). Second, we examined expression in thymocytes from *Myb*$^{f/f}$ *CR* and *Myb*$^{w/f}$ *CR* mice treated with anti-CD3ε in two independent experiments (Figure 23 Experiment 2A and 2B). In Experiment 1, expression of Bcl2a1 is increased in DN4 thymocytes as compared to DN3 thymocytes from control *Myb*$^{w/f}$ *CRT*. Interestingly, expression of Bcl2a1 is greatly increased in DN4 thymocytes in *Myb*$^{f/f}$ *CRT* mice as compared to LMC. It is possible that Bcl2a1 is increased in DN4 thymocytes from *Myb*$^{f/f}$ *CRT* mice in an attempt to survive. In Experiment 2A, Bcl2a1 expression is increased in anti-CD3ε treated control *Myb*$^{w/f}$ CR thymocytes, which was previously reported to occur in the literature [86], whereas in Experiment 2B expression of Bcl2a1 is not increased in anti-CD3ε treated control *Myb*$^{w/f}$ *CR* thymocytes. Interestingly, examination of CD25 expression as a positive control since CD25 decreases as DN3 thymocytes differentiate to the DN4 stage demonstrates that CD25 expression decreases in anti-CD3e treated *Myb*$^{w/f}$ thymocytes in both Experiment 2A and 2B. While we do not understand why Bcl2a1 expression did not increase in response to anti-CD3ε treatment in Experiment 2B, what we can conclude from these experiments is that expression of Bcl2a1 in DN4 thymocytes or anti-CD3ε treated

Figure 23. Expression of Bcl2a1 is not decreased in the absence of c-Myb. Expression of Bcl2a1 and CD25 by quantitative real-time RT-PCR (qPCR) in three separate experiments. In Experiment 1, DN3 and DN4 thymocytes from 2-3 pooled *Myb*$^{w/f}$ and 3-5 pooled *Myb*$^{f/f}$ mice were electronically sorted prior to RNA isolation. Experiment 2A and 2B were two separate experiments where CR mice were treated with anti-CD3ε for 0 and 24 hours prior to RNA isolation. RNA was isolated from sorted cell subsets and reverse transcribed to generate cDNA. Real-time PCR was performed in duplicate wells for each gene and relative expression was normalized according to expression of the GAPDH gene.

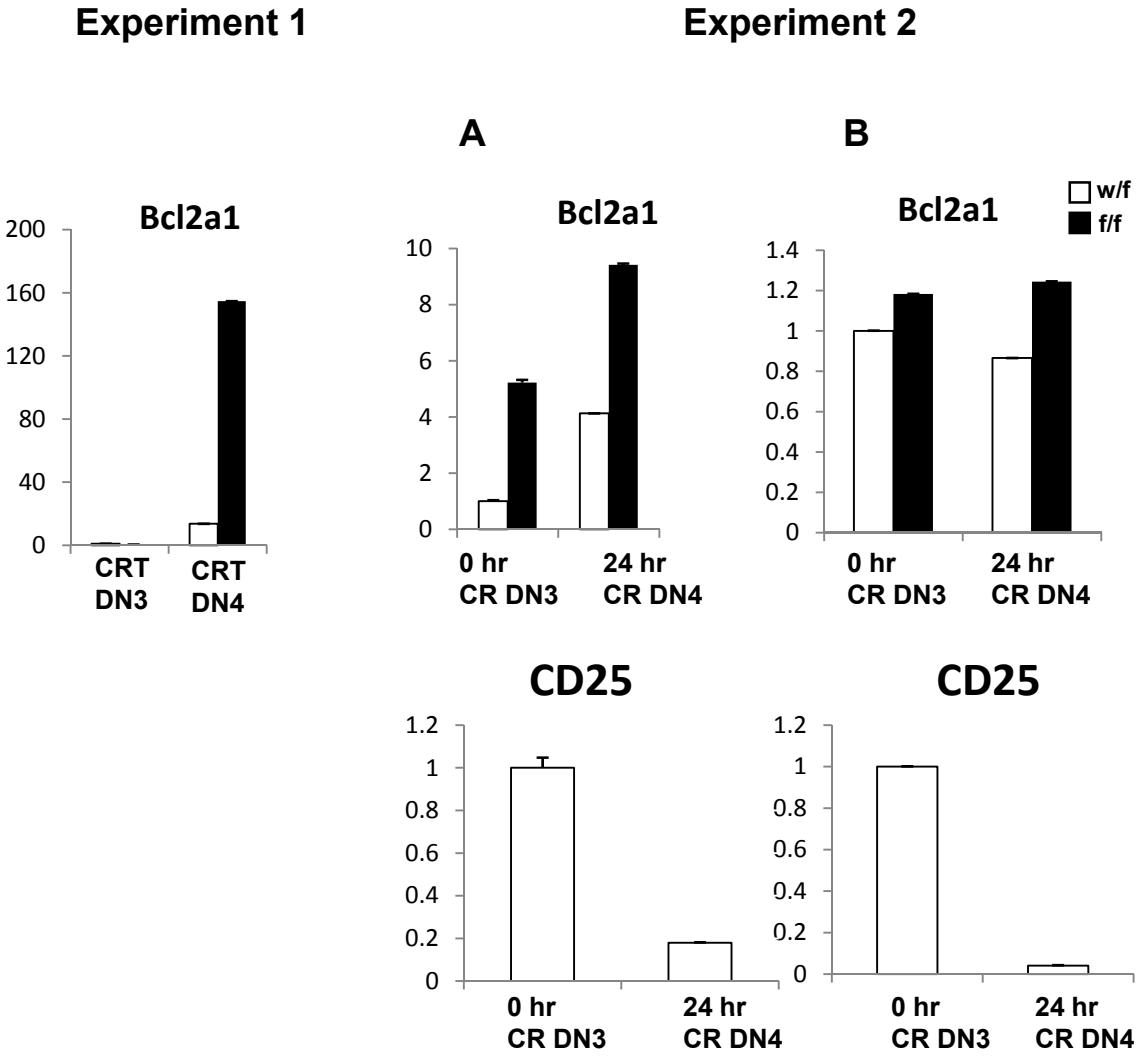
Experiment 1
Experiment 2
A
B
Bcl2a1
200
160
120
80
40
0
CRT DN3
CRT DN4
Bcl2a1
10
8
6
4
2
0
0 hr CR DN3
24 hr CR DN4
Bcl2a1
w/f
f/f
1.4
1.2
1
0.8
0.6
0.4
0.2
0
0 hr CR DN3
24 hr CR DN4
CD25
1.2
1
0.8
0.6
0.4
0.2
0
0 hr CR DN3
24 hr CR DN4
CD25
1.2
1
0.8
0.6
0.4
0.2
0
0 hr CR DN3
24 hr CR DN4

thymocytes is not decreased in the absence of c-Myb. This suggests that Bcl2a1 expression is not compromised in *Myb*-deficient thymocytes undergoing β-selection.

Myb-deficient DN3 thymocytes fail to induce expression of cyclin D3 protein during β-selection. The impaired proliferative expansion that we detect in c-Myb deficient thymocytes that initiate β-selection is either a direct result of massive cell death or the cells do not receive signals to enter the cell cycle, or both. To understand the basis for the impaired proliferative expansion of c-Myb deficient thymocytes that initiate β-selection, we examined events and the expression of proteins that regulate entry from G0 into the G1 phase of the cell cycle. It has been previously reported that DN3L and DN4 thymocytes undergoing β-selection receive signals to enter G1 and hyperphosphorylate Rb [2]. Since we detect few DN4 thymocytes in thymi from $Myb^{f/f}$ *CRT* mice, we measured the phosphorylation status of Rb in sorted DN3 and ISP thymocytes from *CRT* mice (Figure 24A). However, Rb remains hypophosphorylated in DN3 and ISP thymocytes from $Myb^{f/f}$ *CRT* mice. D cyclins contribute to the hyperphosphorylation of Rb and cyclin D3 is required for the proliferative expansion of DN4 and ISP thymocytes [1]. We examined cyclin D3 protein expression and found it severely reduced in DN3 and ISP thymocytes from $Myb^{f/f}$ *CRT* mice as compared to LMC mice (Figure 24B). It has been reported that anti-CD3ε treatment of $Rag2^{-/-}$ mice induced expression of cyclin D3 protein [1] and we readily detect up-regulation of cyclin D3 protein in control mice at 12, 24 and 48 hrs post anti-CD3ε treatment (Figure 24C). However, expression of cyclin D3 is minimally induced in thymocytes from $Myb^{f/f}$

Figure 24. Cyclin D3 protein levels are reduced in DN3 and ISP thymocytes. (A) Thymocytes undergoing β-selection fail to hyperphosphorylate Rb. Western blot analysis of Rb phosphorylation in sorted DN3 and ISP thymocytes from *Myb*$^{w/f}$ and *Myb*$^{f/f}$ *CRT* mice. Data is representative of 3 independent experiments of 3-5 pooled mice for each experiment. **(B)** DN3 and ISP thymocytes do not express cyclin D3 protein. Western blot analysis of cyclin D3 expression in sorted DN3 and ISP thymocytes from *CRT* mice. Blots were stripped and reprobed for ERK1/2. The percentage of reduction in cyclin D3 expression, as determined by densitometry of multiple gels, is listed below the gel picture. Data is representative of 4 independent experiments of 3-5 pooled mice for each experiment. **(C)** Protein expression of cyclin D3 is not induced in response to anti-CD3ε treatment. Western blot analysis of cyclin D3 expression in total thymocytes from *CR* mice treated with anti-CD3ε for 0, 12, 24, or 48 hrs. Blots were stripped and reprobed for β-actin. Data is representative of 4 independent experiments. **(D)** Semi-quantitative RT-PCR of ccnd3 and Actb on RNA from sorted DN3 thymocytes from *Myb*$^{w/f}$ and *Myb*$^{f/f}$ *CRT* mice. Triangles represent concentration of template of 1:3 serial dilutions. Data is representative of 2 independent experiments of at least 4 mice. **(E)** Semi-quantitative RT-PCR of ccnd3 and Actb on RNA from thymocytes from *Myb*$^{w/f}$ and *Myb*$^{f/f}$ *CR* mice that were treated with anti-CD3ε for 0, 12, 24, or 48 hrs. Triangles represent concentration of template of 1:3 serial dilutions. Data is representative of 2 independent experiments of at least 3 mice per timepoint.

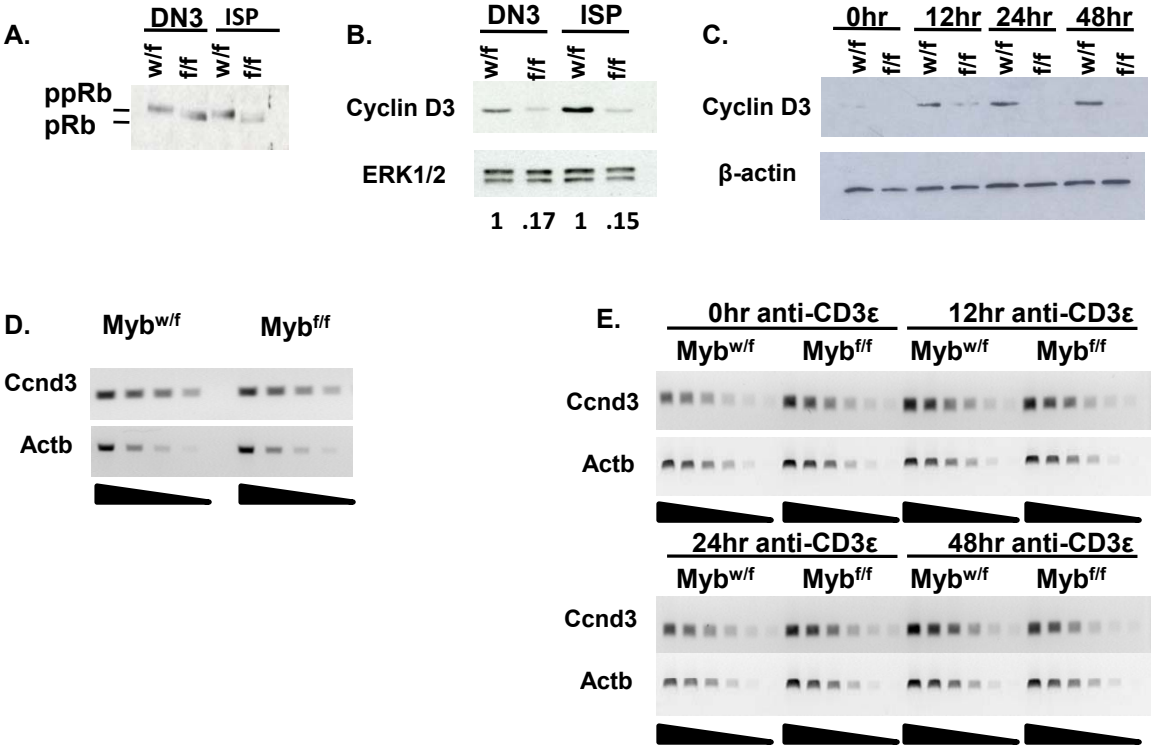
A.
DN3
ISP
w/f
f/f
w/f
f/f
ppRb
pRb
B.
DN3
ISP
w/f
f/f
w/f
f/f
Cyclin D3
ERK1/2
1 .17 1 .15
C.
0hr
12hr
24hr
48hr
w/f
f/f
w/f
f/f
w/f
f/f
w/f
f/f
Cyclin D3
β-actin
D.
Myb^w/f
Myb^f/f
Ccnd3
Actb
E.
0hr anti-CD3ε
12hr anti-CD3ε
Myb^w/f
Myb^f/f
Myb^w/f
Myb^f/f
Ccnd3
Actb
24hr anti-CD3ε
48hr anti-CD3ε
Myb^w/f
Myb^f/f
Myb^w/f
Myb^f/f
Ccnd3
Actb

CR mice 12, 24, and 48 hrs after injection of anti-CD3ε antibody. We detect little difference in the amount of *ccnd3* mRNA detected in DN3 thymocytes from *Myb*$^{f/f}$ *CRT* mice compared to controls as measured by semi-quantitative RT-PCR (Figure 24D). Similarly, we detected little difference in *ccnd3* mRNA in the anti-CD3ε stimulated *Myb*$^{f/f}$ *CR* thymocytes by RT-PCR compared to controls (Figure 24E). Together this data demonstrates that β-selecting thymocytes fail to up-regulate cyclin D3 protein but not *ccnd3* mRNA in the absence of c-Myb.

We also performed one experiment to measure expression of cell cycle components involved in regulation of the G1 phase of the cell cycle such as cyclin dependent kinase 2 (cdk2), 4, and 6 and the cdk-inhibitor p27 in addition to measuring expression of cyclins induced during later phases of the cell cycle to confirm that thymocytes do not receive signals to enter the cell cycle. In *Myb*$^{f/f}$ *CRT* mice, cyclin D3 expression is dramatically decreased and cyclin B1, A and E are also decreased most likely due to the fact that thymocytes do not enter the cell cycle to induce expression of cyclin E later in the G1 phase or cyclin A and cyclin B1 in the G2/S/M phases (Figure 25). During the G1 phase, cyclin D3 forms a complex with either cdk4 or cdk6, and cdk2 forms a complex with cyclin E to phosphorylate Rb. In *Myb*$^{f/f}$ *CRT* DN3 thymocytes, expression of cdk2 is not changed. However, expression of cdk4 is slightly decreased and expression of cdk6 is slightly increased. However, *Cdk4/Cdk2*-null mice contain normal numbers of DN, DP and SP thymocytes [292] suggesting that a reduction in cdk4 does not explain a proliferation defect in *Myb*$^{f/f}$ *CRT* DN3 thymocytes. p27 inhibits all

Figure 25. Expression of cyclins, cdks and the cdk-inhibitor p27 indicate that DN3 thymocytes do not receive signals to enter the cell cycle. DN3 thymocytes from *Myb*$^{f/f}$ *CRT* mice have decreased expression of cyclin D3, cyclin B1, cyclin A, cyclin E and cdk4 and enhanced expression of cdk6 and p27 as compared to the LMC. Western blot analysis of protein expression in sorted DN3 thymocytes. Densitometry of the blots is represented as the percentage of change in protein expression. Data is representative of 1 experiment of thymocyte subsets pooled from 2-5 mice.

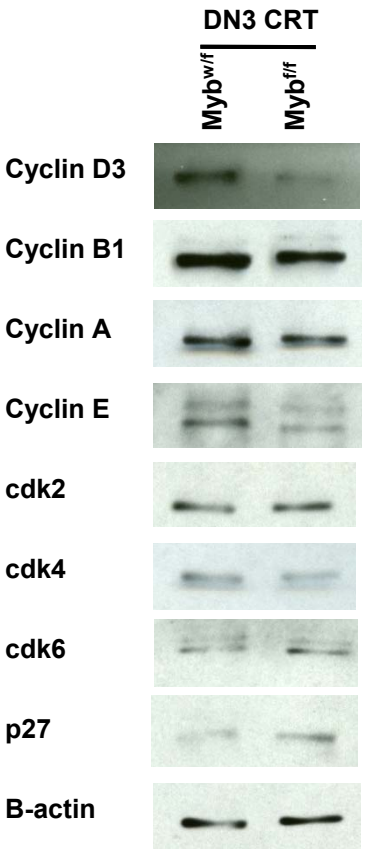
DN3 CRT
Myb^w/f
Myb^f/f
Cyclin D3
Cyclin B1
Cyclin A
Cyclin E
cdk2
cdk4
cdk6
p27
B-actin

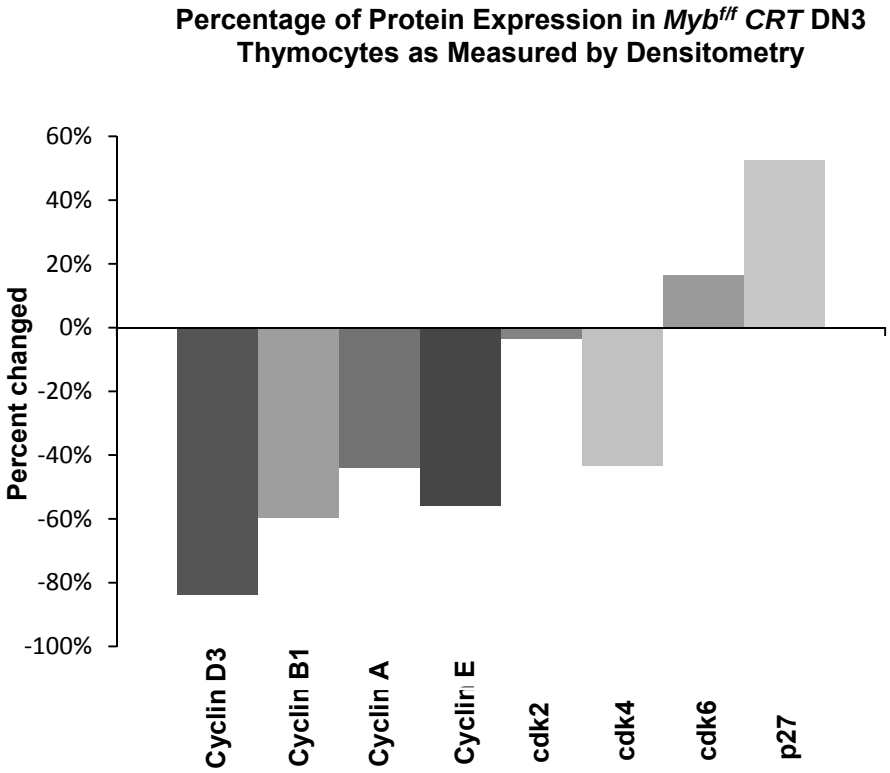
Percentage of Protein Expression in Myb^f/f CRT DN3 Thymocytes as Measured by Densitometry
Percent changed
60%
40%
20%
0%
-20%
-40%
-60%
-80%
-100%
Cyclin D3
Cyclin B1
Cyclin A
Cyclin E
cdk2
cdk4
cdk6
p27

cyclin:cdk complexes with the exception of complexes containing D cyclins [10]. Expression of p27 protein decreases as cells transit from the DN3E to DN3L stage suggesting that the pre-TCR signaling regulates p27 expression to enable thymocytes to proliferate [2]. According to this experiment, expression of p27 is slightly increased in *Myb*$^{f/f}$ *CRT* DN3 thymocytes as compared to LMCs. It is likely that p27 levels are increased since thymocytes fail to receive signals to enter the cell cycle to decrease expression of p27. Together this data suggests that *Myb*$^{f/f}$ *CRT* thymocytes fail to receive signals to enter the cell cycle and undergo apoptosis during β-selection.

Discussion

We have previously reported that tissue specific inactivation of the *Myb* locus in DN2/DN3 thymocytes results in a strong block during differentiation beyond the DN3 stage concomitant with inefficient V(D)J recombination at the *Tcrb* locus [14]. The block in DN3 to DN4 differentiation in *Myb*$^{f/f}$ *C* mice could be explained by defective V(D)J recombination, poor survival of c-Myb deficient DN3 thymocytes or both. *Myb*$^{f/f}$ *CR* thymi did not differ in total cellularity or distribution of DN3 and DN4 subsets as compared to control *Rag2*$^{-/-}$ mice demonstrating that c-Myb is not required for the maintenance of DN3 thymocytes that lack a pre-TCR. Since c-Myb does not appear to be required for maintenance of the DN3 compartment in *Rag2*-deficient thymocytes, defective V(D)J recombination in the *Myb*$^{f/f}$ *C* mice is not simply a consequence of poor

survival and the inability to complete V(D)J recombination in DN3E thymocytes. Furthermore, *Rag2*-deficient thymocytes provided with a *Tcrb*-Tg are able to efficiently differentiate to the DP stage [268]. However, thymocytes from *Myb*$^{f/f}$ *CRT* mice fail to efficiently differentiate beyond the DN3 stage, demonstrating that c-Myb is required for normal β-selection independent of the impairment in V(D)J recombination.

The pre-TCR provides signals during β-selection that initiate events including survival, proliferation, allelic exclusion at the *Tcrb* locus, down-regulation of CD25 to become a DN4 thymocyte and differentiation to the DP stage [40, 42, 55, 280]. We present evidence that c-Myb deficient thymocytes can initiate some events associated with pre-TCR signaling including the up-regulation of surface markers associated with the onset of β-selection including CD5, CD2 and CD27. In addition, anti-CD3ε treatment of *Rag2*$^{-/-}$ mice induces differentiation beyond the DN3 stage including down-regulation of CD25 and up-regulation of CD8 and proliferative expansion [63]. *Myb*$^{f/f}$ *CR* mice are able to respond to anti-CD3ε treatment to down-regulate CD25 and differentiate to the ISP and DP stages of thymocyte differentiation. However, the differentiation of c-Myb deficient DN3 thymocytes appears to be accelerated and they fail to undergo proliferative expansion and die in the absence of c-Myb. It is possible that the accelerated differentiation prevents thymocytes from staying in the DN4 and ISP stages to receive signals to survive and/or proliferate. Thus, the inability of *Myb*-deficient thymocytes to generate a DP compartment is not due to a failure to receive signals to differentiate rather it is due, at least in part, to a failure to survive and proliferate.

c-Myb-deficient DN3 thymocytes that initiate β-selection signaling activate caspase-3 and undergo apoptosis. Mechanisms that mediate survival and suppress apoptosis during β-selection are not well understood. Evidence suggests that the balance of pro-apoptotic and anti-apoptotic Bcl2 family members is important for survival during β-selection [53, 95, 107-110]. Recent studies demonstrate that expression of pro-apoptotic Bcl2 family members Bid and Bim are decreased and expression of pro-survival Bcl2 family member Bcl2a1 is increased in response to pre-TCR signaling [86, 95]. However, we did not detect a decrease in expression of Bcl2a1 mRNA or an increase in expression of Bim in the absence of c-Myb. Expression of Bid is controlled by p53, however, breeding a *p53* null allele onto the $Myb^{f/f}$ C background did not rescue differentiation or thymic cellularity, suggesting that the survival defect in pre-TCR+ thymocytes is not due to a failure to down-regulate p53 or Bid. Interestingly, we detected increased expression of Bcl2a1 mRNA in $Myb^{f/f}$ *CRT* DN4 thymocytes and in anti-CD3ε treated $Myb^{f/f}$ *CR* thymocytes as compared to LMC suggesting that thymocytes may over-express Bcl2a1 in an attempt to rescue survival. Furthermore, we were unable to rescue differentiation and cellularity of $Myb^{f/f}$ *C* DN3 thymocytes with expression of a *Bcl2* transgene which further supports the notion that over-expression of a pro-survival Bcl2 family member is unable to rescue survival of c-Myb-deficient thymocytes. Taken together our data suggests that *Myb*-deficient thymocytes death is independent of altered expression of the Bcl2 family members currently thought to be important for survival during β-selection.

c-Myb-deficient DN3 thymocytes appear to be able to proliferate and enter S-phase but the proportion of DN4 thymocytes in S-phase is reduced and thymocytes undergo apoptosis. In DN4 thymocytes the <2n DNA content is BrdU-negative which suggests that cells do not enter the cell cycle, initiate DNA synthesis and then die, rather they die at the G0/G1 phase. This suggested that perhaps DN4 thymocytes are not receiving signals to enter the cell cycle. We hypothesized that if DN4 thymocytes only had a defect in survival then thymocytes would be cycling and we would detect a BrdU+ <2n DNA population of thymocytes as well. Cyclin D2 is expressed in DN3 thymocytes but is downregulated during β-selection while cyclin D3 expression is induced in response to pre-TCR signaling [1]. However, c-Myb-deficient thymocytes fail to up-regulate cyclin D3 protein in response to pre-TCR signals demonstrating that thymocytes fail to continue proliferating in response to pre-TCR signals. The phenotype of *ccnd3*$^{-/-}$ thymocytes is very similar to *Myb*$^{f/f}$ *C* and *CRT* thymocytes. *Ccnd3*$^{-/-}$ but not *ccnd2*$^{-/-}$ or *ccnd1*$^{-/-}$ mice contain thymi with severely reduced numbers of total and DP thymocytes due to a reduced proportion of DN4 and ISP cells in S-phase while DN3 thymocytes from *ccnd3*$^{-/-}$ mice do not have a decrease in the proportion of cells in S-phase [1, 90]. Since cyclin D2 is expressed in DN3 thymocytes, it may mediate the initial rounds of proliferation of DN3 thymocytes performing β-selection. As DN3 thymocytes differentiate to the DN4 stage cyclin D3 is necessary for efficient entry into S-phase and the proliferation phenotype of DN3 and DN4 thymocytes from *ccnd3*$^{-/-}$ mice correlates with *Myb*$^{f/f}$ *C* and *CRT* mice. Thus, it appears that c-Myb-deficient thymocytes are

unable to perform the transition to dependency on cyclin D3 protein for continued proliferation during β-selection.

Interestingly, the ability of *ccnd3*$^{-/-}$ thymocytes to survive was not addressed and it is possible that the decrease in thymic cellularity in *ccnd3*$^{-/-}$ mice is also due to impaired survival [293]. In addition, *Rag2*$^{-/-}$*ccnd3*$^{-/-}$ mice, like *Myb*$^{f/f}$ *CR* mice, do not increase thymocyte cellularity in response to treatment with anti-CD3ε [1]. However, they did not address if anti-CD3ε treated *Rag2*$^{-/-}$*ccnd3*$^{-/-}$ mice enter S-phase. Based on the requirement for cyclin D3 in DN4 thymocytes but not in DN3 thymocytes and that DN3 thymocytes enter S-phase in the absence of cyclin D3, we would predict that the anti-CD3ε treated *Rag2*$^{-/-}$*ccnd3*$^{-/-}$ DN3 thymocytes initially enter S-phase and proliferate which is what we detect in anti-CD3ε treated *Myb*$^{f/f}$ *CR* mice. However, proliferation in anti-CD3ε treated *Rag2*$^{-/-}$*ccnd3*$^{-/-}$ would decrease as DN3 thymocytes differentiate to DN4 thymocytes which also correlates with the phenotype we detect in anti-CD3ε treated *Myb*$^{f/f}$ *CR* mice. However, despite the fact that DN3 thymocytes proliferate without cyclin D3, thymic cellularity does not increase in anti-CD3ε treated *Rag2*$^{-/-}$*ccnd3*$^{-/-}$ mice supporting the notion that perhaps cell survival is also impaired in the absence of cyclin D3. There is also evidence that cyclin D3 is involved in survival of lymphocytes [1, 294-298]. In peripheral T cell lines, retroviral expression of cyclin-D3 prevented apoptosis induced by phorbol myristate acetate and TCR activation [294]. In addition, reducing cyclin D3 expression through siRNA treatment resulted in cell cycle arrest at the G1 phase and an increase in apoptosis of a myeloma cell line [296]. Interestingly, a

gene expression microarray analysis reported that expression of cyclin D3 in hepatocytes activated transcription of genes involved in cell cycle and cell death pathways [297]. Thus, there is evidence that cyclin D3 is involved in survival supporting the notion that it is possible that a reduction in cyclin D3 in thymocytes performing β-selection may not only cause a reduction in proliferation but in survival as well. β-selection proliferation is also regulated by cdk inhibitors which negatively regulate the cell cycle by inactivating the kinase of the cyclin/cdk complex. The cdk inhibitors p15, p16, and p17 inhibit cyclin D/cdk complexes and p27 and p21 inhibit all other cyclin/cdk complexes [10]. Expression of a $p16^{Ink4\alpha}$ transgene or a $p27^{Kip1}$ transgene in thymocytes blocked differentiation at the DN3 stage [91, 92]. We performed one experiment where we detected an increase in p27 levels in DN3 thymocytes in the absence of c-Myb. However, cdk inhibitors work by inactivating the kinase of the cyclin/cdk complex and do not function by targeting the cyclin for proteosomal degradation. Therefore, an increase in expression of a cdk inhibitor is probably not the cause for the defective cyclin D3 protein expression but is rather an effect of cells not entering the cell cycle.

Expression of cyclin D3 by pre-TCR signaling has been reported to be controlled at the level of transcription [1]. Using RT-PCR, we did not detect an increase in *ccnd3* mRNA in anti-CD3ε treated *Rag2*$^{-/-}$ thymocytes. We also did not detect an increase in expression of *ccnd3* between control DN3 and DN3 *Tcrb*-Tg+ thymocyte subsets according to a gene expression microarray yet we do detect cyclin D3 protein in DN3 *Tcrb*-Tg+ thymocytes and it is in these cells that we detect a decrease in cyclin D3

protein expression in the absence of c-Myb. Expression of *ccnd3* mRNA does not appear to be altered in the absence of c-Myb according to RT-PCR and gene expression microarray analysis performed on control and *Myb*$^{f/f}$ *C* DN3 and DN3 Tcrb-Tg+ thymocyte subsets. Interestingly, previous studies that expressed a dominant negative *Myb* allele in DN thymocytes reported a decrease in expression of cyclin D3, cyclin B1 and cyclin A2 in pooled DN3 and DN4 thymocytes according to an RNase protection assay [265]. However, they defined DN3 and DN4 thymocytes as CD25+ and CD25- thymocytes without gating out CD4/8 expressing cells and we have demonstrated here that c-Myb-deficient DP thymocytes express CD25. DP thymocytes express low levels of cyclin D3 [1] so it appears that the decrease in cyclin D3 expression may only be a reflection of examining expression in two different populations of cells. Expression of cyclin D3 protein is controlled at the level of translation as well as by post-translational signals [299, 300]. Expression of cyclin D3 protein is controlled at the level of translation as well as by post-translational signals [299, 300]. During B-cell development, cyclin D3 protein is stabilized concurrent with pre-BCR signaling demonstrating that translational and post-translational events to control cyclin D3 expression [295]. It is possible that translational or post-translational events occur during β-selection to control cyclin D3 expression that are controlled by c-Myb. Interestingly, thymocyte/stromal cell interactions have also been reported to be involved in regulating cyclin D3 expression. [301]. In peripheral T cells, integrin-dependent spreading is required for cyclin D3 protein expression in response to IL-2 mitogenic stimulation [302]. Perhaps in addition

to the pre-TCR, additional interactions with the microenvironment are also required for cyclin D3 expression and are dependent on c-Myb.

We have demonstrated that c-Myb plays multiple roles during differentiation of DN3 thymocytes (Figure 26). Interestingly, we have identified that these roles are complex and change as the thymocytes differentiate from DN3E to DN3L to DN4 to ISP thymocytes suggesting that these roles are probably mediated by multiple transcriptional targets of c-Myb. DN3E thymocytes do not require c-Myb for survival, but we have provided evidence that c-Myb is required for V(D)J recombination of the *Tcrb* locus. We were able to prove our hypotheses that c-Myb is directly required during the process of V(D)J recombination and that c-Myb is also required for survival during β-selection. Surprisingly, we also discovered that c-Myb is required for proliferation and cyclin D3 expression during β-selection as well which is interesting since c-Myb is not required for proliferation of peripheral B cells [264]. The timing of the impaired survival and proliferation is different when thymocytes are freshly harvested as compared to thymocytes that have been cultured in vitro. Data obtained from freshly isolated thymocytes detected severely impaired survival and proliferation of DN4 thymocytes but not DN3 thymocytes. However, data obtained from thymocytes cultured in vitro detected impaired survival and proliferation of DN3L thymocytes. It is not clear how c-Myb mediates survival during β-selection since survival of *Myb*-deficient thymocytes appears to be independent of expression of the Bcl2 family members currently thought to be important for survival during β-selection. Moreover, it appears that cyclin D3 is

Figure 26. c-Myb roles during differentiation of DN3 thymocytes. Events that are independent of c-Myb during differentiation of DN3E thymocytes to the DN3L, DN4 and ISP stages are listed above the cell subsets. Events that depend on c-Myb during differentiation of DN3E thymocytes to the DN3L, DN4 and ISP stages are listed below the cell subsets.

c-Myb independent:

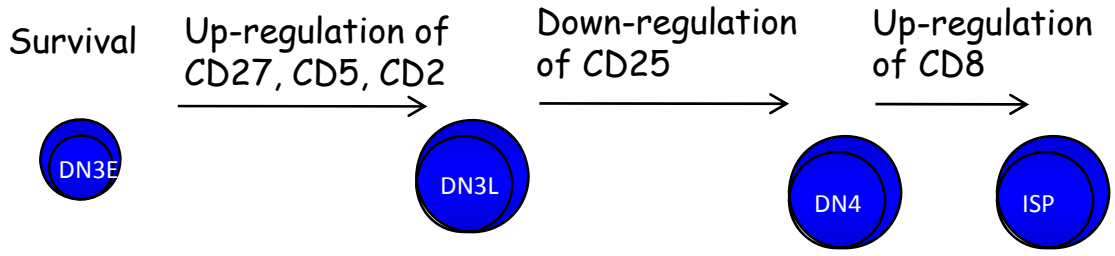

c-Myb dependent:

V(D)J recombination of *Tcrb* locus

Anti-CD3ε mediated differentiation

Survival independent of p53 and Bcl2

Proliferation

Expression of Cyclin D3 protein

Entry into the Cell Cycle

not a transcriptional target of c-Myb since we did not detect altered expression of cyclin D3 mRNA so it is unclear how c-Myb mediates cyclin D3 expression. In addition, it is not clear if thymocytes deficient for cyclin D3 also undergo apoptosis so we do not know if the inability to express cyclin D3 contributes to or is the cause of apoptosis in *Myb*-deficient thymocytes. Now that we have clearly identified the β-selection events that require c-Myb, it is crucial to identify the downstream mediators of c-Myb activity.

Chapter IV. Gene Expression Microarray Analysis on c-Myb Deficient Thymocytes

Introduction

c-Myb is a DNA binding transcription factor that can act as a transcriptional activator or repressor [134-136]. During early thymocyte development, c-Myb is required for β-selection induced survival and proliferation (Chapter III). To gain insight into how c-Myb regulates proliferation and survival it is crucial to identify downstream mediators of c-Myb activity. However, few direct c-Myb transcriptional targets have been defined. Furthermore, few potential c-Myb targets have been tested as mediators of c-Myb activity in physiologically relevant models. Potential c-Myb targets were first identified by scanning promoters for putative Myb binding sites and then testing the ability of exogenously expressed c-Myb to activate these promoters in transient co-transfection assays in cells that normally express low levels of c-Myb [138, 253]. A second approach to identify potential Myb targets used adenoviruses to express each Myb family member in the MCF7 human tumor mammary epithelial cell line and then examine changes in gene expression with gene chip microarrays [154]. Importantly, the microarray chip study also demonstrated that the ability of Myb proteins to activate promoter-reporter gene constructs varied greatly from their ability to activate endogenous genes bringing into question the list of potential Myb target promoters identified with reporter construct assays [154]. Finally, a dominant interfering Myb allele, which is not able to discriminate between Myb family members, was expressed in

leukemic cell lines to identify potential Myb targets by subtractive DNA cloning [245, 254-256]. However, very few of the potential c-Myb targets were tested as mediators of c-Myb activity.

Together, these approaches have identified potential transcriptional targets of c-Myb in T cells that include *Ptcra* [231], *Bcl2* [232-235], *Ada* (Adenosine deaminase) [236, 237], *H2A.Z* (H2A histone Z) [238], *c-Myc* [236, 239-242], *Mat2a* (Methionine adenyl-transferase II, alpha) [236, 243, 244], *Gata-3* [245], *Rag-2* [168, 169, 246], *c-kit* [247-249], *CD4* [245, 250, 251], and *ccnb1* [252]. However, Ptcra, CD4 and Rag-2 are expressed in *Myb*-deficient thymocytes [14, 245]. In addition, recent studies using chromatin immunoprecipitation (ChIP) and gene silencing through c-Myb siRNA to validate potential c-Myb targets, identified c-Myb binding to cis elements of *c-Myc, MAT2A* and *ADA* and not to *Ptcra* and *Ela2* in leukemic cell lines [236]. Interestingly, expression of c-Myb siRNA in these cell lines reduced expression of *c-Myc* and *ADA* but not *MAT2A* demonstrating that c-Myb is important for maintaining expression of ADA and c-Myc but not MAT2A [236]. This list of potential c-Myb transcriptional targets does not explain the impaired survival and proliferation of *Myb*-deficient thymocytes performing β-selection. To begin to identify potential transcriptional targets that regulate survival and proliferation of thymocytes we performed gene expression microarray analysis on several DN thymocyte subsets from $Myb^{f/f}$ *C* and control mice. The $Myb^{f/f}$ *C* mice provide the opportunity to identify global changes in gene expression

across multiple stages of thymopoiesis as well as test potential c-Myb targets in a physiologically relevant model.

Results

Identification of potential c-Myb target genes using cDNA microarrays. Since there are few well characterized c-Myb target promoters and none of the known c-Myb regulated genes provide insight into how c-Myb promotes survival and proliferative expansion during β-selection, we carried out gene chip microarray experiments to compare gene expression between c-Myb deficient and c-Myb sufficient DN thymocytes. We compared gene expression between c-Myb deficient and control thymocytes from three DN subsets. First, we examined gene expression in DN3 thymocytes from *Myb*$^{w/f}$ *cwlckCre Rag2*$^{-/-}$ *Tcrb-Tg+* and *Myb*$^{f/f}$ *cwlckCre Rag2*$^{-/-}$ *Tcrb-Tg+* mice. We initially chose the *Tcrb*-Tg+ DN3 thymocytes to perform the microarray experiments since these mice express a TCRβ chain, were primed to perform β-selection, and were most like wildtype DN4 thymocytes since they expressed markers consistant with cells undergoing β-selection (Chapter III). However, Cre expressed under the proximal lck promoter is detectable in DN2 thymocytes and it is possible that the defects we detect at the β-selection checkpoint could be the result of altered gene expression in DN2 or DN3 thymocytes. Therefore, we also performed gene expression microarrays on DN2 and DN3 thymocytes from *Myb*$^{w/f}$ *cwlckCre* and *Myb*$^{f/f}$ *cwlckCre*

mice. DN2 (Lin-CD4-CD8-CD3-CD117+CD44+CD25+) and DN3 (Lin-CD4-CD8-CD3-CD117-CD44-CD25+) thymocytes were electronically sorted from each mouse and RNA was isolated from each sample. However, since there are very few DN2 (~200,000) and DN3 (~3,500,000) thymocytes per mouse we amplified the RNA prior to making fluorescent labeled cRNA probes. The amplified RNA was sent to the Gene Chip Analysis Core Facility at the University of Virginia for cRNA synthesis, hybridization to Mouse Genome 430 2.0 Affymetrix arrays and data acquisition.

Quality control and statistical analysis was performed by the Bekiranov laboratory by first determining the relative RNA abundance from all of the arrays by quantile normalizing which involves normalizing the signals to a synthetic chip using GCRMA (GC Robust Multi-array Average) [276, 277]. The CEL files were processed using the Affymetrix MAS5 algorithm to obtain presence/absence calls for each array. All possible pairwise comparisons between control and c-Myb deficient DN2, DN3 and DN3 Tcrb-Tg+ samples were performed. Probe sets were eliminated if there was a majority of absence calls made in both pairwise samples being compared indicating a strong likelihood that the transcript could not be detected in either sample. T-tests were performed on the log transformed values to estimate p-values for every probe. These p-values were used to estimate the false discovery rate (FDR) for every probe set [278]. Gene lists of differentially expressed genes were generated by applying a 20% FDR cutoff and requiring the estimated fold change to be greater than 1.1 and a corrected p value of 0.05. In DN3 *Tcrb*-Tg+ thymocytes, expression of 130 genes was increased in the

absence of c-Myb; representing potential c-Myb-activated genes and expression of 209 genes was decreased in the absence of c-Myb, representing potential c-Myb-repressed genes (Appendix Table VI). In DN3 thymocytes, expression of 51 genes was increased in the absence of c-Myb and expression of 82 genes was decreased in the absence of c-Myb (Appendix Table VII) and in DN2 thymocytes, expression of 15 genes was increased in the absence of c-Myb and expression of 182 genes was decreased in the absence of c-Myb (Appendix Table VIII). The DN2, DN3 and DN3 *Tcrb*-Tg+ arrays suggest changes in expression of genes involved in metabolic processes, cell cycle, intracellular signal transduction, protein modification, cell adhesion, and apoptosis which could in part explain the impaired survival and defective expression of cyclin D3 protein that occur in the absence of c-Myb. Interestingly, these arrays provide information about the biology of c-Myb that, based on the literature, we did not expect. For instance, there is no previous evidence to suggest that c-Myb may be involved in regulation of actin cytoskeleton which could, in part, explain the impaired survival and proliferation of *Myb*-deficient thymocytes.

Validation of differential gene and protein expression. To validate that the microarrays are an accurate description of changes in mRNA expression in DN2, DN3, and DN3 Tcrb-Tg+ thymocytes, we performed quantitative real-time RT-PCR on RNA isolated from each sorted thymocyte subset and compared the change in expression between the mutant and the control to that predicted by the microarray data (Figure 27). We examined the expression of genes whose expression is changed over a variety

Figure 27. Validation of DN3 Tcrb-Tg+, DN3 and DN2 gene expression microarrays by quantitative real-time RT-PCR (qPCR). Expression of potential c-Myb transcriptional target genes by qPCR. RNA was isolated from sorted cell subsets from *Myb*$^{w/f}$ and *Myb*$^{f/f}$ *C* and *CRT* mice, and reverse transcribed to generate cDNA. Real-time PCR was performed in duplicate wells for each gene and relative expression was normalized according to expression of the HPRT gene. Dotted blue line indicates relative expression value of control cells. The fold change value for the gene of interest according to microarray analysis is listed above the gene above the graph. **(A)** Gene expression in DN3 Tcrb-Tg+ cells from 2 pooled *Myb*$^{w/f}$ and 4 pooled *Myb*$^{f/f}$ *CRT* mice. **(B)** Gene expression in DN3 cells from 3 pooled *Myb*$^{w/f}$ and 5 pooled *Myb*$^{f/f}$ *C* mice. (C) Gene expression in DN2 cells from 3 pooled *Myb*$^{w/f}$ and 5 pooled *Myb*$^{f/f}$ *C* mice.

A. DN3 Tcrb-Tg+

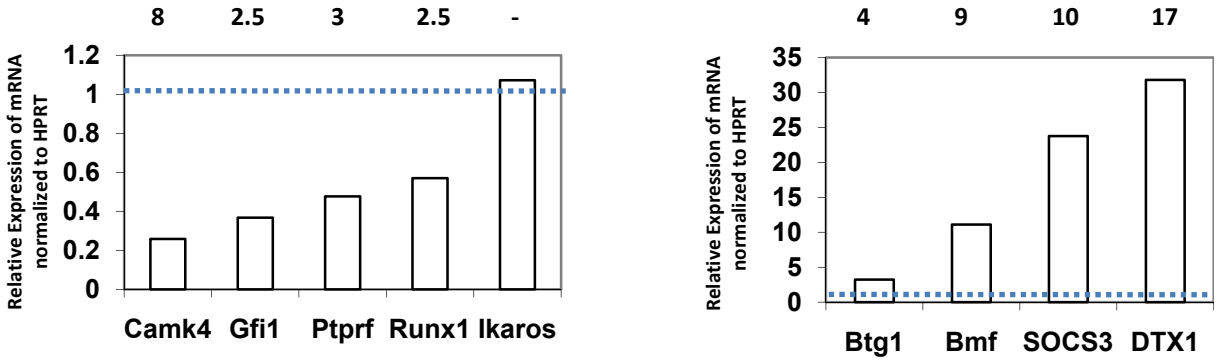

B. DN3

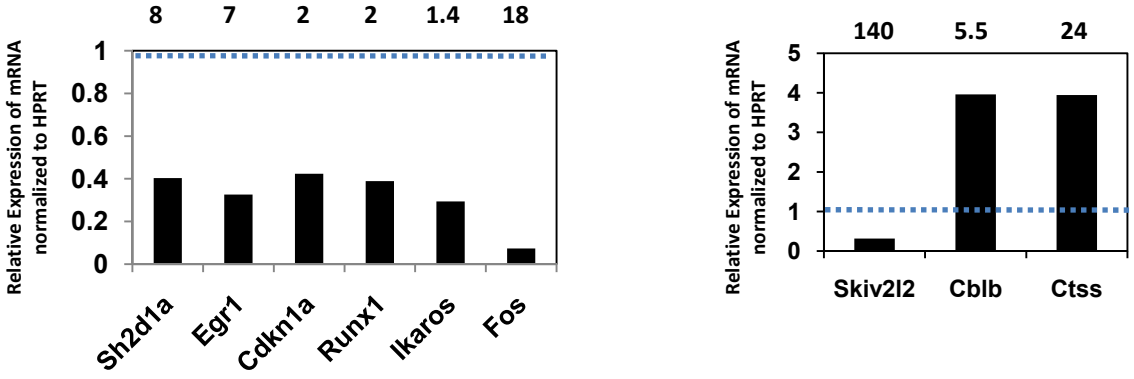

C. DN2

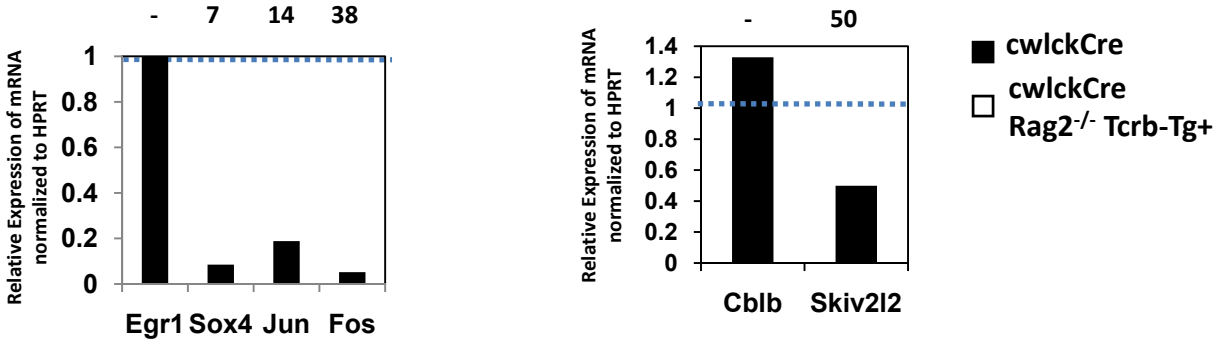

of ranges based on the microarray analysis. According to the DN3 Tcrb-Tg+ microarray, expression of *Camk4, Gfi1, Ptprf,* and *Runx1* is decreased and expression of *Btg1, Bmf, Socs3,* and *Dtx1* are increased (Appendix Table VI). Expression of *Camk4* is decreased 8 fold according to the microarray analysis (MA 8) and is decreased 75% or 4 fold according to the RT-PCR analysis (RT 75% or 4), expression of *Gfi1* is decreased MA 3 and RT 64% or 2.7, expression of *Ptprf* is decreased MA 3 and RT 54% or 2, and *Runx1* is decreased MA 2.5 and RT 45% or 1.5. Interestingly, we also examined expression of *Zfpn1a1* (Ikaros) in DN3 Tcrb-Tg+ thymocytes which is not altered according to the DN3 Tcrb-Tg+ array and we also did not detect a change in expression according to quantitative real-time RT-PCR (Figure 27A). Expression of *Btg1* is increased MA 4 and RT 3, *Bmf* is increased MA 9 and RT 11, *Socs3* is increased MA 11 and RT 23, and *Dtx1* is increased MA 17 and RT 32 in DN3 Tcrb-Tg+ thymocytes. Thus, the DN3 Tcrb-Tg+ microarray prediction of gene expression was very accurate and we were able to obtain very similar fold changes by RT-PCR for genes with low fold changes. The genes with greater fold changes on the DN3 Tcrb-Tg+ microarray appear to be greater according to RT-PCR than the array predicted. The DN3 Tcrb-Tg+ microarray was also accurate in that it did not predict a change in expression of *Ikaros* and we did not detect a change by RT-PCR as well.

According to the DN3 array, expression of *Sh2d1a, Egr1, Cdkn1a, Runx1, Ikaros,* and *Fos* is decreased and expression of *Skiv2l2, Cblb* and *Ctss* is increased (Appendix Table VII). Expression of *Sh2d1a* is decreased MA 8 and RT 60% or 2.5, *Egr1* is decreased

MA 7 and RT 67% or 3, *Cdkn1a* is decreased MA 2 and RT 57% or 2, *Runx1* is decreased MA 2 and RT 64% or 3, *Ikaros* is decreased MA 1.5 and RT 70% or RT 3.4, *Fos* is decreased MA 18 and RT 93% or 13, *Skiv2l2* is increased MA 140 and is decreased RT 70% or 3, *Cblb* is increased MA 6 and RT 4, and *Ctss* is increased MA 24 and RT 4 in DN3 thymocytes (Figure 27B). The quantitative real-time RT-PCR confirmed the changes in gene expression predicted by the DN3 microarray with the exception of Skiv2l2. The DN3 microarray prediction of fold change was very accurate for genes with small fold changes. Genes with greater fold changes like *Sh2d1a* and *Egr1* were not changed to the same extent predicted by the microarray where as the fold change for Fos was accurately predicted. Overall, the DN3 microarray provides an accurate prediction of fold changes in gene expression. Interestingly, expression of *Skiv2l2* is increased on both the DN2 and DN3 microarrays by 50 fold and 140 fold, respectively. No other gene has a fold change in expression that great on any microarrays and we did not detect an increase in expression by quantitative real-time RT-PCR either (Figure 27B, 27C) demonstrating a false positive on the arrays as predicted by a FDR of 20%.

Moreover, we were also able to confirm a reduction in *Sox4, Jun*, and *Fos* expression in DN2 thymocytes by quantitative real-time RT-PCR to validate the DN2 microarray (Appendix Table VIII). Expression of *Sox4* is decreased MA 7 and RT 92% or 11, *Jun* is decreased MA 14 and RT 82% or 5, and *Fos* is decreased MA 28 and RT 93% or 19 in DN2 thymocytes (Figure 27C). We also examined expression of *Egr1* and *Cblb* in DN2 thymocytes which were not changed according to the DN2 microarray but were

changed according to the DN3 microarray. We did not detect a difference in expression of Egr1, however, we did detect a small increase in expression of *Cblb* 1.3 fold according to RT-PCR. The DN2 microarray does predict fairly accurate fold changes in gene expression in DN2 thymocytes. Thus, all three microarrays predict accurate fold changes in gene expression in DN2, DN3 and DN3 Tcrb-Tg+ thymocyte subsets.

Some of the potential c-Myb target genes are cell surface molecules, so we were able to confirm expression by flow cytometry and correlate mRNA expression with protein expression. One cell surface protein that was identified on the DN2 and DN3 Tcrb-Tg+ microarrays is CD53. CD53 is a member of tetraspanin/transmembrane-4 superfamily and it forms a complex with integrin α4β1 and may influence motility [303]. We chose to look at surface expression of CD53 since it was previously identified as a potential Myb target in hematopoietic cells and its expression decreased upon expression of a dominant interfering Myb allele in primary CD8 and CD4 SP thymocytes; however, despite 3 Myb binding sites within the first 2kb of the mRNA start site, CD53 has not been confirmed as a direct c-Myb target [256]. According to our gene expression microarrays, CD53 has an interesting pattern of expression in *Myb*-deficient thymocytes where expression is decreased 2.8 fold in DN2 thymocytes, is unchanged in DN3 thymocytes, and is then increased 2.09 fold in DN3 Tcrb-Tg+ thymocytes (Appendix Tables VI, VII, and VIII). Flow cytometric analysis of CD53 expression in DN2, DN3 and DN4 thymocytes from $Myb^{f/f}$ *C* mice demonstrate a decrease in CD53 expression in *Myb*-deficient DN2 thymocytes (Figure 28A). DN3 thymocytes have a less dramatic decrease

Figure 28. Validation of gene expression microarrays by flow cytometric analysis of CD53, and Integrins α4, β2, and β7 expression. (A) Surface expression of CD53 is decreased in DN2 thymocytes and is increased in DN4 thymocytes confirming the gene expression microarrays. Freshly isolated thymocytes from *Myb*$^{w/f}$ and *Myb*$^{f/f}$ *C* mice were stained for CD53, CD44, CD25 and gated through the DN lineage− gate. n=3 **(B)** Surface expression of integrin α4 is decreased and integrin β2 and β7 are increased. Freshly isolated thymocytes from *Myb*$^{w/f}$ and *Myb*$^{f/f}$ *CRT* mice were gated through the DN lineage− gate to examine Integrin α4, α6, α5 and β1 expression on DN3 thymocytes. Thymocytes from *Myb*$^{w/f}$ and *Myb*$^{f/f}$ *C* mice were gated through the DN lineage− gate to examine Integrin β2, and β7 expression on DN4 thymocytes. n=3

A.

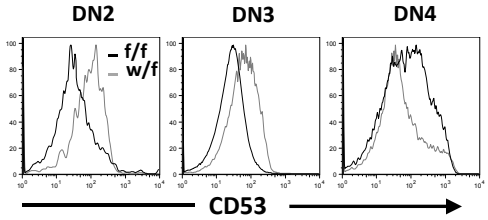

B.

DN3 Tcrb-Tg+

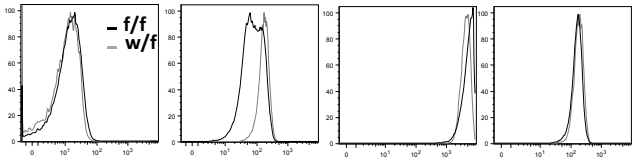

DN4

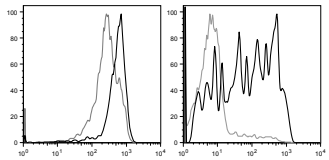

in CD53 expression. Interestingly, in DN4 thymocytes, CD53 expression is increased in *Myb*-deficient thymocytes. The flow cytometric analysis of CD53 in DN2 and DN4 thymocytes correlates with the gene expression microarray performed in DN2 and DN3 Tcrb-Tg+ thymocytes. It also demonstrates that c-Myb may have the potential to activate or repress the same gene and this regulation is very stage specific. Although we did detect a decrease in CD53 surface expression in DN3 thymocytes but we did not detect a decrease in mRNA according to the microarray, this could be a reflection of the transition of the mRNA from being decreased (in DN2) to increased (in DN4) which was not yet reflected in surface protein expression in DN3 thymocytes.

We also chose to look at surface expression of integrins by flow cytometry to see if their expression correlated with the gene expression prediction of the microarrays. Proper integrin receptor signaling is required for DN3 to DN4 differentiation [301]. Transgenic expression of a *trans*-dominant inhibitor of integrin signaling in thymocytes impaired thymocyte adhesion and resulted in a partial block in DN3 differentiation with an increase in cellularity of DN thymocytes but an overall decrease in total thymic cellularity [301]. In addition, *Itga4* was previously identified as a potential c-Myb target in transient co-transfection transcription assays [304]. According to the DN3 array, *Itga9* and *Itgae* are increased 20 and 2.8 fold, respectively (Appendix Table VII) and according to the DN3 Tcrb-Tg+ array, *Itga9, Itgb7,* and *Itgb2* are increased 4.18, 2.74 and 2.32 fold, respectively, and *Itga4* is decreased 2.16 fold (Appendix Table VI). Therefore, we examined surface expression of Integrin α4 in DN3 Tcrb-Tg+ thymocytes (Figure

28B). Flow cytometric analysis of DN3 Tcrb-Tg+ thymocytes confirms the microarray analysis prediction of a decrease in Integrin α4 expression. As a positive control we examined expression of β1, which forms heterodimers with the α-integrins, as well as expression of Integrin α6 and α5 which are expressed in DN thymocytes [127]. However, expression of α6, α5 and β1 was not altered according to the microarray analysis and we did not detect changes in their surface expression. This demonstrates that the reduction in surface expression of Integrin α4 is specific to α4 and reflects an accurate prediction of the microarray analysis. Additionally, we examined surface expression of Integrin β2 and β7 in *Myb*$^{f/f}$ *C* DN4 thymocytes since DN4 thymocytes are TCRβ+ and are most like the DN3 Tcrb-Tg+ thymocytes. According to the Tcrb-Tg+ microarray and flow cytometry of in *Myb*$^{f/f}$ *C* DN4 thymocytes, we detect an increase in expression of β2 and β7 (Figure 28B). Thus, using flow cytometry, we confirm that the microarrays make accurate predictions of gene expression that correlates with protein expression.

Identification of potential c-Myb target genes. Due to the relatively large number of genes that were up or down regulated according to the microarray analyses, we used several criteria to prioritize genes for further study. To identify potential c-Myb target genes that mediate survival and cyclin D3 expression or proliferation, we prioritized the genes that were up or down regulated in c-Myb deficient and sufficient thymocytes into three major groups. First, we scanned the lists of genes identified based on altered expression in c-Myb deficient thymocytes compared to controls and

identified genes with known roles in thymocyte development. In particular, we were interested in identifying genes where phenotypic information based on knockout mice, knock down studies using siRNA approaches or over-expression studies was available that was consistent with the phenotype in *Myb*$^{f/f}$ *C* mice. Genes that fit this description and are known c-Myb targets or had previously been reported to be candidate c-Myb targets would be considered as highest priority. Second, we identified genes with known roles in survival and proliferation. Third, we used Pathway-Express to identify biological pathways that mediate survival and proliferation and are impacted by the loss of c-Myb. We also focused our attention to genes previously reported in the literature as potential c-Myb transcriptional targets and to genes and pathways identified on more than one microarray that may impart survival or proliferation.

The lists of genes that were up or down regulated in c-Myb deficient and sufficient thymocytes revealed a number of genes with established roles in thymocyte development such as *Apc, Hoxa9* on the DN2 array; *Fos, Jun, Sh2d1a, Egr1,* and *Ahr* on the DN3 array; and *Gfra1, Gimap4, Notch3, Capn5, Ets2, Lsp1, Cbl, Smo, Gfi1, Runx1*, *Camk4, Itg4, Zfpn1a1* and *Nr3c1* on the DN3 Tcrb-Tg+ array (Table IV). A subset of these genes are expressed in DN thymocytes and play a role in the DN to DP transition. However, the altered expression of some of these genes gives defined phenotypes at the DN to DP transition but their pattern of expression predicted by the microarrays does not correlate with the phenotype of *Myb*$^{f/f}$ *C* DN thymocytes. Genes such as *Lsp1, Gfra1,* and *Capn5* have roles in migration and survival, and are expressed in DN

Table IV. ***List of thymocyte specific potential c-Myb target genes***

DN2 Microarray	DN3 Microarray	DN3 Tcrb-Tg+ Microarray
Apc	Fos	Gfra1
Hoxa9	Jun	Gimap4
	Sh2d1a	Notch3
	Egr1	Capn5
	Ahr	Ets2
		Lsp1
		Cbl
		Smo
		Gfi1
		Runx1
		Camk4
		Integrin α4
		Ikaros (Zfpn1a1)
		Nr3c1

thymocytes but it is not known if they are required for these processes in DN thymocytes [305-307]. Expression of the transcription factor *Jun* is decreased in DN2 thymocytes in the absence of c-Myb. A recent study demonstrated that thymocyte specific deletion of Jun during the DN2 stage resulted in a partial block in DN3 to DN4 differentiation with impaired survival, but not proliferation, of DN3 and DN4 thymocytes [308]. Jun has the ability to inhibit apoptosis through repression of *Pten* (phosphatase and tensin homolog) mRNA expression leading to activation of the Akt pathway in fibroblasts [309]. Pre-TCR signaling activates Akt to mediate survival through inhibition of transcription factor FoxO3a which leads to a reduction in mRNA and protein expression of pro-apoptotic member Bim [95] or through glucose metabolism and Glut1 expression [310]. Expression of *Jun* mRNA decreases as thymocytes differentiate from the DN to the DP stage [311], however, no link between the pre-TCR and Jun has been made. Although we did not detect a difference in *Pten*, *Bim* or *Glut1* expression according to our microarray analysis, *Jun* is an attractive candidate c-Myb target and will receive high priority for future studies. *Runx1* is also a good candidate gene whose decreased expression in the absence of c-Myb correlates with the impaired differentiation and proliferation in *Myb*-deficient thymocytes. Conditional deletion of *Runx1* in DN2 thymocytes resulted in a partial block in DN3 to DN4 differentiation and impaired DN4 proliferation [284]. We also detect a partial block in DN3 to DN4 differentiation and impaired DN4 proliferation in $Myb^{f/f}$ *C* thymi. Ccnd3 is thought to be a Runx1 target as demonstrated by gel shift assays and transient co-transfection transcription assays in lymphoid cell lines [312]. However, we did not detect a decrease

in expression of ccnd3 or any cyclin on any of the microarrays we performed. According to gene expression microarrays performed on *Runx1*-null embryos, Runx1 targets include genes involved in cell motility, cell proliferation, and cytoskeletal organization according to a biological pathway analysis (Ingenuity Pathways) [313]. It is possible that Runx1 contributes to β-selection proliferation and differentiation through regulation of the actin cytoskeleton and ECM-interactions. Thus, the candidate c-Myb targets identified by our microarray analysis that play known roles in DN thymocyte development and exhibit expression patterns that correlate with impaired survival and proliferation are Jun and Runx1.

The second level of prioritization of genes includes genes involved in apoptosis or proliferation. Genes whose expression correlates with impaired survival include *Casp1* (Caspase 1), and *Dap* (Death associated protein kinase), and *Bmf* (Bcl-2 modifying factor) which are all increased in the absence of c-Myb. Not much is known about the expression of *Casp1* and *Dap* mRNA during apoptosis and it is unclear if an increase in their expression would lead to an increase in apoptosis. However, over-expression of *Bmf* might be expected to correlate with increased cell death during DN thymocyte development. Bmf is a pro-apoptotic member of the Bcl-2 family that interacts with the dynein light chain which associates with the myosin V motor complex in healthy cells. In the absence of cell adhesion which induces apoptosis in MCF7 breast tumor cells referred to as anoikis, Bmf translocates to the mitochondria and binds Bcl2 [314]. During anoikis, expression of *Bmf* mRNA increases demonstrating that Bmf is also

transcriptionally regulated during anoikis [315]. In mice deficient for *Bmf,* thymocyte development is not grossly affected. However, *Bmf*$^{-/-}$ thymocytes are resistant to dexamethasone and histone-deacetylase (HDAC) inhibitor mediated apoptosis and are susceptible to γ irradiation-induced thymic lymphoma [316]. This suggests that over-expression of *Bmf* may play a role during thymocyte development as well.

There are genes on the microarrays whose expression correlates with impaired proliferation, including *Btg1* and *Btla,* which are increased in the absence of c-Myb; *Lig4* and *Cdk6* which are decreased in the absence of c-Myb*;* and genes that are associated with proliferation whose roles are not understood include *Cdca7*, *Bex1*, *Glcci1*, and *Pard6g* which are decreased in the absence of c-Myb. We were able to potentially rule out a few of these genes such as *Lig4* and *Cdk6*. *Lig4*$^{-/-}$ embryos lack DP thymocytes where as *Lig4*$^{+/-}$ embryos do not have a defect in thymocyte development [317]. It is possible that a 3 fold reduction in mRNA may affect T cell development; however, we would need to confirm the reduction in *Lig4* expression by RT-PCR and western blotting in order to determine if *Lig4* is a high priority gene. Additionally, *Cdk6*-null mice do not have abnormal thymocyte development [318] suggesting that a reduction in cdk6 mRNA is not the cause of the severely reduced number of *Myb*-deficient thymocytes. Btla is an inhibitory surface receptor expressed in activated Th1 thymocytes which associates with protein phosphatases SHP1 and SHP2 [319]. *Btla*-null mice do not have a defect in T cell development [320] but that does not rule out the possibility that over-expression of *Btla* may negatively affect T cell development. *Btg1* mRNA decreases as cells enter the cell

cycle [321] and family member Btg2 inhibits expression of cyclin D1 [322]. Perhaps Btg1 works in a similar way to Btg2 during β-selection by inhibiting expression of cyclin D3. Thus, candidate c-Myb targets with known roles in survival and proliferation whose expression best correlates with impaired survival and proliferation include *Bmf* and *Btg1*.

The third level of prioritization of genes includes genes with roles in biological processes that mediate survival and proliferation. Biological processes regulated by c-Myb that mediate survival or proliferation were identified using Pathway-Express [279] (Appendix Tables IX, X, and XI). Pathways that consistently appear on the 3 microarrays that affect survival or proliferation and have high impact factors include Phosphatidylinositol signaling pathway (Figure 29), T cell receptor signaling pathway (Figure 30), Jak-STAT signaling pathway (Figure 31), Regulation of actin cytoskeleton (Figure 32), ECM-receptor interaction (Figure 33), and Cell Adhesion Molecules (Figure 34). The Phosphatidylinositol signaling pathway has the highest impact factor according to all 3 microarrays which suggests that changes in gene expression in the absence of c-Myb greatly affected this pathway. Pre-TCR signaling activates PI3K (phosphatidylinositol-3-OH kinase) [77] which subsequently activates Akt leading to survival [78, 310]. However, as described above, Akt induces survival by mediating a reduction in mRNA and protein expression of pro-apoptotic member Bim [95] or through glucose metabolism and Glut1 expression [310] and we did not detect changes in expression of *Glut1* or *Bim* according to our microarray analyses. The DN3 and DN3

Figure 29. KEGG (Kyoto Encyclopedia of Genes and Genomes) Pathway for Phosphatidylinositol signaling system for the DN3 *Tcrb*-Tg+ microarray. Blue boxed genes represent genes with decreased expression in the absence of c-Myb. Red boxed genes represent genes with increased expression in the absence of c-Myb. Green boxed genes represent genes whose expression is unaltered in the absence of c-Myb.

Phosphatidylinositol signaling system

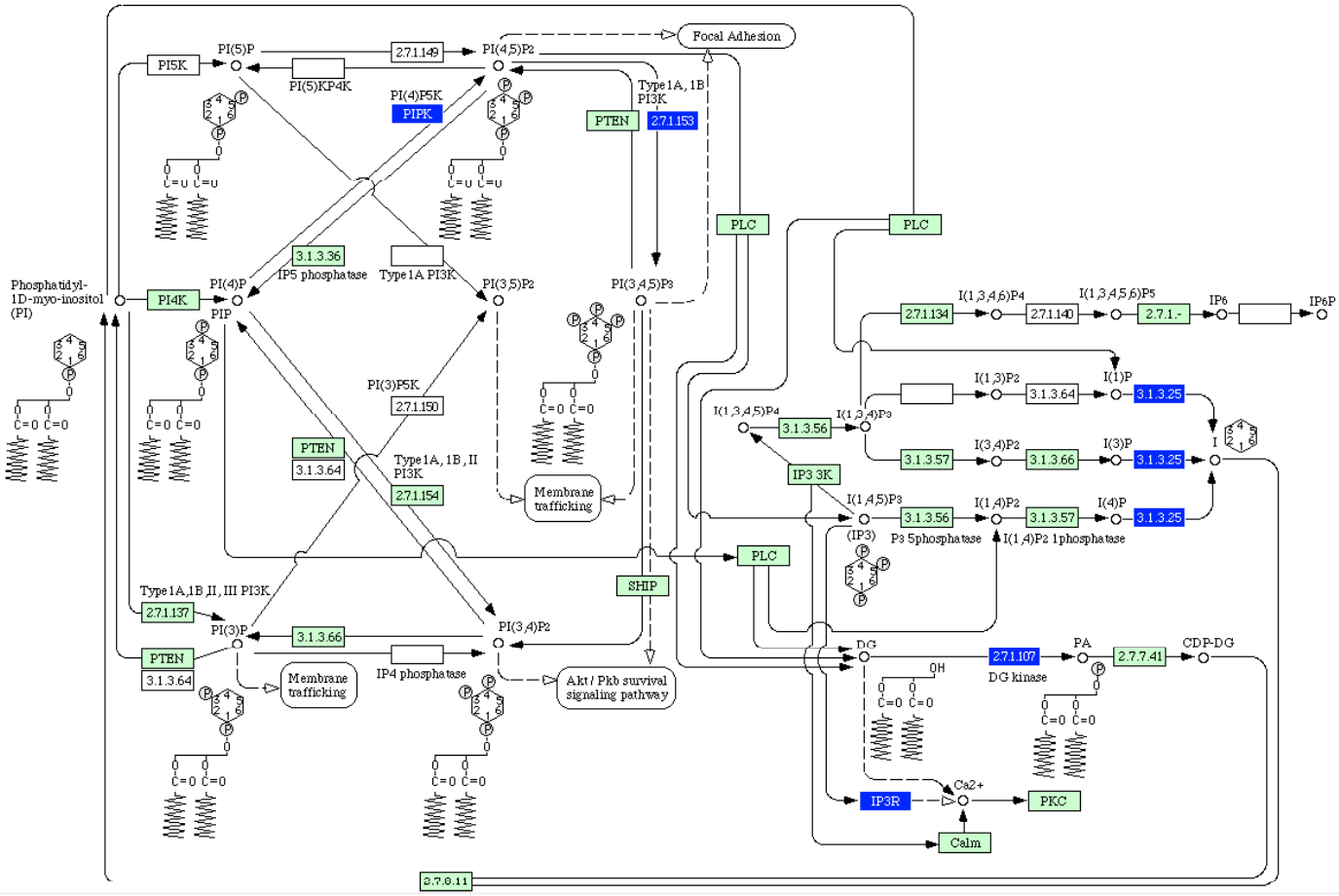

Figure 30. KEGG (Kyoto Encyclopedia of Genes and Genomes) Pathway for T cell Receptor Signaling Pathway. Blue boxed genes represent genes with decreased expression in the absence of c-Myb. Red boxed genes represent genes with increased expression in the absence of c-Myb. Green boxed genes represent genes whose expression is unaltered in the absence of c-Myb.

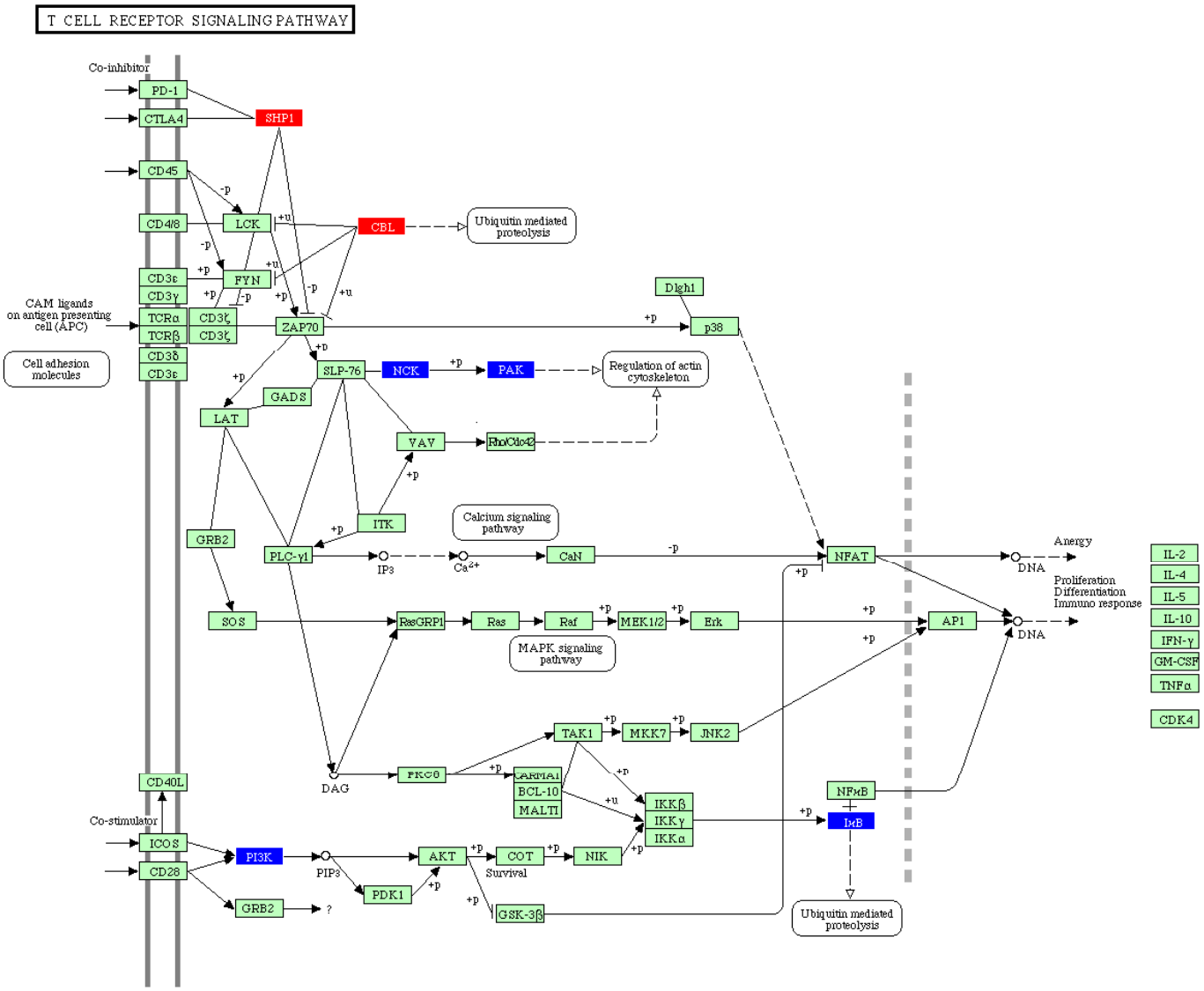
T CELL RECEPTOR SIGNALING PATHWAY
Co-inhibitor
PD-1
CTLA4
SHP1
CD45
CD4/8
LCK
CBL
Ubiquitin mediated proteolysis
CD3ε
CD3γ
FYN
TCRα
TCRβ
CD3ζ
CD3ζ
ZAP70
CAM ligands on antigen presenting cell (APC)
Cell adhesion molecules
CD3δ
CD3ε
Dlgh1
p38
SLP-76
NCK
PAK
Regulation of actin cytoskeleton
GADS
LAT
VAV
Rho/Cdc42
GRB2
ITK
Calcium signaling pathway
PLC-γ1
IP3
Ca2+
CaN
NFAT
Anergy
DNA
Proliferation
Differentiation
Immuno response
IL-2
IL-4
IL-5
IL-10
IFN-γ
GM-CSF
TNFα
CDK4
SOS
RasGRP1
Ras
Raf
MEK1/2
Erk
AP1
DNA
MAPK signaling pathway
TAK1
MKK7
JNK2
DAG
PKCθ
CARMA1
BCL-10
MALT1
IKKβ
IKKγ
IKKα
NFκB
IκB
Ubiquitin mediated proteolysis
CD40L
Co-stimulator
ICOS
CD28
PI3K
PIP3
AKT
COT
NIK
Survival
PDK1
GRB2
?
GSK-3β

Figure 31. KEGG (Kyoto Encyclopedia of Genes and Genomes) Pathway for Jak-STAT signaling pathway for the DN3 *Tcrb*-Tg+ microarray. Blue boxed genes represent genes with decreased expression in the absence of c-Myb. Red boxed genes represent genes with increased expression in the absence of c-Myb. Green boxed genes represent genes whose expression is unaltered in the absence of c-Myb.

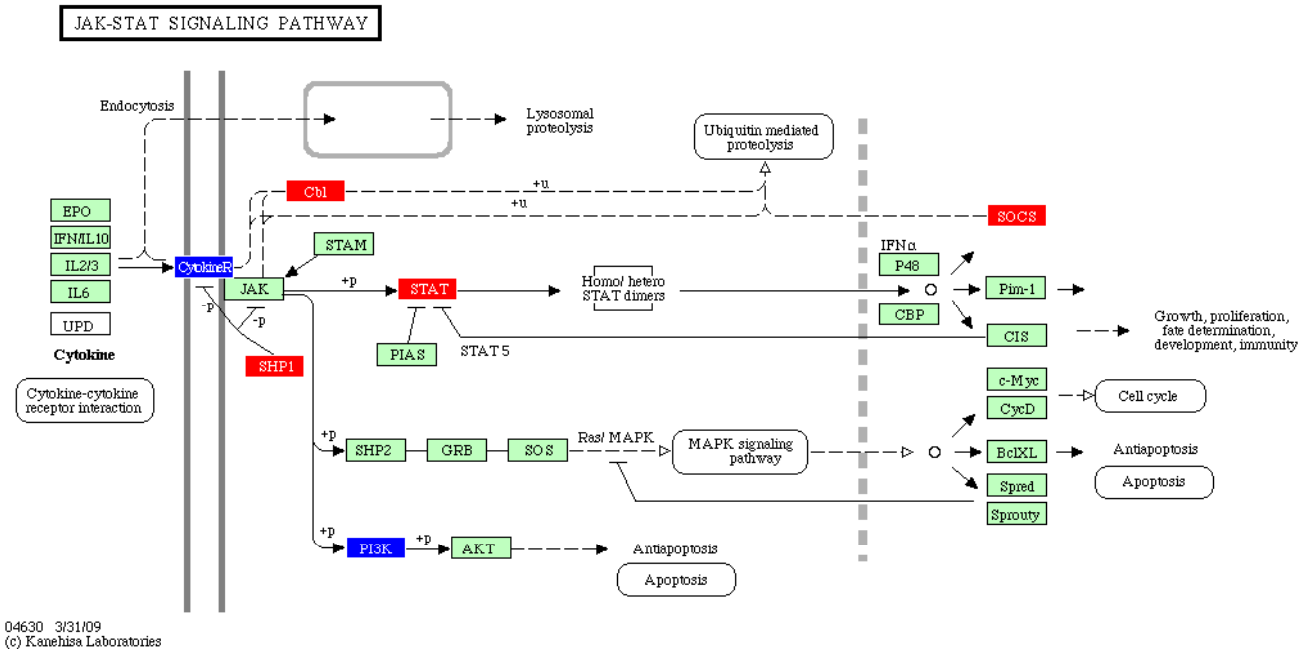

04630 3/31/09
(c) Kanehisa Laboratories

Figure 32. KEGG (Kyoto Encyclopedia of Genes and Genomes) Pathway for Regulation of Actin Cytoskeleton for the DN3 *Tcrb*-Tg+ microarray. Blue boxed genes represent genes with decreased expression in the absence of c-Myb. Red boxed genes represent genes with increased expression in the absence of c-Myb. Green boxed genes represent genes whose expression is unaltered in the absence of c-Myb.

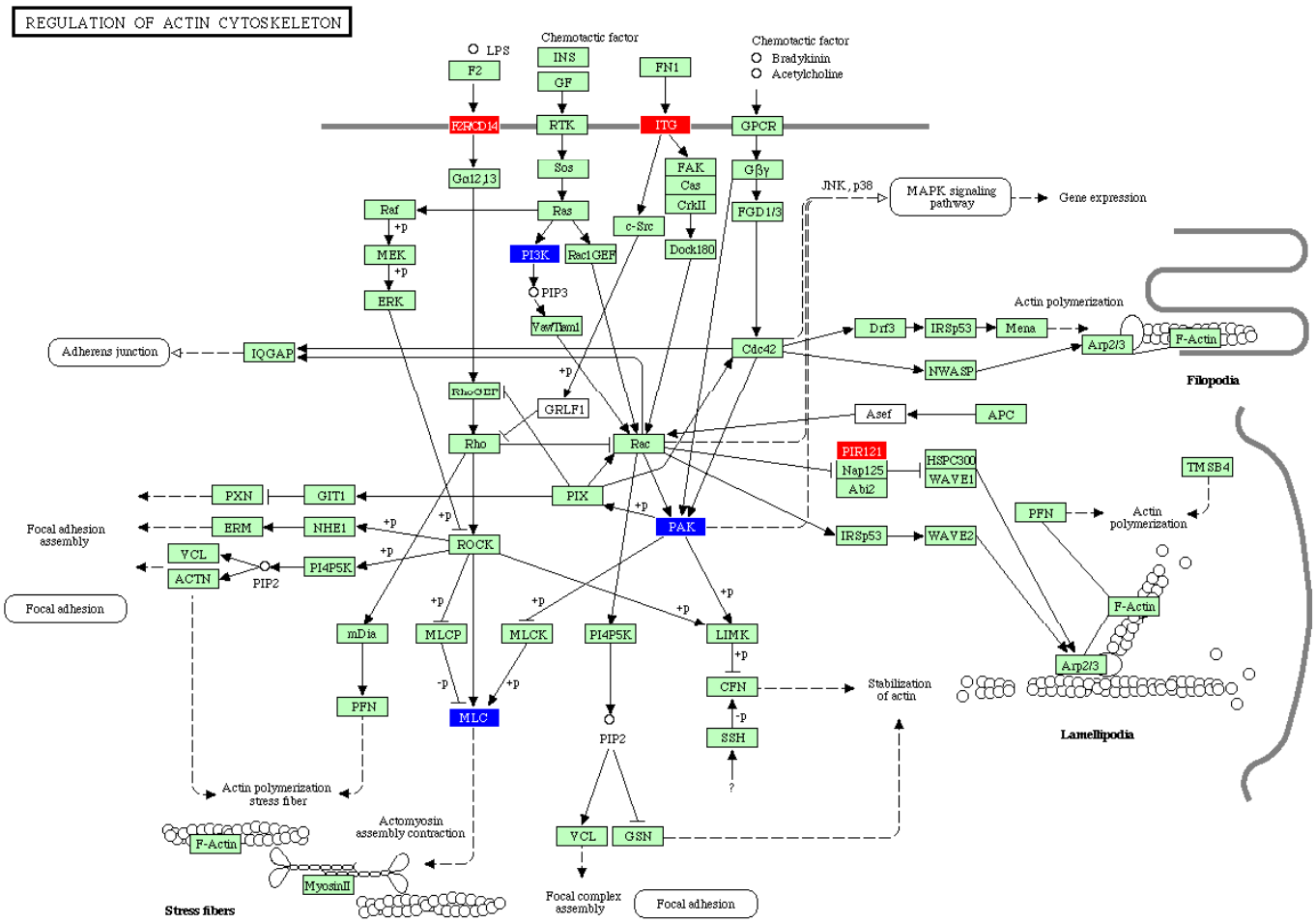
REGULATION OF ACTIN CYTOSKELETON
LPS
Chemotactic factor
Chemotactic factor
Bradykinin
Acetylcholine
INS
GF
F2
FN1
EFKCD14
RTK
ITG
GPCR
Gα12,13
Sos
FAK
Cas
CrkII
Gβγ
JNK, p38
MAPK signaling pathway
Gene expression
Raf
Ras
c-Src
FGD1/3
+p
MEK
PI3K
Rac1GEF
Dock180
+p
ERK
PIP3
Vav/Tiam1
Actin polymerization
Adherens junction
IQGAP
Cdc42
Drf3
IRSp53
Mena
Arp2/3
F-Actin
NWASP
Filopodia
+p
RhoGEF
GRLF1
Asef
APC
Rho
Rac
PIR121
Nap125
Abi2
HSPC300
WAVE1
TMSB4
PXN
GIT1
PIX
+p
+p
PAK
PFN
Actin polymerization
Focal adhesion assembly
ERM
NHE1
+p
+p
IRSp53
WAVE2
ROCK
VCL
ACTN
PIP2
PI4P5K
+p
F-Actin
Focal adhesion
+p
+p
+p
+p
mDia
MLCP
MLCK
PI4P5K
LIMK
+p
Arp2/3
CFN
Stabilization of actin
-p
+p
PFN
MLC
PIP2
-p
SSH
?
Lamellipodia
Actin polymerization stress fiber
Actomyosin assembly contraction
F-Actin
VCL
GSN
MyosinII
Stress fibers
Focal complex assembly
Focal adhesion

Figure 33. KEGG (Kyoto Encyclopedia of Genes and Genomes) Pathway for Extracellular Matrix-Receptor Interactions for the DN3 *Tcrb*-Tg+ microarray. Blue boxed genes represent genes with decreased expression in the absence of c-Myb. Red boxed genes represent genes with increased expression in the absence of c-Myb. Green boxed genes represent genes whose expression is unaltered in the absence of c-Myb.

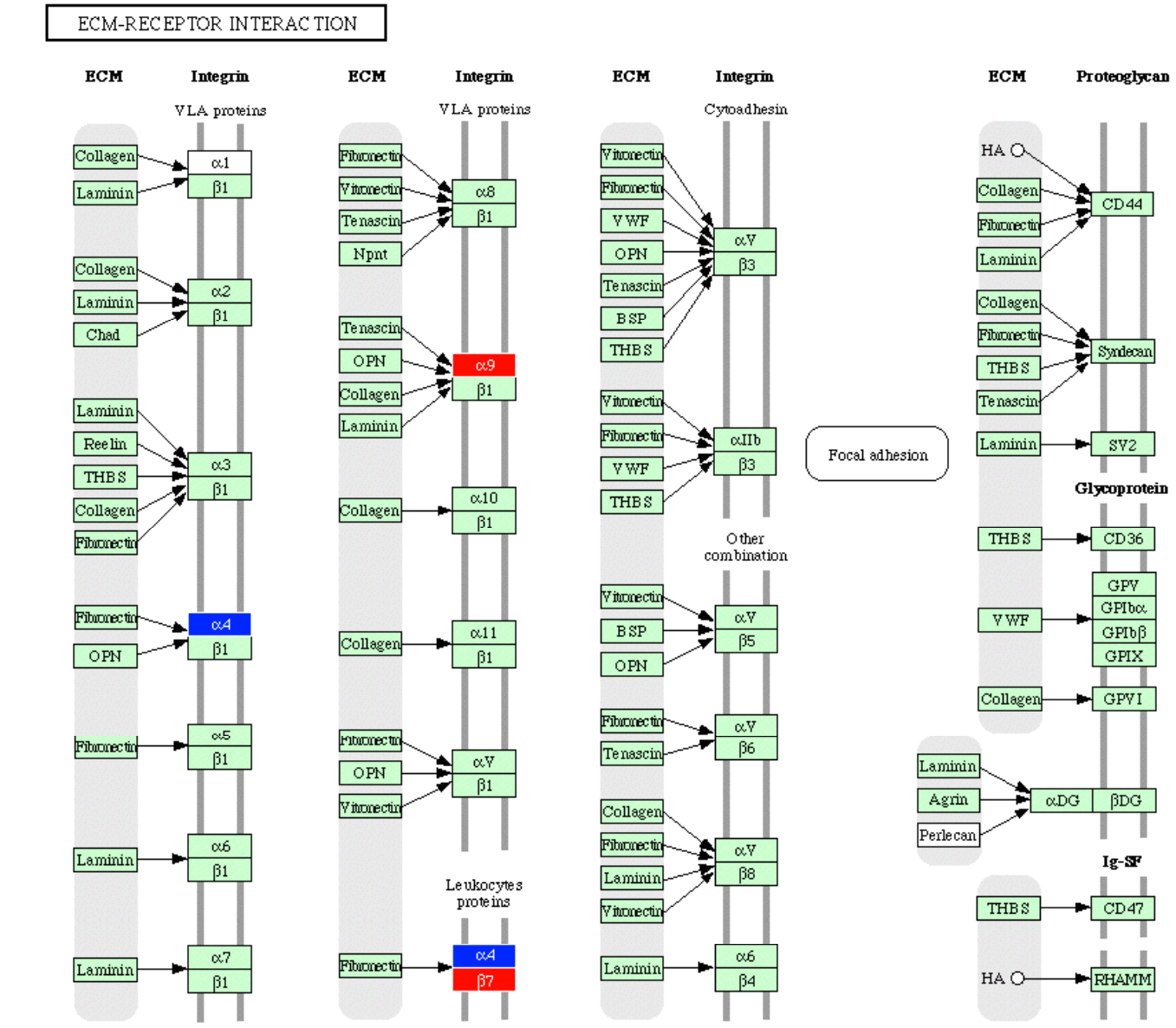
ECM-RECEPTOR INTERACTION
ECM
Integrin
VLA proteins
Collagen
Laminin
α1
β1
Collagen
Laminin
Chad
α2
β1
Laminin
Reelin
THBS
Collagen
Fibronectin
α3
β1
Fibronectin
OPN
α4
β1
Fibronectin
α5
β1
Laminin
α6
β1
Laminin
α7
β1
ECM
Integrin
VLA proteins
Fibronectin
Vitronectin
Tenascin
Npnt
α8
β1
Tenascin
OPN
Collagen
Laminin
α9
β1
Collagen
α10
β1
Collagen
α11
β1
Fibronectin
OPN
Vitronectin
αV
β1
Leukocytes proteins
Fibronectin
α4
β7
ECM
Integrin
Cytoadhesin
Vitronectin
Fibronectin
VWF
OPN
Tenascin
BSP
THBS
αV
β3
Vitronectin
Fibronectin
VWF
THBS
αIIb
β3
Other combination
Vitronectin
BSP
OPN
αV
β5
Fibronectin
Tenascin
αV
β6
Collagen
Fibronectin
Laminin
Vitronectin
αV
β8
Laminin
α6
β4
Focal adhesion
ECM
Proteoglycan
HA
Collagen
Fibronectin
Laminin
CD44
Collagen
Fibronectin
THBS
Tenascin
Syndecan
Laminin
SV2
Glycoprotein
THBS
CD36
VWF
GPV
GPIbα
GPIbβ
GPIX
Collagen
GPVI
Laminin
Agrin
Perlecan
αDG
βDG
Ig-SF
THBS
CD47
HA
RHAMM
04512hsa 03/23/05

Figure 34. KEGG (Kyoto Encyclopedia of Genes and Genomes) Pathway for Cell Adhesion Molecules for the DN3 *Tcrb*-Tg+ microarray. Blue boxed genes represent genes with decreased expression in the absence of c-Myb. Red boxed genes represent genes with increased expression in the absence of c-Myb. Green boxed genes represent genes whose expression is unaltered in the absence of c-Myb.

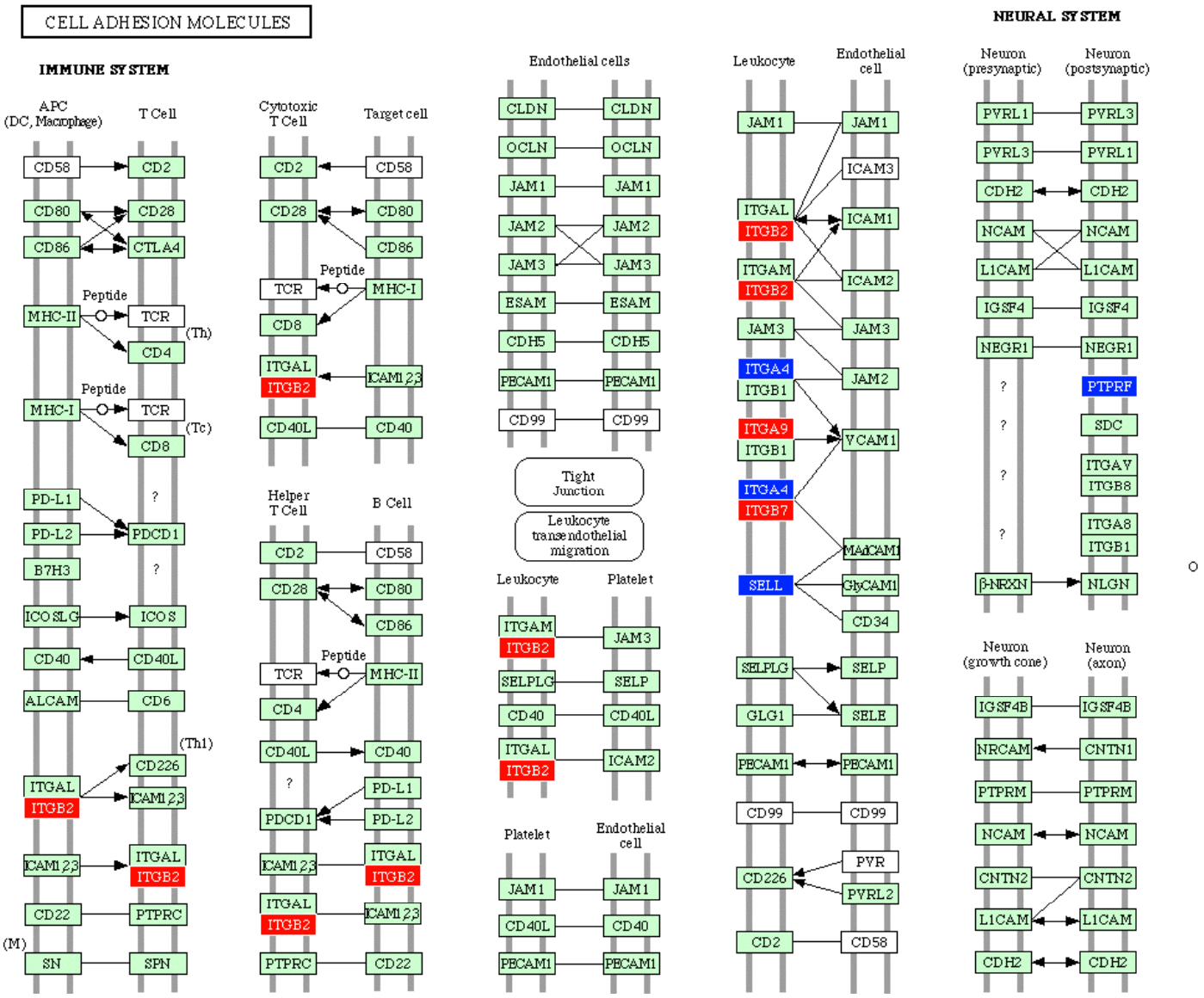
CELL ADHESION MOLECULES
IMMUNE SYSTEM
APC
(DC, Macrophage)
T Cell
CD58
CD2
CD80
CD28
CD86
CTLA4
Peptide
MHC-II
TCR
(Th)
CD4
Peptide
MHC-I
TCR
(Tc)
CD8
PD-L1
PD-L2
B7H3
?
PDCD1
?
ICOSLG
ICOS
CD40
CD40L
ALCAM
CD6
(Th1)
CD226
ITGAL
ITGB2
ICAM1,2,3
ITGAL
ITGB2
ICAM1,2,3
CD22
PTPRC
(M)
SN
SPN
Cytotoxic
T Cell
Target cell
CD2
CD58
CD28
CD80
CD86
Peptide
TCR
MHC-I
CD8
ITGAL
ITGB2
ICAM1,2,3
CD40L
CD40
Helper
T Cell
B Cell
CD2
CD58
CD28
CD80
CD86
Peptide
TCR
MHC-II
CD4
CD40L
CD40
?
PD-L1
PDCD1
PD-L2
ICAM1,2,3
ITGAL
ITGB2
ITGAL
ITGB2
ICAM1,2,3
PTPRC
CD22
Endothelial cells
CLDN
CLDN
OCLN
OCLN
JAM1
JAM1
JAM2
JAM2
JAM3
JAM3
ESAM
ESAM
CDH5
CDH5
PECAM1
PECAM1
CD99
CD99
Tight
Junction
Leukocyte
transendothelial
migration
Leukocyte
Platelet
ITGAM
ITGB2
JAM3
SELPLG
SELP
CD40
CD40L
ITGAL
ITGB2
ICAM2
Platelet
Endothelial
cell
JAM1
JAM1
CD40L
CD40
PECAM1
PECAM1
Leukocyte
Endothelial
cell
JAM1
JAM1
ICAM3
ITGAL
ITGB2
ICAM1
ITGAM
ITGB2
ICAM2
JAM3
JAM3
ITGA4
ITGB1
JAM2
ITGA9
ITGB1
VCAM1
ITGA4
ITGB7
MAdCAM1
SELL
GlyCAM1
CD34
SELPLG
SELP
GLG1
SELE
PECAM1
PECAM1
CD99
CD99
PVR
CD226
PVRL2
CD2
CD58
NEURAL SYSTEM
Neuron
(presynaptic)
Neuron
(postsynaptic)
PVRL1
PVRL3
PVRL3
PVRL1
CDH2
CDH2
NCAM
NCAM
L1CAM
L1CAM
IGSF4
IGSF4
NEGR1
NEGR1
?
PTPRF
?
SDC
?
ITGAV
ITGB8
?
ITGA8
ITGB1
β-NRXN
NLGN
Neuron
(growth cone)
Neuron
(axon)
IGSF4B
IGSF4B
NRCAM
CNTN1
PTPRM
PTPRM
NCAM
NCAM
CNTN2
CNTN2
L1CAM
L1CAM
CDH2
CDH2

Tcrb-Tg+ arrays suggest altered expression of genes involved in the ECM-interaction pathways and the DN2, DN3 and DN3 Tcrb-Tg+ arrays have altered expression of genes involved in the Regulation of actin cytoskeleton pathway. As mentioned above, integrin mediated signaling is required for efficient DN3 to DN4 differentiation suggesting a role for integrin mediated signaling during β-selection [301]. In peripheral T cells, integrin-dependent spreading is required for cyclin D3 protein expression in response to IL-2 mitogenic stimulation [302]. It is possible that integrin mediated ECM-interaction is also required for cyclin D3 expression in response to β-selection signals. Regulation of the actin cytoskeleton is involved in cellular motility and T cell receptor signaling events. Actin polymerization occurs in response to TCR stimulation [323] and in response to CXCL12 stimulation of DN thymocytes (Paul Trampont and Kodi Ravichandran personal communication) suggesting that proper regulation of actin cytoskeleton may be necessary for at least some events associated with β-selection. However, there are currently no published reports that demonstrate that actin polymerization is required for normal β-selection. Interestingly, WASp (Wiskott-Aldrich syndrome protein) interacts with the major mediator of actin polymerization, actin-related protein 2/3 (Arp2/3) complex, and in *WASp*$^{-/-}$ mice or in *WASp*$^{-/-}$ mice that express a transgene encoding a mutated form of WASp such that the VCA domain which interacts with Arp2/3 is deleted, thymocytes are impaired in DN3 to DN4 differentiation [324, 325]. Thus, it is possible that defective regulation of the actin cytoskeleton and thymocyte interactions with the ECM may be involved in impaired survival and proliferation of *Myb*-deficient thymocytes.

Upon examination of the lists of genes that were up or down regulated in c-Myb deficient and sufficient thymocytes, we identified a number of genes previously reported as c-Myb transcriptional targets in other cell types and model systems including *Nras* [326], *Vcl* [154], *CD53* [256], *Cdkn1a* [154], *Cbx4* [256], *Ets2* [327], *Bcl2* [232, 233, 256, 328], and *Itga4* [304]. However, only *Cbx4* and *Bcl2* were reported to be direct c-Myb targets as demonstrated by a ChIP of endogenous c-Myb from promoters in a multipotent hematopoietic cell line FDCP-mix [256]. The fact that these genes have previously been identified as potential targets of c-Myb, and we also detect changes in their expression according to our microarray analysis, suggest that c-Myb may regulate their expression either by direct or indirect mechanisms. In addition, there are genes whose expression is changed on more than one microarray like *Runx1, CD53, Socs3* and *Itga9* (Table V) which also suggests that these genes might be more likely to be a c-Myb transcriptional target since their expression is changed according to multiple microarray analyses. Interestingly, Runx1 is required for DN3 to DN4 differentiation and DN4 proliferation [284] suggesting that *Runx1* may be a c-Myb target that mediates c-Myb biology.

Myb-deficient thymocytes fail to efficiently migrate to CXCL12. By prioritizing the genes with known roles in T cell development, survival, or proliferation and genes that are involved in cellular pathways that mediate survival and proliferation, we generated a focused list with which to generate hypotheses: *Jun, Itga9, Runx1, Bmf*, and

Table V. ***List of potential c-Myb target genes present in multiple microarrays***

DN2 and DN3 Microarrays	DN3 and DN3 Tcrb-Tg+ Microarrays	DN2 and DN3 Tcrb-Tg+ Microarrays
Fos	Tnfrsf18	Pak1
Hspa1b	Ahr	Brd8
Skiv2l2	Dgke	1700097N02Rik
Vpreb1	Edem1	Chchd3
Socs3	Rapgef3	Socs3
	Dnahc8	Cd53
	Zmym1	
	Setd4	
	Cblb	
	Cotl1	
	Slco4a1	
	Lig4	
	A930013B10Rik	
	Runx1	
	Evl	
	D1Ertd564e	
	Depdc6	
	Ctss	
	Btg3 /// LOC640416 /// LOC654432	
	Sh2d1a	
	Arhgap9	
	Pp11r	
	Itga9	
	Prickle1	
	1500009L16Rik	
	LOC632433	
	6430570G24	
	Tsc22d1	
	Tmem16f	
	Lonrf1 /// LOC631639	
	Socs3	

Btg1. We were particularly interested in the reduction in *Itgα4* expression, and the increase in *Itgα9, Itgb2, Itgb7*, *Itgae, Bmf,* and *Mllt4* expression. Mice deficient for Itga9 have impaired granulopoiesis demonstrating a definitive role for integrin α9 during hematopoiesis [329]. Adult mice need Itga4 for development of thymocyte precursor cells in the bone marrow but it does not appear to be required during thymopoiesis [330]. Thus, a decrease in *Itgα4* alone does not explain impaired DN differentiation in *Myb*$^{f/f}$ *C* mice but the combination of altered integrin expression of *Itgb2, Itgb7, Itgae* and *Itgα9* may alter integrin signaling during DN differentiation. Moreover, Mllt4 enhances the inhibition of Integrin β1 adhesion to fibronectin [331] and its expression is increased in the absence of c-Myb suggesting that adhesion and integrin signaling may be impaired in the absence of c-Myb. As mentioned above, integrin receptor signaling is required for DN3 to DN4 differentiation [301] suggesting that impaired integrin signaling correlates with the phenotype of *Myb*$^{f/f}$*C* and *CRT* DN3 thymocytes. There is thymocyte developmental stage specific expression of integrins on thymocytes and patterned expression of their ligands, laminin and fibronectin, in the thymus suggesting stage specific functional roles for integrin mediated signaling [127]. Interestingly, in the absence of laminin-2, DN thymocytes are severely reduced in number and undergo apoptosis demonstrating that DN thymocytes require laminin mediated interactions [131]. In addition, blocking laminin-5 interactions with monoclonal antibodies also blocked differentiation of DN thymocytes to the DP stage with an increased proportion of apoptotic DN thymocytes [132] further confirming that laminin/integrin mediated interactions are required during β-selection. The integrins are involved in a number of

biological pathways that were predicted to be disrupted by the DN3 and DN3 Tcrb-Tg+ microarray including Regulation of actin cytoskeleton, Cell adhesion molecules, Focal adhesion, Leukocyte transendothelial migration, and ECM-receptor interaction (Appendix Tables IX and X). Additionally, Bmf is a pro-apoptotic Bcl2 family member which associates with actin motors and is activated by anoikis [314, 315]. Integrin signaling has been linked to actin polymerization and WASp proteins have been immunoprecipitated from Integrin β1 complexes [332, 333]. We hypothesized that the dysregulated integrin expression impaired the ability of β-selecting thymocytes to interact with the thymic microenvironment in the absence of c-Myb possibly resulting in impaired regulation of the actin cytoskeleton leading to an increase in Bmf resulting in anoikis. Based on this hypothesis, we performed a migration assay to test the ability of DN thymocytes to migrate on different extracellular matrices that do or do not support integrin interactions. We chose to do a migration assay over a cell adhesion assay since cell adhesion assays require removal of "non-adhering" cells by washing with PBS and results can vary dramatically with uncontrollable factors such as the force of the wash, angle of the pipette and distance relative to the well. In order for cells to migrate, chemokine receptor signaling and extracellular matrix interaction work together. We chose to test the ability of thymocytes to migrate to the CXCL12 chemokine since it preferentially attracts DN and DP thymocytes. The receptor for CXCL12, CXCR4, is highly expressed in DN and DP thymocytes [334] and is required for cells to traverse the β-selection checkpoint (Paul Trampont and Kodi Ravichandran personal communication).

We predicted that there would be impairment in migration to CXCL12 on an ECM that mediates integrin interaction.

We performed one migration experiment where we tested the ability of thymocytes from 4 *Myb*$^{w/f}$ and 5 *Myb*$^{f/f}$ *cwlckCre* mice to migrate to CXCL12 in a transwell chemotaxis assay where the transwell is coated with either BSA, laminin-1 (LN) or fibronectin (FN). Laminin interacts with Integrins α6β1 and α9β1, fibronectin interacts with Integrins α4β1 and α5β1, and BSA does not interact with integrins. First, we examined expression of the CXCL12 receptor, CXCR4, in DN3 and DN4 thymocytes. DN3 thymocytes do express CXCR4 in the absence of c-Myb; however, expression of CXCR4 is slightly decreased in DN4 *Myb*$^{f/f}$ *C* thymocytes as compared to *Myb*$^{w/f}$ *C* (Figure 35A). The percentage of total random moving cells without chemokine on BSA and FN is not statistically different between *Myb*$^{f/f}$ *C* and *Myb*$^{w/f}$ *C* mice (Figure 35B). However, there is a significant reduction in the percentage of total random moving cells without chemokine on LN in *Myb*$^{f/f}$ *C* mice (Figure 35B). LN is known to interact with Integrin α6β1 and integrin α6 is expressed in the absence of c-Myb (Figure 28B). α9β1 has been reported to be a receptor for laminin in humans [335] and expression of *Itga9* is predicted to be increased in the absence of c-Myb. Thus, it is possible that an increased expression of *Itga9* alters interaction with laminin. The percentage of total thymocytes migrating to CXCL12 is severely reduced in the *Myb*$^{f/f}$ *C* thymocytes regardless of the ECM. However, the greatest difference between *Myb*$^{w/f}$ *C* and *Myb*$^{f/f}$ *C* thymocytes migrating to CXCL12 is on LN. Examination of DN3 and DN4 thymocytes placed on

Figure 35. c-Myb-deficient thymocytes have an impairment in migration to CXCL12. (A) Freshly isolated thymocytes from *Myb*$^{w/f}$ and *Myb*$^{f/f}$ *C* mice were gated through the DN lineage− gate to examine CXCR4 expression in DN3 and DN4 thymocytes. FMO represents a stain that did not include CXCR4. n=2 **(B)** *Myb*-deficient total thymocytes fail to migrate to CXCL12. Total thymocytes from 2 pooled *Myb*$^{w/f}$ and 4 pooled *Myb*$^{f/f}$ *C* mice were added to a transwell coated with either BSA, fibronectin (FN) or laminin-1 (LN) for a chemotaxis assay to CXCL12 or nothing. The percentage of total thymocytes migrating is represented as the percentage of the input thymocytes. * $p \leq 0.05$ **(C)** Examination of the percentage of DN3 and DN4 thymocytes migrating to nothing or CXCL12 on FN, LN or BSA. Data is represented as the percentage of input thymocytes. * $p \leq 0.05$

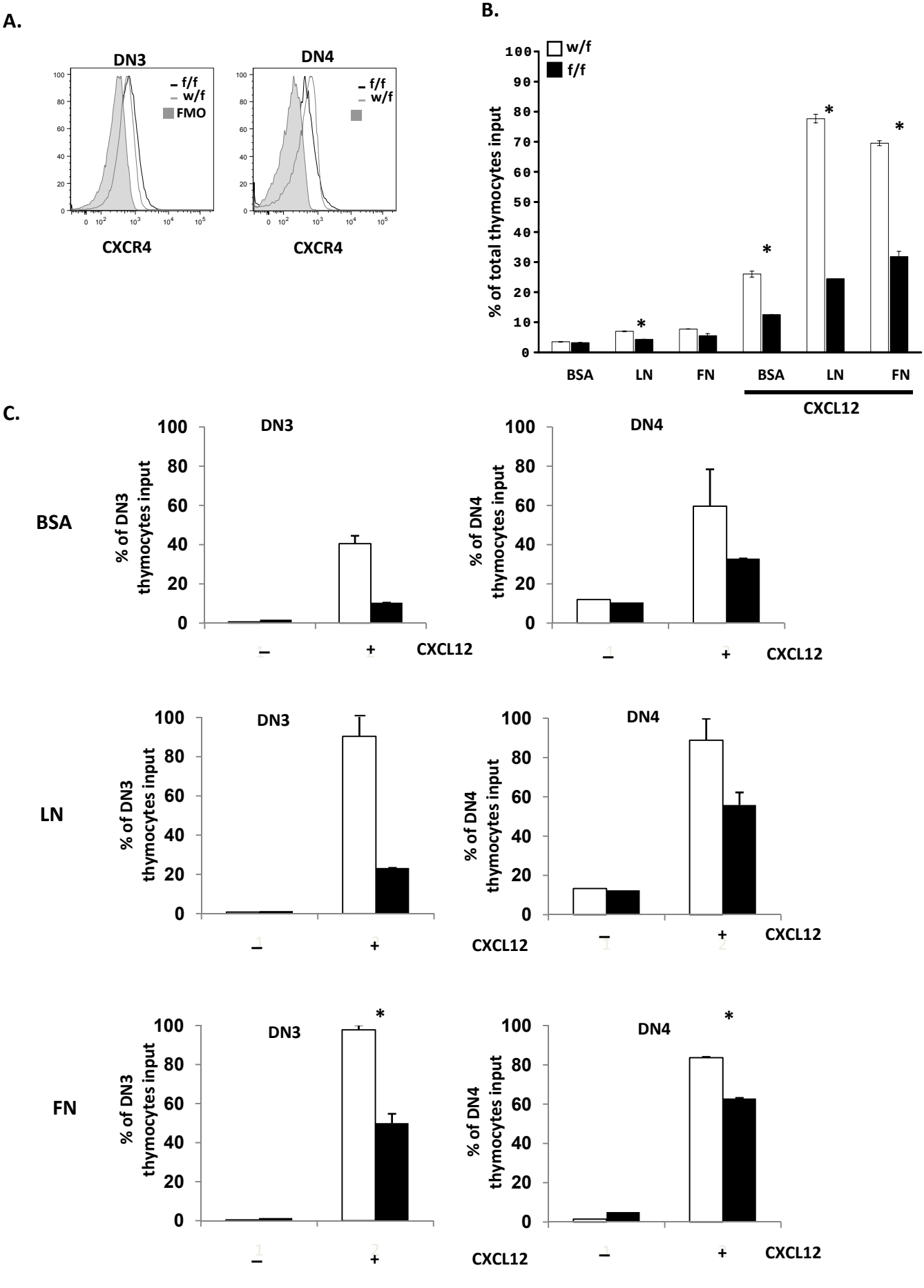
A.
DN3
DN4
f/f
w/f
FMO
CXCR4
CXCR4
B.
w/f
f/f
% of total thymocytes input
BSA
LN
FN
BSA
LN
FN
CXCL12
C.
BSA
LN
FN
DN3
DN4
% of DN3 thymocytes input
% of DN4 thymocytes input
CXCL12

transwells with BSA with and without the addition of CXCL12 reveals a reduction in the proportion of *Myb*$^{f/f}$ *C* DN3 and DN4 thymocytes migrating to CXCL12 (Figure 35C). A reduction in the proportion of *Myb*$^{f/f}$ C DN3 and DN4 thymocytes migrating to CXCL12 is also detected on LN and FN coated transwells. The greatest reduction in migration of *Myb*$^{f/f}$ *C* DN3 thymocytes to CXCL12 is on LN. Although this experiment was only performed once and we are lacking some statistical significance, the trend suggests that *Myb*-deficient DN3 and DN4 thymocytes do not migrate efficiently to CXCL12. This experiment also suggests that *Myb*-deficient thymocytes may be impaired in their ability to interact with laminin. *Myb*-deficient DN4 thymocytes do not express CXCR4 to the same extent as LMC which may contribute to the inefficient migration to CXCL12. However, *Myb*$^{f/f}$ *C* DN3 thymocytes do express CXCR4 and are impaired in migration to CXCL12 suggesting that decreased expression of CXCR4 is not the cause for the impaired migration.

DISCUSSION

c-Myb is required for β-selection induced survival and cyclin D3 expression during T cell development in the thymus. To try to gain further insight into how c-Myb regulates survival and cyclin D3 expression, as well as identify potentially novel roles for c-Myb during T cell development in the thymus, we performed a gene expression microarray on RNA from DN3 Tcrb-Tg+ thymocytes to identify potential c-Myb

transcriptional targets. We also performed microarrays on DN2 and DN3 thymocytes since it is possible that c-Myb is required for an early event that later affects β-selection. It was also possible that changes in gene expression might be masked in DN3 Tcrb-Tg+ thymocytes due to the large proportion of dying cells in this compartment. The microarray experiments identified potential c-Myb target genes that are directly involved in thymocyte development, survival, and proliferation. We identified a number of genes involved in biological pathways that may be affected in the absence of c-Myb. We also detected changes in expression of genes previously reported to be c-Myb targets. However, the majority of the genes identified in these experiments as potential c-Myb targets based simply on changes in expression have not been previously identified. In addition, we provide evidence to suggest that c-Myb has the potential to activate or repress the same gene and that this regulation is very stage specific.

In order to identify potential c-Myb transcriptional target promoters that mediate the biology of c-Myb, we generated a small list of genes by prioritizing genes with known roles in thymocyte development, survival or proliferation as well as genes that are involved in cellular pathways that mediate survival and proliferation in other cell types. Altered expression of *Itga4, Itga9, Itgb2, Itgb7* and *Itgae* fit our criteria of focusing on genes involved in DN thymocyte development since blocking integrin signaling impaired DN3 differentiation [301], genes involved in proliferation since integrin mediated signaling stimulates cyclin D3 expression in peripheral T cells [302], and genes previously suggested to be a c-Myb target since *Itga4* is reported to be a

target of c-Myb [304]. Bmf fit our criteria of regulating survival [314, 315] and its over-expression suggested impaired regulation of actin cytoskeleton which is a pathway that was affected by a c-Myb deficiency. Moreover, overexpression of *Mllt4* suggested that β1 integrin adhesion and signaling may be compromised in the absence of c-Myb. We hypothesized that the altered expression of integrins impaired the ability of *Myb*-deficient thymocytes responding to β-selection signals to interact with the thymic microenvironment. Integrin signaling leads to actin polymerization and reorganization of the actin cytoskeleton [332] and we hypothesized that altered integrin signaling failed to regulate actin organization resulting in an increase in *Bmf* resulting in anoikis. Based on this hypothesis, we performed a migration assay in lieu of an adhesion assay due to the limitations presented by an adhesion assay, to test the ability of *Myb*-deficient thymocytes to interact with extracellular matrices. Interestingly, total, DN3 and DN4 thymocytes deficient for c-Myb do not efficiently migrate to CXCL12 even in the absence of an extracellular matrix protein which suggests an inherent defect in migration. DN3 thymocytes deficient for the receptor for CXCL12, CXCR4, undergo apoptosis during β-selection (Paul Trampont and Kodi Ravichandran personal communication) suggesting that inefficient migration to CXCL12 correlates with the survival defect we detect in the absence of c-Myb. There are three possible explanations for why *Myb*-deficient thymocytes are impaired in responding to CXCL12/CXCR4 signaling. The Jak-STAT signaling pathway is required to mediate signals downstream of CXCR4 in T cell lines through Jak2 and Jak3 activation of STAT 1, 2, 3 and 5 [336], and Jak-STAT signaling is most likely required during β-selection as well. The Jak-STAT pathway is negatively

regulated by Ptpn6 (SHP-1) [337] whose expression is predicted to be increased in the absence of c-Myb which could be affecting CXCR4 signaling. In addition, CXCL12/CXCR4 signaling stimulates actin polymerization and reorganization in order to migrate and there are changes in expression of genes involved in regulation of actin cytoskeleton in *Myb*-deficient thymocytes. Both *Pik3cg* and *Pak1* are predicted to be decreased in the absence of c-Myb and both are shown to mediate actin polymerization [338, 339] which may result in impaired actin cytoskeleton organization which could hamper the ability of thymocytes to migrate to CXCL12. In addition, the third possible explanation for why *Myb*-deficient thymocytes are impaired in migration to CXCL12 is that cellular apoptosis is the cause for impaired migration to CXCL12. We have demonstrated in Chapter III that *Myb*-deficient thymocytes performing β-selection *in vitro* activate caspase-3. It is most likely that *Myb*-deficient thymocytes activate caspase-3 when placed on the BSA, FN and LN. In addition, our preliminary migration experiment also suggests that c-Myb deficient DN3 thymocytes may be impaired in interacting with extracellular matrix protein laminin-1. Laminin interactions are required for differentiation and survival of DN thymocytes [131, 132] and defective laminin interaction correlates with the survival defect detected in the absence of c-Myb. Altered expression of Integrins, Mllt4 and genes that regulate the actin cytoskeleton in thymocytes lacking c-Myb could explain the inability of DN3 thymocytes to interact with laminin-1. Thus, the inability to respond to CXCL12/CXCR4 signals and the inability to interact with extracellular matrix protein laminin, could both contribute to the impaired survival, proliferation and differentiation of *Myb*-deficient preTCR+ DN3 thymocytes.

We have taken the first step in identifying potential c-Myb transcriptional targets that regulate survival and proliferation of β-selecting thymocytes in a physiologically relevant model system. Whole genome expression microarrays are useful for identifying direct and indirect targets that mediate c-Myb activity. Although the phenotype of *Myb*-deficient DN3 thymocytes is complex and is not likely due to altered expression of one gene, the microarrays have identified altered expression of multiple genes involved in pathways that implicate c-Myb in numerous biological processes that could result in impaired survival and proliferation. In addition, we have potentially identified a new potential role for c-Myb in migration to CXCL12 and in interaction with laminin (Figure 36). CXCL12/CXCR4, pre-TCR and integrin/extracellular matrix signaling pathways are all required during β-selection signaling and according to our microarrays, genes involved in these pathways are affected in the absence of c-Myb (Figure 37). The fact that c-Myb may play a role in multiple signaling pathways during β-selection supports the notion that DN3 thymocytes that lack c-Myb display a complex phenotype that cannot be attributed to altered expression of a single gene.

Figure 36. c-Myb roles during differentiation of DN3 thymocytes. Events that are independent of c-Myb during differentiation of DN3E thymocytes to the DN3L, DN4 and ISP stages are listed above the cell subsets. Events that depend on c-Myb during differentiation of DN3E thymocytes to the DN3L, DN4 and ISP stages are listed below the cell subsets. Two new potential roles to add for c-Myb include migration to CXCL12 and interaction with Laminin-1.

c-Myb independent:

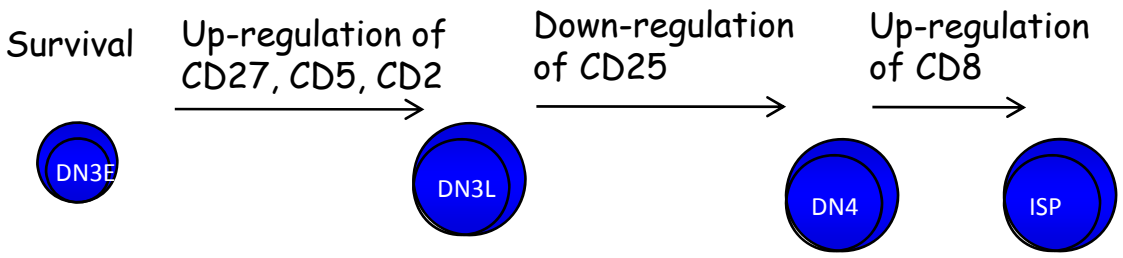

c-Myb dependent:

V(D)J recombination of *Tcrb* locus

Anti-CD3ε mediated differentiation

Survival independent of p53 and Bcl2

Proliferation

Expression of Cyclin D3 protein

Entry into the Cell Cycle

Migration to CXCL12

Interaction with laminin

Figure 37. Receptor mediated events during β-selection required for differentiation, survival, proliferation or migration of DN3 thymocytes that may be affected in the absence of c-Myb. The Green arrows indicate proteins whose gene expression is altered due to the lack of c-Myb. The Red arrows indicate the proteins whose expression we confirmed is altered in the absence of c-Myb. The dashed arrows represent events known to occur downstream of the receptor mediated interaction in other stages of lymphocyte development but have not been specifically demonstrated to occur during β-selection.

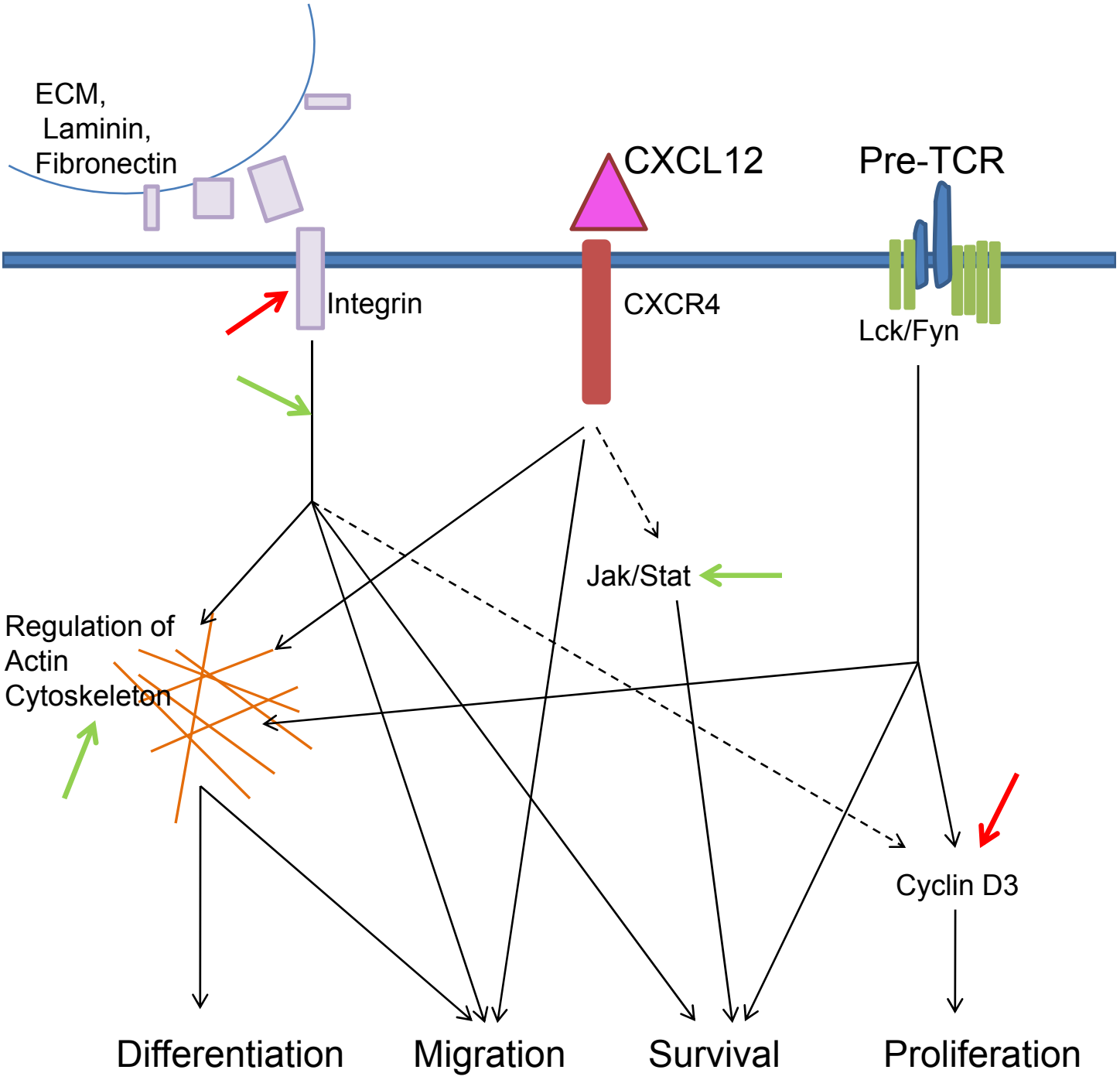
ECM,
Laminin,
Fibronectin
CXCL12
Pre-TCR
Integrin
CXCR4
Lck/Fyn
Jak/Stat
Regulation of
Actin
Cytoskeleton
Cyclin D3
Differentiation
Migration
Survival
Proliferation

Chapter V. Summary and Future Directions

At the time this project was proposed, several groups had used different mutant *Myb* alleles to study the function of c-Myb during thymopoiesis. Due to the embryonic lethality of *Myb*-null mice prior to the initiation of lymphopoiesis [195], homozygous null *Myb/Rag1* chimeric mice were generated which demonstrated a block in differentiation beyond the DN1 stage [225]. However, this model system was not able to differentiate between a role for c-Myb in progenitor cells that later affected thymopoiesis versus a role for c-Myb during thymopoiesis. Since then, several groups, including our own, used conditional mutagenesis to study c-Myb function during thymopoiesis and reported that c-Myb is required for DN3 to DN4 differentiation, survival of pre-selection DP thymocytes, and differentiation of CD4 lineage T cells [14, 266]. Together these studies demonstrate that c-Myb is required at multiple stages during thymopoiesis. Our lab further characterized the block in DN3 differentiation and we did not detect a requirement for c-Myb in DN3 survival or proliferation [14]. Interestingly, intracellular expression of the TCRβ chain was severely reduced in DN3 thymocytes as was Vβ to DJβ recombination of the *Tcrb* locus in the absence of c-Myb. This suggested that the impairment in Vβ to DJβ recombination was the cause of the block in DN3 differentiation. However, a small proportion of DN3 thymocytes expressed a TCRβ protein yet we detected very few DN4 thymocytes in the absence of c-Myb which suggested that c-Myb is required for DN3 differentiation independent of V(D)J recombination. Thus, it was unclear if the impaired Vβ to DJβ recombination observed

in the absence of c-Myb was the sole cause for the block in DN3 differentiation or if c-Myb was required for differentiation of DN3 thymocytes independent of V(D)J recombination. To determine if c-Myb is required for maintenance of DN3E thymocytes prior to V(D)J recombination, which might be expected to affect the efficiency of V(D)J recombination we crossed our *Myb*$^{f/f}$ *cwlckCre* mice with *Rag2*$^{-/-}$ mice to examine survival of DN3E thymocytes in the absence of V(D)J recombination. We predicted that c-Myb is not required for maintenance of DN3E thymocytes and that c-Myb is directly required during the process of V(D)J recombination. We also crossed our *Myb*$^{f/f}$ *cwlckCre* mice with *Tcrb* transgenic mice to determine if expression of a *Tcrb*-transgene (Tg) could rescue DN3 to DN4 differentiation which would demonstrate that defective V(D)J recombination is the sole cause for the block in DN3 differentiation. We predicted that c-Myb is required for DN3 differentiation independent of V(D)J recombination and that the presence of a *Tcrb*-Tg would not rescue DN3 differentiation. Since we did not detect a role for c-Myb in proliferation of peripheral B-cells [264], we predicted that c-Myb is not required for proliferation but it is required for survival and/or differentiation of DN3 pre-TCR+ thymocytes during β-selection.

Characterization of the *Myb*$^{f/f}$ *CR* and *Myb*$^{f/d}$ *CR* mice did not reveal any significant differences in total thymic cellularity or in the absolute number of DN3 and DN4 thymocytes as compared to controls suggesting that c-Myb is not required for the inherent survival of DN3 thymocytes that lack a pre-TCR. Although only 64% of the *Myb* locus is deleted in DN3 thymocytes from *Myb*$^{f/f}$ *CR* mice, if c-Myb was required for their

survival it should be possible to detect impaired survival since over half of the cells do not contain *Myb*. Thus, what we can conclude from these experiments is that c-Myb is required for V(D)J recombination of the *Tcrb* locus but is not required for the inherent survival or maintenance of DN3E thymocytes. It is also possible that c-Myb is required during the DN2 stage of development but we are unable to detect a deficiency in DN2 thymocytes using our current Cre recombinase model system which initiates Cre expression in DN2 thymocytes. Additionally, our microarray analysis performed on DN2 thymocytes from $Myb^{f/f}$ *C* mice revealed a decrease in a number of candidate genes required for differentiation and survival of early DN thymocytes such as *Jun* [308]. DN2 thymocytes themselves are difficult to define and it is not known what signals the DN2 to DN3 transition [340]. It is possible that deletion of the *Myb* locus occurs in late stage DN2 thymocytes and while we detect a decrease in RNA expression of genes involved in differentiation and survival of DN thymocytes, it is possible that the protein levels are not decreased especially proteins with a long half-life. Perhaps with early deletion of the *Myb* locus in DN1 or DN2 thymocytes, we may be able to detect a requirement for c-Myb in the DN1/DN2, or DN2/DN3 stages. To obtain efficient deletion in DN1 and DN2 thymocytes, we could infect $Myb^{f/f}$ $Rag2^{-/-}$ thymocytes with a retrovirus expressing Cre recombinase and culture thymocytes *in vitro*. Our lab has had success with infecting pro-B cells with the Cre-expressing retrovirus and obtaining efficient deletion of the *Myb* locus. In order to test c-Myb function in DN1, DN2 or DN2/DN3 stages, infecting $Myb^{f/f}$ DN1 or DN2 thymocytes with a Cre-expressing retrovirus would lead to efficient *Myb* deletion and may uncover a defect we were not able to previously identify.

In addition, it was unclear if c-Myb was required for DN3 differentiation independent of V(D)J recombination. Interestingly, providing *Myb*$^{f/f}$ *CR* DN3 thymocytes with a *Tcrb* transgene did not rescue DN3 to DN4 differentiation or total, DN3 and DN4 cellularity demonstrating that c-Myb is crucial for normal β-selection independent of V(D)J recombination. We demonstrated that *Myb*-deficient thymocytes initiate pre-TCR signaling and receive pre-TCR signals to down-regulate CD25 and up-regulate CD8 expression. However, differentiation to the DN4 and ISP stages is accelerated in *Myb*- and *Rag2*- doubly deficient thymocytes responding to anti-CD3ε treatment. This suggests that expression of c-Myb is required to keep cells in the DN3L and DN4 proliferating stages and that c-Myb keeps cells in a more immature state. Early studies demonstrated that continuous expression of *Myb* blocked differentiation of murine erythroleukemia cell lines that could otherwise be stimulated to differentiate thus keeping cells in an immature state [210, 213, 341]. In addition, blocking c-Myb activity by the expression of a dominant-negative Myb protein allowed the murine erythroleukemia cell line to differentiate [341]. Recent studies demonstrated that inducible over-expression of c-Myb in *Myb*$^{-/-}$ embryonic stem cell lines prevented terminal differentiation of erythrocytes, megakaryocytes and B-lymphocytes *in vitro* [214]. While these experiments did not reveal an accelerated differentiation upon removal of c-Myb, they support the notion that expression of c-Myb keeps cells in a more immature state and proper levels of c-Myb are required to control differentiation. It is possible that c-Myb is required to keep thymocytes that are performing β-selection

at the appropriate compartment within the thymic microenvironment in order for thymocytes to receive signals to survive and proliferate or it is possible that c-Myb is required to keep a milieu of genes on that somehow mediate thymocyte survival, proliferation and differentiation. Interestingly, we have retrovirally expressed c-Myb and GFP encoding cDNA fragments in *Myb*$^{w/f}$ *CRT* and *Myb*$^{w/f}$ *C* DN3 thymocytes and found that infecting with a large ratio of infectious particles to cells resulted in impaired thymocyte survival as compared to infection with a control vector. Whereas infecting with a small ratio of infectious particles compromised thymocyte survival, it did prolong survival as compared to infection with the large ratio. This suggests that forced c-Myb expression also impairs thymocyte survival. Although we were unable to obtain a large percentage of GFP+ cells to be able to measure the amount of c-Myb protein in the infected cells, these studies suggest that over-expression of c-Myb impairs survival and that proper expression of c-Myb is required for survival of DN3 thymocytes during β-selection.

Our data suggests that *Myb*-deficient thymocytes receive signals to differentiate beyond the DN3 stage but they fail to survive. Using a combination of approaches to measure cell survival, we have clearly demonstrated that upon the acquisition of a pre-TCR, *Myb*$^{f/f}$ *C* and *Myb*$^{f/f}$ *CRT* DN3L thymocytes undergo apoptosis and activate caspase-3 as compared to controls. Thus, we have demonstrated for the first time that c-Myb is required for survival during β-selection. However, data obtained from in vivo experiments detected cell death in DN4 thymocytes, not DN3 thymocytes, where as

data obtained from in vitro experiments detected cell death in DN3L thymocytes. Mechanisms that mediate survival and suppress apoptosis during β-selection are not well understood. Evidence suggests that the balance of pro-apoptotic and anti-apoptotic Bcl2 family members is important for survival during β-selection [53, 95, 107-110]. Recent studies demonstrate that expression of pro-apoptotic Bcl2 family members Bid and Bim are decreased and expression of pro-survival Bcl2 family member Bcl2a1 is increased in response to pre-TCR signaling [86, 95]. Interestingly, the pro-survival molecule Bcl2 was reported to be a c-Myb target [232, 233, 256, 328] and the DN3 Tcrb-Tg+ microarray did predict a minimal 1.35 fold decrease in *Bcl2* expression in the absence of c-Myb but we were unable to detect a decrease in Bcl2 protein expression in DN3 thymocytes by flow cytometry. Moreover, survival of *Myb*-deficient thymocytes was not rescued by expression of a Bcl2-transgene. In addition, expression of Bid is controlled by p53 [95] yet loss of p53 was unable to rescue DN3 cellularity or differentiation in the absence of c-Myb suggesting that the survival defect in pre-TCR+ thymocytes is not due to a failure to down-regulate p53 or Bid. The pre-TCR also mediates survival through up-regulation of Bcl2a1 pro-survival molecule [86]. However, suppression of Bcl2a1 expression using shRNA did not affect survival during β-selection [221]. We did not detect a decrease in Bcl2a1 expression in DN4 thymocytes or in anti-CD3ε treated thymocytes in the absence of c-Myb, rather we detected an increase in expression suggesting that *Myb*-deficient thymocytes may be up-regulating expression of Bcl2a1 in an attempt to survive. Therefore, we conclude that c-Myb is required for survival of thymocytes performing β-selection that is independent of altered expression

of the Bcl2 family members currently thought to be important for survival during β-selection. Thus, it is not known how c-Myb mediates survival during β-selection.

We have also demonstrated that in the absence of c-Myb, DN3 thymocytes performing β-selection enter S-phase but DN4 thymocytes contain a reduced proportion of cells in S-phase with an increase in <2n DNA content. Once again, data obtained from in vivo experiments detected impaired proliferation of DN4 thymocytes, not DN3 thymocytes where as data obtained from in vitro experiments detected impaired proliferation of DN3L thymocytes. Interestingly, the presence of a BrdU-negative <2n DNA content population demonstrated that cells are not entering the cell cycle and then dying, rather they die in G0/G1 which suggested that cells may not be receiving signals to enter the cell cycle. Our data demonstrates that c-Myb-deficient DN3 thymocytes appear to initiate proliferation and enter S-phase in response to pre-TCR generated signals but the proportion of DN4 thymocytes in S-phase is reduced and thymocytes undergo apoptosis. Cyclin D2 is expressed in DN3 thymocytes but is down-regulated during β-selection while cyclin D3 expression is induced in response to pre-TCR signaling [1]. Interestingly, cyclin D3 protein expression is severely reduced in *Myb*$^{f/f}$ DN3 *Tcrb*-Tg+ and anti-CD3ε stimulated *Myb*$^{f/f}$ *CR* thymocytes. The phenotype of *ccnd3*$^{-/-}$ thymocytes is very similar to *Myb*$^{f/f}$ *C* and *CRT* thymocytes in that *ccnd3*$^{-/-}$ mice contain thymi with severely reduced numbers of total thymocytes, reduced proportion of DN4 and ISP thymocytes in S-phase, and anti-CD3ε treatment of *ccnd3*$^{-/-}$*Rag2*$^{-/-}$ thymocytes does not increase thymic cellularity [1] all of which correlates with the proliferation

phenotype in *Myb*$^{f/f}$ *C* mice. Since cyclin D2 is expressed in DN3 thymocytes, it may mediate the initial rounds of proliferation of DN3 thymocytes during β-selection. As DN3 thymocytes differentiate to the DN4 stage cyclin D3 is necessary for efficient entry into S-phase. Thus, c-Myb-deficient thymocytes may be unable to perform the transition to dependency on cyclin D3 protein for continued proliferation during β-selection. The ability of *ccnd3*$^{-/-}$ thymocytes to survive was not addressed and it is possible that the reduction in thymic cellularity is also due to impaired survival in the absence of cyclin D3 [293]. Cyclin D3 has the potential to regulate survival of lymphocytes and retroviral expression of cyclin-D3 prevented apoptosis induced by phorbol myristate acetate and TCR activation of peripheral T cells [294]. In addition, reducing cyclin D3 expression through siRNA treatment resulted in cell cycle arrest at the G1 phase and an increase in apoptosis of a myeloma cell line [296]. Thus, there is evidence to suggest that expression of cyclin D3 can inhibit apoptosis and it is possible that cyclin D3 is also required to inhibit apoptosis in thymocytes performing β-selection.

Since we hypothesized that cyclin D3 has the potential to regulate proliferation and survival during β-selection, we retrovirally expressed cyclin D3 and GFP encoding cDNA fragments in *Myb*$^{f/f}$ *CRT* and *Myb*$^{f/f}$ *C* DN3 thymocytes to test if we could rescue cellularity of DN4 thymocytes. After testing different viral titers and culture conditions, we were unable to consistently detect an increase in the proportion of GFP+ DN4 and DP thymocytes, as compared to control vector, in more than one experiment. Since expression of cyclin D3 protein but not RNA is compromised in the absence of c-Myb

this suggested to us that c-Myb may be regulating cyclin D3 protein stability so we also infected DN3 thymocytes with a proteasomal resistant mutant of cyclin D3 but we were unable to obtain an increase in the proportion of GFP+ DN4 and DP thymocytes. In longer co-cultures containing control DN3 thymocytes that were infected with wildtype cyclin D3 or proteasomal resistant cyclin D3 retroviruses, thymocyte survival dramatically decreased. This could be due to the fact that in the longer co-cultures the majority of the cells were DP thymocytes which do not normally express cyclin D3 suggesting that forced expression of cyclin D3 is detrimental to DP thymocytes. Interestingly, we were unable to obtain a rescue by infecting *Myb*$^{f/f}$ *C* or *Myb*$^{f/f}$ *CRT* DN3 thymocytes with a retrovirus expressing a c-Myb encoding fragment. This suggests that infecting DN3 thymocytes that have developed without c-Myb may be too late for the cells to be able to recover by re-introducing c-Myb or cyclin D3. However, we were unable to efficiently infect *Myb*$^{f/f}$ *C* or *CRT* DN1/DN2 thymocytes to test if infecting earlier stage thymocytes with c-Myb or cyclin D3 may rescue DN3 cellularity. Another approach to using retroviral infection to express a cyclin D3 cDNA encoding fragment in thymocytes is to infect the bone marrow progenitor cells. It is possible that by infecting bone marrow progenitor cells with cyclin D3, these cells then select for cells that have been infected with amounts of cyclin D3 that are not detrimental to the cells. It would be very useful to infect bone marrow progenitor cells with c-Myb and cyclin D3 to try to rescue *Myb*$^{f/f}$ *CRT* thymocyte development. Thus, at this time it is not clear if the inability to express cyclin D3 contributes to or is the cause of apoptosis in *Myb*-deficient thymocytes.

Previous studies correlated expression of *Myb* mRNA with entry into the cell cycle during mid to late G1 or in S-phase [216, 258-260]. Interestingly, cyclin B1 was reported to be a transcriptional target of c-Myb [252], however, cyclin B1 is expressed during the G2/M phase. Here we provide evidence that c-Myb is required for proliferation of a subset of thymocytes and it is required for entry into the cell cycle and cyclin D3 protein expression. In the absence of c-Myb, expression of cyclin D3 does not appear to be altered at the transcriptional level according to RT-PCR and our gene expression microarrays which suggests that c-Myb is required for cyclin D3 protein expression. Cyclin D3 protein expression is repressed translationally by inhibiting translational elongation factor eEF2 and post-translationally by phosphorylation events which target it for proteasomal degradation which are mediated by GSK3β, $p38^{sapk2}$ and PP1 [299, 300]. However, we did not detect altered expression of known mediators of cyclin D3 protein expression according to our microarray analysis. It is possible that c-Myb regulates a mediator of cyclin D3 protein expression that has not been previously characterized. In order to prioritize genes on the microarray that may be involved in regulating translational or post-translational events, it would first be useful to determine if cyclin D3 is targeted for proteasomal degradation in the absence of c-Myb by examining cyclin D3 protein expression and phosphorylation status in anti-CD3ε treated *Rag2*$^{-/-}$ thymocytes cultured in the presence of proteasome inhibitors. However, the amount of protein obtained in these mice is extremely low and it may be better to address these questions in cell lines. The pre-T cell line SCB.29 expresses a TCRβ chain

[342]. c-Myb is expressed in the SCB.29 cell line and we would predict that cyclin D3 is expressed in the SCB.29 cells since cyclin D3 is expressed upon acquisition of a pre-TCR. We could treat SCB.29 cells with c-Myb siRNA to decrease expression of c-Myb and then treat cells with proteasome inhibitors to examine cyclin D3 protein expression and phosphorylation.

Moreover, we performed gene expression microarrays to identify mediators of c-Myb activity in DN2, DN3 and DN3 *Tcrb*-Tg+ thymocytes. By prioritizing genes and pathways involved in survival and proliferation whose expression patterns correlated with the phenotype of $Myb^{f/f}$ *C* mice, we generated hypothesises to test. We were particularly interested in the altered expression of genes involved in cell adhesion and interaction with the thymic microenvironment which include *Itga9, Itga4, Itgb2, Itgb7, Itgae*, *Bmf*, and *Mllt4*. *Bmf* is increased in the absence of c-Myb and since Bmf associates with the cytoskeleton and translocates to the mitochondria to induce apoptosis during anoikis [314], we hypothesized that the altered expression of integrins impaired the ability of *Myb*-deficient DN3 thymocytes to interact with the thymic microenvironment and induced apoptosis. Moreover, expression of *Mllt4* is increased in *Myb*-deficient thymocytes and it inhibits integrin β1 mediated adhesion [331]. Blocking integrin mediated interactions impaired DN3 differentiation [301] suggesting that expression of Mllt4 correlates with the impaired DN3 differentiation of *Myb*-deficient DN thymocytes. Thus, integrin mediated adhesion and signaling may be compromised in the absence of c-Myb. We tested the ability of *Myb*-deficient and control thymocytes

to interact with extracellular matrixes and migrate to CXCL12. Our data suggests that c-Myb-deficient total, DN3 and DN4 thymocytes do not efficiently migrate to CXCL12 even in the absence of an extracellular matrix protein. However, our data also suggests that thymocytes do not efficiently interact with the extracellular protein laminin-1 in the absence of c-Myb. Interactions between thymocytes with laminin and with CXCL12 are both required for DN thymocyte survival during β-selection [131, 132] (Personal communication with Paul Trampont and Kodi Ravichandran). Thus, we have uncovered a potential role for c-Myb during migration to CXCL12 and in interaction with laminin-1 that could either contribute to the impaired survival and proliferation in the absence of c-Myb or the impaired migration could be impaired due to the fact that DN3L and DN4 thymocytes undergo apoptosis. Thus, it is crucial that we rescue survival of *Myb*-deficient thymocytes in order to fully understand what roles c-Myb mediates versus what events are impaired due to cell death.

In conclusion, we have demonstrated that c-Myb is important for multiple events during differentiation of DN3E thymocytes to the DP stage and we have demonstrated for the first time that c-Myb is required for survival and cyclin D3 protein expression during β-selection. We also provide evidence that c-Myb can be required for proliferation of lymphocytes which has been questioned due to the fact that some populations of lymphocytes can proliferate without c-Myb [264]. It is not likely that the mechanism by which c-Myb regulates V(D)J recombination in DN3E thymocytes is similar to the mechanism it mediates during survival of DN3L thymocytes or in

expression of cyclin D3 in DN4 thymocytes. Moreover, cellularity of DN3 and DN4 thymocytes is reduced in *Myb*$^{f/f}$ *C* and *CRT* mice but not in *ccnd3*$^{-/-}$ mice which suggests that the failure to express cyclin D3 protein does not explain the entire phenotype in the absence of c-Myb. The most pressing question to answer now is how c-Myb mediates survival and cyclin D3 expression in DN3L and DN4 thymocytes. We were able to use data obtained from microarrays performed on DN2, DN3 and DN3 *Tcrb*-Tg+ thymocytes to prioritize genes and biological pathways that are greatly affected by the lack of c-Myb that may explain impaired survival and cyclin D3 expression. Testing the ability of these genes to partially rescue survival or proliferation by retroviral expression is the next step in this project. Since we were unable to rescue *Myb*$^{f/f}$ *CRT* DN3 thymocytes by retroviral expression of c-Myb, another approach to retroviral expression is to infect fetal thymic progenitor cells obtained by culturing fetal liver cells or to infect bone marrow progenitor cells from *Myb*$^{f/f}$ *C* or *CRT* mice.

Genes that were identified as high priority genes that will be useful to test if retroviral expression can rescue survival or proliferation include *Jun* and *Runx1*. A recent study reported that thymocyte specific deletion of Jun during the DN2 stage resulted in a partial block in DN3 to DN4 differentiation with impaired survival, but not proliferation, of DN3 and DN4 thymocytes [308]. Jun has the ability to inhibit apoptosis through repression of *Pten* (phosphatase and tensin homolog) mRNA expression leading to activation of the Akt pathway [309]. During pre-TCR signaling, Akt mediates survival by reducing mRNA and protein expression of pro-apoptotic member Bim [95] or through

glucose metabolism and Glut1 expression [310]. Although we did not detect a difference in *Pten*, *Bim* or *Glut1* expression according to our microarray analysis, it is possible that we are unable to detect cells with reduced expression of *Pten*, *Bim* or *Glut1* because they quickly undergo apoptosis. In addition, conditional deletion of *Runx1* in DN2 thymocytes resulted in a partial block in DN3 to DN4 differentiation and impaired DN4 proliferation [284]. A gene expression microarray performed on *Runx1*-null embryos suggested that Runx1 targets also include genes involved in cell motility, cell proliferation, and cytoskeletal organization according to a biological pathway analysis [313]. Since we also detect altered expression of genes involved in similar biological pathways in the absence of c-Myb, it is possible that c-Myb regulation of Runx1 contributes to β-selection proliferation and differentiation through regulation of the actin cytoskeleton and ECM-interactions.

Moreover, *Bmf* is the only Bcl2 family member whose expression is altered in the absence of c-Myb. Bmf induces anoikis and expression of Bmf is increased during anoikis which demonstrates that transcriptional regulation of Bmf can control anoikis [315]. Although there is no direct evidence that Bmf can induce apoptosis in DN3 thymocytes, over-expression of Bmf may contribute to apoptosis of DN3 thymocytes in the absence of c-Myb. Thus, Bmf is an interesting candidate gene to test if retroviral expression of Bmf in wildtype DN3 thymocytes induces apoptosis.

Since we were unable to detect changes in gene expression of genes involved in pre-TCR mediated survival in the absence of c-Myb, the inability to interact with laminin might explain the impaired survival of *Myb*-deficient thymocytes. It also might explain the inability to express cyclin D3 since cyclin D3 protein expression is downstream of integrin mediated signaling in TCR-stimulated peripheral T cells [302]. Moreover, the developmental stage specific expression of integrins on thymocytes and the patterned expression of extracellular matrix proteins in the thymus suggest that these interactions may control stage specific functions [127]. Thus, it is possible that the impaired interaction with laminin contributes to impaired survival, proliferation, and accelerated differentiation of c-Myb-deficient DN3 thymocytes. However, there is more than one gene whose expression is altered that may contribute to the reduced interaction with laminin making it difficult to identify one gene that may partially rescue DN3 differentiation. The best approach is to first identify if the inability to interact with laminin is integrin receptor driven or the result of downstream signaling events since c-Myb appears to regulate expression of genes involved in both processes. Different integrins interact with different laminin isoforms and if c-Myb-deficient thymocytes fail to interact efficiently with multiple isoforms, this would suggest that signaling downstream of integrin interactions is impaired making genes such as Mllt4 which directly inhibits integrin signaling or genes such as Pak1, Byfip1 and Pip5k2b which are involved downstream of integrin signaling to regulate the actin cytoskeleton, high priority genes. It is also possible that c-Myb deficient thymocytes fail to interact with specific isoforms of laminin which would suggest that altered Integrin expression is the

cause for impaired interaction making integrins that interact with the specific laminin isoforms top priority genes. Although integrin α4 has previously been reported to be a c-Myb transcriptional target [304], a functional role for c-Myb during cellular interaction with the microenvironment has not been demonstrated. If c-Myb proves to be required for interaction with the microenvironment during β-selection, this would be the first demonstration that c-Myb functionally mediates interaction with extracellular matrix proteins.

Appendix: Tables for gene expression microarrays

Table VI. List of potential c-Myb target genes in Tcrg-Tg+ DN3 thymocytes.

Gene Title	Gene Symbol	Entrez Gene	FCAbsolute (MT Vs CT)	Mt vs CT
RIKEN cDNA A930013B10 gene	A930013B10Rik	414094	14.20	down
SH2 domain protein 1A	Sh2d1a	20400	9.14	down
calcium/calmodulin-dependent protein kinase IV	Camk4	12326	8.39	down
			8.13	down
expressed sequence BE136769	BE136769	497653	5.70	down
Nebulette	Nebl	74103	5.46	down
RIKEN cDNA A930013B10 gene	A930013B10Rik	414094	5.02	down
RIKEN cDNA 1500009L16 gene	1500009L16Rik	69784	4.93	down
Transcribed locus			4.48	down
diacylglycerol kinase, epsilon	Dgke	56077	4.45	down
solute carrier family 9 (sodium/hydrogen exchanger), isoform 9	Slc9a9	331004	4.35	down
LON peptidase N-terminal domain and ring finger 1 /// similar to CG32369-PB, isoform B	Lonrf1 /// LOC631639	244421 /// 631639	4.19	down
annexin A2	Anxa2	12306	4.13	down
RIKEN cDNA 1700097N02 gene	1700097N02Rik	67522	4.12	down
aquaporin 11	Aqp11	66333	4.09	down
zinc finger protein 36, C3H type-like 2	Zfp36l2	12193	4.01	down
nuclear factor of kappa light polypeptide gene enhancer in B-cells inhibitor, epsilon	Nfkbie	18037	4.01	down
RIKEN cDNA 1700097N02 gene	1700097N02Rik	67522	3.96	down
lectin, galactose binding, soluble 9	Lgals9	16859	3.74	down
metal response element binding transcription factor 2	Mtf2	17765	3.66	down
coiled-coil domain containing 18	Ccdc18	73254	3.55	down
metal response element binding transcription factor 2	Mtf2	17765	3.54	down
placental protein 11 related	Pp11r	19011	3.50	down
brain expressed gene 1	Bex1	19716	3.49	down
RIKEN cDNA 1190002N15 gene	1190002N15Rik	68861	3.48	down
CD96 antigen	Cd96	84544	3.44	down
nuclear receptor subfamily 3, group C, member 1	Nr3c1	14815	3.40	down
transmembrane protein 16F	Tmem16f	105722	3.40	down
placental protein 11 related	Pp11r	19011	3.34	down
Aquaporin 11	Aqp11	66333	3.31	down
metal response element binding transcription factor 2	Mtf2	17765	3.29	down
nuclear receptor subfamily 3, group C, member 1	Nr3c1	14815	3.26	down
RIKEN cDNA D330017J20 gene	D330017J20Rik	320609	3.23	down
CREBBP/EP300 inhibitory protein 2	Cri2	386655	3.19	down
spermatogenesis associated, serine-rich 2	Spats2	72572	3.18	down
transmembrane protein 16F	Tmem16f	105722	3.12	down
ligase IV, DNA, ATP-dependent	Lig4	319583	3.06	down
nuclear receptor subfamily 3, group C, member 1	Nr3c1	14815	3.04	down
aquaporin 11	Aqp11	66333	3.01	down
nuclear factor of kappa light polypeptide gene enhancer in B-cells inhibitor, epsilon	Nfkbie	18037	3.01	down
gene model 323, (NCBI)	Gm323	210573	2.94	down
protein tyrosine phosphatase, receptor type, F	Ptprf	19268	2.93	down
membrane-spanning 4-domains, subfamily A, member 6B	Ms4a6b	69774	2.93	down
CD24a antigen	Cd24a	12484	2.92	down
Aquaporin 11	Aqp11	66333	2.76	down
			2.71	down
integrin alpha 4	Itga4	16401	2.70	down
ER degradation enhancer, mannosidase alpha-like 1	Edem1	192193	2.68	down
metal response element binding transcription factor 2	Mtf2	17765	2.68	down
calmodulin regulated spectrin-associated protein 1-like 1	Camsap1l1	67886	2.67	down
RIKEN cDNA 5830468F06 gene	5830468F06Rik	76082	2.65	down
RIKEN cDNA 1190002N15 gene	1190002N15Rik	68861	2.60	down
tubulin, beta 2b	Tubb2b	73710	2.60	down
hypothetical protein 6430570G24	6430570G24	327989	2.58	down
myristoylated alanine rich protein kinase C substrate	Marcks	17118	2.56	down

RIKEN cDNA C330011F01 gene /// RIKEN cDNA 6430706D22 gene	C330011F01Rik /// 6430706D22Rik	381280 /// 78605	2.56	down
N-myc downstream regulated gene 1	Ndrg1	17988	2.51	down
kinesin family member 11	Kif11	16551	2.51	down
cyclic AMP-regulated phosphoprotein, 21	Arpp21	74100	2.49	down
non-catalytic region of tyrosine kinase adaptor protein 2	Nck2	17974	2.49	down
solute carrier family 30 (zinc transporter), member 4	Slc30a4	22785	2.49	down
runt related transcription factor 1	Runx1	12394	2.49	down
troponin T1, skeletal, slow	Tnnt1	21955	2.49	down
Rap guanine nucleotide exchange factor (GEF) 3	Rapgef3	223864	2.48	down
growth factor independent 1	Gfi1	14581	2.45	down
myosin light chain 2, precursor lymphocyte-specific	Mylc2pl	59310	2.45	down
platelet-activating factor acetylhydrolase, isoform 1b, alpha1 subunit	Pafah1b3	18476	2.43	down
ceramide kinase-like	Cerkl	228094	2.43	down
Rap guanine nucleotide exchange factor (GEF) 3	Rapgef3	223864	2.42	down
RIKEN cDNA B430201A12 gene	B430201A12Rik	329739	2.41	down
Casitas B-lineage lymphoma	Cbl	12402	2.40	down
CCR4-NOT transcription complex, subunit 2	Cnot2	72068	2.38	down
nuclear receptor interacting protein 1	Nrip1	268903	2.37	down
Cut-like 1 (Drosophila)	Cutl1	13047	2.37	down
dynein, axonemal, heavy chain 8	Dnahc8	13417	2.30	down
potassium channel tetramerisation domain containing 1	Kctd1	106931	2.30	down
CCR4-NOT transcription complex, subunit 2	Cnot2	72068	2.29	down
FYN binding protein	Fyb	23880	2.27	down
oxysterol binding protein-like 1A	Osbpl1a	64291	2.27	down
Rho GTPase activating protein 9	Arhgap9	216445	2.26	down
brain abundant, membrane attached signal protein 1	Basp1	70350	2.22	down
prickle like 1 (Drosophila)	Prickle1	106042	2.21	down
small EDRK-rich factor 1	Serf1	20365	2.19	down
0 day neonate cerebellum cDNA, RIKEN full-length enriched library, clone:C230070N19 product:myristoylated alanine rich protein kinase C substrate, full insert sequence			2.18	down
zinc and ring finger 1	Znrf1	170737	2.18	down
Casitas B-lineage lymphoma	Cbl	12402	2.18	down
interleukin 17 receptor B	Il17rb	50905	2.18	down
hypothetical protein 6430570G24	6430570G24	327989	2.18	down
Kruppel-like factor 9	Klf9	16601	2.17	down
cut-like 1 (Drosophila)	Cutl1	13047	2.17	down
integrin alpha 4	Itga4	16401	2.16	down
6-phosphogluconolactonase	Pgls	66171	2.15	down
smoothened homolog (Drosophila)	Smo	319757	2.15	down
CKLF-like MARVEL transmembrane domain containing 7	Cmtm7	102545	2.15	down
DNA segment, Chr 9, University of California at Los Angeles 1	D9Ucla1	102644	2.13	down
cyclic AMP-regulated phosphoprotein, 21	Arpp21	74100	2.11	down
Coiled-coil-helix-coiled-coil-helix domain containing 3	Chchd3	66075	2.11	down
src family associated phosphoprotein 1	Scap1	78473	2.10	down
cut-like 1 (Drosophila)	Cutl1	13047	2.10	down
cerebellar degeneration-related 2	Cdr2	12585	2.09	down
cyclin-dependent kinase 6	Cdk6	12571	2.08	down
solute carrier family 22 (organic cation transporter), member 3	Slc22a3	20519	2.07	down
expressed sequence AI834762	AI834762	98429	2.06	down
inositol 1,4,5-triphosphate receptor 2	Itpr2	16439	2.06	down
Rho GTPase activating protein 9	Arhgap9	216445	2.05	down
neuroligin 2	Nlgn2	216856	2.04	down
amyotrophic lateral sclerosis 2 (juvenile) homolog (human)	Als2	74018	2.04	down
expressed sequence AI504432	AI504432	229694	2.03	down
RIKEN cDNA 3110001A13 gene	3110001A13Rik	66540	2.02	down
selectin, lymphocyte	Sell	20343	2.02	down
palmitoyl-protein thioesterase 1	Ppt1	19063	2.02	down
prostaglandin E receptor 4 (subtype EP4)	Ptger4	19219	2.01	down
phosphoinositide-3-kinase, catalytic, gamma polypeptide	Pik3cg	30955	2.00	down
RIKEN cDNA 1500031L02 gene	1500031L02Rik	66994	2.00	down
CCR4-NOT transcription complex, subunit 2	Cnot2	72068	2.00	down
RIKEN cDNA 3110001A13 gene	3110001A13Rik	66540	1.97	down
RIKEN cDNA 2700083E18 gene	2700083E18Rik	72640	1.97	down

Prohibitin	Phb	18673	1.96	down
A kinase (PRKA) anchor protein (gravin) 12	Akap12	83397	1.95	down
RIKEN cDNA A830010M20 gene	A830010M20Rik	231570	1.94	down
solute carrier family 43, member 1	Slc43a1	72401	1.93	down
inositol 1,4,5-triphosphate receptor 2	Itpr2	16439	1.92	down
SET and MYND domain containing 3	Smyd3	69726	1.92	down
B-cell translocation gene 3 /// similar to BTG3 protein (Tob5 protein) (Abundant in neuroepithelium area protein) /// B-cell translocation gene 3 pseudogene	Btg3 /// LOC640416 /// LOC654432	12228 /// 640416 /// 654432	1.90	down
Rho GTPase activating protein 26	Arhgap26	71302	1.90	down
Transcribed locus			1.88	down
calponin 3, acidic	Cnn3	71994	1.85	down
myocyte enhancer factor 2A	Mef2a	17258	1.84	down
glucocorticoid induced transcript 1	Glcci1	170772	1.83	down
DNA segment, Chr 15, Wayne State University 75, expressed	D15Wsu75e	28075	1.83	down
FCH domain only 1	Fcho1	74015	1.82	down
par-6 partitioning defective 6 homolog gamma (C. elegans)	Pard6g	93737	1.81	down
Tax1 (human T-cell leukemia virus type I) binding protein 1	Tax1bp1	52440	1.81	down
expressed sequence AI504432	AI504432	229694	1.80	down
tubulin, alpha 1	Tuba1	22142	1.80	down
selectin, lymphocyte	Sell	20343	1.79	down
ADP-ribosylation factor-like 6 interacting protein 1	Arl6ip1	54208	1.77	down
cell division cycle associated 7	Cdca7	66953	1.77	down
protein regulator of cytokinesis 1	Prc1	233406	1.76	down
catenin (cadherin associated protein), alpha 1	Ctnna1	12385	1.75	down
RIKEN cDNA 4930427A07 gene	4930427A07Rik	104732	1.75	down
aryl-hydrocarbon receptor	Ahr	11622	1.74	down
zinc finger, MYM domain containing 1	Zmym1	68310	1.73	down
hairy and enhancer of split 6 (Drosophila)	Hes6	55927	1.72	down
leucine rich repeat containing 42	Lrrc42	77809	1.72	down
vascular endothelial zinc finger 1	Vezf1	22344	1.72	down
			1.69	down
RAB27A, member RAS oncogene family	Rab27a	11891	1.69	down
DNA segment, Chr 17, human D6S56E 5	D17H6S56E-5	110956	1.67	down
catenin (cadherin associated protein), alpha 1	Ctnna1	12385	1.67	down
galactokinase 1	Galk1	14635	1.66	down
death associated protein 3	Dap3	65111	1.65	down
interleukin 17 receptor A	Il17ra	16172	1.63	down
expressed sequence AA536743	AA536743	100532	1.61	down
cytoskeleton associated protein 2	Ckap2	80986	1.61	down
DNA segment, Chr 15, Wayne State University 75, expressed	D15Wsu75e	28075	1.60	down
sialophorin	Spn	20737	1.59	down
RIKEN cDNA 4930534B04 gene	4930534B04Rik	75216	1.59	down
single-stranded DNA binding protein 3	Ssbp3	72475	1.59	down
metastasis associated 3	Mta3	116871	1.58	down
protein phosphatase 2 (formerly 2A), catalytic subunit, beta isoform	Ppp2cb	19053	1.57	down
transcription termination factor, RNA polymerase II	Ttf2	74044	1.56	down
regulatory factor X-associated protein	Rfxap	170767	1.56	down
hypothetical protein A730046J16	A730046J16	329124	1.56	down
inositol (myo)-1(or 4)-monophosphatase 2	Impa2	114663	1.54	down
zinc finger, DHHC domain containing 14	Zdhhc14	224454	1.54	down
three prime histone mRNA exonuclease 1	Thex1	67276	1.54	down
RE1-silencing transcription factor	Rest	19712	1.53	down
transforming, acidic coiled-coil containing protein 3	Tacc3	21335	1.52	down
Fgfr1 oncogene partner	Fgfr1op	75296	1.52	down
interleukin enhancer binding factor 3	Ilf3	16201	1.51	down
RIKEN cDNA 4930427A07 gene	4930427A07Rik	104732	1.51	down
zinc finger, DHHC domain containing 14	Zdhhc14	224454	1.50	down
hydroxysteroid dehydrogenase like 1	Hsdl1	72552	1.50	down
RIKEN cDNA 9130023F12 gene	9130023F12Rik	216549	1.49	down
kelch-like 6 (Drosophila)	Klhl6	239743	1.49	down
protein regulator of cytokinesis 1	Prc1	233406	1.48	down
bromodomain containing 8	Brd8	78656	1.48	down
M-phase phosphoprotein 9	Mphosph9	269702	1.47	down
brix domain containing 1	Bxdc1	67239	1.47	down

Serpine1 mRNA binding protein 1	Serbp1	66870	1.46	down
YY1 transcription factor	Yy1	22632	1.45	down
SET domain containing 4	Setd4	224440	1.45	down
centaurin, beta 1	Centb1	216859	1.45	down
RIKEN cDNA 2410001C21 gene	2410001C21Rik	66404	1.44	down
E2F transcription factor 6	E2f6	50496	1.44	down
cell division cycle associated 4	Cdca4	71963	1.43	down
src family associated phosphoprotein 1	Scap1	78473	1.42	down
G-protein signalling modulator 2 (AGS3-like, C. elegans)	Gpsm2	76123	1.42	down
Wolf-Hirschhorn syndrome candidate 1 (human)	Whsc1	107823	1.41	down
p21 (CDKN1A)-activated kinase 1	Pak1	18479	1.40	down
synapse defective 1, Rho GTPase, homolog 2 (C. elegans) /// similar to synapse defective 1, Rho GTPase, homolog 1	Syde2 /// LOC639654	214804 /// 639654	1.40	down
cleavage stimulation factor, 3' pre-RNA subunit 2	Cstf2	108062	1.38	down
zinc finger protein 496	Zfp496	268417	1.36	down
Terf1 (TRF1)-interacting nuclear factor 2	Tinf2	28113	1.36	down
B-cell leukemia/lymphoma 2	Bcl2	12043	1.35	down
surfeit gene 5	Surf5	20933	1.33	down
interleukin 7 receptor	Il7r	16197	1.32	down
F-box and leucine-rich repeat protein 14	Fbxl14	101358	1.31	down
exocyst complex component 6	Exoc6	107371	1.31	down
glyoxalase 1	Glo1	109801	1.31	down
RIKEN cDNA F730047E07 gene	F730047E07Rik	212377	1.30	down
myelin basic protein expression factor 2, repressor	Myef2	17876	1.29	down
zinc finger, A20 domain containing 2	Za20d2	22682	1.29	down
receptor accessory protein 5	Reep5	13476	1.29	down
Rho GTPase activating protein 15	Arhgap15	76117	1.27	down
ribonuclease III, nuclear	Rnasen	14000	1.27	down
chromobox homolog 5 (Drosophila HP1a)	Cbx5	12419	1.26	down
nucleolar complex associated 4 homolog (S. cerevisiae)	Noc4l	100608	1.24	down
MARVEL (membrane-associating) domain containing 1	Marveld1	277010	1.16	down
glial cell line derived neurotrophic factor family receptor alpha 1	Gfra1	14585	18.32	up
deltex 1 homolog (Drosophila)	Dtx1	14357	16.52	up
myeloid/lymphoid or mixed lineage-leukemia translocation to 4 homolog (Drosophila)	Mllt4	17356	16.48	up
stanniocalcin 1	Stc1	20855	14.54	up
DEP domain containing 6	Depdc6	97998	11.97	up
DEP domain containing 6	Depdc6	97998	11.35	up
suppressor of cytokine signaling 3	Socs3	12702	10.97	up
GTPase, IMAP family member 4	Gimap4	107526	10.61	up
suppressor of cytokine signaling 3	Socs3	12702	10.60	up
CD160 antigen	Cd160	54215	9.49	up
DEP domain containing 6	Depdc6	97998	9.07	up
Bcl2 modifying factor	Bmf	171543	9.05	up
B and T lymphocyte associated	Btla	208154	6.71	up
Ena-vasodilator stimulated phosphoprotein	Evl	14026	6.52	up
bromodomain, testis-specific	Brdt	114642	6.26	up
cathepsin S	Ctss	13040	5.59	up
tissue inhibitor of metalloproteinase 2	Timp2	21858	5.40	up
ADP-ribosylation factor-like 4C /// similar to ADP-ribosylation factor-like protein 7	Arl4c /// LOC632433	320982 /// 632433	5.21	up
hepatoma-derived growth factor, related protein 3	Hdgfrp3	29877	4.93	up
calpain 5	Capn5	12337	4.93	up
tissue inhibitor of metalloproteinase 2	Timp2	21858	4.90	up
			4.74	up
dopa decarboxylase	Ddc	13195	4.68	up
sporulation protein, meiosis-specific, SPO11 homolog (S. cerevisiae) /// similar to Meiotic recombination protein SPO11	Spo11 /// LOC675982	26972 /// 675982	4.35	up
HIV-1 Rev binding protein	Hrb	15463	4.25	up
integrin alpha 9	Itga9	104099	4.18	up
B-cell translocation gene 1, anti-proliferative	Btg1	12226	4.10	up
tissue inhibitor of metalloproteinase 2	Timp2	21858	4.08	up
HIV-1 Rev binding protein	Hrb	15463	4.05	up
B-cell translocation gene 1, anti-proliferative	Btg1	12226	3.98	up
hemogen	Hemgn	93966	3.94	up

			3.92	up
HIV-1 Rev binding protein	Hrb	15463	3.90	up
HIV-1 Rev binding protein	Hrb	15463	3.77	up
hepatoma-derived growth factor, related protein 3 /// transmembrane 6 superfamily member 1	Hdgfrp3 /// Tm6sf1	107769 /// 29877	3.51	up
serine (or cysteine) peptidase inhibitor, clade B, member 1a	Serpinb1a	66222	3.44	up
DNA segment, Chr 1, ERATO Doi 564, expressed	D1Ertd564e	52347	3.42	up
hepatoma-derived growth factor, related protein 3	Hdgfrp3	29877	3.37	up
v-myc myelocytomatosis viral related oncogene, neuroblastoma derived (avian)	Mycn	18109	3.37	up
solute carrier organic anion transporter family, member 4a1	Slco4a1	108115	3.27	up
prostaglandin E receptor 3 (subtype EP3)	Ptger3	19218	3.25	up
caspase 1	Casp1	12362	3.21	up
similar to ADP-ribosylation factor-like protein 7	LOC632433	632433	3.16	up
fatty acid binding protein 4, adipocyte	Fabp4	11770	3.15	up
Notch gene homolog 3 (Drosophila)	Notch3	18131	3.13	up
Transcribed locus			3.11	up
tribbles homolog 2 (Drosophila)	Trib2	217410	3.08	up
Nuclear antigen Sp100	Sp100	20684	2.98	up
RIKEN cDNA C130080N23 gene	C130080N23Rik	226829	2.97	up
fatty acid binding protein 5, epidermal	Fabp5	16592	2.94	up
DEP domain containing 6	Depdc6	97998	2.92	up
GRAM domain containing 3	Gramd3	107022	2.91	up
Notch gene homolog 3 (Drosophila)	Notch3	18131	2.90	up
lymphocyte specific 1	Lsp1	16985	2.83	up
Coactosin-like 1 (Dictyostelium)	Cotl1	72042	2.83	up
matrilin 2	Matn2	17181	2.79	up
selenoprotein P, plasma, 1	Sepp1	20363	2.79	up
GRP1 (general receptor for phosphoinositides 1)-associated scaffold protein	Grasp	56149	2.77	up
CD52 antigen	Cd52	23833	2.77	up
coactosin-like 1 (Dictyostelium)	Cotl1	72042	2.74	up
integrin beta 7	Itgb7	16421	2.74	up
S100 calcium binding protein A4	S100a4	20198	2.68	up
lymphocyte antigen 6 complex, locus C	Ly6c	17067	2.66	up
transmembrane 6 superfamily member 1	Tm6sf1	107769	2.65	up
			2.62	up
ecotropic viral integration site 2a	Evi2a	14017	2.60	up
matrilin 2	Matn2	17181	2.58	up
Kruppel-like factor 2 (lung)	Klf2	16598	2.53	up
DNA segment, Chr 8, ERATO Doi 82, expressed	D8Ertd82e	244418	2.52	up
G protein-coupled receptor 177	Gpr177	68151	2.51	up
Tnf receptor-associated factor 1	Traf1	22029	2.43	up
RIKEN cDNA A630077B13 gene	A630077B13Rik	215900	2.43	up
hepatoma-derived growth factor, related protein 3	Hdgfrp3	29877	2.43	up
Transcribed locus			2.41	up
Casitas B-lineage lymphoma b	Cblb	208650	2.40	up
tescalcin	Tesc	57816	2.38	up
E26 avian leukemia oncogene 2, 3' domain	Ets2	23872	2.37	up
Max dimerization protein 4	Mxd4	17122	2.36	up
recombination activating gene 1	Rag1	19373	2.34	up
integrin beta 2	Itgb2	16414	2.32	up
CD160 antigen	Cd160	54215	2.31	up
purinergic receptor P2Y, G-protein coupled, 5	P2ry5	67168	2.30	up
SH3-domain binding protein 5 (BTK-associated)	Sh3bp5	24056	2.29	up
zinc finger protein 53	Zfp53	24132	2.25	up
B-cell CLL/lymphoma 9-like	Bcl9l	80288	2.25	up
Abelson helper integration site	Ahi1	52906	2.24	up
aldehyde dehydrogenase 1 family, member B1	Aldh1b1	72535	2.24	up
tocopherol (alpha) transfer protein	Ttpa	50500	2.22	up
death-associated protein	Dap	223453	2.21	up
DENN/MADD domain containing 2D	Dennd2d	72121	2.21	up
coactosin-like 1 (Dictyostelium)	Cotl1	72042	2.16	up
neuron specific gene family member 2	Nsg2	18197	2.13	up
CD53 antigen	Cd53	12508	2.09	up
expressed sequence C85492	C85492	215494	2.08	up

mitogen-activated protein kinase-activated protein kinase 3	Mapkapk3	102626	2.04	up
coactosin-like 1 (Dictyostelium)	Cotl1	72042	2.00	up
coagulation factor II (thrombin) receptor	F2r	14062	2.00	up
lysosomal acid lipase 1	Lip1	16889	1.98	up
dehydrogenase/reductase (SDR family) member 8	Dhrs8	114664	1.97	up
B-cell CLL/lymphoma 9-like	Bcl9l	80288	1.93	up
RIKEN cDNA C920005C14 gene	C920005C14Rik	338368	1.93	up
RIKEN cDNA 2310043N10 gene	2310043N10Rik	66961	1.92	up
anthrax toxin receptor 1	Antxr1	69538	1.92	up
signal transducer and activator of transcription 4	Stat4	20849	1.91	up
solute carrier organic anion transporter family, member 4a1	Slco4a1	108115	1.87	up
ATP-binding cassette, sub-family C (CFTR/MRP), member 5	Abcc5	27416	1.86	up
threonine aldolase 1	Tha1	71776	1.85	up
RIKEN cDNA 5330431N19 gene	5330431N19Rik	226162	1.85	up
cytoplasmic FMR1 interacting protein 1	Cyfip1	20430	1.84	up
			1.80	up
protein tyrosine phosphatase, non-receptor type 6	Ptpn6	15170	1.79	up
synaptic nuclear envelope 1	Syne1	64009	1.76	up
ATPase, Na+/K+ transporting, beta 1 polypeptide	Atp1b1	11931	1.76	up
ATPase, Na+/K+ transporting, beta 1 polypeptide	Atp1b1	11931	1.75	up
plakophilin 4	Pkp4	227937	1.74	up
cDNA sequence BC031353	BC031353	235493	1.71	up
neuron specific gene family member 2	Nsg2	18197	1.71	up
tumor necrosis factor receptor superfamily, member 18	Tnfrsf18	21936	1.70	up
runt related transcription factor 3	Runx3	12399	1.70	up
pleckstrin homology, Sec7 and coiled-coil domains, binding protein	Pscdbp	227929	1.69	up
RAS-like, family 11, member B	Rasl11b	68939	1.65	up
acyl-Coenzyme A dehydrogenase, very long chain	Acadvl	11370	1.64	up
somatostatin receptor 2	Sstr2	20606	1.63	up
RIKEN cDNA 1200003I10 gene /// RIKEN cDNA 1200015M12 gene /// RIKEN cDNA 1200016E24 gene /// RIKEN cDNA A130040M12 gene /// RIKEN cDNA E430024C06 gene	1200003I10Rik /// 1200015M12Rik /// 1200016E24Rik /// A130040M12Rik /// E430024C06Rik	319202 /// 319269 /// 319443 /// 71719 /// 71739	1.58	up
transcription factor 4	Tcf4	21413	1.52	up
HRAS like suppressor 3	Hrasls3	225845	1.51	up
solute carrier family 12, member 7	Slc12a7	20499	1.46	up
TSC22 domain family, member 1	Tsc22d1	21807	1.45	up
RIKEN cDNA 2610002F03 gene	2610002F03Rik	72091	1.39	up
vacuolar protein sorting 41 (yeast)	Vps41	218035	1.37	up
transmembrane protein 24	Tmem24	71764	1.35	up
DNA segment, Chr 7, Wayne State University 128, expressed	D7Wsu128e	28018	1.30	up
carbonyl reductase 4	Cbr4	234309	1.22	up
RIKEN cDNA B330012G18 gene	B330012G18Rik	320419	1.21	up
eukaryotic translation initiation factor 2, subunit 2 (beta)	Eif2s2	67204	1.12	up

Table VII. ***List of potential c-Myb target genes in DN3 thymocytes***

Gene Title	Gene Symbol	Entrez Gene	FCAbsolute (MT Vs CT)	Mt vs CT	Corrected Pvalue (MT Vs CT)
superkiller viralicidic activity 2-like 2 (S. cerevisiae)	Skiv2l2	72198	139.95087	up	0.00437433
heat shock protein 1B	Hspa1b	15511	33.748985	down	0.1205879
heat shock protein 1B	Hspa1b	15511	31.114056	down	0.16061288
heat shock protein 1B	Hspa1b	15511	29.747513	down	0.13120921
cathepsin S	Ctss	13040	24.409958	up	0.19388737
integrin alpha 9	Itga9	104099	20.368328	up	0.12956084
FBJ osteosarcoma oncogene	Fos	14281	18.081896	down	0.14619021
carbonic anhydrase 8 /// similar to Carbonic anhydrase-related protein (CARP) (CA-VIII)	Car8 /// LOC676792	12319 /// 676792	15.884071	up	0.19265634
Heparanase	Hpse	15442	14.112086	up	0.18007219
DEP domain containing 6	Depdc6	97998	11.83638	up	0.12956084
glutamate receptor, ionotropic, AMPA2 (alpha 2)	Gria2	14800	11.002369	up	0.16061288
expressed sequence AI593864	AI593864	103794	10.788857	up	0.1857715
naked cuticle 1 homolog (Drosophila) /// similar to naked cuticle 1 homolog /// similar to naked cuticle 1 homolog	Nkd1 /// LOC634379 /// LOC671838	634379 /// 671838 /// 93960	10.101104	up	0.16061288
Epstein-Barr virus induced gene 2	Ebi2	321019	9.515759	up	0.19930862
DEP domain containing 6	Depdc6	97998	9.293585	up	0.11540385
RIKEN cDNA A930013B10 gene	A930013B10Rik	414094	9.237827	down	0.12956084
SH2 domain protein 1A	Sh2d1a	20400	8.181489	down	0.18087949
integrin alpha 9	Itga9	104099	8.156744	up	0.02481114
early growth response 1	Egr1	13653	7.1913385	down	0.19535129
amyotrophic lateral sclerosis 2 (juvenile) chromosome region, candidate 12 (human)	Als2cr12	108812	6.517745	up	0.19218668
RIKEN cDNA A930013B10 gene	A930013B10Rik	414094	6.4343796	down	0.13078395
ubiquitin-conjugating enzyme E2E 2 (UBC4/5 homolog, yeast)	Ube2e2	218793	6.130635	up	0.12956084
Casitas B-lineage lymphoma b	Cblb	208650	5.5174794	up	0.19535129
diacylglycerol kinase, epsilon	Dgke	56077	5.4765525	down	0.18721637
suppressor of cytokine signaling 3	Socs3	12702	5.358732	up	0.1917803
Ras-related GTP binding D	Rragd	52187	5.2051725	down	0.16952358
Beta-2 microglobulin	B2m	12010	4.7806807	up	0.13209315
leucine-rich repeats and immunoglobulin-like domains 1	Lrig1	16206	4.7529726	up	0.1720623
fibroblast growth factor 13	Fgf13	14168	4.7329936	down	0.16061288
suppressor of cytokine signaling 3	Socs3	12702	4.714256	up	0.12956084
DNA segment, Chr 1, ERATO Doi 564, expressed	D1Ertd564e	52347	4.626779	up	0.194536
RIKEN cDNA 2010300C02 gene /// similar to Y59A8B.19	2010300C02Rik /// LOC639555	639555 /// 72097	4.5162177	up	0.19388737
neural precursor cell expressed, developmentally down-regulated gene 9	Nedd9	18003	4.5138855	up	0.16061288
RIKEN cDNA 6820402I19 gene	6820402I19Rik	74509	4.419848	up	0.17178465
Coactosin-like 1 (Dictyostelium)	Cotl1	72042	4.353042	up	0.19535129
			4.332885	up	0.13120921
placental protein 11 related	Pp11r	19011	4.326833	down	0.07479045
			4.3014574	up	0.1917803
RIKEN cDNA 1500009L16 gene	1500009L16Rik	69784	4.190327	down	0.12956084
zinc finger protein, subfamily 1A, 3 (Aiolos)	Zfpn1a3	22780	4.086614	down	0.19535129
phosphatidic acid phosphatase type 2B	Ppap2b	67916	4.0094934	up	0.12956084
DNA segment, Chr 10, Brigham & Women's Genetics 1379 expressed	D10Bwg1379e	215821	3.9756334	up	0.17577663
diacylglycerol kinase, epsilon	Dgke	56077	3.8861399	down	0.18909477
dynein, axonemal, heavy chain 8	Dnahc8	13417	3.861198	down	0.1857715
cDNA sequence BC035044	BC035044	232406	3.632033	down	0.1857715
hypothetical protein 6430570G24	6430570G24	327989	3.5026073	down	0.19930862
Cd200 antigen	Cd200	17470	3.4172463	down	0.11170884
thymocyte selection-associated HMG box gene	Tox	252838	3.399171	down	0.19535129
neural precursor cell expressed, developmentally down-regulated gene 9	Nedd9	18003	3.3940742	up	0.14687656
LON peptidase N-terminal domain and ring finger 1 /// similar to CG32369-PB, isoform B	Lonrf1 /// LOC631639	244421 /// 631639	3.3593605	down	0.18007219
Wolfram syndrome 1 homolog (human)	Wfs1	22393	3.3529649	up	0.12956084
placental protein 11 related	Pp11r	19011	3.327945	down	0.11540385
Kruppel-like factor 4 (gut)	Klf4	16600	3.3164701	down	0.13120921

RIKEN cDNA 2310042L06 gene	2310042L06Rik	76457	3.1629298	up	0.19388737
SKI-like	Skil	20482	3.1305223	down	0.1917803
similar to ADP-ribosylation factor-like protein 7	LOC632433	632433	3.1001225	up	0.1668137
ligase IV, DNA, ATP-dependent	Lig4	319583	3.0965648	down	0.19535129
angiopoietin 1	Angpt1	11600	3.0916622	down	0.18932593
RIKEN cDNA 4631427C17 gene	4631427C17Rik	74340	3.085995	down	0.13120921
RIKEN cDNA A630001G21 gene	A630001G21Rik	319997	2.994173	up	0.19535129
tumor necrosis factor, alpha-induced protein 8-like 1	Tnfaip8l1	66443	2.9719565	down	0.12956084
0 day neonate thymus cDNA, RIKEN full-length enriched library, clone:A430066P15 product:hypothetical protein, full insert sequence			2.853143	down	0.1857715
meiosis-specific nuclear structural protein 1	Mns1	17427	2.851746	down	0.13120921
Casitas B-lineage lymphoma b	Cblb	208650	2.7965171	up	0.16061288
integrin, alpha E, epithelial-associated	Itgae	16407	2.7814999	up	0.11170884
solute carrier organic anion transporter family, member 4a1	Slco4a1	108115	2.7650347	up	0.15757187
Rap guanine nucleotide exchange factor (GEF) 3	Rapgef3	223864	2.7623765	down	0.19535129
neuropilin 1	Nrp1	18186	2.7471693	down	0.1857715
CD82 antigen	Cd82	12521	2.744474	up	0.1668137
prickle like 1 (Drosophila)	Prickle1	106042	2.6979766	down	0.12956084
RIKEN cDNA 4632418H02 gene	4632418H02Rik	78265	2.6317568	up	0.1857715
zinc finger protein 623	Zfp623	78834	2.6258576	down	0.1857715
Casitas B-lineage lymphoma b	Cblb	208650	2.61517	up	0.12956084
TBC1 domain family, member 24	Tbc1d24	224617	2.45189	down	0.1857715
transmembrane protein 16F	Tmem16f	105722	2.4169276	down	0.16061288
WW domain-containing oxidoreductase	Wwox	80707	2.2705238	down	0.1720623
RIKEN cDNA 2900002H16 gene	2900002H16Rik	75695	2.2477043	down	0.19535129
Heterogeneous nuclear ribonucleoprotein U	Hnrpu	51810	2.2076535	up	0.16061288
tumor necrosis factor receptor superfamily, member 18	Tnfrsf18	21936	2.193958	up	0.06781627
retinol dehydrogenase 10 (all-trans)	Rdh10	98711	2.190228	up	0.11540385
ankyrin repeat domain 25	Ankrd25	235041	2.116379	down	0.1857715
transforming, acidic coiled-coil containing protein 1	Tacc1	320165	2.1039746	down	0.19265634
runt related transcription factor 1	Runx1	12394	2.0848548	down	0.13120921
abhydrolase domain containing 4	Abhd4	105501	2.0509849	down	0.19535129
death associated protein kinase 1	Dapk1	69635	2.0477953	down	0.1857715
			2.0295503	down	0.07479045
ER degradation enhancer, mannosidase alpha-like 1	Edem1	192193	1.9900616	down	0.19535129
aryl-hydrocarbon receptor	Ahr	11622	1.9876124	down	0.19535129
cyclin-dependent kinase inhibitor 1A (P21)	Cdkn1a	12575	1.9692839	down	0.11540385
Rho GTPase activating protein 9	Arhgap9	216445	1.967703	down	0.16061288
leucine-rich repeats and IQ motif containing 2	Lrriq2	74201	1.9653497	down	0.16061288
B-cell translocation gene 3 /// similar to BTG3 protein (Tob5 protein) (Abundant in neuroepithelium area protein) /// B-cell translocation gene 3 pseudogene	Btg3 /// LOC640416 /// LOC654432	12228 /// 640416 /// 654432	1.9642142	down	0.05773552
Mitogen-activated protein kinase associated protein 1	Mapkap1	227743	1.961991	up	0.18570605
zinc finger, MYM domain containing 1	Zmym1	68310	1.9484218	down	0.12956084
lysosomal-associated protein transmembrane 5 /// similar to Lysosomal-associated multitransmembrane protein (Retinoic acid-inducible E3 protein)	Laptm5 /// LOC669058	16792 /// 669058	1.924141	down	0.13120921
nuclear receptor coactivator 1	Ncoa1	17977	1.9237827	down	0.1917803
Transcribed locus			1.8882208	up	0.11170884
RIKEN cDNA 4732474O15 gene	4732474O15Rik	238455	1.875781	up	0.1857715
RIKEN cDNA 6430598A04 gene	6430598A04Rik	243300	1.8466141	down	0.13209315
Transcribed locus			1.8255105	down	0.1720623
interferon regulatory factor 2 binding protein 2 /// similar to interferon regulatory factor 2 binding protein 2	Irf2bp2 /// LOC672960	270110 /// 672960	1.7994026	down	0.19535129
fatty acid desaturase 2	Fads2	56473	1.7866704	up	0.19535129
spermatid perinuclear RNA binding protein	Strbp	20744	1.7721509	down	0.19535129
expressed sequence C76798	C76798	97127	1.7317202	up	0.19535129
expressed sequence AU021025	AU021025	105285	1.7303556	up	0.18721637
SAM and SH3 domain containing 1	Sash1	70097	1.7042077	down	0.13120921
ectonucleoside triphosphate diphosphohydrolase 5	Entpd5	12499	1.69828	down	0.1857715
copine V	Cpne5	240058	1.6885595	down	0.11540385
solute carrier family 27 (fatty acid transporter), member 2	Slc27a2	26458	1.6863036	down	0.12956084
RIKEN cDNA 2610035D17 gene	2610035D17Rik	72386	1.673881	down	0.19535129
SET domain containing 4	Setd4	224440	1.6678201	down	0.19930862
RIKEN cDNA A430108E01 gene	A430108E01Rik	384382	1.6633605	up	0.19535129
lectin, mannose-binding 2-like	Lman2l	214895	1.6397102	down	0.12956084

TSC22 domain family, member 1	Tsc22d1	21807	1.6343299	down	0.17577663
nuclear factor I/C	Nfic	18029	1.623268	down	0.16061288
pre-B lymphocyte gene 1	Vpreb1	22362	1.6212374	down	0.194536
chloride channel 5	Clcn5	12728	1.6211678	down	0.17577663
glia maturation factor, gamma	Gmfg	63986	1.6026528	down	0.1857715
Traf3 interacting protein 2	Traf3ip2	103213	1.5941008	up	0.17577663
TRAF-interacting protein	Traip	22036	1.5714785	down	0.194536
RIKEN cDNA 2700049A03 gene	2700049A03Rik	76967	1.5475457	down	0.12956084
nuclear factor of activated T-cells, cytoplasmic, calcineurin-dependent 2 interacting protein	Nfatc2ip	18020	1.5430505	down	0.12956084
RIKEN cDNA 9830147J24 gene	9830147J24Rik	229900	1.535216	up	0.01514666
tripartite motif protein 37	Trim37	68729	1.5248642	down	0.12956084
chromobox homolog 4 (Drosophila Pc class)	Cbx4	12418	1.5154564	down	0.13298446
WD repeat domain 33	Wdr33	74320	1.5067347	down	0.1720623
RIKEN cDNA 9530033F24 gene	9530033F24Rik	268469	1.458627	down	0.13120921
YTH domain family 2	Ythdf2	213541	1.4504417	down	0.19535129
serine (or cysteine) peptidase inhibitor, clade E, member 2	Serpine2	20720	1.4267101	down	0.12956084
synaptojanin 2 binding protein	Synj2bp	24071	1.3904783	down	0.1857715
plasma membrane proteolipid	Pllp	67801	1.372868	down	0.10111927
zinc finger protein, subfamily 1A, 1 (Ikaros)	Zfpn1a1	22778	1.3489431	down	0.17577663
zinc finger protein 566	Zfp566	72556	1.3423828	down	0.1857715
zinc finger protein 319	Zfp319	79233	1.286001	down	0.1720623
myeloid/lymphoid or mixed-lineage leukemia (trithorax homolog, Drosophila); translocated to, 11	Mllt11	56772	1.2391255	up	0.1857715
Acidic nuclear phosphoprotein 32 family, member B	Anp32b	67628	1.195885	up	0.1857715
Ena-vasodilator stimulated phosphoprotein	Evl	14026	1.1800323	up	0.13120921

Table VIII. ***List of potential c-Myb target genes in DN2 thymocytes***

Gene Title	Gene Symbol	Entrez Gene	FCAbsolute (MT Vs CT)	Mt vs CT	Corrected Pvalue (MT Vs CT)
superkiller viralicidic activity 2-like 2 (S. cerevisiae)	Skiv2l2	72198	49.915585	up in MT	0.01606334
FBJ osteosarcoma oncogene	Fos	14281	37.90121	down	0.09931164
heat shock protein 1B	Hspa1b	15511	35.89665	down	0.12309026
Jun oncogene	Jun	16476	13.619337	down	0.15269223
Jun oncogene	Jun	16476	12.593312	down	0.16248038
homeo box A9	Hoxa9	15405	12.29368	down	0.13563594
RIKEN cDNA C630010D07 gene /// similar to methylenetetrahydrofolate dehydrogenase (NADP+ dependent) 2-like /// region containing RIKEN cDNA C630010D07 gene; RIKEN cDNA 1110019K23 gene	C630010D07Rik /// LOC665563 /// LOC674367	503860 /// 665563 /// 674367	8.085352	down	0.12309026
RIKEN cDNA E130309D02 gene	E130309D02Rik	231868	7.9445496	down	0.10898781
Transcribed locus			6.6013775	down	0.12309026
SRY-box containing gene 4 /// similar to Transcription factor SOX-4	Sox4 /// LOC672274	20677 /// 672274	6.499265	down	0.15269223
dedicator of cytokinesis 8	Dock8	76088	6.4892883	down	0.10898781
glutamate oxaloacetate transaminase 2, mitochondrial	Got2	14719	6.3033013	down	0.15694605
endothelial differentiation, sphingolipid G-protein-coupled receptor, 3	Edg3	13610	5.912275	down	0.12309026
RNA binding motif protein 5	Rbm5	83486	5.894149	down	0.12309026
brix domain containing 5	Bxdc5	70285	5.807275	down	0.17922762
Transcobalamin 2	Tcn2	21452	5.762501	down	0.19144724
lactamase, beta 2	Lactb2	212442	5.457429	down	0.12309026
formin binding protein 1-like	Fnbp1l	214459	5.441247	down	0.0530811
single-stranded DNA binding protein 2	Ssbp2	66970	5.4242363	down	0.12309026
ST8 alpha-N-acetyl-neuraminide alpha-2,8-sialyltransferase 1	St8sia1	20449	5.2093477	down	0.17522609
downstream of Stk11	Dos	216164	5.1686473	down	0.12309026
Bone marrow macrophage cDNA, RIKEN full-length enriched library, clone:I830003K21 product:unclassifiable, full insert sequence			5.034254	down	0.13563594
zinc finger, AN1-type domain 2A	Zfand2a	100494	4.6774263	down	0.17103879
transmembrane protein 40	Tmem40	94346	4.6103916	down	0.16248038
ankyrin repeat and KH domain containing 1	Ankhd1	108857	4.5784006	down	0.15372995
ATPase, Class V, type 10D	Atp10d	231287	4.481681	down	0.09455363
spastic paraplegia 20, spartin (Troyer syndrome) homolog (human)	Spg20	229285	4.43132	down	0.12461345
cDNA sequence BC018601	BC018601	104479	4.4281716	down	0.17984402
synaptobrevin like 1	Sybl1	20955	4.367285	down	0.1425723
t-complex 11 (mouse) like 2	Tcp11l2	216198	4.2739863	down	0.12309026
phosphoribosyl pyrophosphate synthetase-associated protein 2	Prpsap2	212627	4.2723265	down	0.12309026
myeloid cell leukemia sequence 1	Mcl1	17210	4.0981	down	0.13563594
Gene model 237, (NCBI)	Gm237	211488	4.068734	down	0.03613977
non-catalytic region of tyrosine kinase adaptor protein 1	Nck1	17973	4.0533504	down	0.15331252
RIKEN cDNA E130308A19 gene	E130308A19Rik	230259	4.0282187	down	0.04839424
cDNA sequence BC024969	BC024969	240442	3.9673288	down	0.02827073
RIKEN cDNA 4930488E11 gene	4930488E11Rik	399591	3.963002	down	0.18512924
RIKEN cDNA 1200009F10 gene	1200009F10Rik	67454	3.889808	down	0.12309026
pre-B lymphocyte gene 1	Vpreb1	22362	3.8399568	down	0.1965496
Wolf-Hirschhorn syndrome candidate 1-like 1 (human)	Whsc1l1	234135	3.790115	down	0.14694817
nuclear receptor subfamily 4, group A, member 2	Nr4a2	18227	3.7056396	down	0.17811678
5,10-methylenetetrahydrofolate reductase	Mthfr	17769	3.6951716	down	0.12309026
neuroblastoma ras oncogene	Nras	18176	3.6690536	down	0.15331252
ubiquitin specific peptidase 46	Usp46	69727	3.6320565	down	0.12309026
expressed sequence AU044157	AU044157	100334	3.630645	down	0.05286473
TBC1 domain family, member 23	Tbc1d23	67581	3.6304724	down	0.14847307
zinc finger protein 715	Zfp715	69930	3.5695837	down	0.1965496
kinesin family member 17	Kif17	16559	3.4854555	down	0.1679302
RIKEN cDNA 1700097N02 gene	1700097N02Rik	67522	3.460105	down	0.16776948
ERGIC and golgi 3	Ergic3	66366	3.4522076	down	0.18512924
menage a trois 1	Mnat1	17420	3.448658	down	0.15372995
DCUN1D1 DCN1, defective in cullin neddylation 1, domain containing 1 (S. cerevisiae)	Dcun1d1	114893	3.4116704	down	0.02766798

Nuclear factor of kappa light polypeptide gene enhancer in B-cells inhibitor, zeta	Nfkbiz	80859	3.3675964	down	0.15331252
polymerase (RNA) III (DNA directed) polypeptide G	Polr3g	67486	3.3644123	down	0.08886257
serine palmitoyltransferase, long chain base subunit 1	Sptlc1	268656	3.362357	down	0.19622187
metastasis associated lung adenocarcinoma transcript 1 (non-coding RNA)	Malat1	72289	3.3591673	down	0.12309026
			3.2486107	down	0.18512924
vinculin	Vcl	22330	3.2327259	down	0.17767027
REST corepressor 1	Rcor1	217864	3.2221978	down	0.12309026
forkhead box O3a	Foxo3a	56484	3.220235	down	0.17522609
zinc finger, AN1 type domain 2B	Zfand2b	68818	3.1885278	down	0.12309026
jumonji, AT rich interactive domain 1B (Rbp2 like)	Jarid1b	75605	3.1566923	down	0.12309026
RIKEN cDNA 1110054O05 gene	1110054O05Rik	66209	3.1207798	down	0.19729684
glucose-fructose oxidoreductase domain containing 1	Gfod1	328232	3.1180732	down	0.12309026
RIKEN cDNA C030033M12 gene	C030033M12Rik	77334	3.0802865	down	0.1965496
kelch-like 24 (Drosophila)	Klhl24	75785	3.0722454	down	0.14694817
Ly6/neurotoxin 1	Lynx1	23936	3.0442643	down	0.12309026
zinc finger, A20 domain containing 3	Za20d3	65098	3.0279481	down	0.1679302
RIKEN cDNA 2610305J24 gene /// similar to melanoma antigen /// hypothetical protein LOC669436 /// hypothetical protein LOC670270 /// hypothetical protein LOC672052 /// similar to melanoma antigen /// similar to melanoma antigen	2610305J24Rik /// LOC668904 /// LOC669436 /// LOC670270 /// LOC672052 /// LOC672939 /// LOC677506	668904 /// 669436 /// 670270 /// 672052 /// 672939 /// 677506 /// 72520	3.001472	down	0.03613977
RIKEN cDNA 2610307O08 gene	2610307O08Rik	72512	2.9990718	down	0.19882737
G patch domain containing 4	Gpatc4	66614	2.9798667	up	0.18512924
acyl-CoA thioesterase 2	Acot2	171210	2.9779453	down	0.13563594
suppression of tumorigenicity 7-like	St7l	229681	2.970611	down	0.02766798
ubiquitin-activating enzyme E1-like 2	Ube1l2	231380	2.9682052	down	0.13919428
RIKEN cDNA 4632434I11 gene	4632434I11Rik	74041	2.929621	down	0.17811678
RIKEN cDNA 6820424L24 gene	6820424L24Rik	100515	2.9282758	down	0.1965496
U2 small nuclear RNA auxiliary factor 1-like 4	U2af1l4	233073	2.9108918	down	0.17996162
pleckstrin homology domain containing, family A (phosphoinositide binding specific) member 1	Plekha1	101476	2.9070718	down	0.18634856
RIKEN cDNA 2010003O02 gene	2010003O02Rik	66434	2.8953326	down	0.18558836
peroxiredoxin 4	Prdx4	53381	2.884971	down	0.12309026
RIKEN cDNA 2410004N11 gene	2410004N11Rik	66989	2.8785589	down	0.13563594
solute carrier family 39 (metal ion transporter), member 6	Slc39a6	106957	2.8648343	down	0.12461345
RIKEN cDNA 1200016B10 gene	1200016B10Rik	66875	2.8549294	down	0.13563594
hypothetical LOC433022	LOC433022	433022	2.8473732	down	0.12309026
coatomer protein complex, subunit gamma 2	Copg2	54160	2.825417	down	0.19900602
ethylmalonic encephalopathy 1	Ethe1	66071	2.8124235	down	0.15331252
CD53 antigen	Cd53	12508	2.801546	down	0.12309026
5'-nucleotidase, cytosolic II	Nt5c2	76952	2.790688	down	0.12485109
AT rich interactive domain 4A (Rbp1 like)	Arid4a	238247	2.7841516	down	0.05187233
G patch domain containing 4	Gpatc4	66614	2.7613595	up	0.04775264
phosphatidylinositol 3-kinase, regulatory subunit, polypeptide 1 (p85 alpha)	Pik3r1	18708	2.7435544	down	0.12309026
like-glycosyltransferase	Large	16795	2.7278898	down	0.02686589
ATP synthase mitochondrial F1 complex assembly factor 2	Atpaf2	246782	2.7234926	down	0.13737899
ubiquitin-conjugating enzyme E2G 1 (UBC7 homolog, C. elegans)	Ube2g1	67128	2.719533	down	0.17668547
RIKEN cDNA A430088C08 gene	A430088C08Rik	320892	2.7114646	down	0.12309026
jumonji, AT rich interactive domain 1C (Rbp2 like)	Jarid1c	20591	2.7052813	down	0.17522609
B-cell leukemia/lymphoma 10	Bcl10	12042	2.7034562	down	0.05187233
Kruppel-like factor 6	Klf6	23849	2.667635	down	0.15881358
Actinin alpha 2	Actn2	11472	2.664271	down	0.18512924
acyl-Coenzyme A dehydrogenase, short/branched chain	Acadsb	66885	2.644866	down	0.12309026
RNA binding motif protein 14	Rbm14	56275	2.6268137	down	0.11051951
ORM1-like 1 (S. cerevisiae)	Ormdl1	227102	2.6208127	down	0.19882737
amyloid beta precursor protein (cytoplasmic tail) binding protein 2	Appbp2	66884	2.6123726	down	0.17996162
ganglioside-induced differentiation-associated-protein 2	Gdap2	14547	2.6010036	down	0.12309026
RIKEN cDNA D930036F22 gene	D930036F22Rik	320487	2.5957756	down	0.18094288
			2.5462518	down	0.16165234
BCL2-associated athanogene 4	Bag4	67384	2.5320947	down	0.12309026

membrane protein, palmitoylated 7 (MAGUK p55 subfamily member 7)	Mpp7	75739	2.5211375	down	0.14694817
suppressor of cytokine signaling 3	Socs3	12702	2.5195491	up	0.1865186
sideroflexin 3	Sfxn3	94280	2.5010145	down	0.12309026
DEAD (Asp-Glu-Ala-Asp) box polypeptide 46	Ddx46	212880	2.4879901	down	0.01924309
SET and MYND domain containing 4	Smyd4	319822	2.4805264	down	0.16776948
WW domain containing adaptor with coiled-coil	Wac	225131	2.446973	down	0.18512924
zinc finger protein 451	Zfp451	98403	2.4138868	down	0.03865734
sorting nexin 9	Snx9	66616	2.4133494	down	0.13919428
RIKEN cDNA 4930526I15 gene	4930526I15Rik	75135	2.409905	down	0.14565594
RIKEN cDNA 4631408O11 gene	4631408O11Rik	66693	2.4037516	down	0.15583728
SCY1-like 2 (S. cerevisiae)	Scyl2	213326	2.3861806	down	0.02686589
tripeptidyl peptidase II	Tpp2	22019	2.3485003	down	0.19727188
isochorismatase domain containing 1	Isoc1	66307	2.3296835	down	0.1965496
LIM domain only 4	Lmo4	16911	2.3290188	down	0.16776948
peptidylprolyl isomerase domain and WD repeat containing 1	Ppwd1	238831	2.3002415	down	0.15331252
RIKEN cDNA 2310007F12 gene	2310007F12Rik	69499	2.2889957	down	0.1965496
v-raf murine sarcoma 3611 viral oncogene homolog	Araf	11836	2.286167	down	0.12309026
transducer of ERBB2, 2	Tob2	57259	2.2838154	down	0.12309026
TROVE domain family, member 2	Trove2	20822	2.271896	down	0.17922762
translocation protein 1	Tloc1	69276	2.2585633	down	0.18558836
RIKEN cDNA A330103N21 gene	A330103N21Rik	77773	2.2379148	down	0.12309026
syntaxin 3	Stx3	20908	2.2130466	down	0.17811678
p21 (CDKN1A)-activated kinase 1	Pak1	18479	2.2109134	down	0.16165234
glucosamine	Gne	50798	2.197238	down	0.15583728
pellino 1	Peli1	67245	2.147481	down	0.12309026
Protein phosphatase 2, regulatory subunit B (B56), gamma isoform	Ppp2r5c	26931	2.1385796	down	0.02827073
			2.130126	down	0.18629302
cullin 4B	Cul4b	72584	2.113167	down	0.15881358
chromodomain protein, Y chromosome-like	Cdyl	12593	2.075988	down	0.17996162
RIKEN cDNA 4921505C17 gene	4921505C17Rik	78757	2.0363488	down	0.12309026
RIKEN cDNA 4632417D23 gene	4632417D23Rik	245843	2.0276623	up	0.01155172
nucleolar complex associated 2 homolog (S. cerevisiae)	Noc2l	57741	2.0270324	up	0.1824922
RNA binding motif protein 6	Rbm6	19654	2.0270052	down	0.1824922
retinol dehydrogenase 11	Rdh11	17252	2.0131655	down	0.12461345
ring finger protein 113A1	Rnf113a1	69942	1.9999657	down	0.12309026
Transcribed locus			1.9915036	down	0.12309026
PRP31 pre-mRNA processing factor 31 homolog (yeast)	Prpf31	68988	1.9844816	down	0.17522609
thioredoxin-like 4	Txnl4	27366	1.9809307	down	0.14694817
insulin induced gene 2	Insig2	72999	1.9761147	down	0.17922762
UPF1 regulator of nonsense transcripts homolog (yeast)	Upf1	19704	1.9712161	down	0.1965496
RIKEN cDNA 4930573I19 gene	4930573I19Rik	104859	1.962171	down	0.12309026
p300/CBP-associated factor /// similar to p300/CBP-associated factor	Pcaf /// LOC330129	18519 /// 330129	1.9402153	down	0.13563594
expressed sequence AI448984	AI448984	100124	1.9323536	down	0.13919428
archain 1	Arcn1	213827	1.8996499	down	0.12309026
Sfi1 homolog, spindle assembly associated (yeast) /// similar to spindle assembly associated Sfi1 homolog isoform b /// similar to Sfi1 homolog, spindle assembly associated (yeast)	Sfi1 /// LOC673420 /// LOC673566	673420 /// 673566 /// 78887	1.893512	down	0.17996162
RIKEN cDNA 9430079B08 gene	9430079B08Rik	320481	1.8704658	down	0.13563594
coiled-coil domain containing 94	Ccdc94	72886	1.8604637	down	0.13563594
kelch domain containing 1	Klhdc1	271005	1.8550966	down	0.08531022
zinc and ring finger 3 /// similar to Goliath homolog precursor (Ring finger protein 130) (R-goliath)	Znrf3 /// LOC631806	407821 /// 631806	1.8472387	down	0.12309026
RIKEN cDNA 2610002D18 gene	2610002D18Rik	69885	1.8434565	down	0.17522609
RIKEN cDNA 4933412E12 gene	4933412E12Rik	71086	1.8401062	down	0.15331252
Nuclear respiratory factor 1	Nrf1	18181	1.8360684	down	0.17996162
RIKEN cDNA 2310076G13 gene	2310076G13Rik	71938	1.8352685	down	0.17522609
beclin 1 (coiled-coil, myosin-like BCL2-interacting protein)	Becn1	56208	1.8196083	up	0.18512924
ASF1 anti-silencing function 1 homolog A (S. cerevisiae)	Asf1a	66403	1.8193371	up	0.15269223
RIKEN cDNA 2210018M11 gene	2210018M11Rik	233545	1.7646747	down	0.12309026
RIKEN cDNA 2810454L23 gene	2810454L23Rik	72803	1.7600374	down	0.13318042
Nucleoporin 98	Nup98	269966	1.7500422	down	0.17522609
RIKEN cDNA 4933439F18 gene	4933439F18Rik	66771	1.7357156	down	0.19882737
RIKEN cDNA 4930430F08 gene	4930430F08Rik	68281	1.7275527	up	0.13563594
RIKEN cDNA 1810013L24 gene	1810013L24Rik	69053	1.7243022	down	0.12309026
Axin 1	Axin1	12005	1.7061744	down	0.19882737

HERPUD family member 2	Herpud2	80517	1.696916	down	0.17922762
degenerative spermatocyte homolog 1 (Drosophila)	Degs1	13244	1.6913596	up	0.17522609
RIKEN cDNA 2010004M13 gene	2010004M13Rik	76511	1.6720253	down	0.16165234
growth factor receptor bound protein 2-associated protein 1	Gab1	14388	1.6692672	down	0.1965496
Adult male corpus striatum cDNA, RIKEN full-length enriched library, clone:C030020B06 product:unclassifiable, full insert sequence			1.6663803	down	0.09931164
signal sequence receptor, alpha	Ssr1	107513	1.6622777	down	0.12917191
Coiled-coil-helix-coiled-coil-helix domain containing 3	Chchd3	66075	1.6613253	up	0.12309026
cDNA sequence BC003965	BC003965	214489	1.6291353	up	0.17996162
RIKEN cDNA 2610507B11 gene	2610507B11Rik	72503	1.6219219	up	0.1824922
bobby sox homolog (Drosophila)	Bbx	70508	1.6194224	down	0.1965496
zinc finger CCCH type containing 11A	Zc3h11a	70579	1.6188921	down	0.12309026
MOCO sulphurase C-terminal domain containing 2	Mosc2	67247	1.6135603	up	0.1865186
similar to PDZ and LIM domain protein 5 (Enigma homolog) (Enigma-like PDZ and LIM domains protein)	LOC669660	669660	1.6064879	down	0.12309026
triple functional domain (PTPRF interacting)	Trio	223435	1.5864819	down	0.12309026
X-ray repair complementing defective repair in Chinese hamster cells 3	Xrcc3	74335	1.5838869	down	0.1824922
basic transcription factor 3-like 4	Btf3l4	70533	1.5330924	down	0.12461345
synovial sarcoma translocation gene on chromosome 18-like 1	Ss18l1	269397	1.5314841	down	0.13919428
RIKEN cDNA E130016E03 gene	E130016E03Rik	623474	1.5247271	down	0.05187233
adenomatosis polyposis coli	Apc	11789	1.5081093	down	0.17922762
Transcribed locus			1.5071025	down	0.12309026
RIKEN cDNA 5730596P11 gene	5730596P11Rik	77012	1.5010681	up	0.08531022
Expressed sequence AI663975	AI663975	103819	1.4823654	down	0.1824922
RIKEN cDNA 6330415G19 gene	6330415G19Rik	320020	1.4586152	down	0.15881358
leucine zipper, down-regulated in cancer 1-like	Ldoc1l	223732	1.4281262	down	0.01723915
ash1 (absent, small, or homeotic)-like (Drosophila)	Ash1l	192195	1.4100885	down	0.18512924
nucleolar protein 8	Nol8	70930	1.4092861	down	0.14694817
two pore channel 1	Tpcn1	252972	1.3360527	down	0.12309026
spectrin beta 2	Spnb2	20742	1.3317744	down	0.1679302
leucine rich repeat containing 20	Lrrc20	216011	1.319025	down	0.13919428
bromodomain containing 8	Brd8	78656	1.1849959	down	0.12461345
adducin 3 (gamma)	Add3	27360	1.1477915	down	0.05258514

Table IX. ***List of Kegg Pathways involving potential Myb targets in DN3 Tcrb-Tg+ thymocytes***

Rank	Pathway Name	Impact Factor	#Genes in Pathway	#Input Genes in Pathway	Gene	Fold change
1	Phosphatidylinositol signaling system	34.558	73	5		
					Dgke	-4.45
					Impa2	-1.54
					Itpr2	-2.06
					Pik3cg	-2.00
					Pip5k2b	-1.90
2	T cell receptor signaling pathway	9.584	94	7		
					Cbl	-2.18
					Cblb	2.40
					Nck2	-2.49
					Nfkbie	-3.01
					Pak1	-1.40
					Pik3cg	-2.00
					Ptpn6	1.79
3	Type II diabetes mellitus	9.55	45	2		
					Pik3cg	-2.00
					Socs3	10.60
4	Jak-STAT signaling pathway	8.897	151	7		
					Cbl	-2.18
					Cblb	2.40
					Il7r	-1.32
					Pik3cg	-2.00
					Ptpn6	1.79
					Socs3	10.60
					Stat4	1.91
5	Regulation of actin cytoskeleton	8.456	199	9		
					Cyfip1	1.84
					F2r	2.00
					Itga4	-2.16
					Itga9	4.18
					Itgb2	2.32
					Itgb7	2.74
					Pak1	-1.40
					Pik3cg	-2.00
					Pip5k2b	-1.90
6	Natural killer cell mediated cytotoxicity	7.418	117	5		
					Itgb2	2.32
					Pak1	-1.40
					Pik3cg	-2.00
					Ptpn6	1.79
					Sh2d1a	-9.14
7	Long-term potentiation	7.153	63	3		
					Camk4	-8.39
					Itpr2	-2.06
					Rapgef3	-2.42
8	Adipocytokine signaling pathway	6.612	69	2		
					Nfkbie	-3.01
					Socs3	10.60
9	Notch signaling pathway	6.459	46	2		
					Dtx1	16.52
					Notch3	3.13
10	Leukocyte transendothelial migration	6.424	117	5		
					Ctnna1	-1.75
					Itga4	-2.16
					Itgb2	2.32
					Pik3cg	-2.00
					Rapgef3	-2.42

11	Cell adhesion molecules (CAMs)	5.971	147	6		
					Itga4	-2.16
					Itga9	4.18
					Itgb2	2.32
					Itgb7	2.74
					Ptprf	-2.93
					Sell	-2.02
12	Insulin signaling pathway	5.891	133	5		
					Cbl	-2.18
					Cblb	2.40
					Pik3cg	-2.00
					Ptprf	-2.93
					Socs3	10.60
13	Neurodegenerative disorders	5.536	33	3		
					Als2	-2.04
					Bcl2	-1.35
					Casp1	3.21
14	Calcium signaling pathway	5.281	174	4		
					Camk4	-8.39
					F2r	2.00
					Itpr2	-2.06
					Ptger3	3.25
15	Focal adhesion	5.139	190	6		
					Bcl2	-1.35
					Itga4	-2.16
					Itga9	4.18
					Itgb7	2.74
					Pak1	-1.40
					Pik3cg	-2.00
16	Amyotrophic lateral sclerosis (ALS)	4.47	17	2		
					Als2	-2.04
					Bcl2	-1.35
17	B cell receptor signaling pathway	4.446	64	3		
					Nfkbie	-3.01
					Pik3cg	-2.00
					Ptpn6	1.79
18	Adherens junction	4.264	74	3		
					Ctnna1	-1.75
					Ptpn6	1.79
					Ptprf	-2.93
19	Antigen processing and presentation	3.792	91	2		
					Ctss	5.59
					Rfxap	-1.56
20	ECM-receptor interaction	3.458	85	3		
					Itga4	-2.16
					Itga9	4.18
					Itgb7	2.74
21	Dentatorubropallidoluysian atrophy (DRPLA)	2.992	14	1		
					Casp1	3.21
22	Prion disease	2.959	11	1		
					Bcl2	-1.35
23	Neuroactive ligand-receptor interaction	2.829	311	6		
					F2r	2.00
					Nr3c1	-3.40
					P2ry5	2.30
					Ptger3	3.25
					Ptger4	-2.01
					Sstr2	1.63
24	Tight junction	2.795	117	3		
					Ctnna1	-1.75
					Pard6g	-1.81

					Ppp2cb	-1.57
25	Long-term depression	2.774	72	2		
					Itpr2	-2.06
					Ppp2cb	-1.57
26	VEGF signaling pathway	2.77	71	2		
					Mapkapk3	2.04
					Pik3cg	-2.00
27	GnRH signaling pathway	2.587	93	1		
					Itpr2	-2.06
28	Apoptosis	2.583	81	2		
					Bcl2	-1.35
					Pik3cg	-2.00
29	Axon guidance	2.464	132	2		
					Nck2	-2.49
					Pak1	-1.40
30	Huntington's disease	2.35	28	1		
					Casp1	3.21
31	Hedgehog signaling pathway	2.226	53	1		
					Smo	-2.15
32	MAPK signaling pathway	2.187	231	3		
					Casp1	3.21
					Mapkapk3	2.04
					Pak1	-1.40
33	Fc epsilon RI signaling pathway	1.976	75	1		
					Pik3cg	-2.00
34	Gap junction	1.905	90	2		
					Itpr2	-2.06
					Tuba2	-1.80
35	Cytokine-cytokine receptor interaction	1.758	241	4		
					Il17ra	-1.63
					Il17rb	-2.18
					Il7r	-1.32
					Tnfrsf18	1.70
36	Toll-like receptor signaling pathway	1.703	91	1		
					Pik3cg	-2.00
37	Wnt signaling pathway	1.658	143	2		
					Ppp2cb	-1.57
					Prickle1	-2.21
38	TGF-beta signaling pathway	1.566	83	1		
					Ppp2cb	-1.57
39	mTOR signaling pathway	1.482	49	1		
					Pik3cg	-2.00
40	Complement and coagulation cascades	1.261	71	1		
					F2r	2.00
41	Colorectal cancer	0.941	77	1		
					Bcl2	-1.35

Table X. List of Kegg Pathways involving potential Myb targets in DN3 thymocytes

Rank	Pathway Name	Impact Factor	#Genes in Pathway	#Input Genes in Pathway	Gene	Fold change
1	Phosphatidylinositol signaling system	37.006	73	1		
					Dgke	-5.48
2	Antigen processing and presentation	7.982	91	2		
					B2m	4.78
					Ctss	24.41
3	Colorectal cancer	7.95	77	1		
					Fos	-18.08
4	Toll-like receptor signaling pathway	7.909	91	1		
					Fos	-18.08
5	Long-term depression	7.403	72	1		
					Gria2	11.00
6	Long-term potentiation	6.817	63	2		
					Gria2	11.00
					Rapgef3	-2.76
7	Type II diabetes mellitus	4.915	45	1		
					Socs3	4.71
8	B cell receptor signaling pathway	4.68	64	1		
					Fos	-18.08
9	T cell receptor signaling pathway	4.507	94	2		
					Cblb	2.80
					Fos	-18.08
10	Natural killer cell mediated cytotoxicity	4.199	117	1		
					Sh2d1a	-8.18
11	Regulation of actin cytoskeleton	4.027	199	3		
					Fgf13	-4.73
					Itga9	8.16
					Itgae	2.78
12	Jak-STAT signaling pathway	3.703	151	2		
					Cblb	2.80
					Socs3	4.71
13	Wnt signaling pathway	3.596	143	2		
					Nkd1	10.10
					Prickle1	-2.70
14	MAPK signaling pathway	3.596	231	2		
					Fgf13	-4.73
15	Adipocytokine signaling pathway	3.29	69	1		
					Socs3	4.71
16	Leukocyte transendothelial migration	2.889	117	1		
					Rapgef3	-2.76
17	Insulin signaling pathway	2.871	133	2		
					Cblb	2.80
					Socs3	4.71
18	ECM-receptor interaction	2.541	85	1		
					Itga9	8.16
19	Neuroactive ligand-receptor interaction	2.344	311	1		
					Gria2	11.00
20	Cell adhesion molecules (CAMs)	2.199	147	1		
					Itga9	8.16
21	Focal adhesion	2.001	190	1		
					Itga9	8.16
22	Gap junction	1.361	90	1		
					Tuba8	-2.03
23	Axon guidance	1.172	132	1		
					Nrp1	-2.75

24	Cytokine-cytokine receptor interaction	0.76	241	1		
					Tnfrsf18	2.19

Table XI. List of Kegg Pathways involving potential Myb targets in DN2 thymocytes

Rank	Pathway Name	Impact Factor	#Genes in Pathway	#Input Genes in Pathway	Gene	Fold change
1	Phosphatidylinositol signaling system	28.105	73	1		
					Pik3r1	-2.74
2	T cell receptor signaling pathway	13.69	94	7		
					Bcl10	-2.70
					Fos	-37.90
					Jun	-12.59
					Nck1	-4.05
					Nras	-3.67
					Pak1	-2.21
					Pik3r1	-2.74
3	Colorectal cancer	13.665	77	5		
					Apc	-1.51
					Axin1	-1.71
					Fos	-37.90
					Jun	-12.59
					Pik3r1	-2.74
4	Toll-like receptor signaling pathway	13.259	91	3		
					Fos	-37.90
					Jun	-12.59
					Pik3r1	-2.74
5	B cell receptor signaling pathway	11.822	64	5		
					Bcl10	-2.70
					Fos	-37.90
					Jun	-12.59
					Nras	-3.67
					Pik3r1	-2.74
6	Tight junction	8.825	117	6		
					Actn2	-2.66
					Ash1l	-1.41
					Jam3	-2.55
					Nras	-3.67
					Ppp2r3a	-2.41
					Spnb2	-1.33
7	Long-term depression	7.952	72	1		
					Nras	-3.67
8	MAPK signaling pathway	7.461	231	4		
					Fos	-37.90
					Jun	-12.59
					Nras	-3.67
					Pak1	-2.21
9	Focal adhesion	6.675	190	5		
					Actn2	-2.66
					Jun	-12.59
					Pak1	-2.21
					Pik3r1	-2.74
					Vcl	-3.23
10	Long-term potentiation	6.499	63	1		
					Nras	-3.67
11	mTOR signaling pathway	6.31	49	3		
					4921505C17R	-2.04
					Pik3r1	-2.74
					Stk11	-5.17
12	Gap junction	6.123	90	1		
					Nras	-3.67
13	Regulation of actin cytoskeleton	6.091	199	6		
					Actn2	-2.66
					Apc	-1.51

					Nras	-3.67
					Pak1	-2.21
					Pik3r1	-2.74
					Vcl	-3.23
14	Leukocyte transendothelial migration	5.482	117	4		
					Actn2	-2.66
					Jam3	-2.55
					Pik3r1	-2.74
					Vcl	-3.23
15	Natural killer cell mediated cytotoxicity	5.399	117	3		
					Nras	-3.67
					Pak1	-2.21
					Pik3r1	-2.74
16	GnRH signaling pathway	4.894	93	2		
					Jun	-12.59
					Nras	-3.67
17	Fc epsilon RI signaling pathway	4.834	75	2		
					Nras	-3.67
					Pik3r1	-2.74
18	Adipocytokine signaling pathway	4.793	69	2		
					Socs3	2.52
					Stk11	-5.17
19	Type II diabetes mellitus	4.639	45	2		
					Pik3r1	-2.74
					Socs3	2.52
20	Insulin signaling pathway	4.536	133	3		
					Nras	-3.67
					Pik3r1	-2.74
					Socs3	2.52
21	VEGF signaling pathway	4.409	71	2		
					Nras	-3.67
					Pik3r1	-2.74
22	SNARE interactions in vesicular transport	4.256	36	2		
					Stx3	-2.21
					Sybl1	-4.37
23	Cell adhesion molecules (CAMs)	4.22	147	1		
					Jam3	-2.55
24	Axon guidance	4.089	132	3		
					Nck1	-4.05
					Nras	-3.67
					Pak1	-2.21
25	Wnt signaling pathway	3.999	143	3		
					Apc	-1.51
					Axin1	-1.71
					Jun	-12.59
26	Adherens junction	3.978	74	2		
					Actn2	-2.66
					Vcl	-3.23
27	Jak-STAT signaling pathway	2.839	151	2		
					Pik3r1	-2.74
					Socs3	2.52
28	Apoptosis	2.449	81	1		
					Pik3r1	-2.74
29	Neuroactive ligand-receptor interaction	1.751	311	1		
					Edg3	-5.91
30	Notch signaling pathway	1.673	46	1		
					Pcaf	-1.94

Literature Cited

1. Sicinska, E., et al., *Requirement for cyclin D3 in lymphocyte development and T cell leukemias.* Cancer Cell, 2003. **4**(6): p. 451-61.
2. Hoffman, E.S., et al., *Productive T-cell receptor beta-chain gene rearrangement: coincident regulation of cell cycle and clonality during development in vivo.* Genes Dev, 1996. **10**(8): p. 948-62.
3. Lipsick, J.S. and D.M. Wang, *Transformation by v-Myb.* Oncogene, 1999. **18**(19): p. 3047-55.
4. Ness, S.A., *Myb binding proteins: regulators and cohorts in transformation.* Oncogene, 1999. **18**(19): p. 3039-3046.
5. Petrie, H.T. and P.W. Kincade, *Many roads, one destination for T cell progenitors.* J Exp Med, 2005. **202**(1): p. 11-3.
6. Pelayo, R., et al., *Lymphoid progenitors and primary routes to becoming cells of the immune system.* Curr Opin Immunol, 2005. **17**(2): p. 100-7.
7. Bhandoola, A., et al., *Early T lineage progenitors: new insights, but old questions remain.* J Immunol, 2003. **171**(11): p. 5653-8.
8. Zuniga-Pflucker, J.C., *T-cell development made simple.* Nat Rev Immunol, 2004. **4**(1): p. 67-72.
9. Xu, G. and Y. Shi, *Apoptosis signaling pathways and lymphocyte homeostasis.* Cell Res, 2007. **17**(9): p. 759-71.
10. Giacinti, C. and A. Giordano, *RB and cell cycle progression.* Oncogene, 2006. **25**(38): p. 5220-7.
11. Oltvai, Z.N., C.L. Milliman, and S.J. Korsmeyer, *Bcl-2 heterodimerizes in vivo with a conserved homolog, Bax, that accelerates programmed cell death.* Cell, 1993. **74**(4): p. 609-19.
12. Aifantis, I., et al., *Regulation of T-cell progenitor survival and cell-cycle entry by the pre-T-cell receptor.* Immunol Rev, 2006. **209**: p. 159-69.
13. Staal, F.J. and H.C. Clevers, *WNT signalling and haematopoiesis: a WNT-WNT situation.* Nat Rev Immunol, 2005. **5**(1): p. 21-30.
14. Bender, T.P., et al., *Critical functions for c-Myb at three checkpoints during thymocyte development.* Nat Immunol, 2004. **5**(7): p. 721-9.
15. Godfrey, D.I., et al., *A developmental pathway involving four phenotypically and functionally distinct subsets of CD3-CD4-CD8- triple-negative adult mouse thymocytes defined by CD44 and CD25 expression.* J.Immunol., 1993. **150**(10): p. 4244-4252.
16. Balciunaite, G., R. Ceredig, and A.G. Rolink, *The earliest subpopulation of mouse thymocytes contains potent T, significant macrophage, and natural killer cell but no B-lymphocyte potential.* Blood, 2005. **105**(5): p. 1930-6.

17. Petrie, H.T. and J.C. Zuniga-Pflucker, *Zoned out: functional mapping of stromal signaling microenvironments in the thymus.* Annu Rev Immunol, 2007. **25**: p. 649-79.
18. Rothenberg, E.V., J.E. Moore, and M.A. Yui, *Launching the T-cell-lineage developmental programme.* Nat Rev Immunol, 2008. **8**(1): p. 9-21.
19. Shortman, K., et al., *The generation and fate of thymocytes.* Semin Immunol, 1990. **2**(1): p. 3-12.
20. Capone, M., R.D. Hockett, Jr., and A. Zlotnik, *Kinetics of T cell receptor beta, gamma, and delta rearrangements during adult thymic development: T cell receptor rearrangements are present in CD44(+)CD25(+) Pro-T thymocytes.* Proc Natl Acad Sci U S A, 1998. **95**(21): p. 12522-7.
21. Livak, F., et al., *Characterization of TCR gene rearrangements during adult murine T cell development.* J Immunol, 1999. **162**(5): p. 2575-80.
22. Wilson, A., W. Held, and H.R. MacDonald, *Two waves of recombinase gene expression in developing thymocytes.* J Exp Med, 1994. **179**(4): p. 1355-60.
23. Shinkai, Y., et al., *RAG-2-deficient mice lack mature lymphocytes owing to inability to initiate V(D)J rearrangement.* Cell, 1992. **68**(5): p. 855-867.
24. Mombaerts, P., et al., *RAG-1-deficient mice have no mature B and T lymphocytes.* Cell, 1992. **68**(5): p. 869-877.
25. Tillman, R.E., et al., *Cutting edge: targeting of V beta to D beta rearrangement by RSSs can be mediated by the V(D)J recombinase in the absence of additional lymphoid-specific factors.* J.Immunol., 2003. **170**(1): p. 5-9.
26. Bergman, Y., *Allelic exclusion in B and T lymphopoiesis.* Semin.Immunol., 1999. **11**(5): p. 319-328.
27. Malissen, M., et al., *Altered T cell development in mice with a targeted mutation of the CD3-epsilon gene.* EMBO J., 1995. **14**(19): p. 4641-4653.
28. Mallick, C.A., et al., *Rearrangement and diversity of T cell receptor beta chain genes in thymocytes: a critical role for the beta chain in development.* Cell, 1993. **73**(3): p. 513-9.
29. Dudley, E.C., et al., *T cell receptor beta chain gene rearrangement and selection during thymocyte development in adult mice.* Immunity, 1994. **1**(2): p. 83-93.
30. Mombaerts, P., et al., *Mutations in T-cell antigen receptor genes alpha and beta block thymocyte development at different stages.* Nature, 1992. **360**(6401): p. 225-231.
31. Michie, A.M. and J.C. Zuniga-Pflucker, *Regulation of thymocyte differentiation: pre-TCR signals and beta-selection.* Semin.Immunol., 2002. **14**(5): p. 311-323.
32. Wolfer, A., et al., *Inactivation of Notch1 impairs VDJbeta rearrangement and allows pre-TCR-independent survival of early alpha beta Lineage Thymocytes.* Immunity., 2002. **16**(6): p. 869-879.
33. Hozumi, K., et al., *Delta-like 4 is indispensable in thymic environment specific for T cell development.* J Exp Med, 2008. **205**(11): p. 2507-13.

34. Plotkin, J., et al., *Critical role for CXCR4 signaling in progenitor localization and T cell differentiation in the postnatal thymus.* J Immunol, 2003. **171**(9): p. 4521-7.
35. Ioannidis, V., et al., *The beta-catenin--TCF-1 pathway ensures CD4(+)CD8(+) thymocyte survival.* Nat Immunol, 2001. **2**(8): p. 691-7.
36. van Genderen, C., et al., *Development of several organs that require inductive epithelial-mesenchymal interactions is impaired in LEF-1-deficient mice.* Genes Dev, 1994. **8**(22): p. 2691-703.
37. Mulroy, T., et al., *Wnt-1 and Wnt-4 regulate thymic cellularity.* Eur J Immunol, 2002. **32**(4): p. 967-71.
38. Staal, F.J., et al., *Wnt signaling is required for thymocyte development and activates Tcf-1 mediated transcription.* Eur J Immunol, 2001. **31**(1): p. 285-93.
39. Staal, F.J., et al., *Wnt target genes identified by DNA microarrays in immature CD34+ thymocytes regulate proliferation and cell adhesion.* J Immunol, 2004. **172**(2): p. 1099-108.
40. von Boehmer, H. and H.J. Fehling, *Structure and function of the pre-T cell receptor.* Annu Rev Immunol, 1997. **15**: p. 433-52.
41. Levelt, C.N. and K. Eichmann, *Receptors and signals in early thymic selection.* Immunity, 1995. **3**(6): p. 667-72.
42. Levin, S.D., et al., *A dominant-negative transgene defines a role for p56lck in thymopoiesis.* EMBO J., 1993. **12**(4): p. 1671-1680.
43. Wiest, D.L., M.A. Berger, and M. Carleton, *Control of early thymocyte development by the pre-T cell receptor complex: A receptor without a ligand?* Semin Immunol, 1999. **11**(4): p. 251-62.
44. Clevers, H., et al., *The T cell receptor/CD3 complex: a dynamic protein ensemble.* Annu Rev Immunol, 1988. **6**: p. 629-62.
45. von Boehmer, H., H.S. Teh, and P. Kisielow, *The thymus selects the useful, neglects the useless and destroys the harmful.* Immunol Today, 1989. **10**(2): p. 57-61.
46. Robey, E. and B.J. Fowlkes, *Selective events in T cell development.* Annu Rev Immunol, 1994. **12**: p. 675-705.
47. Sebzda, E., et al., *Selection of the T cell repertoire.* Annu Rev Immunol, 1999. **17**: p. 829-74.
48. Singer, A., S. Adoro, and J.H. Park, *Lineage fate and intense debate: myths, models and mechanisms of CD4- versus CD8-lineage choice.* Nat Rev Immunol, 2008. **8**(10): p. 788-801.
49. Bosma, G.C., R.P. Custer, and M.J. Bosma, *A severe combined immunodeficiency mutation in the mouse.* Nature, 1983. **301**(5900): p. 527-30.
50. von Boehmer, H., et al., *Pleiotropic changes controlled by the pre-T-cell receptor.* Curr Opin Immunol, 1999. **11**(2): p. 135-42.
51. Penit, C., B. Lucas, and F. Vasseur, *Cell expansion and growth arrest phases during the transition from precursor (CD4-8-) to immature (CD4+8+) thymocytes in normal and genetically modified mice.* J.Immunol., 1995. **154**(10): p. 5103-5113.

52. Falk, I., et al., *Proliferation kinetics associated with T cell receptor-beta chain selection of fetal murine thymocytes.* J Exp Med, 1996. **184**(6): p. 2327-39.
53. Haks, M.C., et al., *Pre-TCR signaling and inactivation of p53 induces crucial cell survival pathways in pre-T cells.* Immunity., 1999. **11**(1): p. 91-101.
54. Hozumi, K., et al., *Evidence of stage-specific element for germ-line transcription of the TCR alpha gene located upstream of J alpha49 locus.* Eur J Immunol, 1998. **28**(4): p. 1368-78.
55. Levelt, C.N., et al., *Regulation of T cell receptor (TCR)-beta locus allelic exclusion and initiation of TCR-alpha locus rearrangement in immature thymocytes by signaling through the CD3 complex.* Eur.J.Immunol., 1995. **25**(5): p. 1257-1261.
56. Villey, I., et al., *Defect in rearrangement of the most 5' TCR-J alpha following targeted deletion of T early alpha (TEA): implications for TCR alpha locus accessibility.* Immunity, 1996. **5**(4): p. 331-42.
57. Borowski, C., et al., *Pre-TCRalpha and TCRalpha are not interchangeable partners of TCRbeta during T lymphocyte development.* J Exp Med, 2004. **199**(5): p. 607-15.
58. Berger, M.A., et al., *Subunit composition of pre-T cell receptor complexes expressed by primary thymocytes: CD3 delta is physically associated but not functionally required.* J Exp Med, 1997. **186**(9): p. 1461-7.
59. Dave, V.P., et al., *CD3 delta deficiency arrests development of the alpha beta but not the gamma delta T cell lineage.* EMBO J, 1997. **16**(6): p. 1360-70.
60. Yamasaki, S., et al., *Mechanistic basis of pre-T cell receptor-mediated autonomous signaling critical for thymocyte development.* Nat Immunol, 2006. **7**(1): p. 67-75.
61. Yamasaki, S. and T. Saito, *Molecular basis for pre-TCR-mediated autonomous signaling.* Trends Immunol, 2007. **28**(1): p. 39-43.
62. Levelt, C.N., et al., *Restoration of early thymocyte differentiation in T-cell receptor beta-chain-deficient mutant mice by transmembrane signaling through CD3 epsilon.* Proc.Natl.Acad.Sci.U.S.A, 1993. **90**(23): p. 11401-11405.
63. Shinkai, Y. and F.W. Alt, *CD3 epsilon-mediated signals rescue the development of CD4+CD8+ thymocytes in RAG-2-/- mice in the absence of TCR beta chain expression.* Int Immunol, 1994. **6**(7): p. 995-1001.
64. Saint-Ruf, C., et al., *Different initiation of pre-TCR and gammadeltaTCR signalling.* Nature, 2000. **406**(6795): p. 524-7.
65. Aifantis, I., et al., *Constitutive pre-TCR signaling promotes differentiation through Ca2+ mobilization and activation of NF-kappaB and NFAT.* Nat Immunol, 2001. **2**(5): p. 403-9.
66. van Oers, N.S., et al., *alpha beta T cell development is abolished in mice lacking both Lck and Fyn protein tyrosine kinases.* Immunity., 1996. **5**(5): p. 429-436.

67. Cheng, A.M., et al., *The Syk and ZAP-70 SH2-containing tyrosine kinases are implicated in pre-T cell receptor signaling.* Proc Natl Acad Sci U S A, 1997. **94**(18): p. 9797-801.
68. Zhang, W., et al., *Essential role of LAT in T cell development.* Immunity, 1999. **10**(3): p. 323-32.
69. Clements, J.L., et al., *Requirement for the leukocyte-specific adapter protein SLP-76 for normal T cell development.* Science, 1998. **281**(5375): p. 416-9.
70. Wu, J., et al., *Vav and SLP-76 interact and functionally cooperate in IL-2 gene activation.* Immunity, 1996. **4**(6): p. 593-602.
71. Gomez, M., V. Tybulewicz, and D.A. Cantrell, *Control of pre-T cell proliferation and differentiation by the GTPase Rac-I.* Nat Immunol, 2000. **1**(4): p. 348-52.
72. Motto, D.G., et al., *Implication of the GRB2-associated phosphoprotein SLP-76 in T cell receptor-mediated interleukin 2 production.* J Exp Med, 1996. **183**(4): p. 1937-43.
73. Swat, W., et al., *Activated Ras signals differentiation and expansion of CD4+8+ thymocytes.* Proc Natl Acad Sci U S A, 1996. **93**(10): p. 4683-7.
74. Gartner, F., et al., *Immature thymocytes employ distinct signaling pathways for allelic exclusion versus differentiation and expansion.* Immunity., 1999. **10**(5): p. 537-546.
75. Iritani, B.M., et al., *Distinct signals mediate maturation and allelic exclusion in lymphocyte progenitors.* Immunity, 1999. **10**(6): p. 713-22.
76. Fischer, A.M., et al., *The role of erk1 and erk2 in multiple stages of T cell development.* Immunity, 2005. **23**(4): p. 431-43.
77. Swat, W., et al., *Essential role of PI3Kdelta and PI3Kgamma in thymocyte survival.* Blood, 2006. **107**(6): p. 2415-22.
78. Mao, C., et al., *Unequal contribution of Akt isoforms in the double-negative to double-positive thymocyte transition.* J Immunol, 2007. **178**(9): p. 5443-53.
79. Galandrini, R., S.W. Henning, and D.A. Cantrell, *Different functions of the GTPase Rho in prothymocytes and late pre-T cells.* Immunity, 1997. **7**(1): p. 163-74.
80. Henning, S.W., et al., *The GTPase Rho has a critical regulatory role in thymus development.* EMBO J, 1997. **16**(9): p. 2397-407.
81. Costello, P.S., et al., *The GTPase rho controls a p53-dependent survival checkpoint during thymopoiesis.* J.Exp.Med., 2000. **192**(1): p. 77-85.
82. Williams, B.L., et al., *Phosphorylation of Tyr319 in ZAP-70 is required for T-cell antigen receptor-dependent phospholipase C-gamma1 and Ras activation.* EMBO J, 1999. **18**(7): p. 1832-44.
83. Grakoui, A., et al., *The immunological synapse: a molecular machine controlling T cell activation.* Science, 1999. **285**(5425): p. 221-7.
84. Valge, V.E., et al., *Protein kinase C is required for responses to T cell receptor ligands but not to interleukin-2 in T cells.* Cell, 1988. **55**(1): p. 101-12.

85. Voll, R.E., et al., *NF-kappa B activation by the pre-T cell receptor serves as a selective survival signal in T lymphocyte development.* Immunity, 2000. **13**(5): p. 677-89.
86. Mandal, M., et al., *The BCL2A1 gene as a pre-T cell receptor-induced regulator of thymocyte survival.* J Exp Med, 2005. **201**(4): p. 603-14.
87. Michie, A.M., et al., *Allelic exclusion and differentiation by protein kinase C-mediated signals in immature thymocytes.* Proc.Natl.Acad.Sci.U.S.A, 2001. **98**(2): p. 609-614.
88. Weinberg, R.A., *The retinoblastoma protein and cell cycle control.* Cell, 1995. **81**(3): p. 323-30.
89. Dowdy, S.F., et al., *Physical interaction of the retinoblastoma protein with human D cyclins.* Cell, 1993. **73**(3): p. 499-511.
90. Pagano, M. and P.K. Jackson, *Wagging the dogma; tissue-specific cell cycle control in the mouse embryo.* Cell, 2004. **118**(5): p. 535-8.
91. Lagresle, C., et al., *Transgenic expression of the p16(INK4a) cyclin-dependent kinase inhibitor leads to enhanced apoptosis and differentiation arrest of CD4-CD8- immature thymocytes.* J Immunol, 2002. **168**(5): p. 2325-31.
92. Tsukiyama, T., et al., *Down-regulation of p27Kip1 expression is required for development and function of T cells.* J Immunol, 2001. **166**(1): p. 304-12.
93. Falk, I., et al., *Immature thymocytes that fail to express TCRbeta and/or TCRgamma delta proteins die by apoptotic cell death in the CD44(-)CD25(-) (DN4) subset.* Eur.J.Immunol., 2001. **31**(11): p. 3308-3317.
94. Newton, K., A.W. Harris, and A. Strasser, *FADD/MORT1 regulates the pre-TCR checkpoint and can function as a tumour suppressor.* EMBO J, 2000. **19**(5): p. 931-41.
95. Mandal, M., et al., *Regulation of lymphocyte progenitor survival by the proapoptotic activities of Bim and Bid.* Proc Natl Acad Sci U S A, 2008. **105**(52): p. 20840-5.
96. Roy, N., et al., *The c-IAP-1 and c-IAP-2 proteins are direct inhibitors of specific caspases.* EMBO J, 1997. **16**(23): p. 6914-25.
97. Deveraux, Q.L., et al., *X-linked IAP is a direct inhibitor of cell-death proteases.* Nature, 1997. **388**(6639): p. 300-4.
98. Veis, D.J., et al., *Bcl-2-deficient mice demonstrate fulminant lymphoid apoptosis, polycystic kidneys, and hypopigmented hair.* Cell, 1993. **75**(2): p. 229-40.
99. Ma, A., et al., *Bclx regulates the survival of double-positive thymocytes.* Proc Natl Acad Sci U S A, 1995. **92**(11): p. 4763-7.
100. Strasser, A., et al., *Bcl-2 expression promotes B- but not T-lymphoid development in scid mice.* Nature, 1994. **368**(6470): p. 457-60.
101. Maraskovsky, E., et al., *Bcl-2 can rescue T lymphocyte development in interleukin-7 receptor-deficient mice but not in mutant rag-1-/- mice.* Cell, 1997. **89**(7): p. 1011-1019.
102. Chao, D.T. and S.J. Korsmeyer, *BCL-XL-regulated apoptosis in T cell development.* Int Immunol, 1997. **9**(9): p. 1375-84.

103. Opferman, J.T., et al., *Development and maintenance of B and T lymphocytes requires antiapoptotic MCL-1.* Nature, 2003. **426**(6967): p. 671-6.
104. Dzhagalov, I., A. Dunkle, and Y.W. He, *The anti-apoptotic Bcl-2 family member Mcl-1 promotes T lymphocyte survival at multiple stages.* J Immunol, 2008. **181**(1): p. 521-8.
105. Okada, H., et al., *Survivin loss in thymocytes triggers p53-mediated growth arrest and p53-independent cell death.* J Exp Med, 2004. **199**(3): p. 399-410.
106. Xing, Z., et al., *Essential role of survivin, an inhibitor of apoptosis protein, in T cell development, maturation, and homeostasis.* J Exp Med, 2004. **199**(1): p. 69-80.
107. Jiang, D., M.J. Lenardo, and C. Zuniga-Pflucker, *p53 prevents maturation to the CD4+CD8+ stage of thymocyte differentiation in the absence of T cell receptor rearrangement.* J. Exp. Med., 1996. **183**(4): p. 1923-1928.
108. Guidos, C.J., et al., *V(D)J recombination activates a p53-dependent DNA damage checkpoint in scid lymphocyte precursors.* Genes Dev., 1996. **10**(16): p. 2038-2054.
109. Nacht, M., et al., *Mutations in the p53 and SCID genes cooperate in tumorigenesis.* Genes Dev, 1996. **10**(16): p. 2055-66.
110. Bogue, M.A., et al., *p53 is required for both radiation-induced differentiation and rescue of V(D)J rearrangement in scid mouse thymocytes.* Genes Dev, 1996. **10**(5): p. 553-65.
111. Yasutomo, K., et al., *The Fas-deficient SCID mouse exhibits the development of T cells in the thymus.* J Immunol, 1997. **158**(10): p. 4729-33.
112. Kabra, N.H., et al., *T cell-specific FADD-deficient mice: FADD is required for early T cell development.* Proc Natl Acad Sci U S A, 2001. **98**(11): p. 6307-12.
113. Salmena, L., et al., *Essential role for caspase 8 in T-cell homeostasis and T-cell-mediated immunity.* Genes Dev, 2003. **17**(7): p. 883-95.
114. Kuida, K., et al., *Decreased apoptosis in the brain and premature lethality in CPP32-deficient mice.* Nature, 1996. **384**(6607): p. 368-72.
115. Ciofani, M. and J.C. Zuniga-Pflucker, *Notch promotes survival of pre-T cells at the beta-selection checkpoint by regulating cellular metabolism.* Nat Immunol, 2005. **6**(9): p. 881-8.
116. Felli, M.P., et al., *Expression pattern of notch1, 2 and 3 and Jagged1 and 2 in lymphoid and stromal thymus components: distinct ligand-receptor interactions in intrathymic T cell development.* Int Immunol, 1999. **11**(7): p. 1017-25.
117. Koch, U., et al., *Delta-like 4 is the essential, nonredundant ligand for Notch1 during thymic T cell lineage commitment.* J Exp Med, 2008. **205**(11): p. 2515-23.
118. Mancini, S.J., et al., *Jagged1-dependent Notch signaling is dispensable for hematopoietic stem cell self-renewal and differentiation.* Blood, 2005. **105**(6): p. 2340-2.

119. Jiang, R., et al., *Defects in limb, craniofacial, and thymic development in Jagged2 mutant mice.* Genes Dev, 1998. **12**(7): p. 1046-57.
120. Radtke, F., et al., *Deficient T cell fate specification in mice with an induced inactivation of Notch1.* Immunity, 1999. **10**(5): p. 547-58.
121. Pui, J.C., et al., *Notch1 expression in early lymphopoiesis influences B versus T lineage determination.* Immunity., 1999. **11**(3): p. 299-308.
122. Taghon, T., et al., *Developmental and molecular characterization of emerging beta- and gammadelta-selected pre-T cells in the adult mouse thymus.* Immunity, 2006. **24**(1): p. 53-64.
123. Huang, E.Y., et al., *Surface expression of Notch1 on thymocytes: correlation with the double-negative to double-positive transition.* J Immunol, 2003. **171**(5): p. 2296-304.
124. Goux, D., et al., *Cooperating pre-T-cell receptor and TCF-1-dependent signals ensure thymocyte survival.* Blood, 2005. **106**(5): p. 1726-33.
125. Xu, Y., et al., *Deletion of beta-catenin impairs T cell development.* Nat Immunol, 2003. **4**(12): p. 1177-82.
126. Cobas, M., et al., *Beta-catenin is dispensable for hematopoiesis and lymphopoiesis.* J Exp Med, 2004. **199**(2): p. 221-9.
127. Savino, W., et al., *Molecular mechanisms governing thymocyte migration: combined role of chemokines and extracellular matrix.* J Leukoc Biol, 2004. **75**(6): p. 951-61.
128. Misslitz, A., et al., *Thymic T cell development and progenitor localization depend on CCR7.* J Exp Med, 2004. **200**(4): p. 481-91.
129. Benz, C., K. Heinzel, and C.C. Bleul, *Homing of immature thymocytes to the subcapsular microenvironment within the thymus is not an absolute requirement for T cell development.* Eur J Immunol, 2004. **34**(12): p. 3652-63.
130. Wadsworth, S., M.J. Halvorson, and J.E. Coligan, *Developmentally regulated expression of the beta 4 integrin on immature mouse thymocytes.* J Immunol, 1992. **149**(2): p. 421-8.
131. Magner, W.J., et al., *Aberrant development of thymocytes in mice lacking laminin-2.* Dev Immunol, 2000. **7**(2-4): p. 179-93.
132. Kim, M.G., et al., *Epithelial cell-specific laminin 5 is required for survival of early thymocytes.* J Immunol, 2000. **165**(1): p. 192-201.
133. Klempnauer, K.H. and J.M. Bishop, *Neoplastic transformation by E26 leukemia virus is mediated by a single protein containing domains of gag and myb genes.* J.Virol., 1984. **50**(1): p. 280-283.
134. Ness, S.A., A. Marknell, and T. Graf, *The v-myb oncogene product binds to and activates the promyelocyte-specific mim-1 gene.* Cell, 1989. **59**(6): p. 1115-1125.
135. Weston, K. and J.M. Bishop, *Transcriptional activation by the v-myb oncogene and its cellular progenitor, c-myb.* Cell, 1989. **58**(1): p. 85-93.
136. Ibanez, C.E. and J.S. Lipsick, *trans activation of gene expression by v-myb.* Mol.Cell Biol., 1990. **10**(5): p. 2285-2293.
137. Lipsick, J.S., *One billion years of Myb.* Oncogene, 1996. **13**(2): p. 223-235.

138. Oh, I.H. and E.P. Reddy, *The myb gene family in cell growth, differentiation and apoptosis.* Oncogene, 1999. **18**(19): p. 3017-3033.
139. Dudek, H. and E.P. Reddy, *Identification of two translational products for c-myb.* Oncogene, 1989. **4**(9): p. 1061-6.
140. Dudek, H. and E.P. Reddy, *Murine myeloid leukemias with aberrant myb loci show heterogeneous expression of novel myb proteins.* Oncogene, 1989. **4**(12): p. 1489-95.
141. Sakura, H., et al., *Delineation of three functional domains of the transcriptional activator encoded by the c-myb protooncogene.* Proc.Natl.Acad.Sci.U.S.A, 1989. **86**(15): p. 5758-5762.
142. Saikumar, P., R. Murali, and E.P. Reddy, *Role of tryptophan repeats and flanking amino acids in Myb-DNA interactions.* Proc.Natl.Acad.Sci.U.S.A, 1990. **87**(21): p. 8452-8456.
143. Ogata, K., et al., *Solution structure of a DNA-binding unit of Myb: a helix-turn-helix-related motif with conserved tryptophans forming a hydrophobic core.* Proc.Natl.Acad.Sci.U.S.A, 1992. **89**(14): p. 6428-6432.
144. Ogata, K., et al., *Comparison of the free and DNA-complexed forms of the DNA-binding domain from c-Myb.* Nat.Struct.Biol., 1995. **2**(4): p. 309-320.
145. Mo, X., et al., *Histone H3 tail positioning and acetylation by the c-Myb but not the v-Myb DNA-binding SANT domain.* Genes Dev, 2005. **19**(20): p. 2447-57.
146. Frampton, J., et al., *DNA-binding domain ancestry.* Nature, 1989. **342**(6246): p. 134.
147. Ogata, K., et al., *Solution structure of a specific DNA complex of the Myb DNA-binding domain with cooperative recognition helices.* Cell, 1994. **79**(4): p. 639-648.
148. Biedenkapp, H., et al., *Viral myb oncogene encodes a sequence-specific DNA-binding activity.* Nature, 1988. **335**(6193): p. 835-837.
149. Tahirov, T.H., et al., *Mechanism of c-Myb-C/EBP beta cooperation from separated sites on a promoter.* Cell, 2002. **108**(1): p. 57-70.
150. Ness, S.A., *The Myb oncoprotein: regulating a regulator.* Biochim.Biophys.Acta, 1996. **1288**(3): p. F123-F139.
151. Ramsay, R.G., S. Ishii, and T.J. Gonda, *Interaction of the Myb protein with specific DNA binding sites.* J.Biol.Chem., 1992. **267**(8): p. 5656-5662.
152. Howe, K.M. and R.J. Watson, *Nucleotide preferences in sequence-specific recognition of DNA by c-myb protein.* Nucleic Acids Res., 1991. **19**(14): p. 3913-3919.
153. Kalkbrenner, F., S. Guehmann, and K. Moelling, *Transcriptional activation by human c-myb and v-myb genes.* Oncogene, 1990. **5**(5): p. 657-661.
154. Lei, W., et al., *Positive and negative determinants of target gene specificity in myb transcription factors.* J Biol Chem, 2004. **279**(28): p. 29519-27.
155. Klempnauer, K.H., T.J. Gonda, and J.M. Bishop, *Nucleotide sequence of the retroviral leukemia gene v-myb and its cellular progenitor c-myb: the architecture of a transduced oncogene.* Cell, 1982. **31**(2 Pt 1): p. 453-463.

156. Gonda, T.J. and J.M. Bishop, *Structure and transcription of the cellular homolog (c-myb) of the avian myeloblastosis virus transforming gene (v-myb).* J.Virol., 1983. **46**(1): p. 212-220.
157. Dash, A.B., F.C. Orrico, and S.A. Ness, *The EVES motif mediates both intermolecular and intramolecular regulation of c-Myb.* Genes Dev., 1996. **10**(15): p. 1858-1869.
158. Kanei-Ishii, C., et al., *Transactivation and transformation by Myb are negatively regulated by a leucine-zipper structure.* Proc.Natl.Acad.Sci.U.S.A, 1992. **89**(7): p. 3088-3092.
159. Dubendorff, J.W. and J.S. Lipsick, *Transcriptional regulation by the carboxyl terminus of c-Myb depends upon both the Myb DNA-binding domain and the DNA recognition site.* Oncogene, 1999. **18**(23): p. 3452-3460.
160. Woo, C.H., L. Sopchak, and J.S. Lipsick, *Overexpression of an alternatively spliced form of c-Myb results in increases in transactivation and transforms avian myelomonoblasts.* J.Virol., 1998. **72**(8): p. 6813-6821.
161. Nomura, T., et al., *Negative autoregulation of c-Myb activity by homodimer formation through the leucine zipper.* J.Biol.Chem., 1993. **268**(29): p. 21914-21923.
162. Nomura, T., et al., *Oncogenic activation of c-Myb correlates with a loss of negative regulation by TIF1beta and Ski.* J Biol Chem, 2004. **279**(16): p. 16715-26.
163. Tavner, F.J., et al., *Molecular cloning reveals that the p160 Myb-binding protein is a novel, predominantly nucleolar protein which may play a role in transactivation by Myb.* Mol.Cell Biol., 1998. **18**(2): p. 989-1002.
164. Dudek, H., et al., *Myb and Ets proteins cooperate in transcriptional activation of the mim-1 promoter.* Proc.Natl.Acad.Sci.U.S.A, 1992. **89**(4): p. 1291-1295.
165. Shapiro, L.H., *Myb and Ets proteins cooperate to transactivate an early myeloid gene.* J Biol Chem, 1995. **270**(15): p. 8763-71.
166. Hernandez-Munain, C. and M.S. Krangel, *c-Myb and core-binding factor/PEBP2 display functional synergy but bind independently to adjacent sites in the T-cell receptor delta enhancer.* Mol Cell Biol, 1995. **15**(6): p. 3090-9.
167. Carabana, J., E. Ortigoza, and M.S. Krangel, *Regulation of the murine Ddelta2 promoter by upstream stimulatory factor 1, Runx1, and c-Myb.* J Immunol, 2005. **174**(7): p. 4144-52.
168. Kishi, H., et al., *Cooperative binding of c-Myb and Pax-5 activates the RAG-2 promoter in immature B cells.* Blood, 2002. **99**(2): p. 576-83.
169. Jin, Z.X., et al., *Lymphoid enhancer-binding factor-1 binds and activates the recombination-activating gene-2 promoter together with c-Myb and Pax-5 in immature B cells.* J Immunol, 2002. **169**(7): p. 3783-92.
170. Oelgeschlager, M., et al., *C/EBP, c-Myb, and PU.1 cooperate to regulate the neutrophil elastase promoter.* Mol Cell Biol, 1996. **16**(9): p. 4717-25.

171. Ness, S.A., et al., *Myb and NF-M: combinatorial activators of myeloid genes in heterologous cell types.* Genes Dev., 1993. **7**(5): p. 749-759.
172. Leverson, J.D., et al., *Pim-1 kinase and p100 cooperate to enhance c-Myb activity.* Mol.Cell, 1998. **2**(4): p. 417-425.
173. Sano, Y. and S. Ishii, *Increased affinity of c-Myb for CREB-binding protein (CBP) after CBP-induced acetylation.* J.Biol.Chem., 2001. **276**(5): p. 3674-3682.
174. Dai, P., et al., *CBP as a transcriptional coactivator of c-Myb.* Genes Dev., 1996. **10**(5): p. 528-540.
175. Tomita, A., et al., *c-Myb acetylation at the carboxyl-terminal conserved domain by transcriptional co-activator p300.* Oncogene, 2000. **19**(3): p. 444-51.
176. Oelgeschlager, M., et al., *Interaction of the co-activator CBP with Myb proteins: effects on Myb-specific transactivation and on the cooperativity with NF-M.* EMBO J., 1996. **15**(11): p. 2771-2780.
177. Luscher, B. and R.N. Eisenman, *New light on Myc and Myb. Part II. Myb.* Genes Dev., 1990. **4**(12B): p. 2235-2241.
178. Aziz, N., et al., *Modulation of c-Myb-induced transcription activation by a phosphorylation site near the negative regulatory domain.* Proc.Natl.Acad.Sci.U.S.A, 1995. **92**(14): p. 6429-6433.
179. Tomita, A., et al., *c-Myb acetylation at the carboxyl-terminal conserved domain by transcriptional co-activator p300.* Oncogene, 2000. **19**(3): p. 444-451.
180. Bies, J. and L. Wolff, *Oncogenic activation of c-Myb by carboxyl-terminal truncation leads to decreased proteolysis by the ubiquitin-26S proteasome pathway.* Oncogene, 1997. **14**(2): p. 203-212.
181. Bies, J., J. Markus, and L. Wolff, *Covalent attachment of the SUMO-1 protein to the negative regulatory domain of the c-Myb transcription factor modifies its stability and transactivation capacity.* J.Biol.Chem., 2002. **277**(11): p. 8999-9009.
182. Kanei-Ishii, C., et al., *Wnt-1 signal induces phosphorylation and degradation of c-Myb protein via TAK1, HIPK2, and NLK.* Genes Dev, 2004. **18**(7): p. 816-29.
183. Pani, E. and S. Ferrari, *p38MAPK delta controls c-Myb degradation in response to stress.* Blood Cells Mol Dis, 2008. **40**(3): p. 388-94.
184. Bies, J., et al., *Hyperphosphorylation and increased proteolytic breakdown of c-Myb induced by the inhibition of Ser/Thr protein phosphatases.* Oncogene, 2000. **19**(24): p. 2846-54.
185. Feikova, S., L. Wolff, and J. Bies, *Constitutive ubiquitination and degradation of c-myb by the 26S proteasome during proliferation and differentiation of myeloid cells.* Neoplasma, 2000. **47**(4): p. 212-8.
186. Kitagawa, K., et al., *Fbw7 promotes ubiquitin-dependent degradation of c-Myb: involvement of GSK3-mediated phosphorylation of Thr-572 in mouse c-Myb.* Oncogene, 2009.
187. Aziz, N., et al., *c-Myb and v-Myb are differentially phosphorylated by p42mapk in vitro.* Oncogene, 1993. **8**(8): p. 2259-2265.

188. Miglarese, M.R., et al., *Differential regulation of c-Myb-induced transcription activation by a phosphorylation site in the negative regulatory domain.* J.Biol.Chem., 1996. **271**(37): p. 22697-22705.
189. Winn, L.M., W. Lei, and S.A. Ness, *Pim-1 phosphorylates the DNA binding domain of c-Myb.* Cell Cycle, 2003. **2**(3): p. 258-62.
190. Gu, W. and R.G. Roeder, *Activation of p53 sequence-specific DNA binding by acetylation of the p53 C-terminal domain.* Cell, 1997. **90**(4): p. 595-606.
191. Nomura, N., et al., *Isolation of human cDNA clones of myb-related genes, A-myb and B-myb.* Nucleic Acids Res., 1988. **16**(23): p. 11075-11089.
192. Toscani, A., et al., *Arrest of spermatogenesis and defective breast development in mice lacking A-myb.* Nature, 1997. **386**(6626): p. 713-717.
193. Golay, J., et al., *The A-Myb transcription factor is a marker of centroblasts in vivo.* J.Immunol., 1998. **160**(6): p. 2786-2793.
194. Westin, E.H., et al., *Differential expression of the amv gene in human hematopoietic cells.* Proc.Natl.Acad.Sci.U.S.A, 1982. **79**(7): p. 2194-2198.
195. Mucenski, M.L., et al., *A functional c-myb gene is required for normal murine fetal hepatic hematopoiesis.* Cell, 1991. **65**(4): p. 677-689.
196. Tanaka, Y., et al., *B-myb is required for inner cell mass formation at an early stage of development.* J.Biol.Chem., 1999. **274**(40): p. 28067-28070.
197. Rushton, J.J., et al., *Distinct changes in gene expression induced by A-Myb, B-Myb and c-Myb proteins.* Oncogene, 2003. **22**(2): p. 308-13.
198. Ness, S.A., *Myb protein specificity: evidence of a context-specific transcription factor code.* Blood Cells Mol Dis, 2003. **31**(2): p. 192-200.
199. Brown, K.E., M.S. Kindy, and G.E. Sonenshein, *Expression of the c-myb proto-oncogene in bovine vascular smooth muscle cells.* J.Biol.Chem., 1992. **267**(7): p. 4625-4630.
200. Rosenthal, M.A., et al., *Colonic expression of c-myb is initiated in utero and continues throughout adult life.* Cell Growth Differ, 1996. **7**(7): p. 961-7.
201. Ess, K.C., et al., *Diverse developing mouse lineages exhibit high-level c-Myb expression in immature cells and loss of expression upon differentiation.* Oncogene, 1999. **18**(4): p. 1103-1111.
202. Griffin, C.A. and S.B. Baylin, *Expression of the c-myb oncogene in human small cell lung carcinoma.* Cancer Res., 1985. **45**(1): p. 272-275.
203. Alitalo, K., et al., *Aberrant expression of an amplified c-myb oncogene in two cell lines from a colon carcinoma.* Proc.Natl.Acad.Sci.U.S.A, 1984. **81**(14): p. 4534-4538.
204. Guerin, M., et al., *Strong association between c-myb and oestrogen-receptor expression in human breast cancer.* Oncogene, 1990. **5**(1): p. 131-5.
205. Thiele, C.J., P.S. Cohen, and M.A. Israel, *Regulation of c-myb expression in human neuroblastoma cells during retinoic acid-induced differentiation.* Mol Cell Biol, 1988. **8**(4): p. 1677-83.
206. Clappier, E., et al., *The C-MYB locus is involved in chromosomal translocation and genomic duplications in human T-cell acute leukemia (T-*

ALL), the translocation defining a new T-ALL subtype in very young children. Blood, 2007. **110**(4): p. 1251-61.
207. Lahortiga, I., et al., *Duplication of the MYB oncogene in T cell acute lymphoblastic leukemia.* Nat Genet, 2007. **39**(5): p. 593-5.
208. Bender, T.P. and W.M. Kuehl, *Differential expression of the c-myb proto-oncogene marks the pre-B cell/B cell junction in murine B lymphoid tumors.* J.Immunol., 1987. **139**(11): p. 3822-3827.
209. Gonda, T.J. and D. Metcalf, *Expression of myb, myc and fos proto-oncogenes during the differentiation of a murine myeloid leukaemia.* Nature, 1984. **310**(5974): p. 249-251.
210. Kuehl, W.M., et al., *Expression and function of the c-myb oncogene during hematopoietic differentiation.* Curr.Top.Microbiol.Immunol., 1988. **141:318-23.**: p. 318-323.
211. Clarke, M.F., et al., *Constitutive expression of a c-myb cDNA blocks Friend murine erythroleukemia cell differentiation.* Mol.Cell Biol., 1988. **8**(2): p. 884-892.
212. Yanagisawa, H., et al., *Constitutive expression of exogenous c-myb gene causes maturation block in monocyte-macrophage differentiation.* Biochim Biophys Acta, 1991. **1088**(3): p. 380-4.
213. Todokoro, K., et al., *Down-regulation of c-myb gene expression is a prerequisite for erythropoietin-induced erythroid differentiation.* Proc.Natl.Acad.Sci.U.S.A, 1988. **85**(23): p. 8900-8904.
214. Sakamoto, H., et al., *Proper levels of c-Myb are discretely defined at distinct steps of hematopoietic cell development.* Blood, 2006. **108**(3): p. 896-903.
215. Bender, T.P., C.B. Thompson, and W.M. Kuehl, *Differential expression of c-myb mRNA in murine B lymphomas by a block to transcription elongation.* Science, 1987. **237**(4821): p. 1473-1476.
216. Thompson, C.B., et al., *Expression of the c-myb proto-oncogene during cellular proliferation.* Nature, 1986. **319**(6052): p. 374-380.
217. Toth, C.R., et al., *Members of the nuclear factor kappa B family transactivate the murine c-myb gene.* J.Biol.Chem., 1995. **270**(13): p. 7661-7671.
218. McCann, S., et al., *Repression of the c-myb gene by WT1 protein in T and B cell lines.* J.Biol.Chem., 1995. **270**(40): p. 23785-23789.
219. Sullivan, J., et al., *Identification of the major positive regulators of c-myb expression in hematopoietic cells of different lineages.* J Biol Chem, 1997. **272**(3): p. 1943-9.
220. Xiao, C., et al., *MiR-150 controls B cell differentiation by targeting the transcription factor c-Myb.* Cell, 2007. **131**(1): p. 146-59.
221. Monticelli, S., et al., *MicroRNA profiling of the murine hematopoietic system.* Genome Biol, 2005. **6**(8): p. R71.
222. Zhao, H., et al., *The c-myb proto-oncogene and microRNA-15a comprise an active autoregulatory feedback loop in human hematopoietic cells.* Blood, 2009. **113**(3): p. 505-16.

223. Luscher, B. and R.N. Eisenman, *c-myc and c-myb protein degradation: effect of metabolic inhibitors and heat shock.* Mol Cell Biol, 1988. **8**(6): p. 2504-12.
224. Sumner, R., et al., *Initiation of adult myelopoiesis can occur in the absence of c-Myb whereas subsequent development is strictly dependent on the transcription factor.* Oncogene, 2000. **19**(30): p. 3335-42.
225. Allen, R.D., III, T.P. Bender, and G. Siu, *c-Myb is essential for early T cell development.* Genes Dev., 1999. **13**(9): p. 1073-1078.
226. Badiani, P., et al., *Dominant interfering alleles define a role for c-Myb in T-cell development.* Genes Dev., 1994. **8**(7): p. 770-782.
227. White, J.R. and K. Weston, *Myb is required for self-renewal in a model system of early hematopoiesis.* Oncogene, 2000. **19**(9): p. 1196-1205.
228. Emambokus, N., et al., *Progression through key stages of haemopoiesis is dependent on distinct threshold levels of c-Myb.* EMBO J, 2003. **22**(17): p. 4478-88.
229. Carpinelli, M.R., et al., *Suppressor screen in Mpl-/- mice: c-Myb mutation causes supraphysiological production of platelets in the absence of thrombopoietin signaling.* Proc Natl Acad Sci U S A, 2004. **101**(17): p. 6553-8.
230. Sandberg, M.L., et al., *c-Myb and p300 regulate hematopoietic stem cell proliferation and differentiation.* Dev Cell, 2005. **8**(2): p. 153-66.
231. Reizis, B. and P. Leder, *The upstream enhancer is necessary and sufficient for the expression of the pre-T cell receptor alpha gene in immature T lymphocytes.* J Exp Med, 2001. **194**(7): p. 979-90.
232. Taylor, D., P. Badiani, and K. Weston, *A dominant interfering Myb mutant causes apoptosis in T cells.* Genes Dev., 1996. **10**(21): p. 2732-2744.
233. Salomoni, P., et al., *Resistance to apoptosis in CTLL-2 cells constitutively expressing c-Myb is associated with induction of BCL-2 expression and Myb-dependent regulation of bcl-2 promoter activity.* Proc Natl Acad Sci U S A, 1997. **94**(7): p. 3296-301.
234. Frampton, J., T. Ramqvist, and T. Graf, *v-Myb of E26 leukemia virus up-regulates bcl-2 and suppresses apoptosis in myeloid cells.* Genes Dev., 1996. **10**(21): p. 2720-2731.
235. Peng, S., et al., *c-Maf interacts with c-Myb to down-regulate Bcl-2 expression and increase apoptosis in peripheral CD4 cells.* Eur J Immunol, 2007. **37**(10): p. 2868-80.
236. Berge, T., et al., *Revisiting a selection of target genes for the hematopoietic transcription factor c-Myb using chromatin immunoprecipitation and c-Myb knockdown.* Blood Cells Mol Dis, 2007. **39**(3): p. 278-86.
237. Ess, K.C., et al., *A central role for a single c-Myb binding site in a thymic locus control region.* Mol.Cell Biol., 1995. **15**(10): p. 5707-5715.
238. Hooper, J., et al., *Myb proteins regulate expression of histone variant H2A.Z during thymocyte development.* Immunology, 2008. **123**(2): p. 282-9.

239. Schmidt, M., et al., *Regulation of the resident chromosomal copy of c-myc by c-Myb is involved in myeloid leukemogenesis.* Mol Cell Biol, 2000. **20**(6): p. 1970-81.
240. Cogswell, J.P., et al., *Mechanism of c-myc regulation by c-Myb in different cell lineages.* Mol Cell Biol, 1993. **13**(5): p. 2858-69.
241. Nakagoshi, H., et al., *Transcriptional activation of the c-myc gene by the c-myb and B-myb gene products.* Oncogene, 1992. **7**(6): p. 1233-40.
242. Zobel, A., et al., *Interaction of the v-and c-Myb proteins with regulatory sequences of the human c-myc gene.* Oncogene, 1991. **6**(8): p. 1397-407.
243. Yang, H., et al., *The role of c-Myb and Sp1 in the up-regulation of methionine adenosyltransferase 2A gene expression in human hepatocellular carcinoma.* FASEB J, 2001. **15**(9): p. 1507-16.
244. Zeng, Z., et al., *The role of c-Myb in the up-regulation of methionine adenosyltransferase 2A expression in activated Jurkat cells.* Biochem J, 2001. **353**(Pt 1): p. 163-168.
245. Maurice, D., et al., *c-Myb regulates lineage choice in developing thymocytes via its target gene Gata3.* EMBO J, 2007. **26**(15): p. 3629-40.
246. Wang, Q.F., J. Lauring, and M.S. Schlissel, *c-Myb binds to a sequence in the proximal region of the RAG-2 promoter and is essential for promoter activity in T-lineage cells.* Mol.Cell Biol., 2000. **20**(24): p. 9203-9211.
247. Ratajczak, M.Z., et al., *Myb and ets proteins are candidate regulators of c-kit expression in human hematopoietic cells.* Blood, 1998. **91**(6): p. 1934-46.
248. Hogg, A., et al., *Inactivation of a c-Myb/estrogen receptor fusion protein in transformed primary cells leads to granulocyte/macrophage differentiation and down regulation of c-kit but not c-myc or cdc2.* Oncogene, 1997. **15**(24): p. 2885-98.
249. Vandenbark, G.R., et al., *Complex regulation of human c-kit transcription by promoter repressors, activators, and specific myb elements.* Cell Growth Differ, 1996. **7**(10): p. 1383-92.
250. Allen, R.D., 3rd, et al., *Negative regulation of CD4 gene expression by a HES-1-c-Myb complex.* Mol Cell Biol, 2001. **21**(9): p. 3071-82.
251. Siu, G., *Linking CD4 gene expression and T cell development.* Curr Mol Med, 2001. **1**(5): p. 523-32.
252. Nakata, Y., et al., *c-Myb contributes to G2/M cell cycle transition in human hematopoietic cells by direct regulation of cyclin B1 expression.* Mol Cell Biol, 2007. **27**(6): p. 2048-58.
253. Muller, C., et al., *c-myb transactivates the human cyclin A1 promoter and induces cyclin A1 gene expression.* Blood, 1999. **94**(12): p. 4255-62.
254. Chen, J., C.S. Kremer, and T.P. Bender, *The carbonic anhydrase I locus contains a c-Myb target promoter and modulates differentiation of murine erythroleukemia cells.* Oncogene, 2006. **25**(19): p. 2758-72.
255. Chen, J. and T.P. Bender, *A novel system to identify Myb target promoters in friend murine erythroleukemia cells.* Blood Cells Mol.Dis., 2001. **27**(2): p. 429-436.

256. Lang, G., et al., *Myb proteins regulate the expression of diverse target genes.* Oncogene, 2005. **24**(8): p. 1375-84.
257. Gonda, T.J., D.K. Sheiness, and J.M. Bishop, *Transcripts from the cellular homologs of retroviral oncogenes: distribution among chicken tissues.* Mol Cell Biol, 1982. **2**(6): p. 617-24.
258. Stern, J.B. and K.A. Smith, *Interleukin-2 induction of T-cell G1 progression and c-myb expression.* Science, 1986. **233**(4760): p. 203-6.
259. Catron, K.M., et al., *Constitutive versus cell cycle regulation of c-myb mRNA expression correlates with developmental stages in murine B lymphoid tumors.* J.Immunol., 1992. **148**(3): p. 934-942.
260. Golay, J., et al., *Expression of c-myb and B-myb, but not A-myb, correlates with proliferation in human hematopoietic cells.* Blood, 1991. **77**(1): p. 149-58.
261. Gewirtz, A.M. and B. Calabretta, *A c-myb antisense oligodeoxynucleotide inhibits normal human hematopoiesis in vitro.* Science, 1988. **242**(4883): p. 1303-1306.
262. Citro, G., et al., *Inhibition of leukemia cell proliferation by receptor-mediated uptake of c-myb antisense oligodeoxynucleotides.* Proc Natl Acad Sci U S A, 1992. **89**(15): p. 7031-5.
263. Burgess, T.L., et al., *The antiproliferative activity of c-myb and c-myc antisense oligonucleotides in smooth muscle cells is caused by a nonantisense mechanism.* Proc.Natl.Acad.Sci.U.S.A, 1995. **92**(9): p. 4051-4055.
264. Thomas, M.D., et al., *c-Myb is critical for B cell development and maintenance of follicular B cells.* Immunity, 2005. **23**(3): p. 275-86.
265. Pearson, R. and K. Weston, *c-Myb regulates the proliferation of immature thymocytes following beta-selection.* EMBO J., 2000. **19**(22): p. 6112-6120.
266. Lieu, Y.K., et al., *Requirement of c-myb in T cell development and in mature T cell function.* Proc Natl Acad Sci U S A, 2004. **101**(41): p. 14853-8.
267. Barnden, M.J., et al., *Defective TCR expression in transgenic mice constructed using cDNA-based alpha- and beta-chain genes under the control of heterologous regulatory elements.* Immunol Cell Biol, 1998. **76**(1): p. 34-40.
268. Shinkai, Y., et al., *Restoration of T cell development in RAG-2-deficient mice by functional TCR transgenes.* Science, 1993. **259**(5096): p. 822-825.
269. Schmitt, T.M. and J.C. Zuniga-Pflucker, *Induction of T cell development from hematopoietic progenitor cells by delta-like-1 in vitro.* Immunity., 2002. **17**(6): p. 749-756.
270. Sun, Z., et al., *Requirement for RORgamma in thymocyte survival and lymphoid organ development.* Science, 2000. **288**(5475): p. 2369-73.
271. Pear, W.S., et al., *Efficient and rapid induction of a chronic myelogenous leukemia-like myeloproliferative disease in mice receiving P210 bcr/abl-transduced bone marrow.* Blood, 1998. **92**(10): p. 3780-3792.

272. De Santa, F., et al., *pRb-dependent cyclin D3 protein stabilization is required for myogenic differentiation.* Mol Cell Biol, 2007. **27**(20): p. 7248-65.
273. Pear, W.S., et al., *Production of high-titer helper-free retroviruses by transient transfection.* Proc.Natl.Acad.Sci.U.S.A, 1993. **90**(18): p. 8392-8396.
274. Kotani, H., et al., *Improved methods of retroviral vector transduction and production for gene therapy.* Hum Gene Ther, 1994. **5**(1): p. 19-28.
275. Parker, B.A. and G.R. Stark, *Regulation of simian virus 40 transcription: sensitive analysis of the RNA species present early in infections by virus or viral DNA.* J Virol, 1979. **31**(2): p. 360-9.
276. Bolstad, B.M., et al., *A comparison of normalization methods for high density oligonucleotide array data based on variance and bias.* Bioinformatics, 2003. **19**(2): p. 185-93.
277. Wu, Z., et al., *A Model-Based Background Adjustment for Oligonucleotide Expression Arrays.* Journal of the American Statistical Association, 2004. **99**(468): p. 909-917.
278. Reiner, A., D. Yekutieli, and Y. Benjamini, *Identifying differentially expressed genes using false discovery rate controlling procedures.* Bioinformatics, 2003. **19**(3): p. 368-75.
279. Khatri, P., et al., *New Onto-Tools: Promoter-Express, nsSNPCounter and Onto-Translate.* Nucleic Acids Res, 2006. **34**(Web Server issue): p. W626-31.
280. Fehling, H.J. and H. von Boehmer, *Early alpha beta T cell development in the thymus of normal and genetically altered mice.* Curr Opin Immunol, 1997. **9**(2): p. 263-75.
281. Chen, F., et al., *Differential transcriptional regulation of individual TCR V beta segments before gene rearrangement.* J.Immunol., 2001. **166**(3): p. 1771-1780.
282. Azzam, H.S., et al., *CD5 expression is developmentally regulated by T cell receptor (TCR) signals and TCR avidity.* J Exp Med, 1998. **188**(12): p. 2301-11.
283. Rodewald, H.R., et al., *Fc gamma RII/III and CD2 expression mark distinct subpopulations of immature CD4-CD8- murine thymocytes: in vivo developmental kinetics and T cell receptor beta chain rearrangement status.* J Exp Med, 1993. **177**(4): p. 1079-92.
284. Egawa, T., et al., *The role of the Runx transcription factors in thymocyte differentiation and in homeostasis of naive T cells.* J Exp Med, 2007. **204**(8): p. 1945-57.
285. Fehling, H.J., et al., *Crucial role of the pre-T-cell receptor alpha gene in development of alpha beta but not gamma delta T cells.* Nature, 1995. **375**(6534): p. 795-798.
286. Irving, B.A., F.W. Alt, and N. Killeen, *Thymocyte development in the absence of pre-T cell receptor extracellular immunoglobulin domains.* Science, 1998. **280**(5365): p. 905-8.

287. Crompton, T., et al., *Double-negative thymocyte subsets in CD3 zeta chain-deficient mice: absence of HSA+CD44-CD25- cells.* Eur J Immunol, 1994. **24**(8): p. 1903-7.
288. Kennedy, N.J., et al., *Caspase activation is required for T cell proliferation.* J Exp Med, 1999. **190**(12): p. 1891-6.
289. Ciofani, M., et al., *Obligatory role for cooperative signaling by pre-TCR and Notch during thymocyte differentiation.* J Immunol, 2004. **172**(9): p. 5230-9.
290. Freeden-Jeffry, U., et al., *The earliest T lineage-committed cells depend on IL-7 for Bcl-2 expression and normal cell cycle progression.* Immunity., 1997. **7**(1): p. 147-154.
291. Akashi, K., et al., *Bcl-2 rescues T lymphopoiesis in interleukin-7 receptor-deficient mice.* Cell, 1997. **89**(7): p. 1033-41.
292. Barriere, C., et al., *Mice thrive without Cdk4 and Cdk2.* Mol Oncol, 2007. **1**(1): p. 72-83.
293. Diehl, J.A., *The cyclin D3 knockout: a pound of redundancy with a dash of tissue specificity.* Cancer Biol Ther, 2004. **3**(2): p. 162-4.
294. Boonen, G.J., et al., *Cyclin D3 regulates proliferation and apoptosis of leukemic T cell lines.* J Biol Chem, 1999. **274**(49): p. 34676-82.
295. Cooper, A.B., et al., *A unique function for cyclin D3 in early B cell development.* Nat Immunol, 2006. **7**(5): p. 489-97.
296. Taniguchi, I., H. Hata, and T. Sonoki, *Down-regulation of Cyclin D3 by Small-interfering RNA Induces Cell Cycle Arrest and Apoptosis through the Dissociation of p27Kip1 in a t(6 ; 14) (p21 ; q32) Positive Myeloma Cell Line.* Journal of Clinical and Experimental Hematopathology, 2005. **45**(2): p. 81-87.
297. Mullany, L.K., et al., *Distinct proliferative and transcriptional effects of the D-type cyclins in vivo.* Cell Cycle, 2008. **7**(14): p. 2215-24.
298. Mendelsohn, A.R., et al., *Cyclin D3 activates Caspase 2, connecting cell proliferation with cell death.* Proc Natl Acad Sci U S A, 2002. **99**(10): p. 6871-6.
299. Gutzkow, K.B., et al., *Cyclic AMP inhibits translation of cyclin D3 in T lymphocytes at the level of elongation by inducing eEF2-phosphorylation.* Cell Signal, 2003. **15**(9): p. 871-81.
300. Lahne, H.U., et al., *Degradation of cyclin D3 independent of Thr-283 phosphorylation.* Oncogene, 2006. **25**(17): p. 2468-76.
301. Schmeissner, P.J., et al., *Integrin functions play a key role in the differentiation of thymocytes in vivo.* J Immunol, 2001. **167**(7): p. 3715-24.
302. Geginat, J., et al., *Anchorage dependence of mitogen-induced G1 to S transition in primary T lymphocytes.* J Immunol, 1999. **162**(9): p. 5085-93.
303. Mannion, B.A., et al., *Transmembrane-4 superfamily proteins CD81 (TAPA-1), CD82, CD63, and CD53 specifically associated with integrin alpha 4 beta 1 (CD49d/CD29).* J Immunol, 1996. **157**(5): p. 2039-47.
304. Postigo, A.A., et al., *c-Myb and Ets proteins synergize to overcome transcriptional repression by ZEB.* EMBO J., 1997. **16**(13): p. 3924-3934.

305. Palker, T.J., et al., *Developmental regulation of lymphocyte-specific protein 1 (LSP1) expression in thymus during human T-cell maturation.* Hybridoma, 1998. **17**(6): p. 497-507.
306. Kondo, S., et al., *Possible involvement of glial cell line-derived neurotrophic factor and its receptor, GFRalpha1, in survival and maturation of thymocytes.* Eur J Immunol, 2003. **33**(8): p. 2233-40.
307. Franz, T., et al., *Capn5 is expressed in a subset of T cells and is dispensable for development.* Mol Cell Biol, 2004. **24**(4): p. 1649-54.
308. Riera-Sans, L. and A. Behrens, *Regulation of alphabeta/gammadelta T cell development by the activator protein 1 transcription factor c-Jun.* J Immunol, 2007. **178**(9): p. 5690-700.
309. Hettinger, K., et al., *c-Jun promotes cellular survival by suppression of PTEN.* Cell Death Differ, 2007. **14**(2): p. 218-29.
310. Juntilla, M.M., et al., *Akt1 and Akt2 are required for alphabeta thymocyte survival and differentiation.* Proc Natl Acad Sci U S A, 2007. **104**(29): p. 12105-10.
311. Chen, F., D. Chen, and E.V. Rothenberg, *Specific regulation of fos family transcription factors in thymocytes at two developmental checkpoints.* Int Immunol, 1999. **11**(5): p. 677-88.
312. Bernardin-Fried, F., et al., *AML1/RUNX1 increases during G1 to S cell cycle progression independent of cytokine-dependent phosphorylation and induces cyclin D3 gene expression.* J Biol Chem, 2004. **279**(15): p. 15678-87.
313. Michaud, J., et al., *Integrative analysis of RUNX1 downstream pathways and target genes.* BMC Genomics, 2008. **9**: p. 363.
314. Puthalakath, H., et al., *Bmf: a proapoptotic BH3-only protein regulated by interaction with the myosin V actin motor complex, activated by anoikis.* Science, 2001. **293**(5536): p. 1829-32.
315. Schmelzle, T., et al., *Functional role and oncogene-regulated expression of the BH3-only factor Bmf in mammary epithelial anoikis and morphogenesis.* Proc Natl Acad Sci U S A, 2007. **104**(10): p. 3787-92.
316. Labi, V., et al., *Loss of the BH3-only protein Bmf impairs B cell homeostasis and accelerates gamma irradiation-induced thymic lymphoma development.* J Exp Med, 2008. **205**(3): p. 641-55.
317. Frank, K.M., et al., *Late embryonic lethality and impaired V(D)J recombination in mice lacking DNA ligase IV.* Nature, 1998. **396**(6707): p. 173-7.
318. Malumbres, M., et al., *Mammalian cells cycle without the D-type cyclin-dependent kinases Cdk4 and Cdk6.* Cell, 2004. **118**(4): p. 493-504.
319. Gavrieli, M., et al., *Characterization of phosphotyrosine binding motifs in the cytoplasmic domain of B and T lymphocyte attenuator required for association with protein tyrosine phosphatases SHP-1 and SHP-2.* Biochem Biophys Res Commun, 2003. **312**(4): p. 1236-43.
320. Watanabe, N., et al., *BTLA is a lymphocyte inhibitory receptor with similarities to CTLA-4 and PD-1.* Nat Immunol, 2003. **4**(7): p. 670-9.

321. Rouault, J.P., et al., *BTG1, a member of a new family of antiproliferative genes.* EMBO J, 1992. **11**(4): p. 1663-70.
322. Guardavaccaro, D., et al., *Arrest of G(1)-S progression by the p53-inducible gene PC3 is Rb dependent and relies on the inhibition of cyclin D1 transcription.* Mol Cell Biol, 2000. **20**(5): p. 1797-815.
323. Sechi, A.S. and J. Wehland, *Interplay between TCR signalling and actin cytoskeleton dynamics.* Trends Immunol, 2004. **25**(5): p. 257-65.
324. Zhang, J., et al., *Antigen receptor-induced activation and cytoskeletal rearrangement are impaired in Wiskott-Aldrich syndrome protein-deficient lymphocytes.* J Exp Med, 1999. **190**(9): p. 1329-42.
325. Zhang, J., et al., *WASp verprolin homology, cofilin homology, and acidic region domain-mediated actin polymerization is required for T cell development.* Proc Natl Acad Sci U S A, 2002. **99**(4): p. 2240-5.
326. Ganter, B. and J.S. Lipsick, *Myb binding sites within the N-ras promoter repress transcription.* Oncogene, 1997. **15**(2): p. 193-202.
327. Wang, D.M., et al., *v-Myb represses the transcription of Ets-2.* Oncogene, 2007. **26**(8): p. 1238-44.
328. Zorbas, M., et al., *c-Myb is critical for murine colon development.* Oncogene, 1999. **18**(42): p. 5821-5830.
329. Chen, C., et al., *The Integrin alpha9beta1 contributes to granulopoiesis by enhancing granulocyte colony-stimulating factor receptor signaling.* Immunity, 2006. **25**(6): p. 895-906.
330. Arroyo, A.G., et al., *Differential requirements for alpha4 integrins during fetal and adult hematopoiesis.* Cell, 1996. **85**(7): p. 997-1008.
331. Su, L., et al., *AF-6 controls integrin-mediated cell adhesion by regulating Rap1 activation through the specific recruitment of Rap1GTP and SPA-1.* J Biol Chem, 2003. **278**(17): p. 15232-8.
332. DeMali, K.A., K. Wennerberg, and K. Burridge, *Integrin signaling to the actin cytoskeleton.* Curr Opin Cell Biol, 2003. **15**(5): p. 572-82.
333. Sturge, J., J. Hamelin, and G.E. Jones, *N-WASP activation by a beta1-integrin-dependent mechanism supports PI3K-independent chemotaxis stimulated by urokinase-type plasminogen activator.* J Cell Sci, 2002. **115**(Pt 4): p. 699-711.
334. Annunziato, F., et al., *Chemokines and lymphopoiesis in human thymus.* Trends Immunol, 2001. **22**(5): p. 277-81.
335. Kutlesa, S., et al., *Developmentally regulated interactions of human thymocytes with different laminin isoforms.* Immunology, 2002. **105**(4): p. 407-18.
336. Vila-Coro, A.J., et al., *The chemokine SDF-1alpha triggers CXCR4 receptor dimerization and activates the JAK/STAT pathway.* FASEB J, 1999. **13**(13): p. 1699-710.
337. Yi, T., et al., *Hematopoietic cell phosphatase associates with the interleukin-3 (IL-3) receptor beta chain and down-regulates IL-3-induced tyrosine phosphorylation and mitogenesis.* Mol Cell Biol, 1993. **13**(12): p. 7577-86.

338. Rodriguez-Viciana, P., et al., *Role of phosphoinositide 3-OH kinase in cell transformation and control of the actin cytoskeleton by Ras.* Cell, 1997. **89**(3): p. 457-67.
339. Sells, M.A., et al., *Human p21-activated kinase (Pak1) regulates actin organization in mammalian cells.* Curr Biol, 1997. **7**(3): p. 202-10.
340. Ceredig, R., N. Bosco, and T. Rolink, *Problems defining DN2 thymocytes.* Immunol Cell Biol, 2008. **86**(7): p. 545-7.
341. Chen, J., C.S. Kremer, and T.P. Bender, *A Myb dependent pathway maintains Friend murine erythroleukemia cells in an immature and proliferating state.* Oncogene, 2002. **21**(12): p. 1859-1869.
342. Groettrup, M., et al., *A novel disulfide-linked heterodimer on pre-T cells consists of the T cell receptor beta chain and a 33 kd glycoprotein.* Cell, 1993. **75**(2): p. 283-94.